GEND-INF-090
June 1989

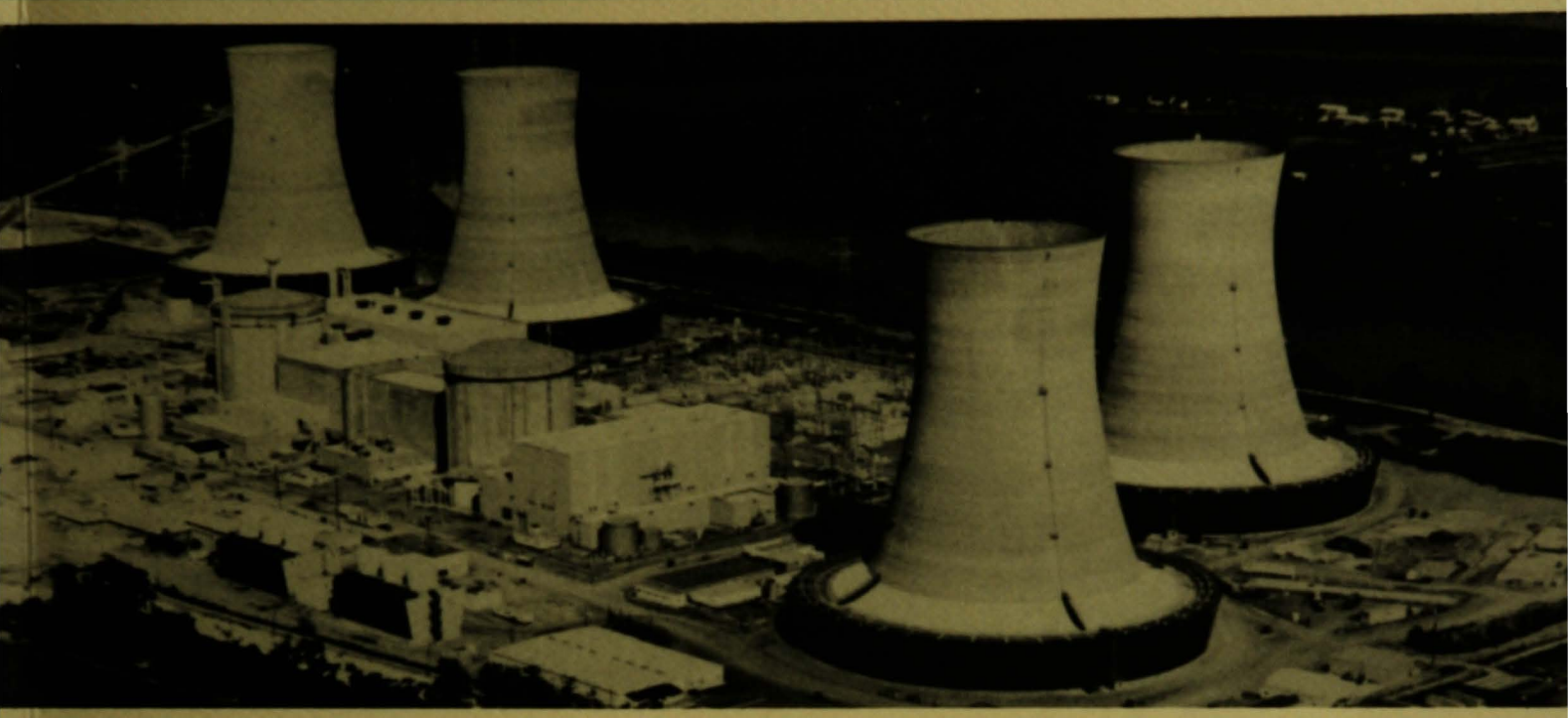

This is an informal report intended for use as a preliminary or working document

GEND
General Public Utilities • Electric Power Research Institute • U.S. Nuclear Regulatory Commission • U.S. Department of Energy

TMI-2 B-LOOP STEAM GENERATOR TUBE SHEET LOOSE DEBRIS EXAMINATION AND ANALYSIS

T. L. Hardt
G.O. Hayner

Prepared for the
U.S. Department of Energy
Three Mile Island Operations Office
Under Contract No. DE-AC07-76ID01570

GEND-INF-090

TMI-2 B-LOOP STEAM GENERATOR TUBE SHEET LOOSE DEBRIS EXAMINATION AND ANALYSIS

G. O. Hayner
T. L. Hardt

Published June 1989

Babcock & Wilcox
A McDermott Company
Contract Research Division
3315 Old Forest Road
P.O. Box 10935
Lynchburg, Virginia 24506

Prepared for EG&G Idaho, Inc.
Under Subcontract No. C86-130971
and the U.S. Department of Energy
Under Contract No. DE-AC07-76ID01570

ABSTRACT

The debris recovered from the upper tube sheet of the TMI-2 B-loop steam generator was analyzed in an effort to determine the concentration and distribution of the chemical and radiochemical species. The debris is of special interest because it is believed to have been transported from the core region during the core damage sequence between 174 and 192 min after accident initiation when a B-loop reactor coolant pump was restarted. Characterization of five size fractions and 10 of the largest particles was accomplished by destructive (chemical, radiochemical, metallography, and SEM/EDS) and nondestructive (photographic examination and density) methods of analysis.

ACKNOWLEDGMENTS

This report was prepared by The Babcock & Wilcox Company (B&W) for EG&G Idaho (EG&G) as an account of work sponsored by the United States Department of Energy (DOE). The authors gratefully acknowledge the many helpful discussions with Mr. M. L. Russell of EG&G during the course of this project. We would like to thank Mr. Harold E. Collins, Mr. Keith S. Doran, and Mr. John E. Bullard for their assistance with the chemical analysis portions, Mr. Robert L. Farmer for his help with the metallurgical portions of the work, and Dr. C. S. Olsen of EG&G for his help with the estimates of prior peak temperature of the individual particles. A special acknowledgment is due to Ms. Bea H. Putney for her assistance with the manuscript preparation. This work was supported by the U.S. Department of Energy under Subcontract Number C86-130971.

PROGRAM SUMMARY

The loose debris taken from the upper tube sheet of the TMI-2 B steam generator was examined at the Babcock & Wilcox hot cell and radiochemistry laboratory facility in Lynchburg, Virginia. The primary objective of this work was to determine the overall chemical and metallurgical characteristics of the debris material and, in particular, the characteristics of 10 large particles selected from the bulk of the sample.

The examinations conducted on the debris samples included detailed chemical, radiochemical, metallurgical, and scanning electron microscope analyses. The results obtained from this program are as follows:

- The 10 large particles chosen for analysis included reaction products composed of uranium and zirconium oxides, two particles that were identified as portions of control rods, and one particle that is a piece of a fuel pellet.

- The 10 large particles did not include any specimens of previously molten stainless steel or Inconel from the fuel assembly upper end fittings or the upper grid. All sample compositions had below-core-average concentrations of the iron, nickel, and chrome aggregate.

- The prior peak temperatures of five of the 10 large particles is estimated to be at least 2800 K.

CONTENTS

FIGURES

TABLES

TMI-2 B-LOOP STEAM GENERATOR TUBE SHEET LOOSE DEBRIS EXAMINATION AND ANALYSIS

1. INTRODUCTION

One of the major objectives of the technical data acquisition program for the Three Mile Island Unit-2 (TMI-2) reactor[a] is to provide information on the release, transport, and deposition of fission products and other radionuclides during severe core damage accidents. This information is being obtained by a detailed characterization of material deposited within the TMI-2 reactor coolant system during the accident.

This report describes the nondestructive and destructive examination and analysis of loose core debris recovered from the B-loop steam generator upper tube sheet to determine the overall chemical and metallurgical characteristics of the debris material and, in particular, the characteristics of large particles selected from the bulk of the sample. The results of these examinations are expressed in terms of TMI-2 accident information.

1.1 Background

The examination of core debris from the B-loop steam generator upper tube sheet is a small part of a large and complex TMI-2 Accident Evaluation Program Sample Acquisition and Examination Plan.[b]

Although the March 28, 1979, accident at TMI-2 involved severe damage to the core of the reactor, the accident had no observable effects on the health and safety of the public in the area. That such a severe core-disruption accident would have no consequent health or safety effects

---

a. E. L. Tolman et al., TMI-2 Accident Evaluation Program, EGG-TMI-7048, February 1986.

b. M. L. Russell et al., TMI-2 Accident Evaluation Program Sample Acquisition and Examination Plan - Executive Summary, EG&G-TMI-7121, EG&G Idaho, Inc., December 1985.

has led to questions concerning earlier light water reactor (LWR) safety studies and estimates. In an effort to resolve these questions, several major research programs have been initiated by organizations concerned with nuclear power plant safety. The U.S. Nuclear Regulatory Commission (NRC) has embarked on a thorough review of reactor safety issues, particularly the causes and effects of core-damage accidents. Industrial organizations have conducted the Industry Degraded Core Rulemaking (IDCOR) Program. The U.S. Department of Energy (DOE) has established the TMI-2 Program to develop technology for recovery from a serious reactor accident and to conduct relevant research and development that will enhance nuclear power plant safety.

Immediately after the TMI-2 accident, four organizations with interests in both plant recovery and accident data acquisition formally agreed to cooperate in these areas. These organizations, commonly referred to as the GEND Group--GPU Nuclear Corporation, Electric Power Research Institute, Nuclear Regulatory Commission, and Department of Energy, are actively involved in reactor recovery and accident research. At present, the DOE is providing a portion of the funds for reactor recovery (in those areas where accident recovery knowledge will be of generic benefit to the U.S. LWR industry) as well as the preponderance of funds for severe accident technical data acquisition (such as the examination of the damaged core).

This work by Babcock & Wilcox is part of the DOE program to involve private laboratories in the United States in the TMI-2 Accident Evaluation Program,[a] which is coordinated by EG&G Idaho, Inc. (EG&G). The TMI-2 Accident Evaluation Program report[a] defines the program required to implement the DOE assignments and contains the guidelines and requirements for TMI-2 sample acquisition and examinations.

The already-completed portion of the Sample Acquisition and Examination (SA&E) Plan[b] includes in situ measurements, and sample

---

a. Ibid. p.1, footnote a.

b. Ibid. p.1, footnote b.

acquisition and examinations involving private organizations and state and federal agencies. It has provided postaccident core and fission product end-state data that indicate the following:

- The current estimate of damage and reconfiguration of the core is as follows:

Core Region	Percent of Core Material
Still standing rod bundle geometry	33
Loose debris (unmelted and previously molten core material mixture) below the cavity in the upper core region (the cavity was 26% of the original core volume)	20
Previously molten core material:	47:
Retained in core boundary	25
Escaped from core boundary:	22:
	(47)
Bypass region	3
Core support assembly	4
Lower plenum	15
	(22)

- Some uranium dioxide fuel melting occurred with temperatures greater than 2800 K.

- Fission product retention by the core materials is significant with fission product retention outside the core primarily by the reactor coolant system water and the reactor building basement water and concrete.

Examination and analysis of loose debris from the B-loop steam generator is part of the Reactor Coolant System Fission Product Inventory portion of the TMI-2 Accident Evaluation Program SA&E Plan. This part of the plan also includes examination of additional loose deposits from

reactor coolant system horizontal and low-point surfaces; examinations of the pressurizer and steam generator manway cover backing plate surface deposits; in situ video and boroscope surveys of the reactor coolant system vessels and piping for locating core material deposits; and in situ gamma spectrometer surveys for locating uranium in the reactor coolant system. The TMI-2 AEP requirements and/or objective for the RCS FPI Sample Acquisition and Examination Program are stated as follows:

> "All present experience in characterizing the plant indicates relatively small fission product deposition on the reactor system surfaces external to the reactor vessel. However, the primary cooling system surface deposition may provide the only benchmark for the fission product transport during the core degradation phase of the accident. Analysis of the core material debris deposited in the RCS will be conducted to enhance our understanding of the plant hydraulic conditions during or shortly after the accident."

> "For each sample, the following characteristics should be determined:

- Physical appearance,
- Elemental and chemical composition,
- Particle size distributions, density, and surface texture, and
- Radiochemical measurements of retained fission product concentrations and chemical forms."

1.2 B-Loop Steam Generator Loose Debris History

1.2.1 RCS Description

TMI-2 reactor coolant system piping and components are shown in Figure 1 and include the following:

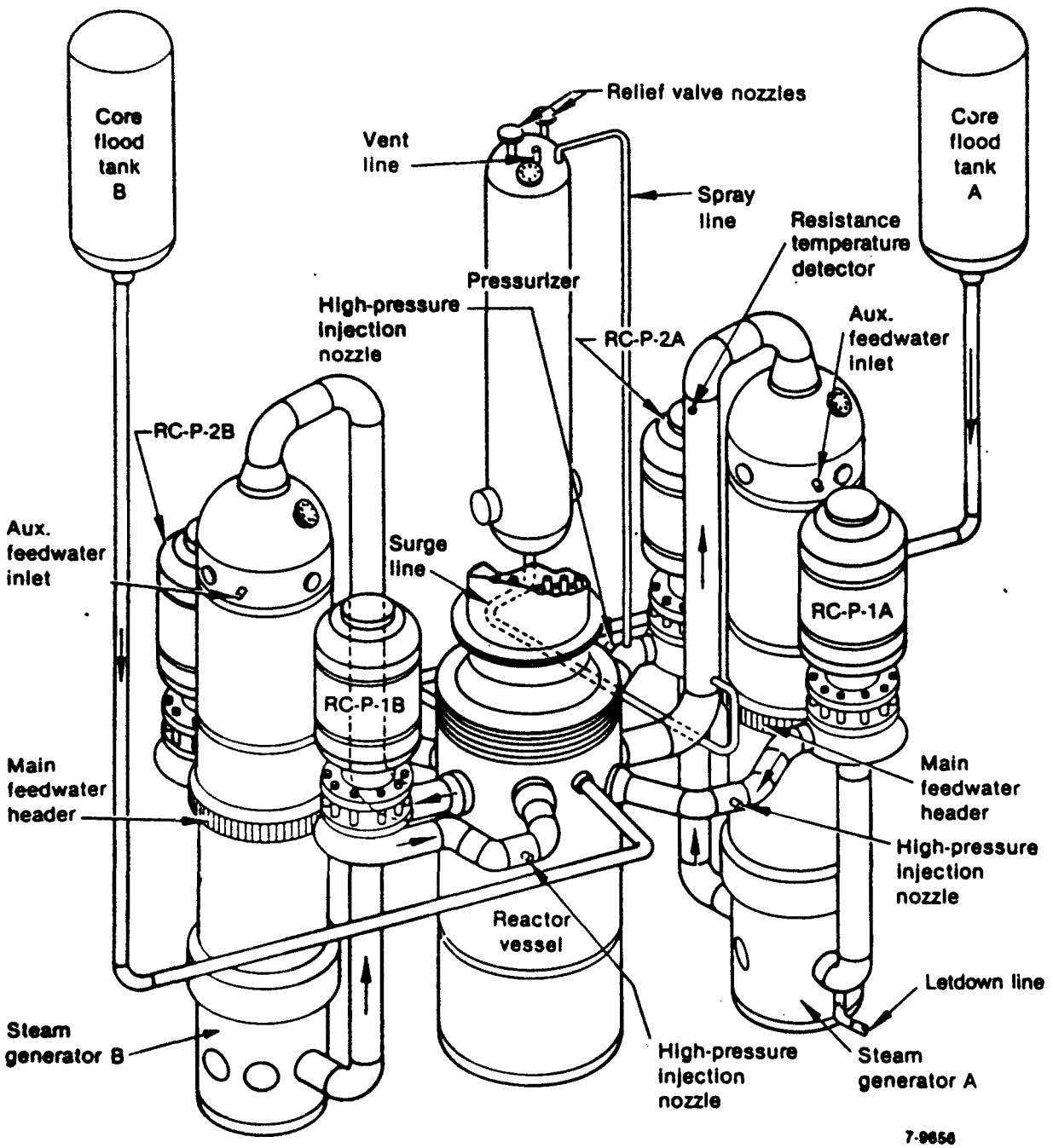

Figure 1. TMI-2 reactor coolant system piping and components.

- A reactor vessel containing the uranium-fueled core.

- Dual reactor cooling loops (A and B) consisting of the candy-cane shaped hot legs from the reactor vessel upper plenum to the steam generator tops, two single-pass type steam generators (Figure 2), dual (four total) cold legs from the steam generator bottom back to the reactor vessel via the four reactor coolant pumps.

- A pressurizer connected to the cooling loops by a surge line from the A-loop hot leg to the pressurizer bottom and a spray line from the A-loop cold leg (downstream of pump RC-P-2A) to the pressurizer top.

- Dual core flood tanks connected to the reactor vessel.

1.2.2 TMI-2 Accident and Recovery Period Environment

During and after the TMI-2 accident sequence that lasted until natural circulation cooling commenced (approximately 30 days after accident initiation), many events occurred that affected the character and distribution of core materials and fission products that escaped from the reactor vessel to the reactor coolant system. The most significant events include the following:

- Fission product and a small uranium fraction release commenced in the reactor vessel at approximately 138 min after accident initiation when fuel rod cladding failure commenced. Reactor coolant pump operation had ceased, and the available escape paths were (a) through the A-loop hot leg, surge line, and pressurizer because the pilot-operated relief valve (PORV) was stuck open, releasing reactor coolant to the reactor basement through the reactor coolant drain tank, and (b) through the A-loop cold leg to the letdown line (upstream of reactor coolant pump RCP-P-1A).

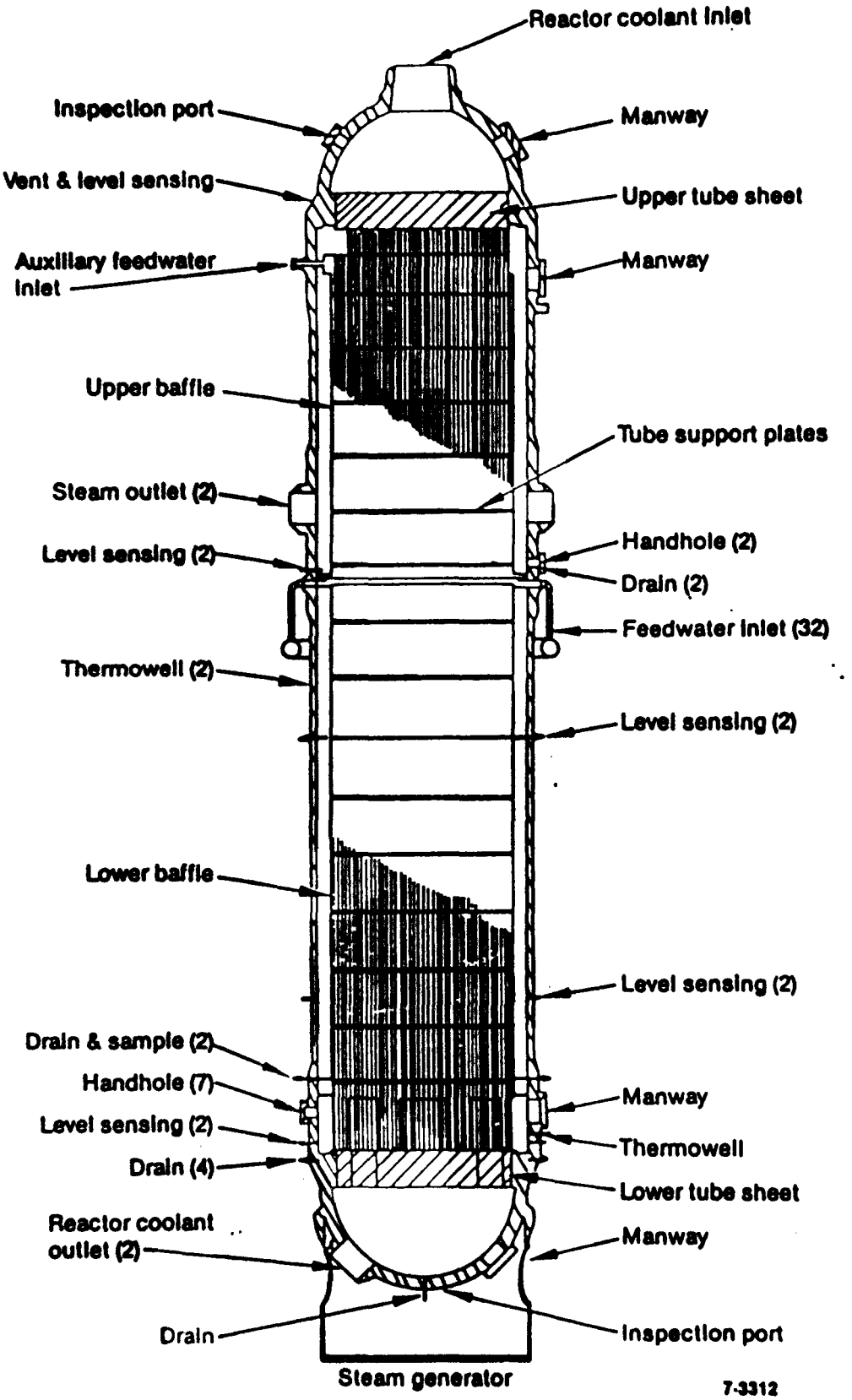

Figure 2. TMI-2 steam generator diagram.

- Reactor coolant system temperatures exceeded the coolant saturation temperature from 136 min to approximately 16 h after accident initiation in the hot legs and occasionally in the cold legs. Measured coolant temperatures did not exceed 725 K.

- The PORV/pressurizer escape path was closed at 142 min after accident initiation.

- Zircaloy-steam reaction became significant at 144 min, releasing hydrogen and other chemical reaction products into the coolant in the reactor vessel. Core material temperatures continued to rise and reached temperatures exceeding 2800 K, which could (a) generate aerosols from low volatility materials and chemical reactions and (b) accelerate the escape of fission products from the uranium dioxide. Noncondensable gases collected in the steam generator and hot leg piping upper regions.

- A reactor coolant sample taken at 163 min contained 140 μCi/mL gross activity.

- Reactor coolant pump RC-P-2B was energized from 174 to 192 min after accident initiation. This event is believed to have reflooded the overheated core region, fragmented most of the standing fuel in the upper core region, and caused circulation of core material particles and fission products throughout the B-loop components.

- The PORV/pressurizer escape path was reopened from 192 to 197 min and from 220 to 318 min.

- At 227 min, a significant relocation of core material into the flooded reactor vessel lower plenum region occurred, which would likely increase the escape of core material and fission products to the letdown system escape path.

- A sustained high pressure injection period commenced at 267 min and continued to 544 min.

- A reactor coolant sample taken at 283 min contained >500 μCi/mL gross activity.

- The PORV/pressurizer escape path was cycled open repeatedly during the 340- to 458-min period to prevent RCS overpressurization and was also opened from 458 to 550, 565 to 589, 600 to 668, 756 to 767, and 772 to 780 min to depressurize the RCS for core flood injection.

- Core flood tank injection probably occurred from 511 to 550 min after accident initiation. This event is believed to have caused a back flow leak path to develop from the reactor coolant system to Flood Tank B due to incomplete check valve reseating.

- A reactor coolant system pressurization in the 840- to 900-min period probably forced coolant and core material aerosols and volatile fission products from the reactor vessel into Flood Tank B.

- Forced circulation cooling of the reactor was resumed at 949 min (15 h 49 min) through the A-loop with reactor coolant pump RC-P-1A. This action flushed the noncondensable gases from the A-loop steam generator and hot leg upper regions.

- Letdown flow was lost from 18 h 34 min to 26 h 30 min.

- A reactor coolant sample taken at 36 h and 15 min measured >1000 R/h on contact.

- At 6 days after accident initiation, the noncondensable gas bubble in the B-loop upper region appeared to be gone.

- Natural circulation cooling of the reactor commenced, using both coolant loops, 30 days and 10 h after accident initiation. Steam generator B was later isolated.

- Reactor coolant water cleanup using the SDS/EPICOR-II system commenced 2 yr and 106 days (7/12/81) after accident initiation and included cleanup of an equivalent of four reactor coolant system volumes of reactor coolant water.

- After the accident, the reactor coolant was a water solution with the following target specifications:

  - pH 7.5 to 7.7

  - Boron 5000 to 5350 ppm

  - Buffer NaOH.

- The RCS liquid volume was drawn down for initial reactor disassembly in July 1982, uncovering the pressurizer and steam generator upper regions. Figure 3 shows video still-images of the conditions at the top of the steam generator tube sheet when the manway covers were removed in March 1986.

1.2.3 Loose Debris Sample Retrieval and Handling

In September 1986, the loose debris sample was retrieved with a vacuum apparatus from the top of the B-loop steam generator upper tube sheet. The vacuum apparatus, shown schematically in Figure 4, used a "pickup" nozzle (Figure 5) consisting of an 8-ft-long tube with a 0.622-in. inside diameter. The nozzle with an attached video camera was inserted into the steam generator upper region through the manway opening.

The sample was transferred from the top of the tube sheet through the nozzle tube and vacuum hose into a polypropylene sock-type filter supported

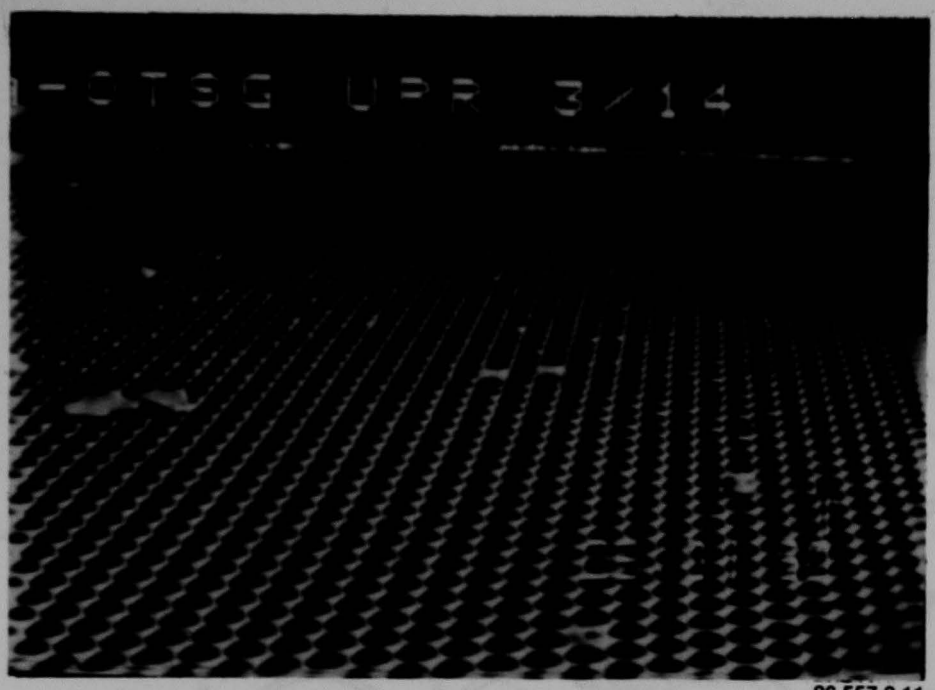

86-557-2-11

A-loop steam generator tube sheet top

86-557-3-6

B-loop steam generator tube sheet top

Figure 3. Video still-image views of TMI-2 steam generator tube sheet tops in March 1986.

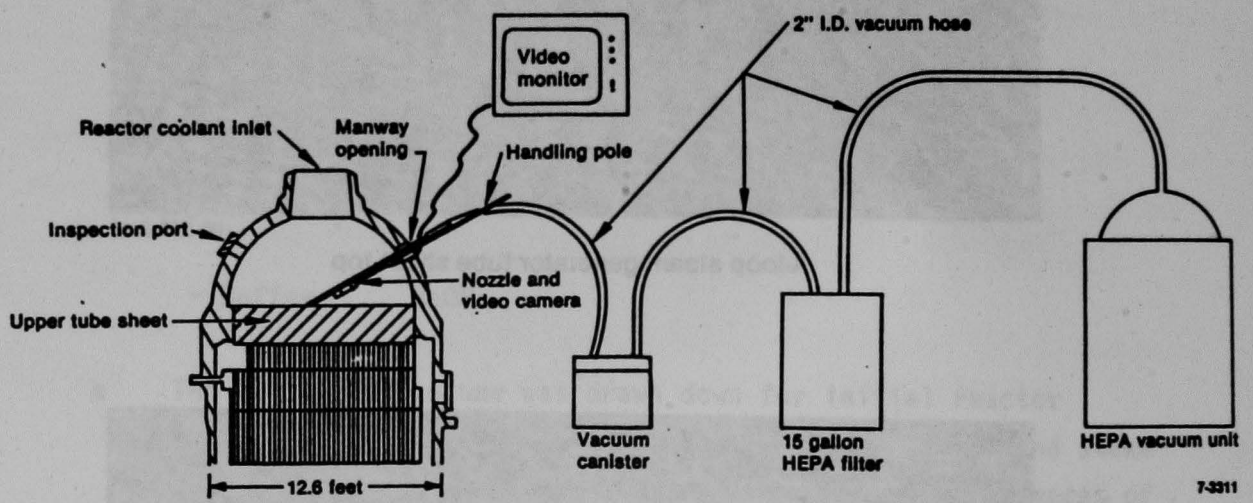

Figure 4. Loose debris sample collection apparatus - schematic.

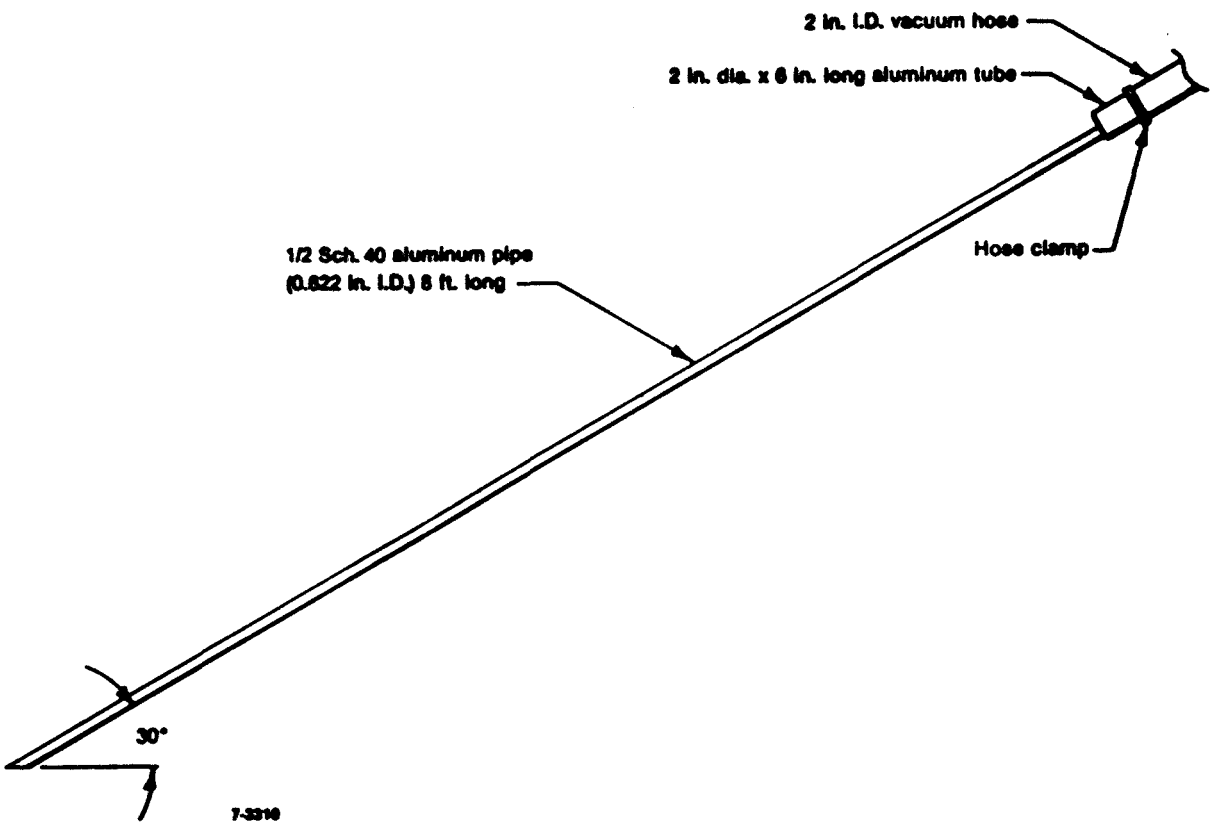

Figure 5. Vacuum nozzle arrangement.

by a perforated stainless steel canister 4 in. in diameter by 8 in. long. The perforated canister was located inside an outer filter canister that included lead shielding and special features so that it could be used as a DOT 7A Type A shipping package. The polypropylene sock may have broken near the tip during the vacuuming, allowing an unknown quantity of the sample to escape.

The vacuum canister was shipped to the INEL where the sample was unloaded, separated into sieve fractions, and weighed. The sample of loose debris is shown (Figure 6) in a plastic cup. The filter sleeve and filter canister are shown, after separation from the 81-g sample, in Figure 7. The filter sleeve, moisture, and embedded debris weighed 28.8 g. The weights of the sieve fractions from the loose debris sample were as follows:

Particle Size (μm)	Mass (g)
>1000	75.60
710 to 1000	1.35
300 to 710	2.20
150 to 300	0.80
<150	1.08
Total	81.03

The filter sleeve and approximately one-half of the sieved loose debris, including the largest single particle, were repackaged into the vacuum canister and shipped via air freight to Babcock & Wilcox in Lynchburg, Virginia, for examination.

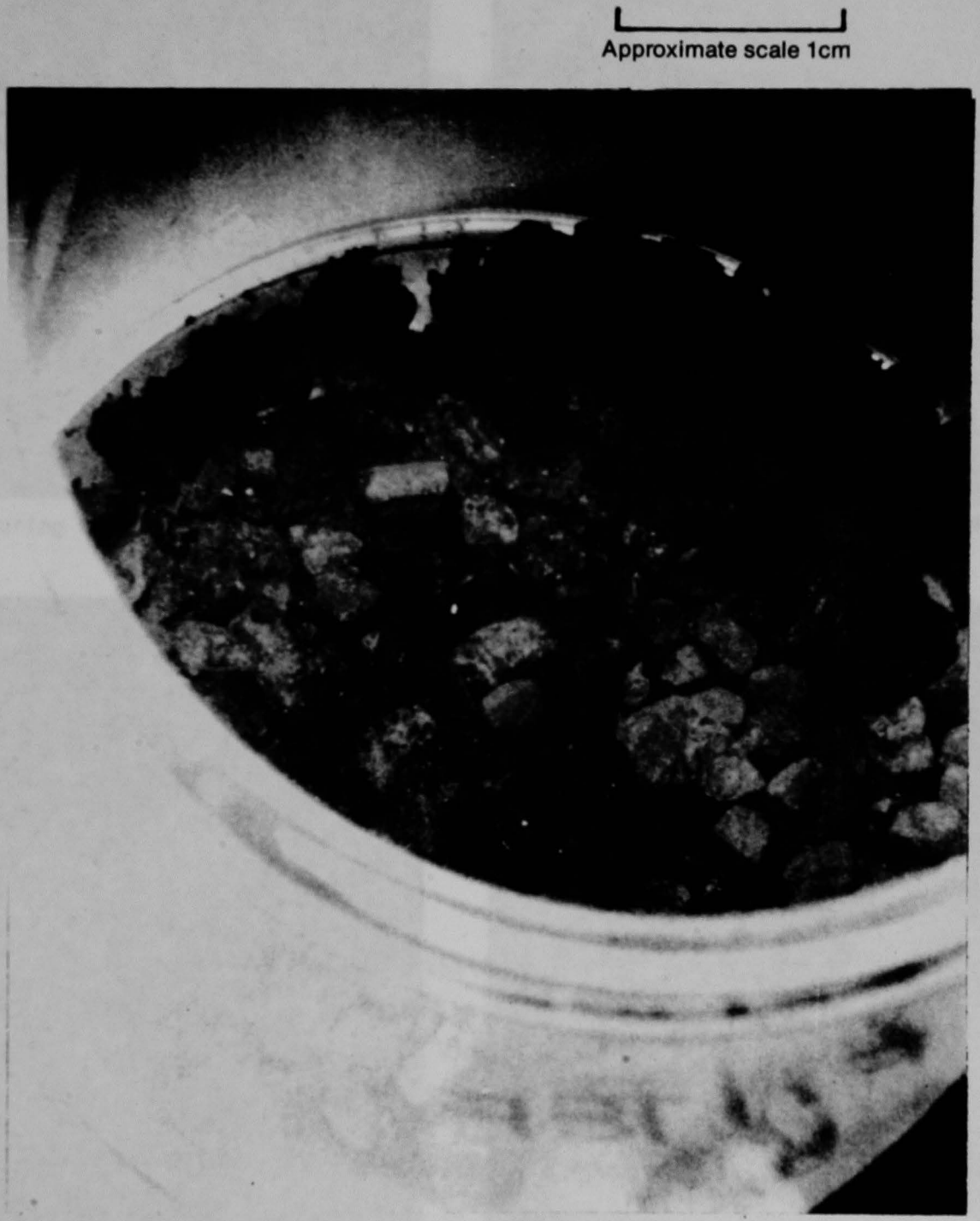

Figure 6. B-loop steam generator tube sheet top loose debris.

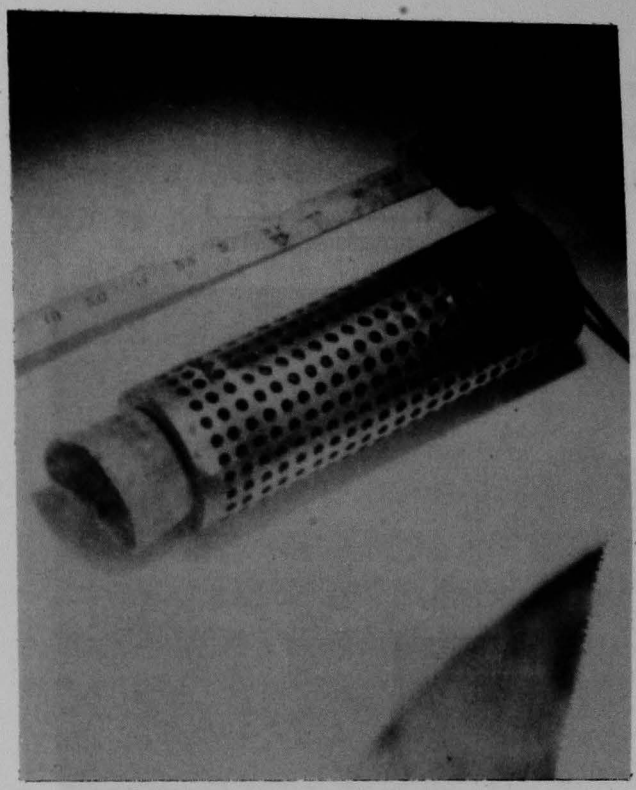

Filter canister

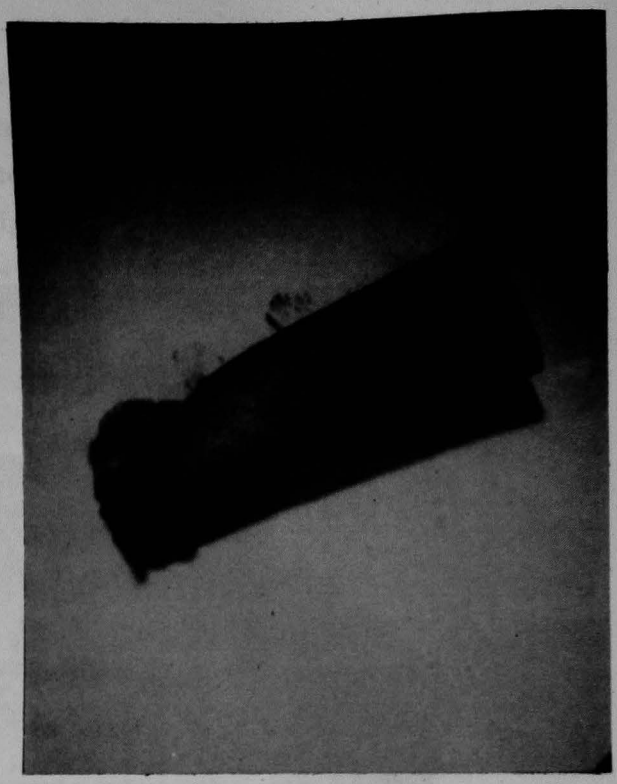

Filter fabric sleeve

Filter fabric sleeve-opened

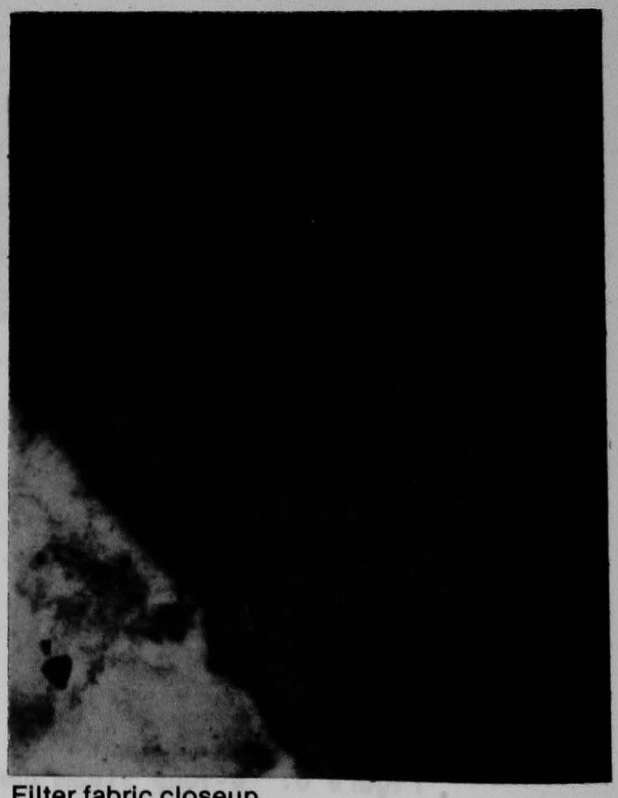

Filter fabric closeup

Figure 7. Filter and filter canister used to collect the loose debris from the B-loop steam generator upper tube sheet.

2. EXAMINATION AND RESULTS

Table 1 shows in summary form the analysis program that was performed on each sample.

2.1 Sample Receipt and Initial Inspection

The sample shipment containing the TMI-2 B-loop steam generator debris samples from EG&G Idaho, Inc., was received in a shielded 55-gal drum on March 17, 1987, at the Babcock & Wilcox Lynchburg Research Center in Lynchburg, Virginia. Five vials containing the size fractions of the debris material and a filter sleeve were removed from the shielded container and transferred to the hot cell. During the transfer of the 300 to 710 μm sample to the hot cell, we noticed that the lid of the sample bottle was unattached. Other lids were also found to be loose. Most of the debris from the open sample was recovered from the plastic bag used during the transfer.

The shipping container was found to be very contaminated on the inside surfaces. Radiation survey results indicated a reading of about 500 mR/h ($\beta + \gamma$) at 6 in. from the center of the shipping container cavity. Based on the weighing results and the loose lids, it is estimated that approximately 0.1 g of debris material may have escaped and is present as contamination on the inside of the shipping container.

2.1.1 Gross Radiation Levels

As each sample fraction and the filter were removed from the shipping container, a radiation measurement was made at distances of 2 and 12 in. from each sample container. Open window ($\beta + \gamma$) and closed window (γ) readings were made with two handheld ion chamber instruments. The 2-in. reading was taken with an Eberline RO-7 survey meter and the 12-in. reading was taken with a larger volume Eberline RO-3A instrument. A summary of the radiation survey results is given in Table 2.

TABLE 1. MATRIX CHART LISTING ALL SAMPLES AND EXAMINATIONS PERFORMED

	Particle Size Group (μm)						Individual Particle Number ("large")											
Analysis	>1000	700-1000	310-700	150-310	<150	Filter	1	2	3	4	5	6	7	8	9	10	11	12
Initial radiation levels	x	x	x	x	x	x	--	--	--	--	--	--	--	--	--	--	--	--
Weight	x	x	x	x	x	x	x	x	x	x	x	x	x	x	--	--	x	x
Appearance	--	--	--	--	--	--	x	x	x	x	x	x	x	x	x	x	x	x
Photographs	x	x	x	x	x	x	x	x	x	x	x	x	x	x	x	x	x	x
Immersion density	--	--	--	--	--	--	x	x	x	x	x	x	x	x	--	--	x	x
Metallography	--	--	--	--	--	--	x	x	x	x	x	x	x	x	--	--	x	x
SEM photos	--	--	--	--	--	--	x	x	x	x	x	x	x	x	--	--	x	x
SEM dot maps	--	--	--	--	--	--	x	x	x	x	x	x	x	x	--	--	x	x
EDS analysis	--	--	--	--	--	--	x	x	x	x	x	x	x	x	--	--	x	x
Gross radiation measurement	x	x	x	x	x	x	x	x	x	x	x	x	x	x	--	--	x	x
Elemental composition	x	x	x	x	x	x	x	x	x	x	x	x	x	x	--	--	x	x
Fission product analysis	x	x	x	x	x	x	x	x	x	x	x	x	x	x	--	--	x	x
Sr-90	x	x	x	x	x	x	x	x	x	x	x	x	x	x	--	--	x	x
I-129	--	x	x	x	x	x	x	x	x	--	x	--	--	x	--	--	--	--

TABLE 2. B-LOOP DEBRIS WEIGHT AND RADIATION SURVEY INFORMATION

Loose Debris Particle Size[b]	Estimated Weight[b] (g)	As-Received Weight (g)	Radiation Survey Results[a] (mR/h)			
			At 2-Inch Distance		At 12-Inch Distance	
			β + γ	γ	β + γ	γ
>1000	36.07	36.055	8,800	6,800	1,000	700
1000 to 710	0.811	0.726	200	100	50	23
710 to 300	1.137	1.139	400	200	60	27
300 to 150	0.522	0.520	120	110	35	20
<150	0.456	0.399	200	200	50	25
Total Weight	38.996	38.839				
Filters	28.8	17.13	60,000	700	7,000	500

a. Readings based on survey data made with two hand-held ion chambers of different chamber volumes used as appropriate. Samples were in glass bottles when survey performed.

b. Based on EG&G information supplied.

2.1.2 Some Physical Characteristics

Each sample fraction was put into a tared weighing dish and weighed on a Mettler balance in the hot cell. A summary of the as-received weights is presented in Table 2 and compares very favorably with the weights provided by EG&G prior to shipment, except for the filter that may have dried during handling and shipping to B&W. Following weighing, each debris sample was put into a Teflon dish for photographic examination. The photographs in Appendix A show each size fraction under varying magnification.

2.2 Examination of Large Particles

2.2.1 Particle Selection and Division

Twelve large particles from the >1000 μm size fraction were selected for further examination using a selection criterion based on largest size and potential for being a product of core material interaction. This was done on April 9, 1987 with the aid of M. L. Russell during his visit on behalf of EG&G. A preliminary physical description of all 12 particles is documented in Table 3. The 12 particles were later reduced to the 10 specified in the subcontract by removing Samples 9 and 10. These two particles were removed because they seemed to be similar to Sample 3, which appeared to be a fragment of a fuel pellet. The radiation survey results for each of the 10 selected particles are given in Table 4. The maximum dimension of the 12 particles from scaling photographs ranges from 4.4 mm (Particles 10 and 11) to 7.9 mm (Particle 6). Photographic documentation of the 10 particles is given in Appendix B.

Following the immersion density work described in the next paragraph, each particle was cut into two sections with a diamond saw. One of the sections was metallographically mounted and the other was reserved for radiochemistry. If the second section was large enough, it was also cut so that one part could be used for I-129 analysis and the remainder dissolved for all other chemical analysis.

TABLE 3. APPEARANCE OF 12 B-LOOP DEBRIS SAMPLES SELECTED DURING EG&G VISIT

Sample Number	Remarks
1	Orange-brown coating; possible metallic material; probable core material reaction product
2	Orange-brown coating; possible machine tool mark; curved surface; some type of cladding
3	Curved surface on one side with grinding marks, probable fuel pellet fragment
4	Small melted metallic nugget
5	Core material reaction product with surface porosity
6	Orange-brown coating; larger piece, interaction zone; surface porosity, possible core material reaction product
7	Orange-brown surface deposit, some surface porosity; probable core material reaction product
8	Orange-brown surface deposit; some surface porosity; probable core material reaction product
9	Similar to 3
10	Orange-brown deposit layer; probable fuel pellet fragment
11	Square-shaped particle, orange-brown deposit layer; surface porosity; metallic appearance
12	Irregular shape, orange-brown spots; probable core material reaction product

TABLE 4. RADIATION SURVEY--10 B-LOOP DEBRIS SAMPLES SELECTED FOR FURTHER EXAMINATION

	Radiation Survey Results[a] (mR/h)			
	At 2-Inch Distance		At 12-Inch Distance	
Sample Number	β + γ	γ	β + γ	γ
1	240	140	11	8
2	5	2.5	1.1	0.9
3	500	400	15	12
4	3	1.5	0.7	0.6
5	360	240	20	14
6	23	11	2	1.6
7	180	90	9	6
8	280	150	14	10
11	35	12	3	1.5
12	230	180	10	8

a. Survey results obtained with RO-3C hand-held ion chamber. Samples were in glass bottles when survey performed.

2.2.2 Particle Density

Immersion density measurements were performed on each of the 10 particles selected from the coarsest (>1000 μm particle size) sieve fraction sample provided. The immersion densities were obtained using ASTM C373-72 as a guide. Deviations from this procedure were as follows:

1. The particles were saturated by water immersion in a vacuum bell jar.

2. Following blotting of the particles with both dry and wet towels, saturated weights were recorded.

3. The density of water was not assumed to be constant and was corrected for fluid density based on the temperature of water or air.

4. Three replicates were performed on each particle to establish precision.

The immersion density results are given in Table 5.

2.2.3 Metallographic Examination

The samples for metallographic examination were mounted, ground and polished using SiC and Al_2O_3 abrasives. An outline describing this procedure is given in Appendix C. The cut surface of each sample was examined with an Olympus microscope. Black and white optical photomicrographs of the polished surfaces were made for each particle. These are shown in Appendix D. The letter "M," shown on these photos, indicates a typical representation of mounting material location. The mounting material used was either a low temperature Pb, Sn, Bi alloy or epoxy resin.

TABLE 5. IMMERSION DENSITIES OF THE 10 SELECTED PARTICLES

	A	D	S	M	E	F	V	P	G	J	T
Cycle 1 @ 25.9 C											
Sample	Fluid Density (g/cc)	Dry Wt (g)	Susp. Wt (g)	(W)[a] Sat. Wt (g)	(D)[b] Sat. Wt (g)	Open[c] Porosity (cc)	Pellet[d] Volume (cc)	Open[e] Porosity (%)	Bulk[f] Density (g/cc)	Matrix[g] Volume (cc)	Matrix[h] Density (g/cc)
1	0.996809	0.42709	0.37355	0.43887	0.43804	0.01182	0.06553	18.03429	6.51756	0.05371	7.95157
2	0.996809	0.16190	0.13480	0.16369	0.16330	0.00180	0.02898	6.19592	5.58613	0.02719	5.95511
3	0.996809	0.68023	0.61507	0.68057	0.68024	0.00034	0.06571	0.51908	10.35205	0.06537	10.40607
4	0.996809	0.06256	0.05625	0.06282	0.06270	0.00026	0.00659	3.95738	9.49169	0.00633	9.88278
5	0.996809	0.73123	0.64019	0.75255	0.75201	0.02139	0.11272	18.97472	6.48715	0.09133	8.00633
Cycle 2 @ 25.1 C											
Sample	Fluid Density (g/cc)	Dry Wt (g)	Susp. Wt (g)	(W) Sat. Wt (g)	(D) Sat. Wt (g)	Open Porosity (cc)	Pellet Volume (cc)	Open Porosity (%)	Bulk Density (g/cc)	Matrix Volume (cc)	Matrix Density (g/cc)
1	0.997018	0.42685	0.37334	0.43995	0.43792	0.01314	0.06681	19.66672	6.38909	0.05367	7.95323
2	0.997018	0.16185	0.13485	0.16353	0.16340	0.00169	0.02877	5.85774	5.62648	0.02708	5.97657
3	0.997018	0.68012	0.61493	0.68083	0.68020	0.00071	0.06610	1.07739	10.28971	0.06538	10.40178
4	0.997018	0.06252	0.05623	0.06285	0.06272	0.00033	0.00664	4.98489	9.41595	0.00631	9.90995
5	0.997018	0.73088	0.63933	0.75151	0.75045	0.02069	0.11252	18.39009	6.49581	0.09182	7.95959
Cycle 3 @ 24.4 C											
Sample	Fluid Density (g/cc)	Dry Wt (g)	Susp. Wt (g)	(W) Sat. Wt (g)	(D) Sat. Wt (g)	Open Porosity (cc)	Pellet Volume (cc)	Open Porosity (%)	Bulk Density (g/cc)	Matrix Volume (cc)	Matrix Density (g/cc)
1	0.997196	0.42678	0.37214	0.43650	0.43620	0.00975	0.06454	15.10255	6.61254	0.05479	7.78886
2	0.997196	0.16179	0.13460	0.16405	0.16324	0.00227	0.02953	7.67402	5.47831	0.02727	5.93366
3	0.997196	0.68004	0.61520	0.68109	0.68040	0.00105	0.06608	1.59357	10.29190	0.06502	10.45856
4	0.997196	0.06249	0.05623	0.06290	0.06281	0.00041	0.00669	6.14693	9.34255	0.00628	9.95444
5	0.997196	0.73079	0.63862	0.75221	0.74870	0.02148	0.11391	18.85729	6.41554	0.09243	7.90649
Cycle 1 @ 24.8 C											
Sample	Fluid Density (g/cc)	Dry Wt (g)	Susp. Wt (g)	(W) Sat. Wt (g)	(D) Sat. Wt (g)	Open Porosity (cc)	Pellet Volume (cc)	Open Porosity (%)	Bulk Density (g/cc)	Matrix Volume (cc)	Matrix Density (g/cc)
6	0.997095	0.54378	0.44705	0.58765	0.58464	0.04400	0.14101	31.20199	3.85633	0.09701	5.60530
7	0.997095	0.30001	0.26734	0.31661	0.31575	0.01665	0.04941	33.69190	6.07141	0.03277	9.15637
8	0.997095	0.72339	0.63282	0.73427	0.73325	0.01091	0.10175	10.72449	7.10979	0.09083	7.96388
11	0.997095	0.15184	0.13288	0.15511	0.15424	0.00328	0.02229	14.70985	6.81057	0.01902	7.98517
12	0.997095	0.29742	0.26448	0.30139	0.30076	0.00398	0.03702	10.75589	8.03457	0.03304	9.00291

TABLE 5. (continued)

	A	D	S	M	E	F	V	P	G	J	T
Cycle 2 @ 24.3											
Sample	Fluid Density (g/cc)	Dry Wt (g)	Susp. Wt (g)	(W) Sat. Wt (g)	(D) Sat. Wt (g)	Open Porosity (cc)	Pellet Volume (cc)	Open Porosity (%)	Bulk Density (g/cc)	Matrix Volume (cc)	Matrix Density (g/cc)
6	0.997221	0.54306	0.44659	0.58402	0.58203	0.04107	0.13781	29.80426	3.94056	0.09674	5.61367
7	0.997221	0.29963	0.26631	0.31558	0.31500	0.01599	0.04941	32.37264	6.06449	0.03341	8.96751
8	0.997221	0.72316	0.63204	0.73316	0.73275	0.01003	0.10140	9.88924	7.13163	0.09137	7.91429
11	0.997221	0.15180	0.13310	0.15510	0.15459	0.00331	0.02206	15.00000	6.88082	0.01875	8.09509
12	0.997221	0.29694	0.26416	0.30059	0.30021	0.00366	0.03653	10.01921	8.12832	0.03287	9.03340
Cycle 3 @ 24.7 C											
Sample	Fluid Density (g/cc)	Dry Wt (g)	Susp. Wt (g)	(W) Sat. Wt (g)	(D) Sat. Wt (g)	Open Porosity (cc)	Pellet Volume (cc)	Open Porosity (%)	Bulk Density (g/cc)	Matrix Volume (cc)	Matrix Density (g/cc)
6	0.997120	0.54283	0.44357	0.58606	0.58256	0.04335	0.14290	30.33897	3.79863	0.09955	5.45302
7	0.997120	0.29969	0.26253	0.31091	0.31041	0.01125	0.04852	23.19140	6.17666	0.03727	8.04163
8	0.997120	0.72308	0.63160	0.73251	0.73186	0.00946	0.10120	9.34496	7.14496	0.09174	7.88148
11	0.997120	0.15185	0.13335	0.15420	0.15365	0.00236	0.02091	11.27098	7.26200	0.01855	8.18447
12	0.997120	0.29697	0.26370	0.30051	0.30017	0.00355	0.03692	9.61695	8.04441	0.03337	8.90035

a. (W) Sat. Wt = saturated weight after blotting with wet towel.

b. (D) Sat. Wt = saturated weight after blotting with dry towel. This term is not used for calculations but is included for reference only.

c. $F = \frac{M - D}{A}$.

d. $V = \frac{M - S}{A}$.

e. $P = \frac{F}{V}(100)$.

f. $G = \frac{D}{V}$.

g. $J = \frac{D - S}{A}$.

h. $T = \frac{D}{J}$.

2.2.4 SEM/EDS Examination

A Perkin-Elmer Etec Autoscan Model U-2 SEM with a Kevex Super 8005 detector (for EDS) was used to identify the composition of the matrix as well as minor elements in the large particle samples.

Examination of the particles showed that most are reaction products consisting of uranium and zirconium oxides. Fe, Ni, and Cr were most often observed as trace elements in the matrix of the samples. Two particles (Nos. 4 and 12) were mainly Ag, In, and Cd, which indicates a control rod origin. Particle No. 3 appears to be a fuel pellet fragment. Particle No. 2 exhibited only Zr and O, indicating a possible piece from fuel assembly instrumentation or guide tubes or fuel cladding. A brief comparative description of the examination results is given in Table 6. A comparison of arbitrary EDS peak heights for the matrix material is given in Table 7. The SEM photographic results and EDS spectra are given in Appendix D.

2.3 Radiochemical Analysis

Upon receipt of the debris samples in the radiochemistry laboratory, a portion of each sample of sufficient size was removed, weighed, and stored in a marked vial for subsequent I-129 analysis. The remainder of the samples was weighed and dissolved for the gamma spectroscopy and elemental composition analysis.

After a review of dissolution methods and previous knowledge of the TMI-2 debris composition, dissolution of the B-loop steam generator debris was accomplished with mineral acids. Each sample dissolved to this point has been treated with 8M nitric acid and heat, and subsequently filtered to remove the undissolved residue. The residue and filter were ashed and treated with concentrated sulfuric and hydrofluoric acids in platinum. Weights were obtained before and after treatment to determine the loss of silica (if any). Finally, the residue was treated with hydrofluoric, hydrochloric, and nitric acids until dissolution was complete. All

TABLE 6. COMPARATIVE SUMMARY OF SEM/EDS RESULTS

Sample Number	Average Density (g/cc)	Matrix Composition	Minor/Trace Composition	Comments
1	7.9	U, Zr, O	Cr, Fe, Ni, Cu	Large interconnected pores, reaction product
2	6.0	Zr/Zr, O	--	Piece of cladding with oxidized layer
3	10.4	U, O	--	Piece of UO_2 fuel
4	9.9	Ag, In, Cd	Zr, O, Ni, Cr, Fe, Al, Mn	Piece of control rod
5	8.0	U, Zr, O	Al, Zr, Cr, Fe, Ni, Cu	Large porosity, reaction product
6	5.6	U, Zr, O	Fe, Zr, Al, Ni, Cr, Ag, C	Composite structure, low density probably due to large internal porosity
7	8.7	U, Zr, O	Cu, Al, Cr, Fe, Ni	Foamed reaction product
8	7.9	U, Zr, O	Cu, Al, Cr, Bi, Pb, Fe, Ni	Large interconnected pores, reaction product
11	8.1	U, Zr, O, Cr, Fe	Cu, Al, C	Large interconnected pores, reaction product
12	9.0	Ag, In, Cd	Cu, Al	Piece of control rod

Note: Cu probably originates from slight smearing of Cu mount jacket during grinding. Al probably originates from Al_2O_3 polishing compound. Pb and Bi originate from mounting material. C originates from C evaporated layer on pieces 6 and 11.

TABLE 7. ARBITRARY PEAK HEIGHTS FOR COMPARISON OF MATRIX MATERIAL FOR EACH PARTICLE

Sample Number	Spectrum Number	Accelerated Voltage (kV)	Detector Window	Zr	U	O	Ag	Cd	In	Al	Cr	Fe	Cu
1	035854-2	30	Be	25	75	--	--	--	--	--	--[a]	--[a]	--[a]
1	035858	30	Be	29	71	--	--	--	--	--	--[a]	--[a]	--[a]
1	035854-2A	10	Open	33	49	18	--	--	--	--	--	--	--
2	035818-1	10	Open	100	--	--[b]	--	--	--	--	--	--	--
2	035818-2	10	Open	86	--	14	--	--	--	--	--	--	--
3	037140	30	Be	--	100	--	--	--	--	--	--	--	--
4	035829-1	10	Open	--	--		100	--[a]	--[a]	--[b]	--	--	--
5	035798-2	30	Be	35	65	--	--	--	--	--	--[b]	--[a]	--[a]
5	035795-1	10	Open	42	40	18	--	--	--	--	--	--	--
6	035603-1	30	Be	100	--	--	--	--	--	--	--	--	--
6	035619-1	30	Be	40	60	--	--	--	--	--	--	--	--
6	035619-2	30	Be	83	17	--	--	--	--	--	--	--	--
6	035624-1	10	Open	81	7	12	--	--	--	--	--	--	--
7	035844-1	30	Be	17	83	--	--	--	--	--	--	--	--[a]
7	035844-1A	10	Open	30	54	16	--	--	--	--	--	--	--
7	035839-1	30	Be	8	92	--	--	--	--	--	--	--	--[a]
8	035783-1	30	Be	32	68	--	--	--	--	--[a]	--	--	--[a]
8	035783-1A	10	Open	43	43	14	--	--	--	--	--	--	--
8	035786-1	30	Be	31	69	--	--	--	--	--	--	--[b]	--[a]
11	035719-1	30	Be	37	63	--	--	--	--	--	--[a]	--[a]	--[a]
11	035719-1A	10	Open	47	40	13	--	--	--	--	--	--	--
11	035720-1	30	Be	38	62	--	--	--	--	--	--[b]	--[b]	--
12	035737-3	30	Be	--	--	--	50	50	--	--	--	--	--[a]

a. Trace; Particles 6 and 11 are carbon-coated.

b. Minor.

solutions were then combined. Upon completion of this procedure, the solution was diluted to 100 mL and stored in marked bottles for the chemical and radiochemical analyses.

2.3.1 Gamma Spectroscopy

Solutions of each dissolved sample were analyzed in a known, calibrated geometry by gamma spectroscopy. A 1-mL aliquot of each bulk dissolved solution was further diluted to 125 mL and placed in front of a 16% Ge(Li) detector. Depending on the activity, each sample was counted for a minimum of 3600 s. Table 8 lists the activities for 10 gamma-ray emitting isotopes. Silver-110m and manganese-54 were not detected in any of the samples and were assigned a minimum detectable level based on the Compton background in the spectral area of their peaks. All activities have been decay-corrected to April 1, 1987, to make data comparison easier.

2.3.2 Strontium-90 Analysis

An aliquot was removed from the stock dissolved solution of each sample for Sr-90 analysis. The aliquots ranged from 0.1 to 10 mL depending on the weight of the sample that was dissolved. Each sample was subjected to a standard $SrCO_3$ precipitation separation followed by liquid scintillation counting for strontium-90 activity. Chemical yield was determined from the atomic absorption measurement of strontium carrier added prior to the chemical separation. For all samples, the scavenge and purification procedures were carried out twice in order to obtain counting samples free from trace radioactive contaminants. Table 9 lists the Sr-90 activities for all samples. As with the gamma-ray data, all Sr-90 activities have been decay-corrected to April 1, 1987.

2.3.3 Iodine-129 Analysis

The reserved, weighed portion of 11 of the 16 original solid samples was taken for I-129 analysis. The other five samples were not analyzed because the small amount of sample available required dissolving the entire sample for elemental, Sr-90, and gamma-ray analysis.

TABLE 8. GAMMA-RAY ISOTOPIC ACTIVITY[a] (μCi/g)

Sample	Mn-54	Co-60	Ru-106	Ag-110m	Sb-125	Cs-134	Cs-137	Ce-144	Eu-154	Eu-155
Fraction <150	<1.61	62.6 ± 1.4	63.9 ± 14.5	<10.8	206 ± 9	60.1 ± 1.5	3159 ± 8	96.0 ± 11.6	15.9 ± 1.7	23.4 ± 4.6
Fraction 150-300	<0.96	47.7 ± 0.8	49.2 ± 10.4	<7.3	70.7 ± 4.4	58.0 ± 0.9	2494 ± 5	136 ± 8	26.0 ± 1.1	39.0 ± 3.5
Fraction 300-710	<0.76	25.4 ± 0.5	17.9 ± 6.2	<5.5	60.4 ± 3.9	32.2 ± 0.6	1853 ± 4	104 ± 7	18.6 ± 1.0	24.6 ± 2.4
Fraction 710-1000	<0.89	26.8 ± 0.6	25.1 ± 7.9	<7.4	51.8 ± 3.9	37.4 ± 0.8	2059 ± 5	114 ± 8	23.3 ± 1.1	32.6 ± 3.1
Fraction >1000	<0.97	8.0 ± 0.4	52.3 ± 15.1	<11.2	41.9 ± 5.3	76.4 ± 1.0	4870 ± 7	211 ± 12	32.0 ± 1.3	56.9 ± 4.6
Filter	<0.05	5.7 ± 0.1	3.2 ± 0.4	<0.3	10.9 ± 0.2	3.6 ± 0.1	181 ± 0.1	5.6 ± 0.3	0.9 ± 0.04	1.4 ± 0.1
Particle 1	<2.0	2.8 ± 0.8	<48.9	<14.7	<21.7	44.9 ± 1.7	2022 ± 10	202 ± 2.2	37.3 ± 3.3	52.5 ± 8.0
Particle 2	<0.35	18.9 ± 0.3	<2.6	<0.4	43.8 ± 0.7	<0.3	11.4 ± 0.2	1.4 ± 0.7	<0.5	<0.8
Particle 3	<0.98	0.7 ± 0.2	58.7 ± 16.5	<19.3	43.7 ± 8.1	41.9 ± 1.1	4335 ± 10	125 ± 18	10.1 ± 1.3	35.7 ± 6.2
Particle 4	<0.89	38.8 ± 0.7	<1.7	<0.8	5.6 ± 0.7	<0.8	5.2 ± 0.4	<3.6	<1.2	<1.5
Particle 5	<0.85	2.7 ± 0.3	<9.8	<9.0	<12.7	53.7 ± 1.0	2434 ± 6	146 ± 11	31.7 ± 1.6	39.4 ± 4.4
Particle 6	<0.06	3.7 ± 0.1	1.2 ± 0.4	<0.42	7.0 ± 0.2	2.2 ± 0.1	131 ± 1	2.9 ± 0.3	0.3 ± 0.1	1.2 ± 0.1
Particle 7	<0.58	5.6 ± 0.2	12.4 ± 4.2	<3.8	156 ± 3	15.4 ± 0.4	962 ± 2	230 ± 6	64.2 ± 1.2	152 ± 3
Particle 8	<0.89	14.3 ± 0.6	<21.0	<6.7	<9.0	27.2 ± 0.7	1386 ± 4	148 ± 10	24.7 ± 1.4	40.0 ± 3.6
Particle 11	<0.66	2.1 ± 0.3	<14.2	<4.5	<6.7	10.5 ± 0.6	57.2 ± 2.9	89.7 ± 6.5	13.2 ± 1.1	24.5 ± 2.4
Particle 12	<0.33	4.6 ± 0.2	<10.0	<3.2	720 ± 4	24.2 ± 0.4	1202 ± 2	64.8 ± 3.8	8.8 ± 0.4	19.7 ± 1.6

a. All activities decay-corrected to April 1, 1987.

TABLE 9. SR-90 AND I-129 ISOTOPIC ACTIVITY[a]
(μCi/g)

Sample	Sr-90	I-129
Fraction <150	313 ± 3.1	$3.8 \times 10^{-4} \pm 1.1 \times 10^{-4}$
Fraction 150-300	442 ± 4.4	$3.4 \times 10^{-4} \pm 1.5 \times 10^{-4}$
Fraction 300-710	313 ± 3.1	$3.4 \times 10^{-4} \pm 1.0 \times 10^{-4}$
Fraction 710-1000	363 ± 3.6	$<5.4 \times 10^{-4}$
Fraction >1000	735 ± 7.4	$3.3 \times 10^{-4} \pm 0.6 \times 10^{-4}$
Filter	22.5 ± 0.2	$2.0 \times 10^{-4} \pm 0.4 \times 10^{-4}$
Particle 1	757 ± 7.6	$3.0 \times 10^{-4} \pm 0.8 \times 10^{-4}$
Particle 2	3.24 ± 0.03	$<2.6 \times 10^{-4}$
Particle 3	415 ± 4.2	$7.6 \times 10^{-4} \pm 0.4 \times 10^{-4}$
Particle 4	0.72 ± 0.01	--[b]
Particle 5	616 ± 6.2	$2.4 \times 10^{-4} \pm 0.9 \times 10^{-4}$
Particle 6	6.45 ± 0.06	--[b]
Particle 7	2174 ± 22	--[b]
Particle 8	637 ± 6.4	$<2.5 \times 10^{-4}$
Particle 11	308 ± 3.1	--[b]
Particle 12	212 ± 2.1	--[b]

a. All activities decay-corrected to April 1, 1987.

b. Not measured due to insufficient sample.

Each sample was combined with a known and standardized quantity of stable iodine carrier. The sample and carrier were fused with solid sodium hydroxide (NaOH) for a minimum of 3 h at 600°C. This reduced the sample particles to a fine powder. The fusion was subsequently dissolved in deionized water and filtered. The iodine was extracted into CCl_4, back extracted into the aqueous phase, precipitated as silver iodide, and filtered onto a Millipore paper. The sample was then counted on a calibrated low-energy photon spectrometer (LEPS) for xenon X-ray emitted as a result of the I-129 decay. Chemical yield was determined by gravimetric recovery of the iodine carrier. Table 9 lists the I-129 activities decay-corrected to April 1, 1987.

2.4 Elemental Analysis

Elemental analysis of the dissolved fractions and particles was accomplished with an Applied Research Laboratories Model 3510 Inductively Coupled Plasma Spectrometer (ICP). Te was converted to the gaseous hydride on an Applied Research Laboratories Model 341 hydride generator. Any Te present was then swept into the plasma and analyzed. Prior to analysis, most of the samples were diluted to reduce the activity level. The dilutions used are listed in Table 10. For Te, all samples were diluted 1:20 for optimum acid strength on the hydride generator, except the >1000 fraction, which was diluted 1:100 with the desired concentration of acid.

The standards were prepared from concentrated standard solutions, which were obtained from the National Bureau of Standards or were traceable to the National Bureau of Standards. Selected analytical lines (Table 11) for each element were scanned to determine if background or spectral interferences were present from the other elements expected to be in the samples. Several spectral interferences were observed and corrected for, using the routines available with the instrument. The spectral interferences requiring correction at the selected analytical lines were the interference of U on Cr, Cu, Gd, and Si, and the interference of Zr on Al. Background correction points were chosen from background scans at each

TABLE 10. SAMPLE DILUTIONS FOR ELEMENTAL ANALYSIS

Sample	Dilution Ratio
Fraction <150	11:100
Fraction 150-300	11:100
Fraction 300-710	5:100
Fraction 710-1000	10:100
Fraction >1000	1:100
Filter	20:100
Particle 1	10:100
Particle 2	25:100
Particle 3	20:100
Particle 4	None
Particle 5	10:100
Particle 6	25:50
Particle 7	20:100
Particle 8	10:100
Particle 11	None
Particle 12	25:100

TABLE 11. ANALYTICAL LINES USED FOR ELEMENTAL ANALYSIS

Element	Wavelength (nm)	LQD (ppm)
Sn	189.989	0.150
Mo	202.03	0.025
Te	214.275	0.020
Cd	226.502	0.015
Ni	231.604	0.010
B	249.678	0.013
Mn	257.61	0.001
Cr	267.716	0.015
Fe	273.955	0.020
Mg	279.553	0.0004
Si	288.158	0.100
Nb	316.34	0.100
Cu	324.754	0.006
In	230.606	0.200
Ag	338.289	0.050
Gd	342.247	0.050
Zr	343.823	0.010
Al	396.152	0.075
U	409.014	0.500

element wavelength for two of the samples assumed to contain representative concentrations of the elements of interest. The majority of background shifts and spectral interferences observed were due to the presence of U.

The results of the sample analyses are contained in Table 12 with a comparison with the average elemental composition of the TMI-2 core. A less-than value indicates that the level of a particular element is below the lowest quantity determinable (LQD)[a] for that element. The percent element values were calculated using the measured concentration of each element in the sample solution, the final volume and any dilutions made, and the weight of the sample. The errors listed are the relative standard deviation (RSD) of the results, $\pm 1\sigma$. The errors for each element were calculated from the RSD of the analytical curve for that element and the RSD of the measurement of that element in the sample.

The measured recovery of metallic elements by the elemental analysis method is also shown in Table 12. The unaccounted-for composition of the samples is due to (a) the presence of oxygen and other light elements (carbon and hydrogen in the case of the filter) and/or (b) unaccounted sample losses during dissolution.

A control standard containing eight elements was run several times during the actual sample analyses. The difference between the measured values of the elements and the expected values was within acceptable limits (average difference, ±1.7%).

---

a. The LQD is defined as the lowest quantity determinable and the precision at this level is approximately ±10%. The LQD is five times the detection limit.

TABLE 12. ELEMENTAL DISTRIBUTION

Sample	Elemental Distribution (wt%)						
	Cd	Gd	Mn	Mo	Nb	Ni	Te
TMI-2 core average	0.1	0.01	0.08	0.03	0.04	0.9	--a
Fraction <150	0.739 ± 0.012	<0.014	0.051 ± 0.000	0.054 ± 0.000	0.033 ± 0.001	0.774 ± 0.004	<0.012
Fraction 150-300	0.733 ± 0.015	<0.012	0.036 ± 0.000	0.017 ± 0.000	<0.023	0.573 ± 0.005	<0.010
Fraction 300-710	0.325 ± 0.006	<0.011	0.024 ± 0.000	0.020 ± 0.000	<0.023	0.309 ± 0.001	<0.004
Fraction 710-1000	0.640 ± 0.013	<0.008	0.021 ± 0.000	0.020 ± 0.000	0.026 ± 0.001	0.259 ± 0.001	<0.006
Fraction >1000	0.026 ± 0.000	0.016 ± 0.000	0.011 ± 0.000	0.022 ± 0.000	<0.017	0.089 ± 0.001	<0.004
Filter	0.057 ± 0.001	<0.0001	0.0048 ± 0.0000	0.0037 ± 0.0000	<0.0042	0.085 ± 0.000	<0.0034
Particle 1	0.054 ± 0.001	<0.040	0.037 ± 0.000	<0.020	<0.080	0.038 ± 0.000	<0.032
Particle 2	0.020 ± 0.000	<0.032	0.002 ± 0.000	<0.016	<0.063	0.148 ± 0.001	<0.062
Particle 3	<0.004	0.014 ± 0.000	0.009 ± 0.000	0.015 ± 0.000	<0.027	0.010 ± 0.000	<0.022
Particle 4	4.15 ± 0.10	<0.030	0.042 ± 0.001	<0.015	<0.060	0.208 ± 0.002	<0.240
Particle 5	0.040 ± 0.001	<0.012	0.028 ± 0.000	<0.006	0.030 ± 0.001	0.014 ± 0.000	<0.010
Particle 6	0.013 ± 0.000	<0.020	<0.001	<0.010	<0.040	0.036 ± 0.000	<0.080
Particle 7	0.133 ± 0.002	<0.020	0.009 ± 0.000	0.012 ± 0.000	<0.039	0.060 ± 0.000	<0.032
Particle 8	0.018 ± 0.000	<0.020	0.020 ± 0.000	0.025 ± 0.000	0.041 ± 0.001	0.144 ± 0.001	<0.016
Particle 11	0.012 ± 0.000	<0.015	0.020 ± 0.000	<0.007	0.035 ± 0.001	0.032 ± 0.000	<0.118
Particle 12	13.4 ± 0.2	<0.038	0.017 ± 0.000	<0.019	<0.076	0.187 ± 0.002	<0.076

TABLE 12. (continued)

Sample	Elemental Distribution (wt%)					
	U	Zr	Ag	Al	Cu	Fe
TMI-2 core average	65.8	18.0	1.8	0.2	0.001	3.0
Fraction <150	31.5 ± 0.6	9.33 ± 0.17	2.98 ± 0.03	0.340 ± 0.004	0.047 ± 0.000	3.48 ± 0.04
Fraction 150-300	46.5 ± 1.3	10.7 ± 0.2	5.01 ± 0.04	0.150 ± 0.002	0.020 ± 0.000	1.73 ± 0.03
Fraction 300-710	37.6 ± 0.6	9.12 ± 0.16	2.56 ± 0.03	0.101 ± 0.001	0.015 ± 0.000	0.995 ± 0.010
Fraction 710-1000	40.0 ± 0.7	8.89 ± 0.17	1.68 ± 0.03	0.089 ± 0.001	0.011 ± 0.000	0.756 ± 0.011
Fraction >1000	86.1 ± 1.5	0.866 ± 0.021	0.329 ± 0.003	<0.013	0.008 ± 0.0000	0.205 ± 0.002
Filter	2.00 ± 0.04	0.922 ± 0.017	0.201 ± 0.002	0.028 ± 0.000	0.0022 ± 0.0000	0.379 ± 0.004
Particle 1	59.8 ± 0.9	22.1 ± 0.5	0.056 ± 0.000	0.208 ± 0.002	0.011 ± 0.000	1.19 ± 0.02
Particle 2	<0.315	73.8 ± 1.3	<0.032	0.055 ± 0.001	0.006 ± 0.000	0.705 ± 0.007
Particle 3	84.4 ± 1.4	0.006 ± 0.000	<0.013	<0.020	0.005 ± 0.000	0.128 ± 0.001
Particle 4	<0.301	1.35 ± 0.03	73.6 ± 0.6	0.273 ± 0.003	0.059 ± 0.001	0.234 ± 0.005
Particle 5	43.6 ± 0.6	15.8 ± 0.3	0.045 ± 0.000	0.078 ± 0.001	0.005 ± 0.000	0.421 ± 0.005
Particle 6	1.54 ± 0.02	14.1 ± 0.3	0.114 ± 0.001	0.352 ± 0.005	<0.002	0.242 ± 0.002
Particle 7	71.3 ± 1.1	7.92 ± 0.16	0.039 ± 0.000	0.135 ± 0.001	0.018 ± 0.000	0.198 ± 0.002
Particle 8	56.7 ± 0.9	20.3 ± 0.4	0.071 ± 0.000	0.315 ± 0.006	0.007 ± 0.000	1.19 ± 0.01
Particle 11	38.6 ± 0.8	17.2 ± 0.3	0.056 ± 0.000	0.123 ± 0.001	0.021 ± 0.000	0.909 ± 0.008
Particle 12	27.7 ± 0.4	13.2 ± 0.3	0.198 ± 0.015	0.247 ± 0.002	0.059 ± 0.000	1.01 ± 0.01

TABLE 12. (continued)

Sample	Elemental Distribution (wt%)						Metallic Element Recovery (%)
	B	Cr	Si	Sn	Mg	In	
TMI-2 core average	0.1	1.0	0.04	0.3	Negligible	0.3	92
Fraction <150	0.554 ± 0.007	0.410 ± 0.005	1.77 ± 0.02	0.495 ± 0.007	0.018 ± 0.000	0.988 ± 0.009	56
Fraction 150-300	0.053 ± 0.001	0.281 ± 0.2	<0.023	0.323 ± 0.012	0.015 ± 0.000	1.08 ± 0.02	68
Fraction 300-710	0.013 ± 0.000	0.240 ± 0.004	<0.023	0.209 ± 0.003	0.006 ± 0.000	0.548 ± 0.006	52
Fraction 710-1000	0.023 ± 0.000	0.195 ± 0.002	0.031 ± 0.0001	0.174 ± 0.003	0.009 ± 0.000	0.557 ± 0.006	53
Fraction >1000	0.002 ± 0.000	0.043 ± 0.001	<0.017	0.035 ± 0.001	<0.001	0.093 ± 0.001	88
Filter	0.0052 ± 0.0001	0.041 ± 0.001	0.458 ± 0.006	0.034 ± 0.000	0.010 ± 0.0000	0.065 ± 0.001	5
Particle 1	0.042 ± 0.001	0.371 ± 0.004	<0.080	<0.121	0.025 ± 0.000	<0.161	84
Particle 2	<0.008	0.154 ± 0.001	2.48 ± 0.03	1.06 ± 0.02	0.020 ± 0.000	<0.126	78
Particle 3	0.009 ± 0.000	0.030 ± 0.000	0.073 ± 0.001	<0.040	<0.001	<0.054	85
Particle 4	0.672 ± 0.007	0.093 ± 0.001	6.49 ± 0.11	<0.090	0.126 ± 0.003	14.7 ± 0.2	102
Particle 5	0.006 ± 0.000	0.278 ± 0.004	<0.023	<0.035	<0.001	<0.047	60
Particle 6	0.268 ± 0.004	0.011 ± 0.000	2.68 ± 0.05	<0.060	0.031 ± 0.000	<0.080	19
Particle 7	0.017 ± 0.000	0.056 ± 0.001	0.196 ± 0.002	<0.058	0.008 ± 0.000	<0.078	80
Particle 8	0.064 ± 0.001	0.158 ± 0.006	0.143 ± 0.002	<0.059	0.062 ± 0.001	<0.079	79
Particle 11	0.009 ± 0.000	0.252 ± 0.005	1.55 ± 0.05	<0.024	0.009 ± 0.000	<0.059	59
Particle 12	0.223 ± 0.003	0.253 ± 0.002	2.17 ± 0.05	1.74 ± 0.03	0.064 ± 0.001	4.83 ± 0.05	65

a. Fission product.

3. DISCUSSION

The findings based on these examinations are unique and of special interest because the samples represent core conditions at a precise time during the core damage sequence. The debris recovered from the upper tube sheet of the B-loop steam generator is believed to have been carried to that location from the core region when the TMI-2 Reactor Coolant Pump 2B was restarted (174 to 192 min after accident initiation). The B-loop was not used again for forced circulation cooling of the core, and there was more loose debris on the upper tube sheet with possibly different core material compositions compared with the loose debris on the upper tube sheet of the A-loop steam generator. In addition, the debris on the steam generator upper tube sheet appears similar to (a) the sample from 8 cm below the surface of the approximately 0.75-m-deep bed of loose debris found below the cavity at the top of the TMI-2 core that was examined by B&W and (b) some of the individual particles are similar to the rock-size samples of core debris from the reactor vessel lower plenum.

The discussion of the sample elemental composition findings is based on an assumption that the actual ratios of metallic elements present in the sample are the same as the measured ratios. Due to funding constraints, the validity of the assumption was not evaluated by duplicate analysis by an independent laboratory or reanalysis.

3.1 Size Fractions and Filter

The initial radiation levels of the various size fractions correlated roughly with the sample weights. However, it was noted that the larger size fractions exhibited higher beta components (23 to 50%) than the smaller-size fractions (0 to 10%). In fact, the <150-μm-size fraction did not have a measurable beta dose rate. In contrast, the filter sleeve had an intense beta field (60 R/h with a 99% beta component) with gross radiation levels an order of magnitude higher than the >1,000-μm-size fraction that weighed more.

In general, the >1,000-μm-size fraction had the highest fission product inventories (including Sr-90), with the exception of the <150-μm-size fraction, which was highest in Sb-125 and Ru-106. It was noted that Cs-137 constituted the bulk of the retained fission products. The >1,000-μm fraction also had the highest level of Cs-137 retention. The filter material had a much lower fission product inventory (including Sr-90) than the other size fractions. Activation product inventory was also lower for the filter material based on gamma-ray spectroscopy results. I-129 levels were low and approximately the same for all size fractions and the filter.

Elemental analysis indicated that U was the major constituent in all of the samples. The >1,000-μm-size fraction had the highest fraction of U (86.1%). Elemental analysis of the filter material was less than 5% weight (metallic core elements) accountable, of which 2% was U. The other size fractions had U compositions in the range of 30 to 50%. Zr was the second major component in all of the size fractions and the filter. As expected, based on Zircaloy-4 composition, Sn values exhibited the same trend as Zr. Ag and In were somewhat higher, in the 150 to 300-μm-size fraction, indicating a slightly increased contribution of control rod material. It is interesting to note that the analyses for Fe, Ni, Cr, and Mn (also Mg and Mo to a lesser degree) exhibited a trend of increasing weight percentage, going from the largest to the smallest size fractions. Si was randomly present in several samples up to several weight percent. This is most likely due to contamination from the furnace that was used to ash the filter papers during dissolution (i.e., due to SiO_2 dust on the furnace walls).

In summary, all of the size fractions (with the exception of the >1,000-μm fraction) contained all core materials, with the largest contributions coming from the UO_2 fuel and Zircaloy cladding. Smaller weight percentages of other materials, including Ag-In-Cd control rod material and Fe-Cr-Ni alloys such as stainless steel and Inconel, are also present. The trends in the Fe-Cr-Ni analysis indicate a slightly higher contribution of these elements in the finer-size fractions.

The elemental analysis results are consistent with the inventory of core materials (see Table 12). The filtered debris is similar to the size fraction composition with the exception of the filter material itself, which was not quantified and which produced low weight accountability in the elemental analysis results. The high level of beta radiation on the filter is probably due to the lower self-shielding effects associated with the polypropylene filter material. The radiation levels, fission product inventory (especially Cs-137), and elemental analysis all indicate that the >1,000-size fraction contains primarily UO_2 fuel pellet fragments.

3.2 Individual Particles

Out of the 10 large particles selected from the >1,000-μm-size fraction for more detailed analysis, three were positively identified for the reasons outlined in the following paragraphs. These particles included No. 2 (a partially oxidized piece of Zircaloy cladding), No. 3 (a fuel pellet fragment), and No. 4 (a resolidified portion of control rod material). Results among the various analysis techniques were entirely consistent for these particles.

Particle No. 2 was identified as partially oxidized Zircaloy-4 tubing. The particle had the approximate physical shape and dimensions of Zircaloy fuel or burnable poison rod cladding, including a wall thickness of approximately 0.76 mm (nominally 0.67 mm for fuel rods and 0.89 mm for burnable poison rods). The measured matrix density of 6.0 g/cc is consistent with partially oxidized Zr. A heavily oxidized layer was present on both the OD and ID surfaces of the cladding, ranging from 64 μm to 89 μm thick (slightly thicker on the OD). The bulk of the interior metal exhibited large grains (51 to 152 μm diameters) with oxidized Zr at the grain boundaries. The physical and microstructural appearance of the particle indicates that the particle had a relatively low temperature history. Elemental analysis techniques confirmed a high Zr content with smaller amounts of Zircaloy-4 alloying elements. The particle had a relatively low fission product inventory, which is expected.

Particle No. 3 was identified as a portion of a fragmented UO_2 fuel pellet. Early identification of the particle was made during the visual examination when a curved surface with grinding marks was observed. The particle also exhibited the highest gross radiation levels, providing further indication that the particle was mostly UO_2 fuel. The measured matrix density of 10.4 g/cc and low amounts of open porosity are consistent with as-fabricated values for sintered UO_2 fuel pellets. The microstructure exhibited the well developed grain structure and heterogeneous fine porosity typical of UO_2 fuel. Elemental analysis techniques confirmed a high U content (84%) and the absence of other elements, with the exception of trace levels of Fe. If the balance is assumed to be mostly O, then the weight percentages are reasonably close to the stoichiometric O content for UO_2 (possibly a slight O enrichment). The particle had the overall highest level of fission product inventory. This was primarily due to the Cs-137 (4,335 μCi/g). The retention of Cs-137 indicates that the particle had a relatively low temperature history. It was also noted that Gd was only detected (at very low levels) in the >1000 mm size fraction and Particle No. 3, both of which have the highest U content.

Particle No. 4 was identified as a resolidified portion of Ag-In-Cd alloy used in control rod materials. The physical appearance was suggestive of a resolidified metallic nugget. Density measurements were consistent with Ag-In-Cd alloy. The microstructure revealed a dendritic structure with substantial amounts of interdendritic porosity that was partially open (5% open porosity). Small amounts of Zr oxide were observed heterogeneously mixed in with the Ag-In-Cd matrix. This was the only case where elemental analysis was 100% weight accountable, indicating very low levels of oxygen. The relative levels of Ag, In, and Cd are consistent with control rod material. As expected, the fission product inventory was relatively low. The absence of Ag-110 is due to radioactive decay since the time of shutdown (over 10 half-lives for Ag-110). Most of the radioactivity was due to the presence of redeposited activated corrosion products (Co-60).

The other seven particles represented a variety of reaction products between various core structural components. Five of these (Particles 1, 8, 5, 11, and 7) are primarily fuel/clad reaction products. Observations pertaining to these five particles are presented in the following paragraphs.

Particle 1: This particle consisted of large interconnected pores (18% open porosity) with a matrix density of 7.9 g/cc. ICP analysis indicated that Particle 1 was approximately 82% U/Zr (2.7:1) with smaller amounts of Fe, Cr, and Al. SEM/EDS results were consistent with the elemental analysis, indicating a dendritic matrix composed of U/Zr/O with evidence of a eutectic reaction. There was substantial interdendritic porosity partially filled with a lower atomic number phase that was Fe/Ni/Cr rich. Fission product inventory was relatively high, including volatile fission products (i.e., highest 2,022 µCi/g of Cs-137).

Particle 8: This particle consisted of large, interconnected pores (10% open porosity) with a matrix density of 7.9 g/cc. ICP analysis indicated that Particle 8 was approximately 77% U/Zr (2.8:1) with smaller amounts of Fe, Al, Cr, Si, and Ni. SEM/EDS results were consistent with the elemental analysis indicating a dendritic matrix composed of U/Zr/O with evidence of a eutectic reaction. There was substantial interdendritic porosity partially filled with a lower atomic number phase that was Fe/Ni/Cr rich. Fission product inventory was relatively high, including volatile fission products (i.e., highest 1,386 µCi/g of Cs-137).

Particle 5: This particle consisted of large interconnected pores (19% open porosity) with a matrix density of 8.0 g/cc. ICP analysis indicated that Particle 5 was approximately 59% U/Zr (2.8:1) with smaller amounts of Fe and Cr. SEM/EDS results were consistent with the elemental analysis, indicating a dendritic matrix composed of U/Zr/O with evidence of a eutectic reaction. There was substantial interdendritic porosity partially filled with a lower atomic number phase that was Fe/Ni/Cr rich. Fission product inventory was relatively high, including volatile fission products (i.e., highest 2,434 µCi/g of Cs-137).

Particle 11: This particle consisted of large, interconnected pores (14% open porosity) with a matrix density of 8.1 g/cc. ICP analysis indicated that Particle 11 was approximately 56% U/Zr (2.2:1) with smaller amounts of Si, Fe, Cr, and Al. SEM/EDS results were consistent with the elemental analysis, indicating a dendritic matrix composed of U/Zr/O with evidence of a eutectic reaction. There was substantial interdendritic porosity partially filled with a lower atomic number phase that was Fe/Ni/Cr rich. Fission product inventory was relatively low, including volatile fission products (only 57 µCi/g of Cs-137). Sr-90 was highest in this case (308 µCi/g).

Particle 7: This particle exhibited much greater interconnected porosity (both fine and coarse) than the other reaction products, taking on a "foamed" appearance (30% open porosity), although the matrix density was slightly higher (8.7 g/cc). ICP analysis indicated that Particle 7 was approximately 79% U/Zr (9.0:1) with smaller amounts of Si, Fe, Cr, and Al. SEM/EDS results were consistent with the elemental analysis, indicating a dendritic matrix composed of U/Zr/O with evidence of a eutectic reaction. There was substantial interdendritic porosity partially filled with a lower atomic number phase that was Fe/Ni/Cr rich. Fission product inventory was relatively high; however, volatile fission products were lower (962 µCi/g of Cs-137). Sr-90 levels were exceptionally high in this particle (2,174 µCi/g).

All of the above particles were similar in elemental composition--predominantly U, Zr, and O, with smaller amounts of other elements present in core structural materials. Particles 1 and 8 were very similar and had reasonable sample weight accountability, assuming the unaccounted balance was mostly oxygen. Particles 5 and 11, on the other hand, had a lower weight accountability based on elemental analysis (<60%); Particle 5 was otherwise very similar to Particles 1 and 8. Particle 11 had another distinctive trait--a fission product inventory an order of magnitude lower than the other particles. In addition, Sr-90 was the largest contributor to fission product inventory in Particle 11; whereas the other particles (Nos. 1, 8, and 5) were much higher in Cs-137. This may be partially due

to the lower levels of U in this specimen, but there may be other explanations. Low sample weight accountability may indicate a higher percentage of light elements in these particles. However, this could also be due to unaccountable losses during the sample dissolution procedure (especially minute losses in small specimens). Although Particle 7 was basically similar to the other four particles, several differences were noted, including (a) a much higher degree of porosity resulting in a foamed appearance, (b) a much higher ratio of U/Zr, which was reflected in the density measurements, and (c) an order of magnitude higher Sr-90 content than the other reaction products.

The remaining two particles (Nos. 6 and 12) constitute special cases which are discussed below.

Particle 6 had a composite structure consisting mostly of oxidized Zircaloy with some fuel/clad reaction product bonded to it. The particle exhibited very high open porosity (30%) and, compared to most of the other reaction products, a low matrix density of 5.6 g/cc. The matrix density is equivalent to that of ZrO_2. The low density was initially assumed to be due to the existence of closed internal porosity. However, the elemental analysis gave less than 20% accountability of the total sample weight, which is partially due to either the presence of oxygen and possibly other light elements or unaccounted sample losses during dissolution. However, it is still possible that there is an unresolved correlation between the low density measurements and the low weight accountability for Particle 6.

Particle 12 was a very complex reaction product with a high degree of heterogeneity. The particle was divided into two samples: one for the metallurgical analyses and one for the chemistry analyses. The SEM/EDS results indicated a matrix composed chiefly of Ag, In, and Cd with low levels of other elements, although no U or Zr was detected. Sn- and Te-rich particles were also observed in the Ag-In-Cd matrix. However, the chemistry (ICP) results indicated Ag was only present in trace quantities,

and the major components were U, Cd, Zr, and In. Weight accountability for the specimen was also somewhat low (65%). The particle had a fission product inventory similar to the other fuel/clad reaction products.

The lack of prior-molten specimens of Type 304 stainless steel or Inconel from the fuel assembly upper end fittings or the Upper Grid that have regions of ablation and the below-core-average presence of iron and nickel in the particle-size fractions, may indicate that melting of these components at the core exit may not have occurred before the restart of the B-loop reactor coolant pump 174 min after accident initiation.

If the observation is correct that the fuel assembly upper end fittings were not melted when the B-loop pump was restarted, the presence of particles greater than 2.5 mm in diameter on the upper tube sheet of the B-loop steam generator and short segments of rods or tubes in the B-loop hot leg[a] requires one or more of the fuel assembly upper end fittings to have relocated downward sufficiently, before or during the period of forced flow from the restart of the B-loop reactor coolant pump, to allow core component and material interaction products to avoid the spacer grid of the upper end fitting. The spacer grids create a strainer for particles larger than approximately 2.5 mm.

3.3 Peak Temperature Estimates

The prior peak temperatures of the 10 particles extracted from the B-Loop generator were estimated by EG&G Idaho based on one or more of the following characteristics depending on the composition of the particle:

- The grain growth, pore size distribution, and evidence of melting of UO_2

---

a. H. P. Wood, TMI-2 Technical Bulletin TB 87-07 Rev. 0, Sampling and Estimating Sediment Volume in "B" Hot Leg and Attached Decay Heat Line, GPUN, April 20, 1987.

- The presence of prior zirconium phases as determined from the microstructures of the Zircaloy cladding and transformation temperatures from the Zr-Sn phase diagram

- The microstructure of the U-Zr-O ternary material

- The microstructure and evidence of melting of Ag-In-Cd control rod material.

The methods of correlating these characteristics to prior peak temperatures are described in TMI-2 Core Debris Grab Samples--Examination and Analyses, GEND-INF-075, September 1986 by D. W. Akers, et al. The estimated prior peak temperature for the 10 particles is listed in Table 13 along with other relevant data about the particles and key indicators used to estimate peak temperatures.

The prior peak temperature estimation assumed that Particles 1, 5, 7, 8, and 11 were completely oxidized metals. The SEM/EDS data (Tables 6 and 7) indicate oxygen is a principal element in the matrix of Particles 1, 5, 7, 8, and 11.

3.4 Fission Product Behavior

Table 14 shows the fission product isotope composition of the samples normalized to the uranium component of the sample composition as well as a comparison to the average isotopic composition of the TMI-2 core. The ORIGEN2[a] code was used to calculate the average isotopic compositions and assumes that no isotopes were released from the uranium. Overall, the fission product composition shows the greatest retention of the least volatile fission products by the uranium with few exceptions. The finer-size particle collections with the largest surface-to-volume areas

---

a. A. G. Croff, ORIGEN2--A Revised and Updated Version of the Oak Ridge Isotope Generation and Depletion Code, ORNL-5621, Oak Ridge National Laboratory, 1980.

TABLE 13. PRIOR PEAK TEMPERATURE ESTIMATES FOR PARTICLES FROM THE UPPER TUBE SHEET OF THE TMI-2 B-LOOP STEAM GENERATOR

Particle No.	Material Characterisitics	Temp (K)	Key Indicators
1	Homogeneous core material reaction product, 7.9 g/cc, 0.160 U-0.154 Zr-0.013 Fe-0.673 O[a]	>2,800	Minimum melting point of urania/zirconia mixtures
2	Oxidized zircaloy cladding, 6.0 g/cc	≥2,123	Oxide precipitates indicate temperatures exceeding 2,123 K
3	UO_2 pellet fragment, 10.4 g/cc, 5 μm grain size	<1,900	As-fabricated grain size, no pore migration to grain boundaries
4	Near-nominal composition Ag-In-Cd poison material	1,050-1,100	As-fabricated elemental composition, partial melting
5	Homogeneous fuel rod material reaction product, 8.0 g/cc, 0.063 U-0.060 Zr-0.878 O,[a] high porosity	>2,800	Minimum melting point of urania/zirconia mixtures
6	Heterogeneous fuel rod material interaction product	<2,800	Possible interaction of molten urania/zirconia with solid zirconia
7	Homogeneous fuel rod material reaction product, 8.7 g/cc, 0.177 U-0.051 Zr-0.768 O,[a] foamy ceramic	>2,800	Minimum melting point of predominantly uranium, urania/zirconia mixture
8	Homogeneous core material reaction product, 7.9 g/cc, 0.125 U-0.062 Zr-0.011 Fe-0.757 O,[a] high porosity	>2,800	Minimum melting point of urania/zirconia mixtures
11	Homogeneous fuel rod material reaction product, 8.1 g/cc, 0.054 U-0.062 Zr-0.883 O,[a] high porosity	>2,800	Minimum melting point of urania/zirconia mixtures
12	Heterogeneous poison and fuel rod material product	>1,100	Melting of control material

a. Composition in atom percent from ICP data assuming balance of material is oxygen.

TABLE 14. ISOTOPIC COMPOSITION NORMALIZED TO URANIUM

Sample	Mass (g)	Uranium Fraction	Isotope Composition[a] (μCi/g U)								
			Ce-144	Cs-134	Cs-137	Eu-154	Eu-155	I-129	Ru-106	Sb-125	Sr-90
TMI-2 core	126.6×10^6	0.656	214[b]	160[b]	8,680[b]	60.2[b]	125[b]	0.0028[b]	168.0[b]	206[b]	7,540[b]
Fraction <150 μm	0.399	0.315	305	191	10,000	50.5	74.3	0.0012	203	654	994
150 to 300 μm	0.520	0.465	293	125	5,360	55.9	83.9	0.00073	106	152	951
300 to 710 μm	1.140	0.376	277	85.6	4,930	49.5	65.4	0.00090	47.6	161	832
710 to 1000 μm	0.726	0.400	285	93.5	5,150	58.3	81.5	--[c]	62.8	130	908
Fraction >1000 μm:	36.1	--	--	--	--	--	--	--	--	--	--
Bulk	32.70	0.861	245	88.7	5,660	37.2	66.1	0.00038	60.7	48.7	854
Particle 1[e]	0.427	0.598	338	75.1	3,380	62.4	87.8	0.00033	--[c]	--[c]	1,270
Particle 2	0.162	<0.003	--	--	--	--	--	--	--	--	--
Particle 3	0.680	0.844	148	49.6	5,140	12.0	42.3	0.00090	69.5	51.8	492
Particle 4	0.063	<0.003	--	--	--	--	--	--	--	--	--
Particle 5[e]	0.731	0.436	335	123	5,580	72.7	90.4	0.00055	--[c]	--[c]	1,410
Particle 6[e]	0.543	0.015	188	143	8,510	19.5	77.9	--[d]	77.9	455	419
Particle 7[e]	0.300	0.713	323	21.6	1,350	90.0	213	--[d]	17.4	219	3,050
Particle 8[e]	0.723	0.567	261	48.0	2,440	43.6	70.5	--[c]	--[c]	--[c]	1,120
Particle 11[e]	0.152	0.386	232	27.2	182	34.2	63.5	--[d]	--[c]	--[c]	798
Particle 12[e]	0.297	0.277	234	87.4	4,340	31.8	71.1	--[d]	--[c]	2,600	765

a. Radioactivities corrected to April 1, 1987.

b. TMI-2 core average isotope concentration calcuated by ORIGEN2 computer code.

c. Undetectable.

d. Not measured due to insufficient sample.

e. Core material interaction products.

have retained relatively greater concentrations of the most volatile fission products. The data indicate the following about the individual isotopes:

1. High Volatility (Cs-134, Cs-137, and I-129):

   a. Cs-134 and Cs-137. The Cs-134 and -137 isotope composition of the samples indicates (a) increased release from particles with uranium that achieved the highest temperatures during the accident and (b) capture by debris with the highest surface-area/volume (fine particle size) ratios indicating surface deposition.

   b. I-129. All samples are depleted in I-129 with a larger indicated surface deposition on the smallest particle size (<150 μm) fraction as might be expected for the highest surface area/volume samples.

2. Medium Volatility (Ru-106, Sb-125, and Sr-90):

   a. Ru-106. The concentrations of Ru-106 ranged from 0.3 to 0.5 of the expected concentration with the exception of the smallest particle size fraction that has a higher Ru retention and also has high structural material content. The Ru-106 concentrations appear to follow the same release and retention trend with particle size as do the cesium isotopes. Other observations of the association of Ru with metallics have been made.[a]

---

a. G. W. Parker et al., "Source Term Evaluations from Recent Core Melt Experiments," Proceedings IAEA Symposium on Source Term Evaluation for Accident Conditions, Columbus, Ohio, October 28-November 1, 1985, International Atomic Energy Agency, 1986.

b. Sb-125. The Sb-125 is depleted in the individual particle samples that have the highest estimated prior peak temperature. The high retention of Sb-125 by Particle 12 might be associated with the presence of indium; however, the correlation is ambiguous for other particles and particle-size fraction samples with indium present.

c. Sr-90. Strontium-90 is depleted in all samples to about the same degree except for individual Particle 7; however, Particle 7 does not have any distinctive feature that correlates to the preferential retention of Sr-90.

3. Low Volatility (Ce-144, Eu-154, and Eu-155):

a. Ce-144. The Ce-144 is probably still retained by the uranium because, for most of the samples, the composition is close to or above the core average. The above-average Ce-144 composition of most of the samples indicates that much of the material, especially the core material reaction products, came from the above-average power regions of the core. The fuel pellet fragment (Particle 3) below-average cerium composition is consistent with the low prior peak temperature estimate (see Table 13) that indicates it was in a low power region of the core, probably at the core top.

b. Eu-154 and Eu-155. The europium isotope composition of the samples indicates that the isotopes are retained by the uranium like the cerium isotope.

4. CONCLUSIONS

The major conclusions of this report concerning the debris recovered from the upper tube sheet of the TMI-2 B-loop steam generator are listed below.

4.1 Size Fractions and Filter

- The major elemental constituents of all the size fractions are U (highest) and Zr, with smaller amounts of Ag-In-Cd and Fe-Cr-Ni.
- The relative amounts of each element suggest a random contribution from various core materials for all size fractions except the >1,000 μm size fraction.
- The >1,000 μm size fraction consists primarily of UO_2 fuel fragments.

4.2 Individual Particles (Ten Total)

- One particle was a UO_2 fuel pellet fragment (No. 3).
- One particle was partially oxidized Zircaloy cladding (No. 2).
- One particle was a resolidified portion of Ag-In-Cd alloy (i.e., control rod material).
- Three particles (Nos. 1, 8, and 5) were UO_2 fuel/Zircaloy cladding reaction products consisting of large interconnected pores and fine interdendritic inclusions partially filled with lower melting point alloys such as Fe-Cr-Ni, with relatively high levels of volatile fission product retention (Cs-137).

- Particle 11 was a fuel/cladding reaction product similar to the above particles except that it had a lower U content, lower overall fission product inventory, and very low retention of volatile fission products (Cs-137).

- Particle 7 was also a fuel/cladding reaction product, but differed from the other reaction products in the following ways:

  - Higher fission product inventory due to Sr-90 levels

  - Much greater degree of open porosity

  - Higher matrix density due to higher levels of U.

- Particle 6 had a composite structure consisting mostly of highly oxidized Zircaloy cladding with some bonded fuel/cladding reaction product. The particle had a high percentage of open porosity.

- Particle 12 was a complex heterogeneous reaction product between the UO_2 fuel, Zircaloy cladding, and Ag-In-Cd control rod material.

4.3 TMI-2 Accident Sequence of Events

- Between 174 and 192 min after accident initiation, peak temperatures in the core had reached or exceeded 2,800 K and melting of fuel and plenum assembly components at the core exits may not have occurred.

- One or more fuel assembly upper end fittings may have relocated downward sufficiently, before or during the period of forced flow from the restart of the B-loop reactor coolant pump, to allow core component and material interaction products greater than 2.5 mm in diameter to escape from the core by hydraulic levitation.

APPENDIX A

AS RECEIVED PHOTOGRAPHS OF TMI-2 B-LOOP FUEL DEBRIS

Figures A-1 - A-5. TMI-2 B-Loop Fuel Debris,

> 1000 μ Size Fraction (Photographs #19, 20, 21, 22, and 25)

Low Magnification at 0.5X

High Magnification at 2.7X

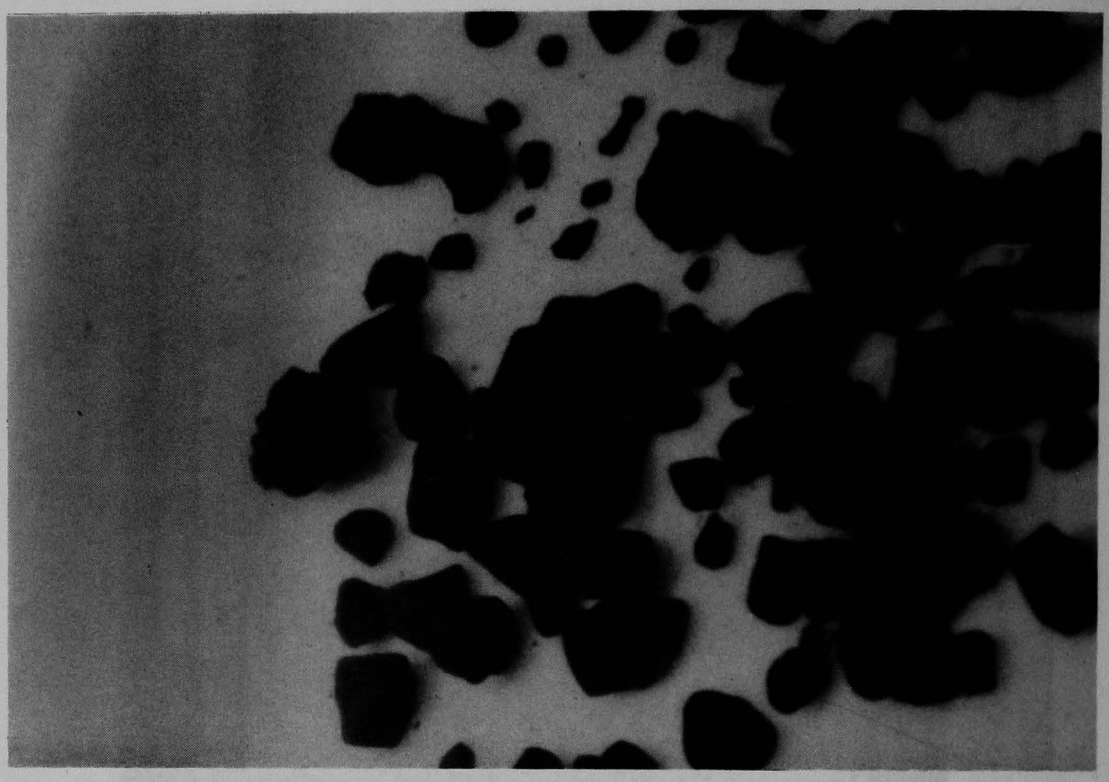

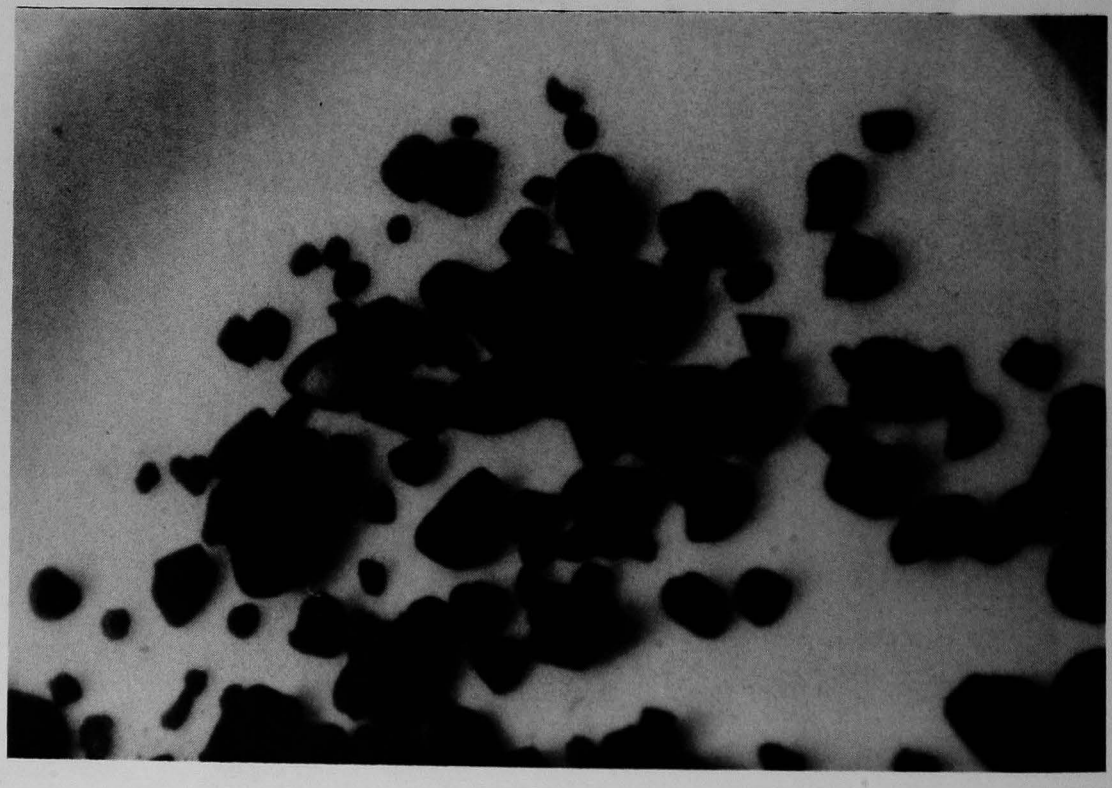

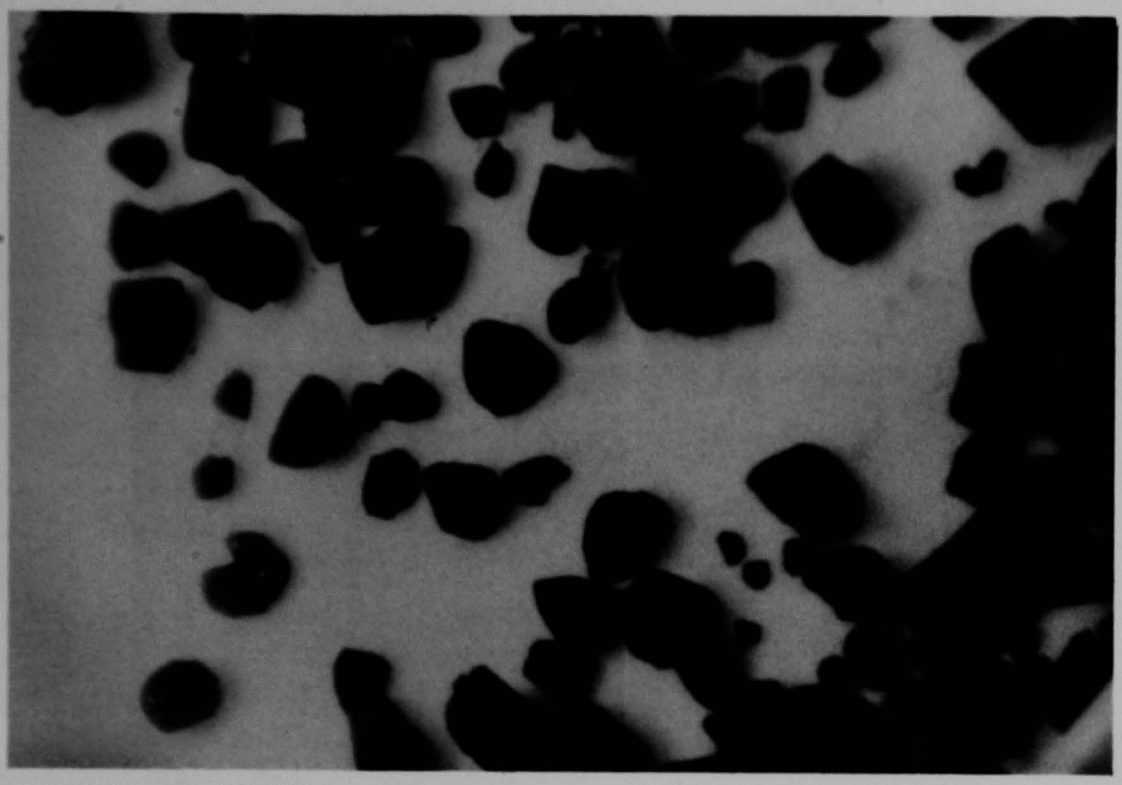

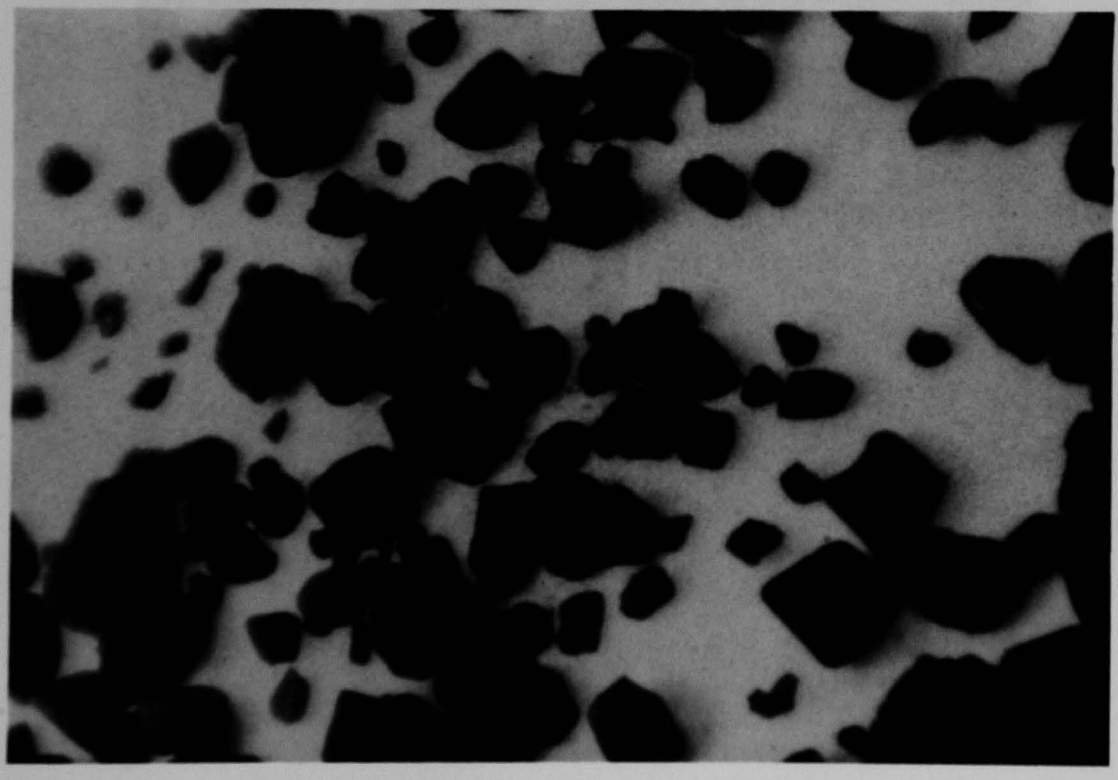

Figures A-6 - A-7. TMI-2 B-Loop Fuel Debris

710 - 1000 μ Size Fraction (Photographs # 7 and 9)

Low Magnification at 0.65X

High Magnification at 3.3X

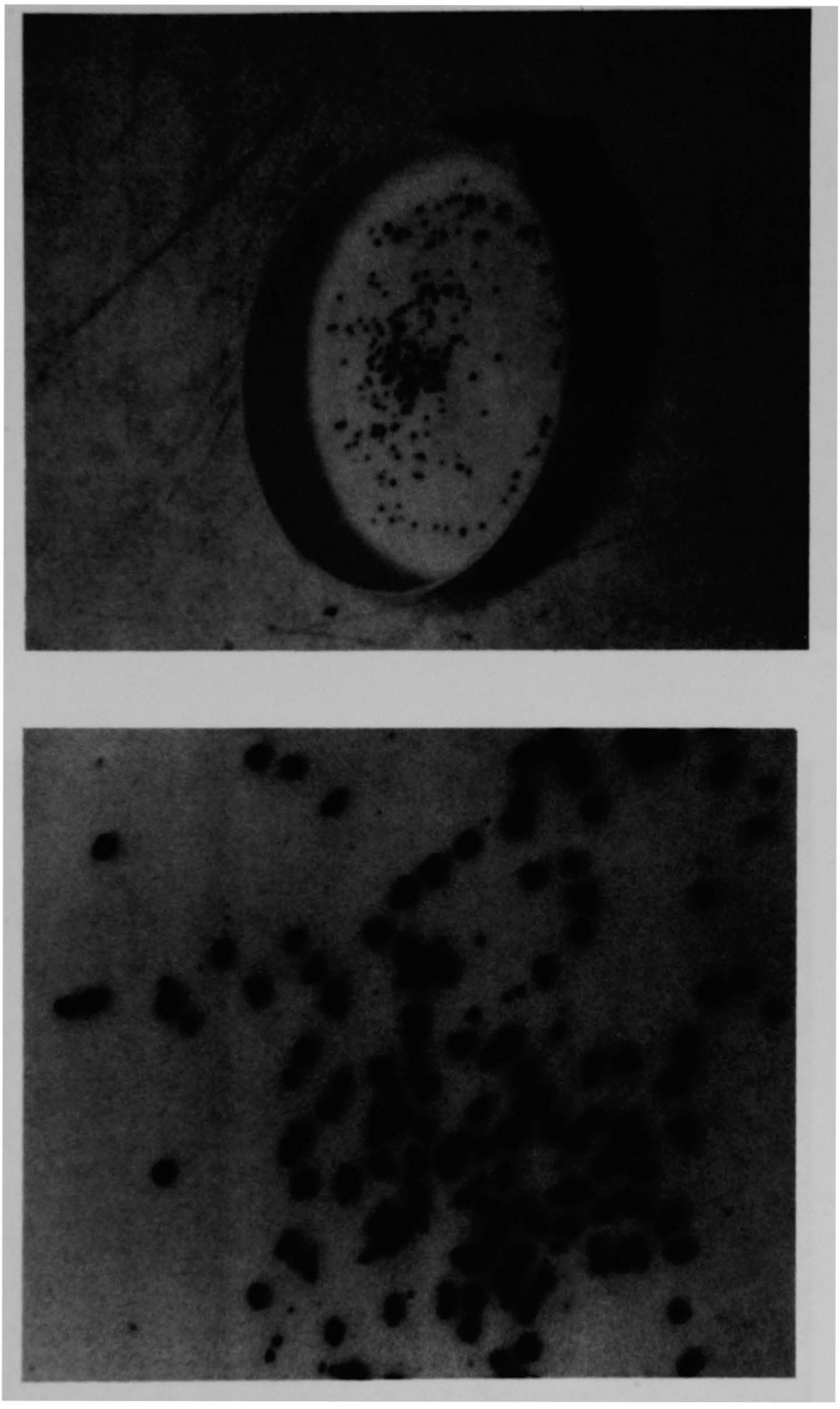

Figures A-8 - A-11. TMI-2 B-Loop Fuel Debris,

300 - 710 μ Size Fraction

Photograph #4 at 0.65X

Photograph #1 at 2.7X

Photographs #3 and 6 at 3.3X

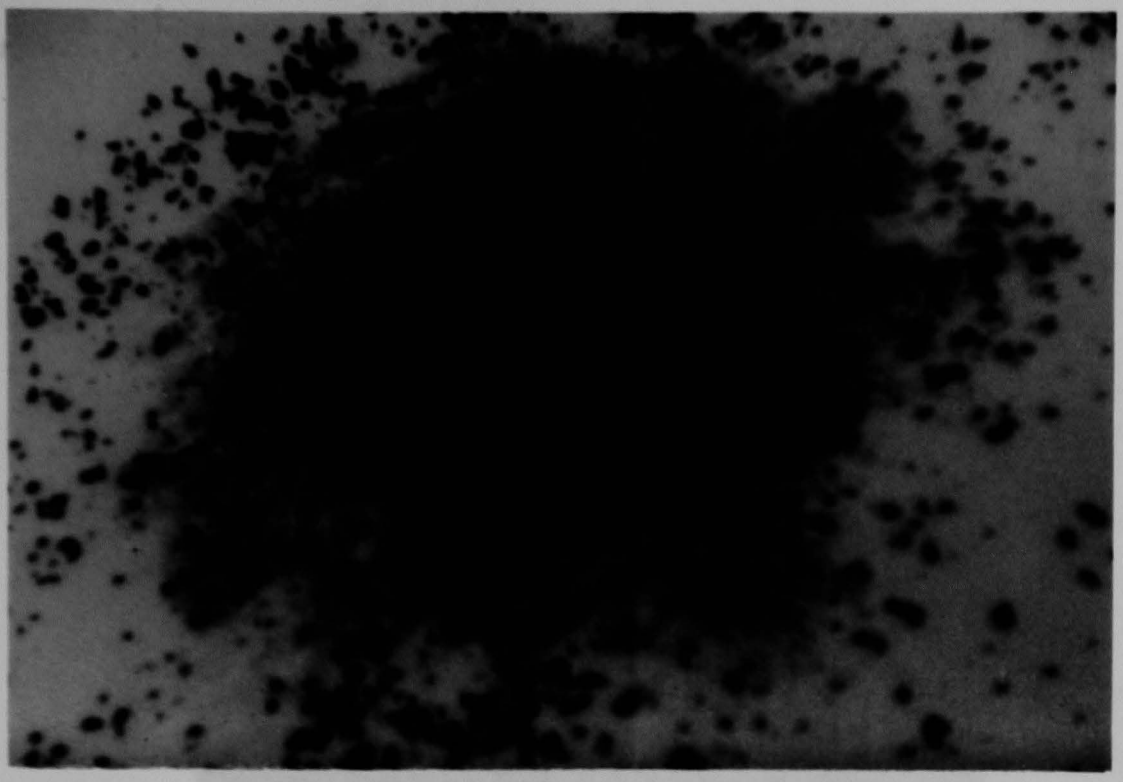

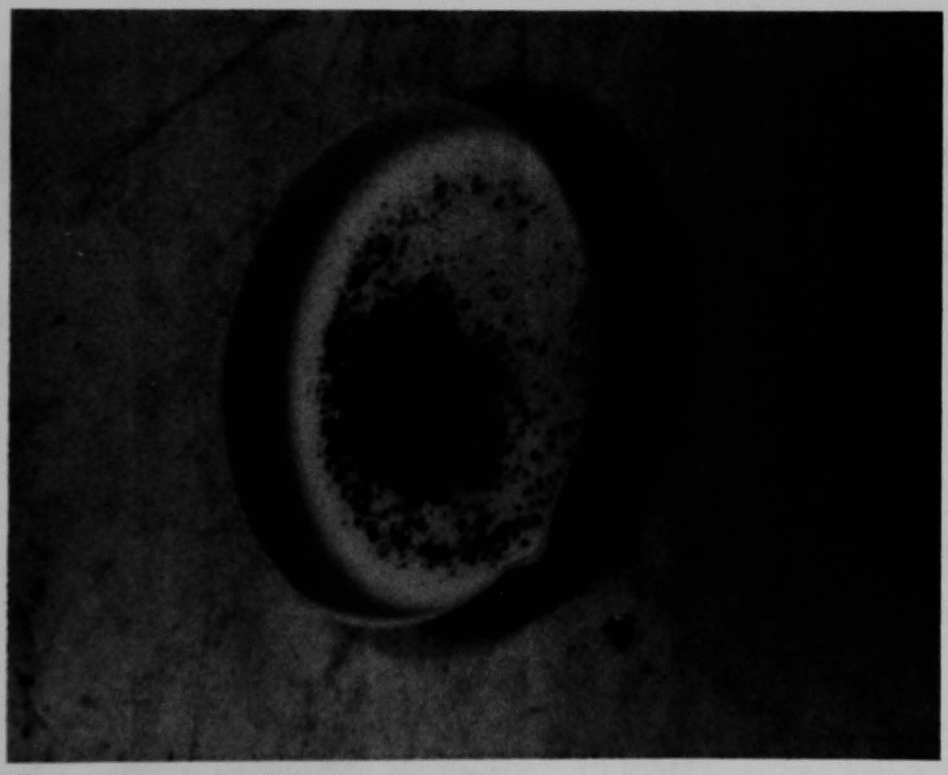

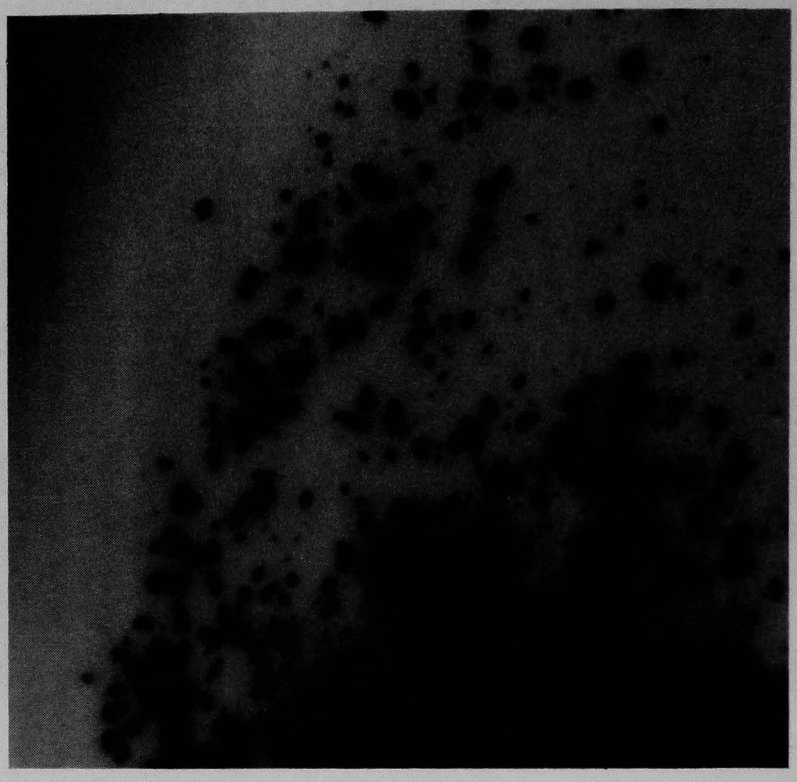

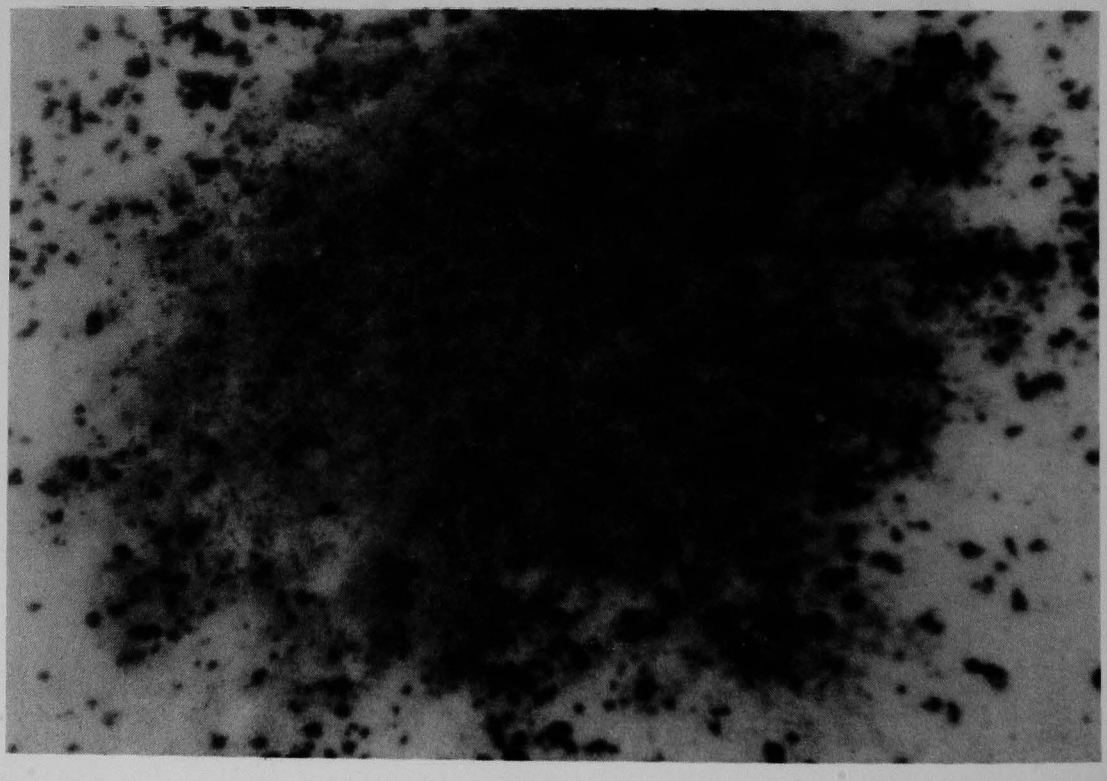

Figures A-12 - A-14. TMI-2 B-Loop

Fuel Debris, 150 - 300 μ Size Fraction

(Photographs #36, 37 and 40)

Low Magnification at 0.65X

High Magnification at 3.3X

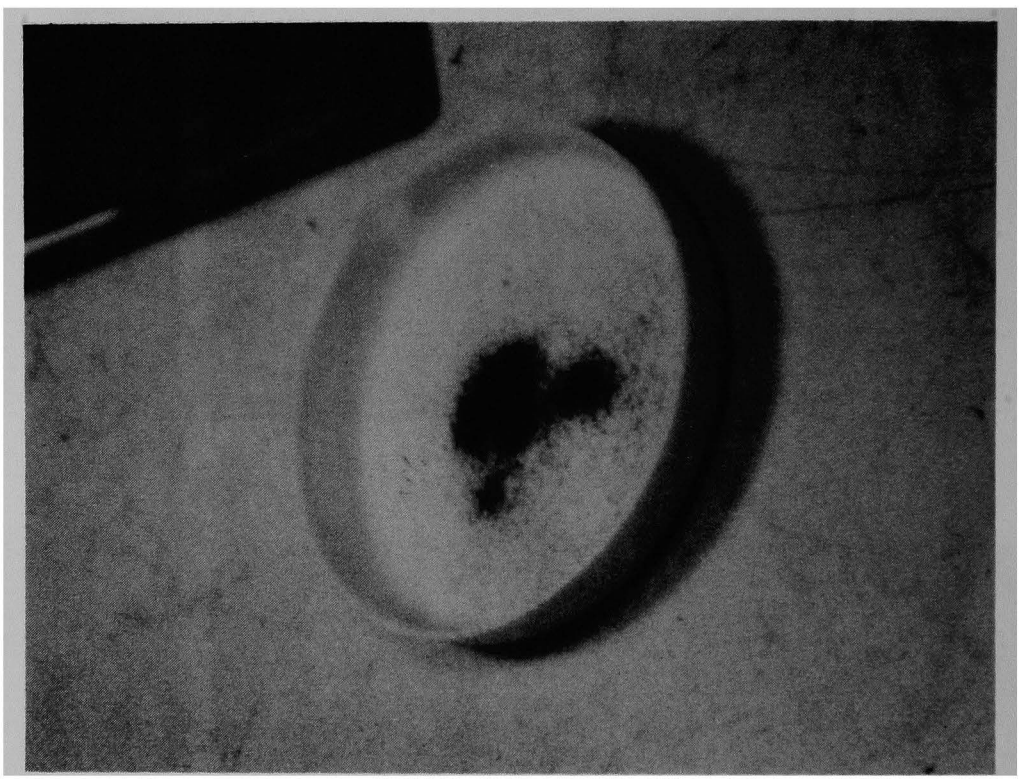

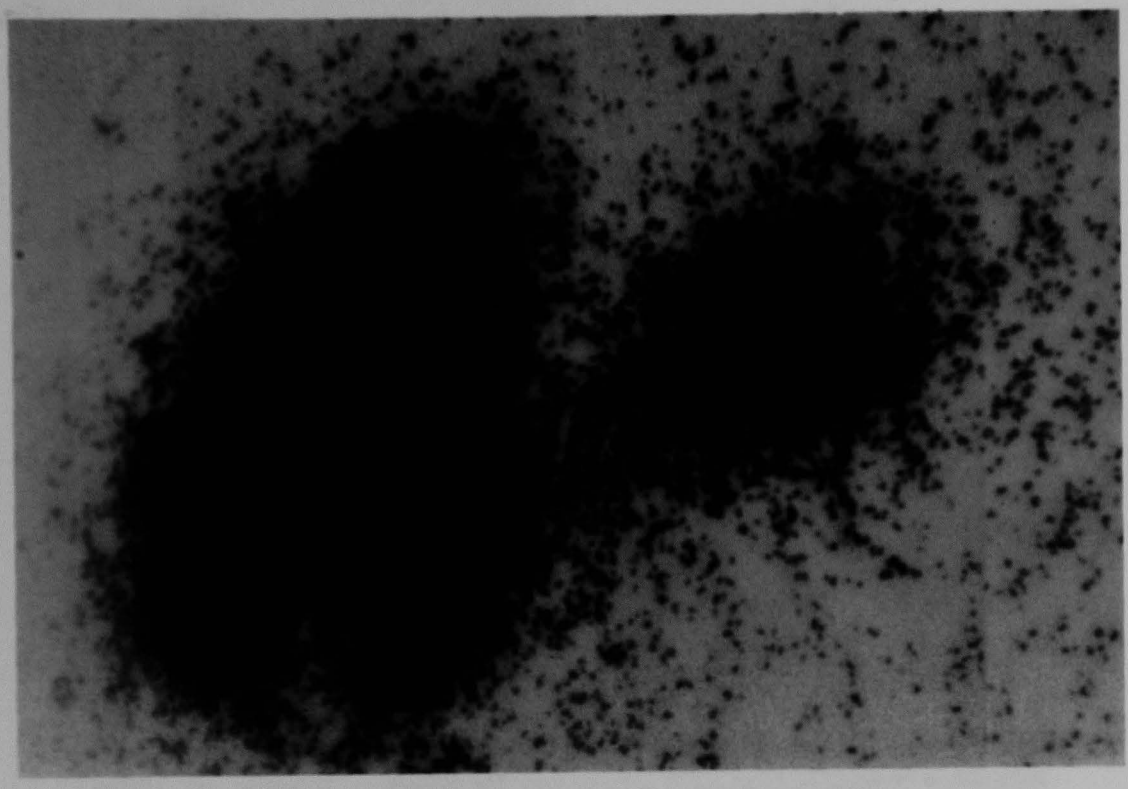

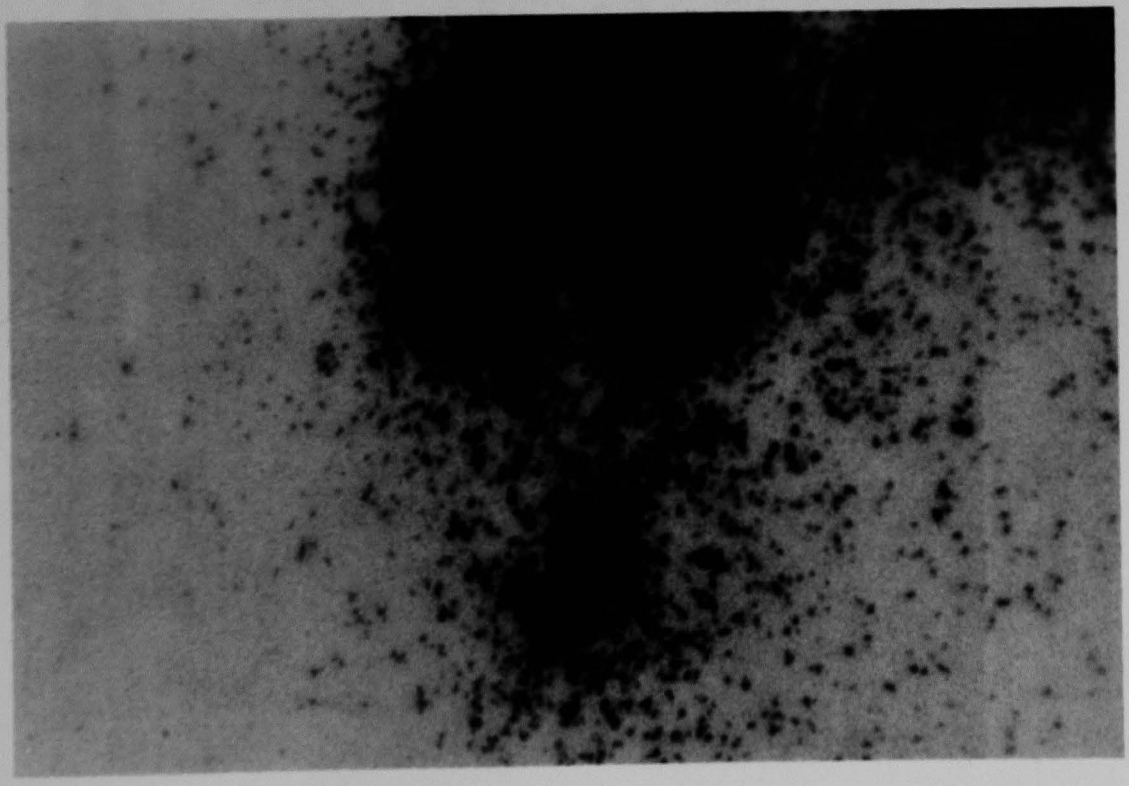

Figures A-15 - A-17 TMI-2 B-Loop

Fuel Debris , < 150 μ Size Fraction

(Photographs #16, 17 and 18)

Photograph 18 at 0.5X

Photograph 17 at 2.7X

Photograph 16 at 3.3X

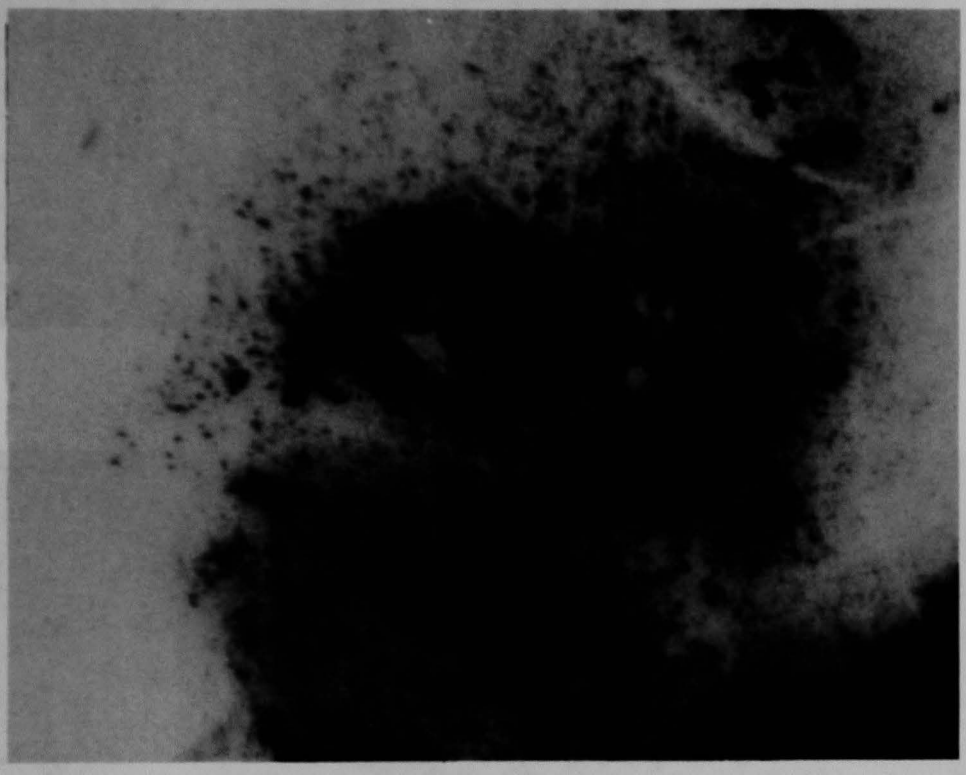

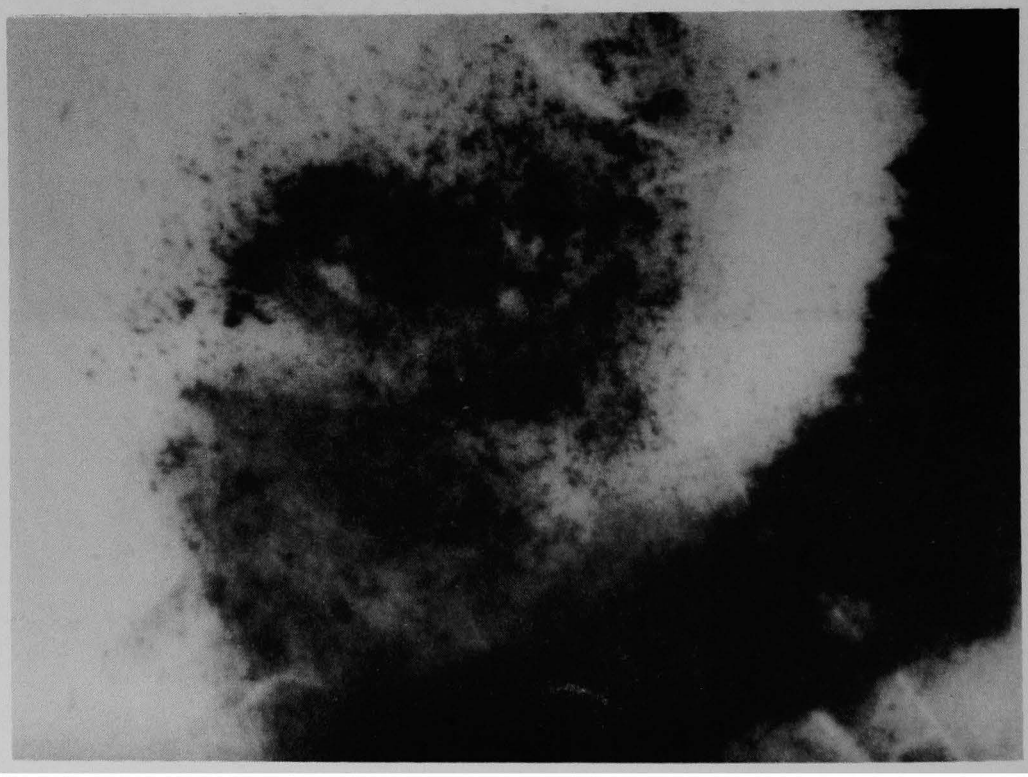

Figures A-18 - A-27 TMI-2 B-Loop Filter Samples

(Photographs # 102-111)

Photograph #102 at 0.65X

Photograph #103 at 3.3X

Photograph #104 at 3.3X

Photograph #105 at 3.3X

Photograph #106 at 2.7X

Photograph #107 at 2.7X

Photograph #108 at 2.7X

Photograph #109 at 2.7X

Photograph #110 at 3.3X

Photograph #111 at 3.3X

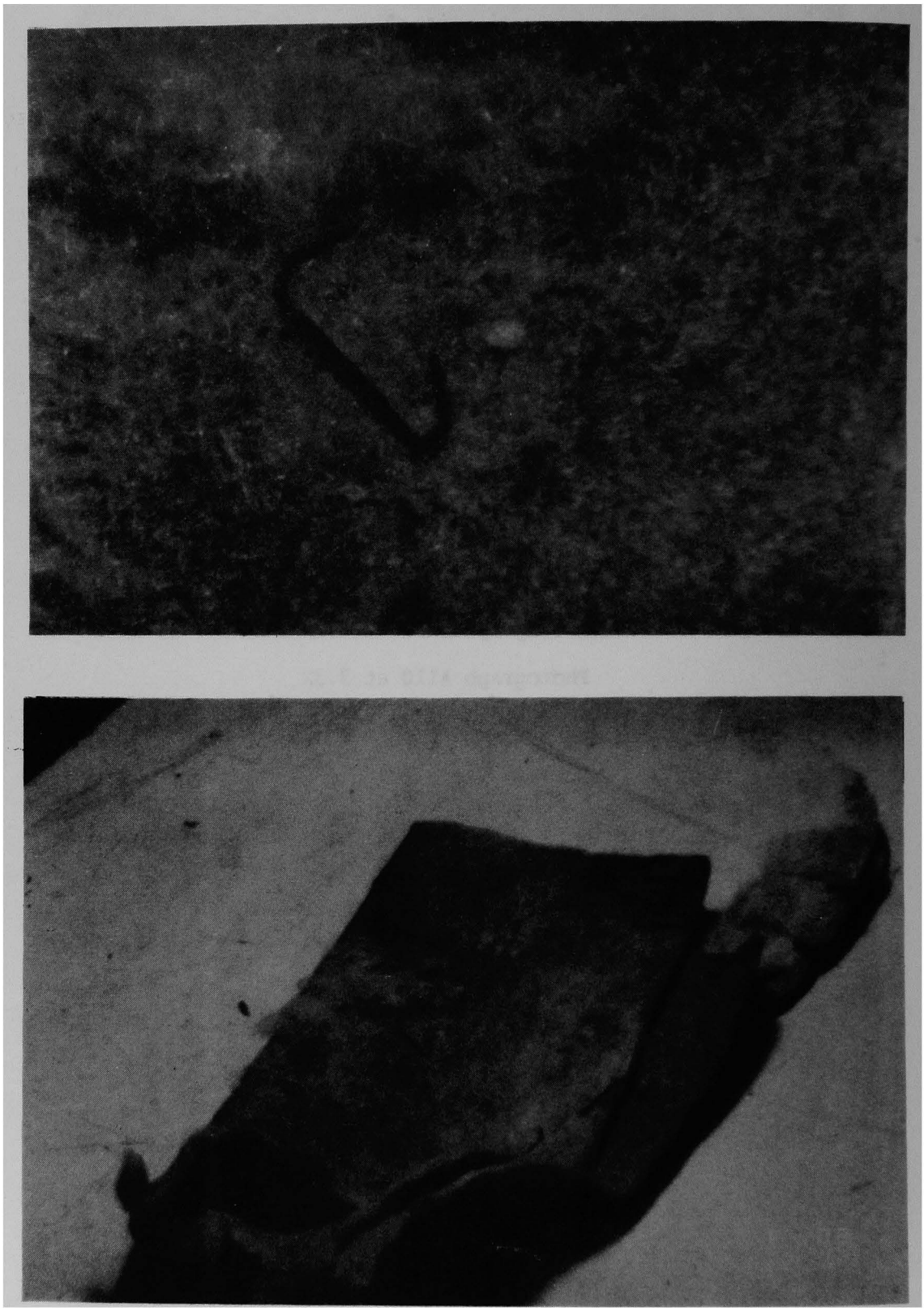

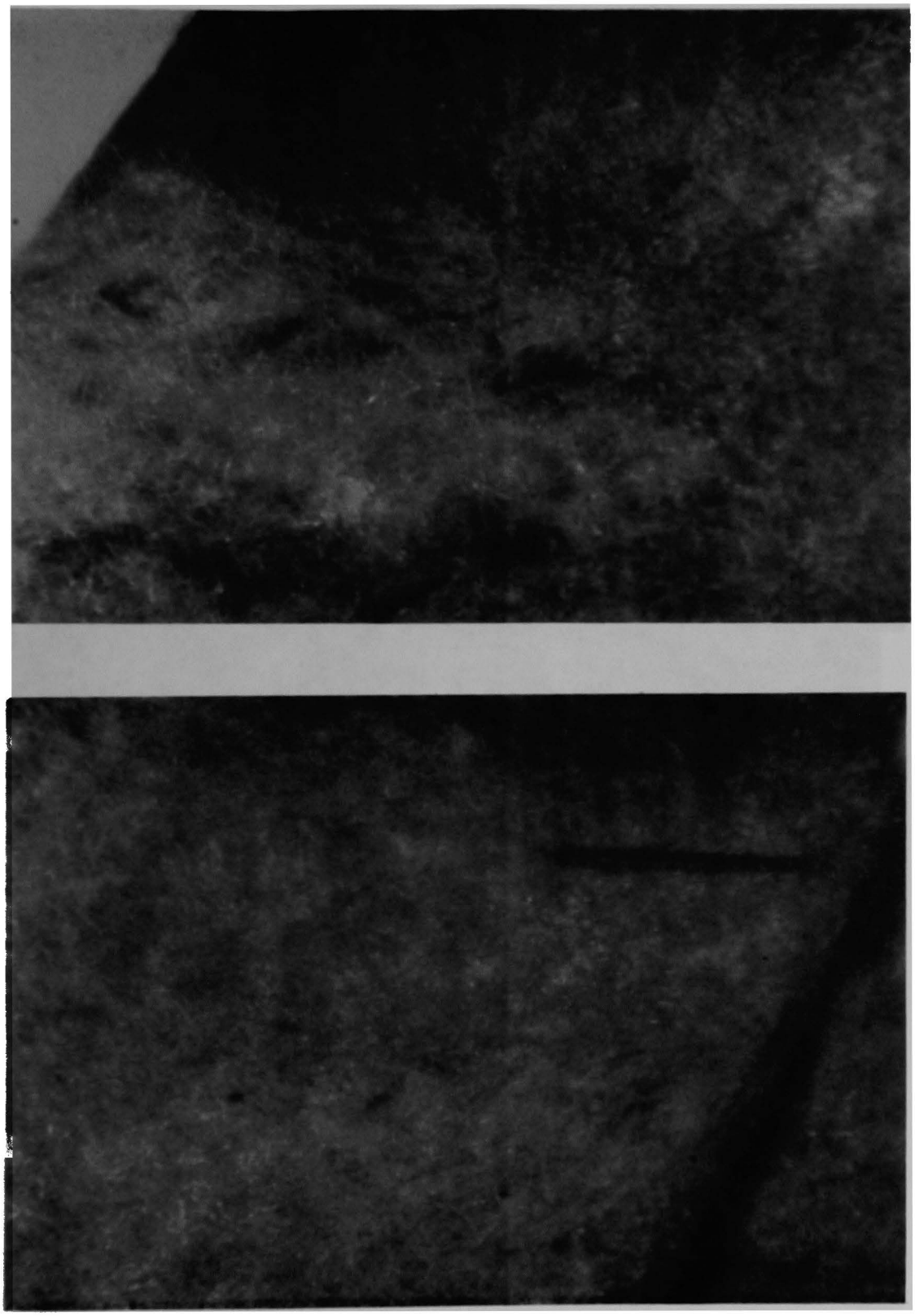

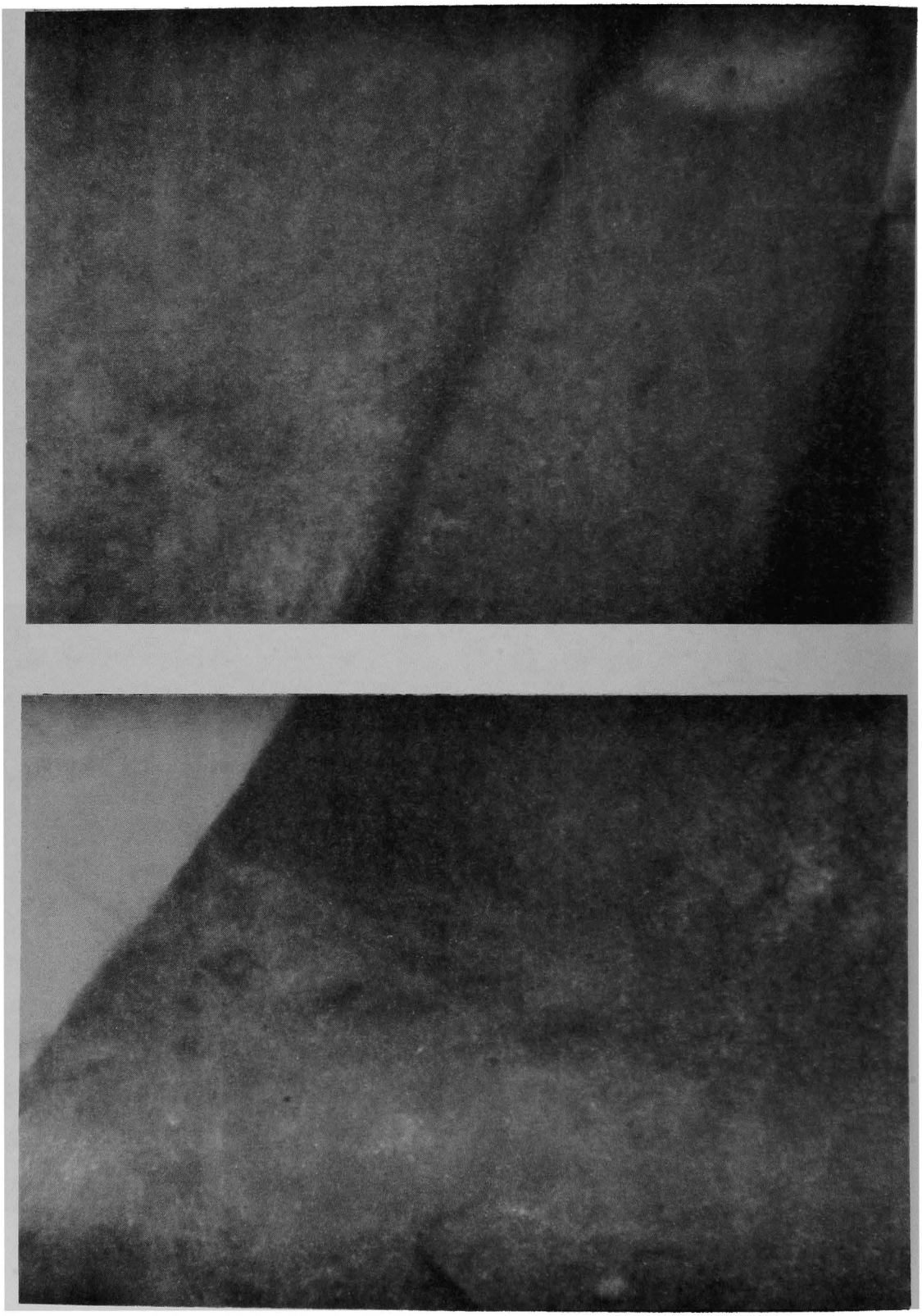

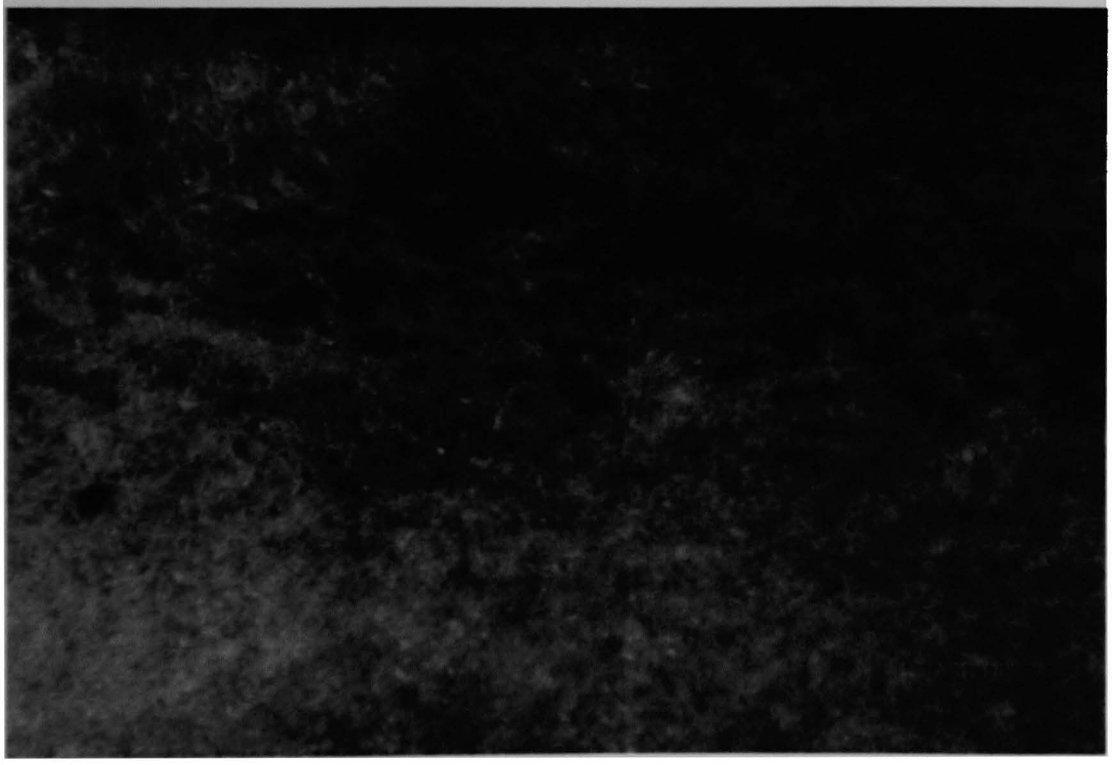

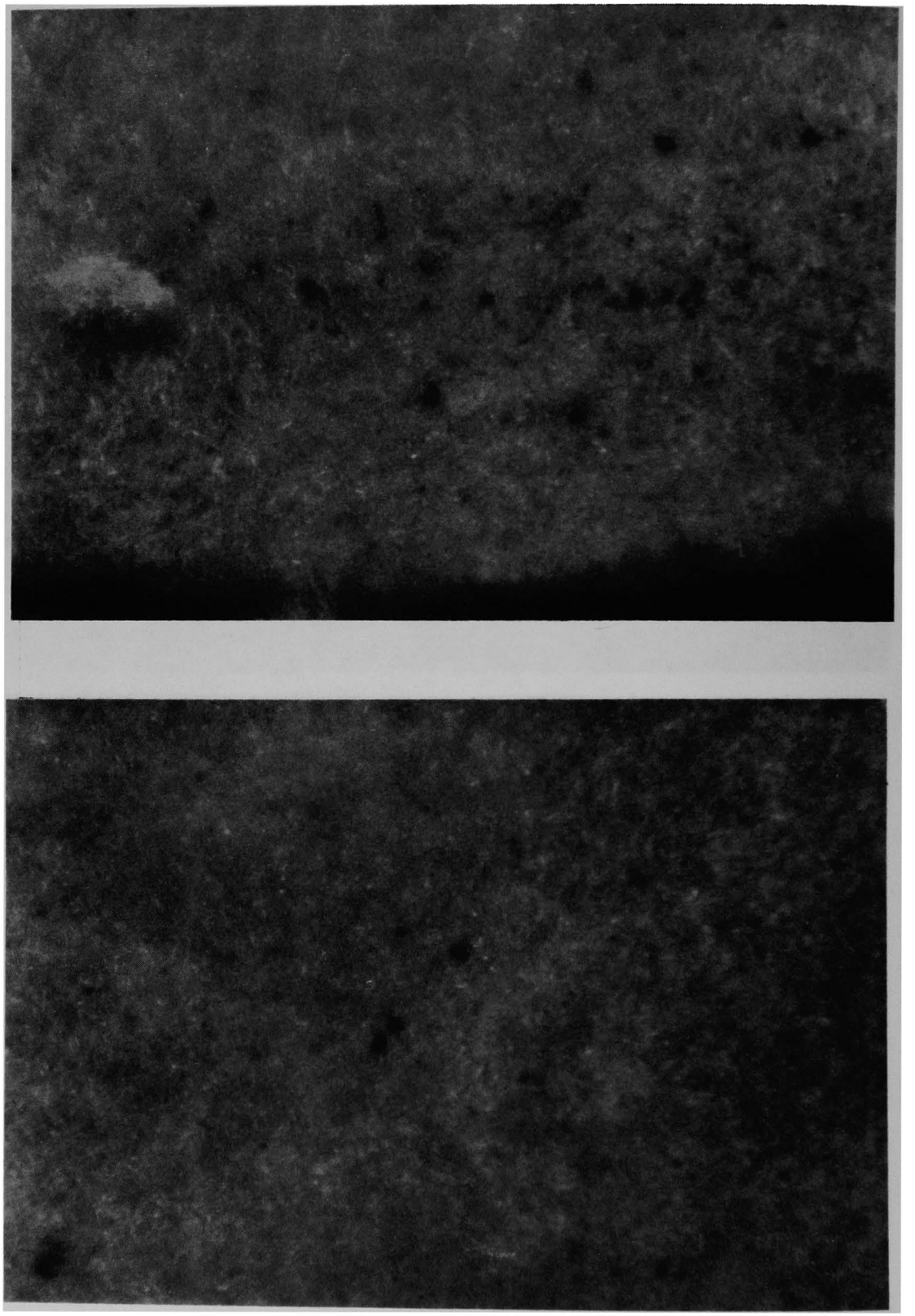

APPENDIX B

PHOTOGRAPHIC EXAMINATION RESULTS OF TEN SELECTED B-LOOP DEBRIS SAMPLES

All black and white prints are 7.5X magnification and all color prints are 9.5X magnification unless marked otherwise.

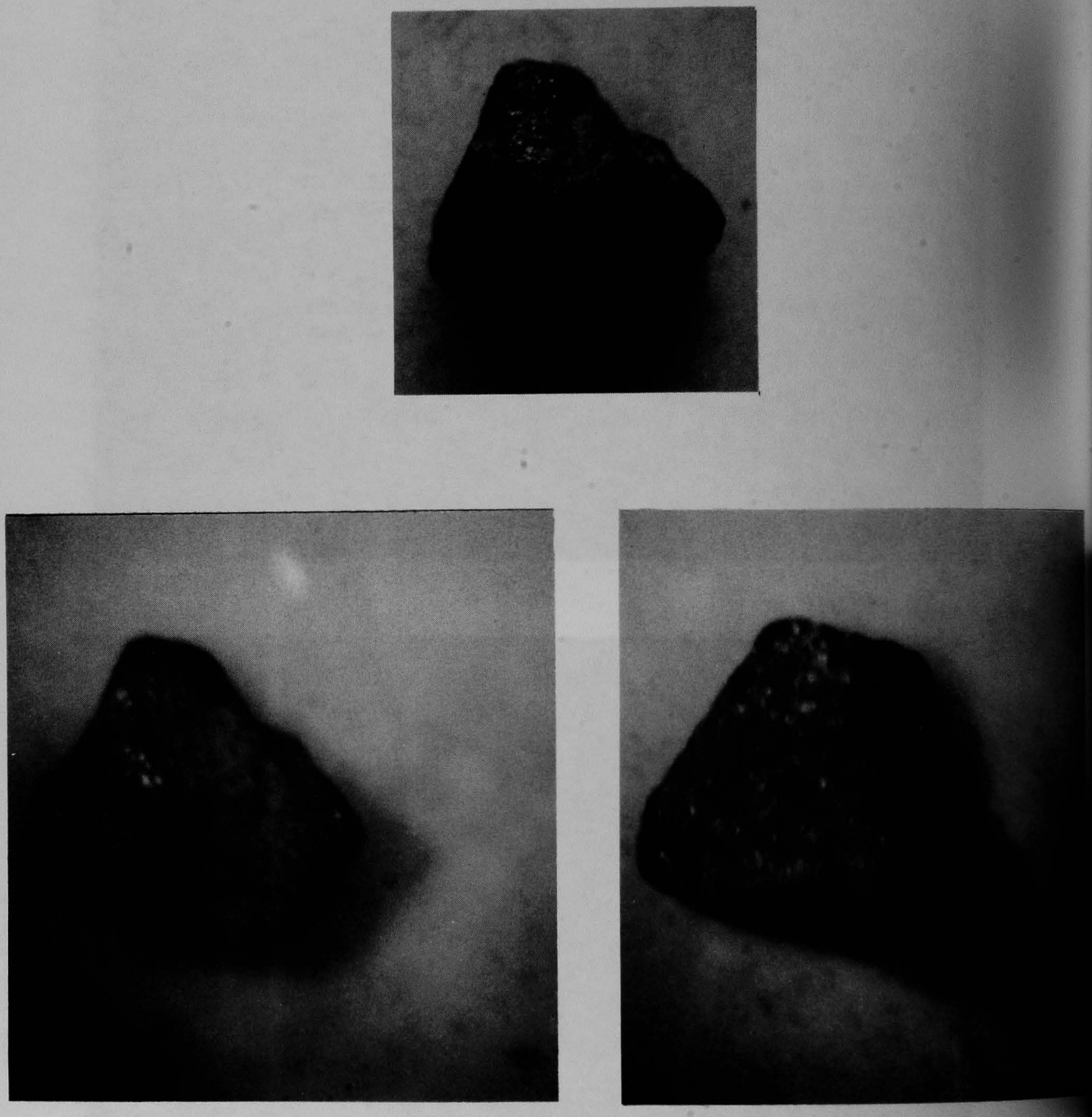

Figure B-1. Sample 1 Photographic Survey Results.

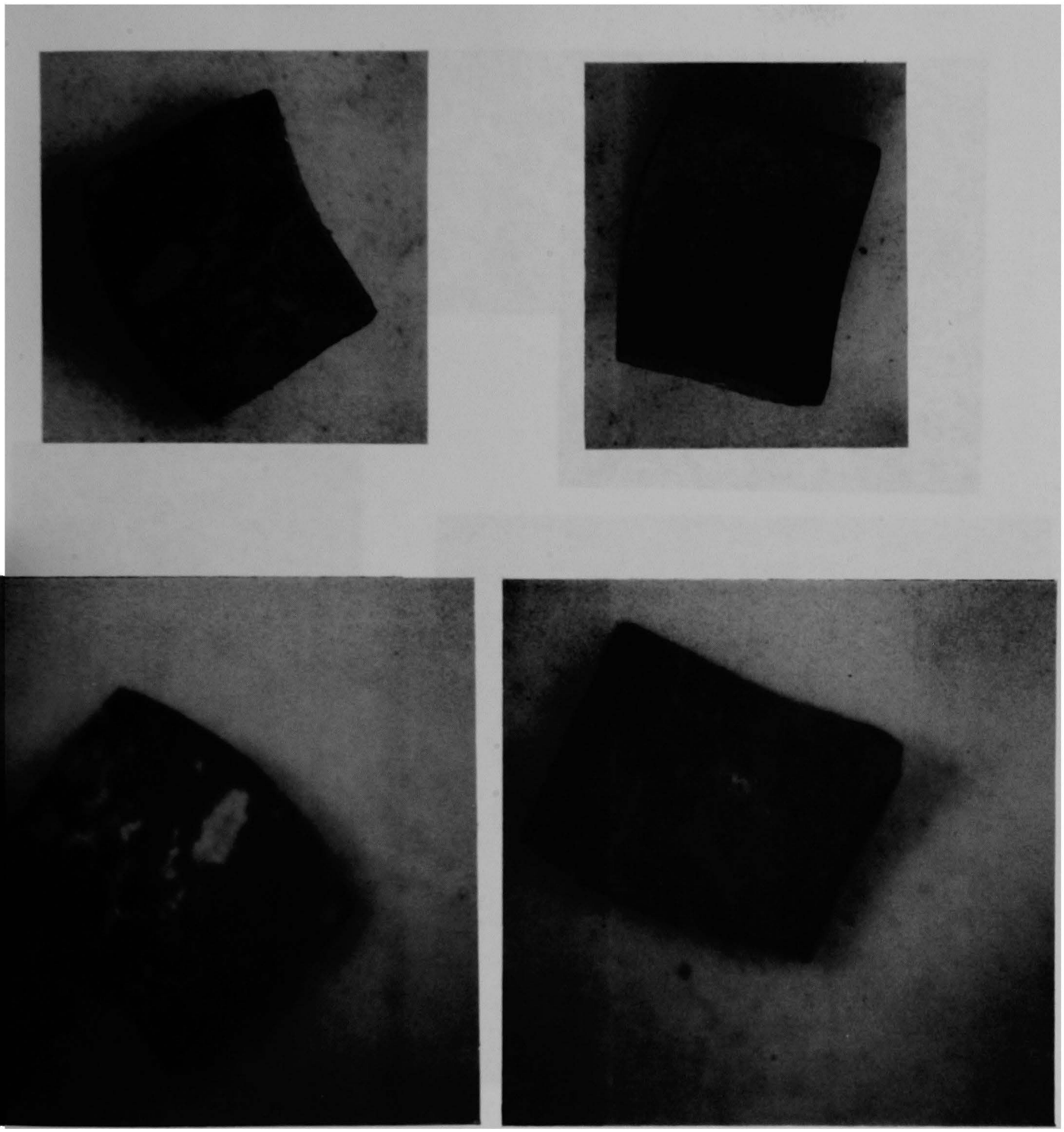

Figure B-2. Sample 2 Photographic Survey Results.

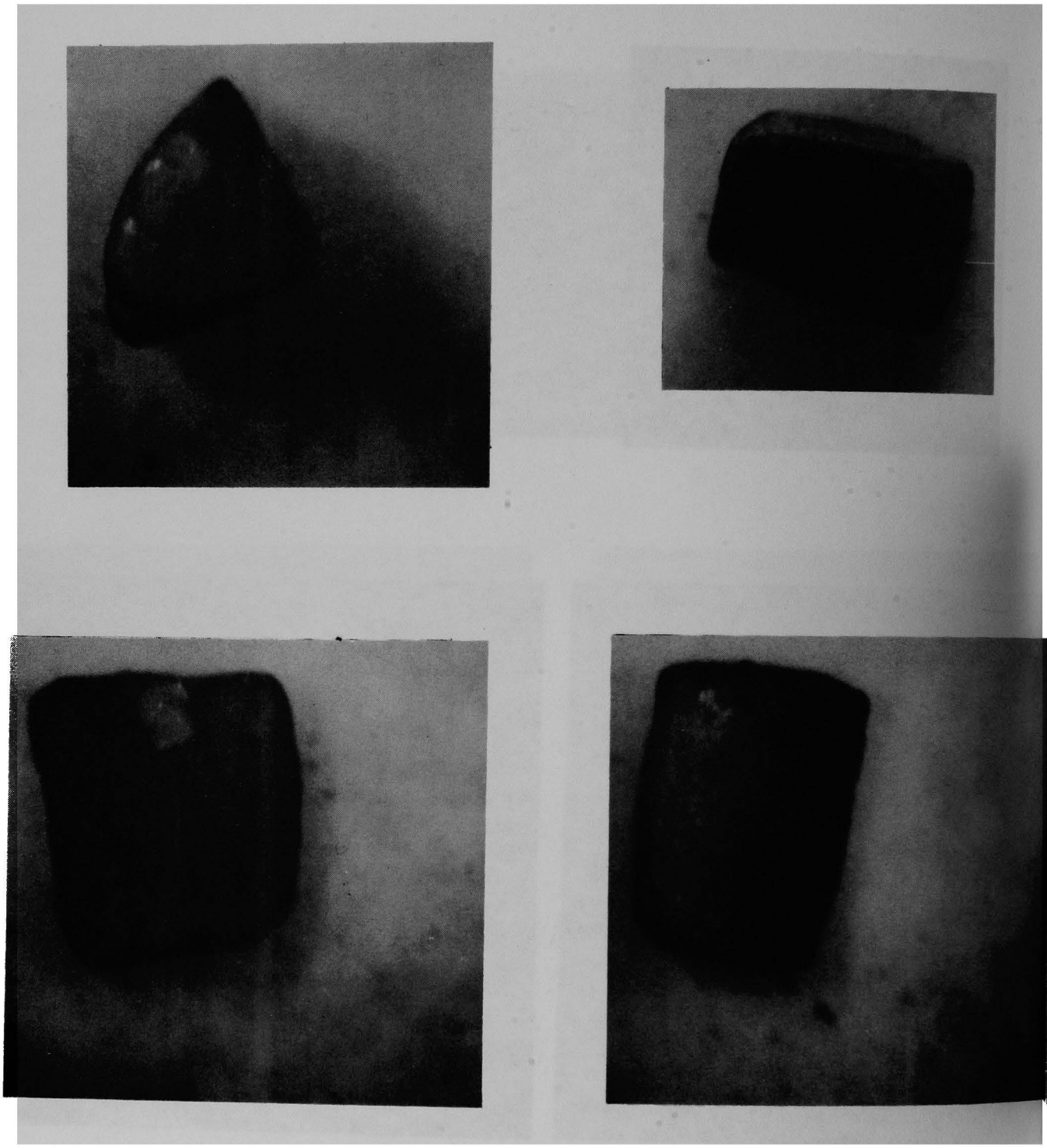

Figure B-3. Sample 3 Photographic Survey Results.

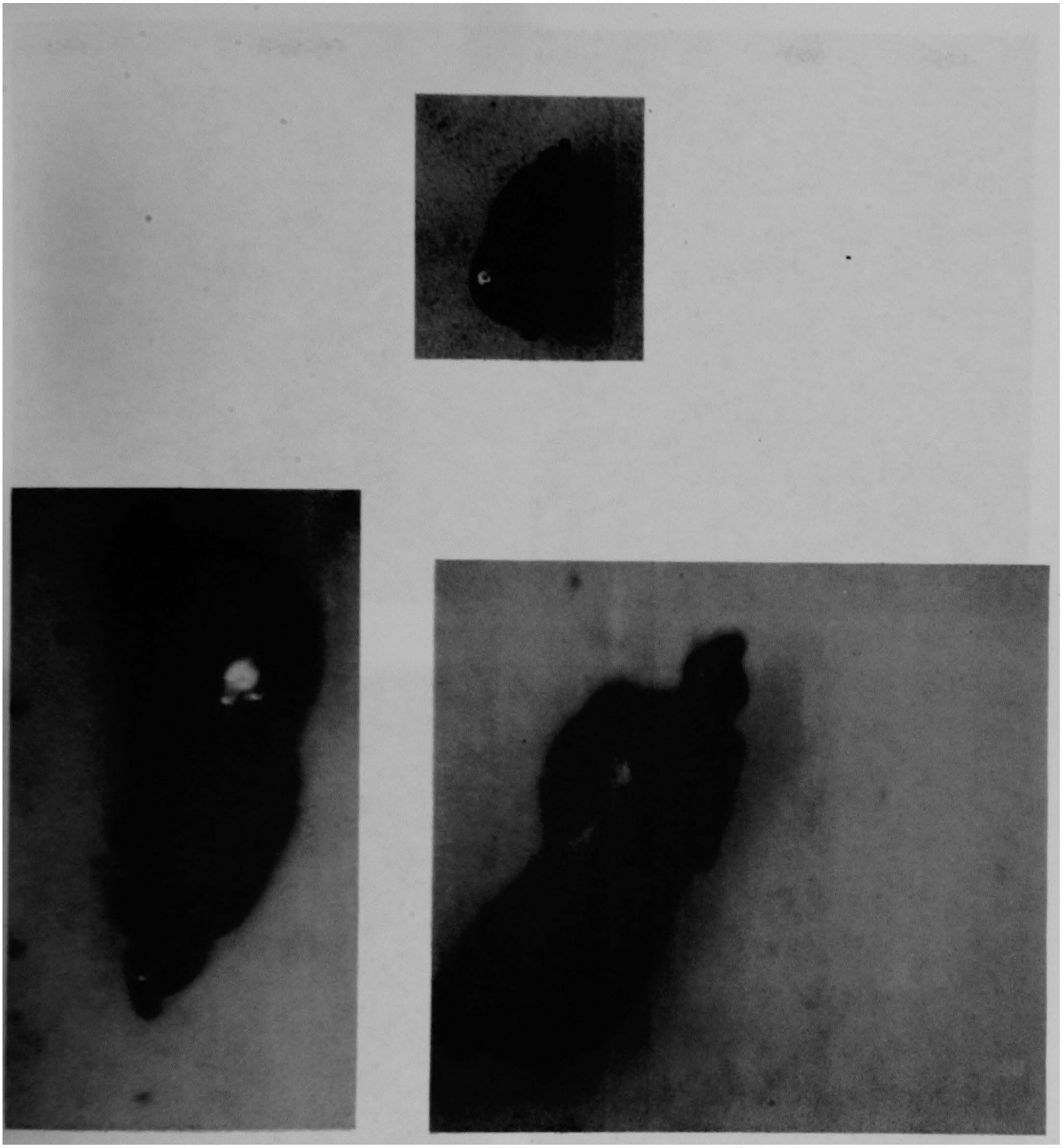

Figure B-4. Sample 4 Photographic Survey Results.
(Color Photographs are 19X).

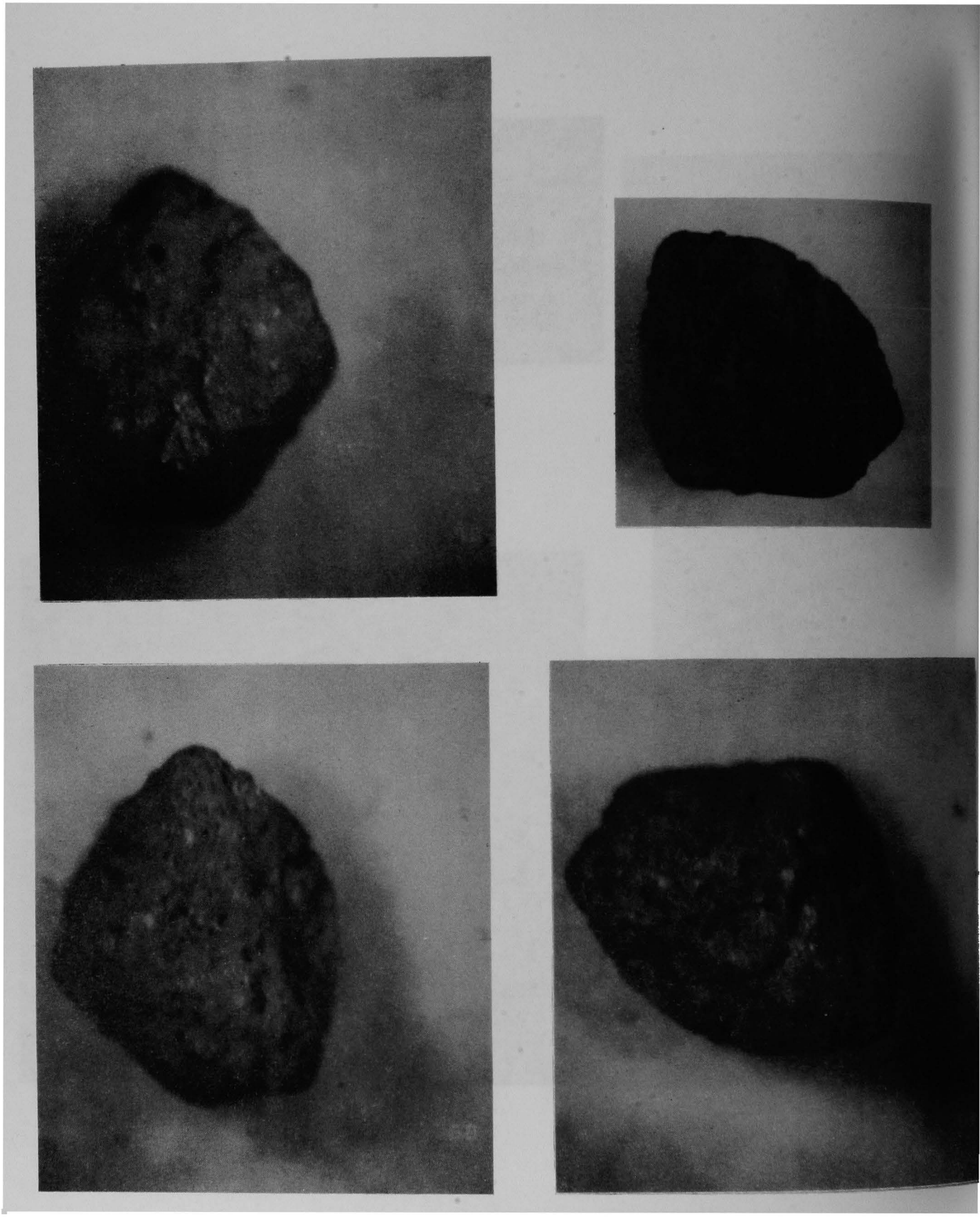

Figure B-5. Sample 5 Photographic Survey Results.

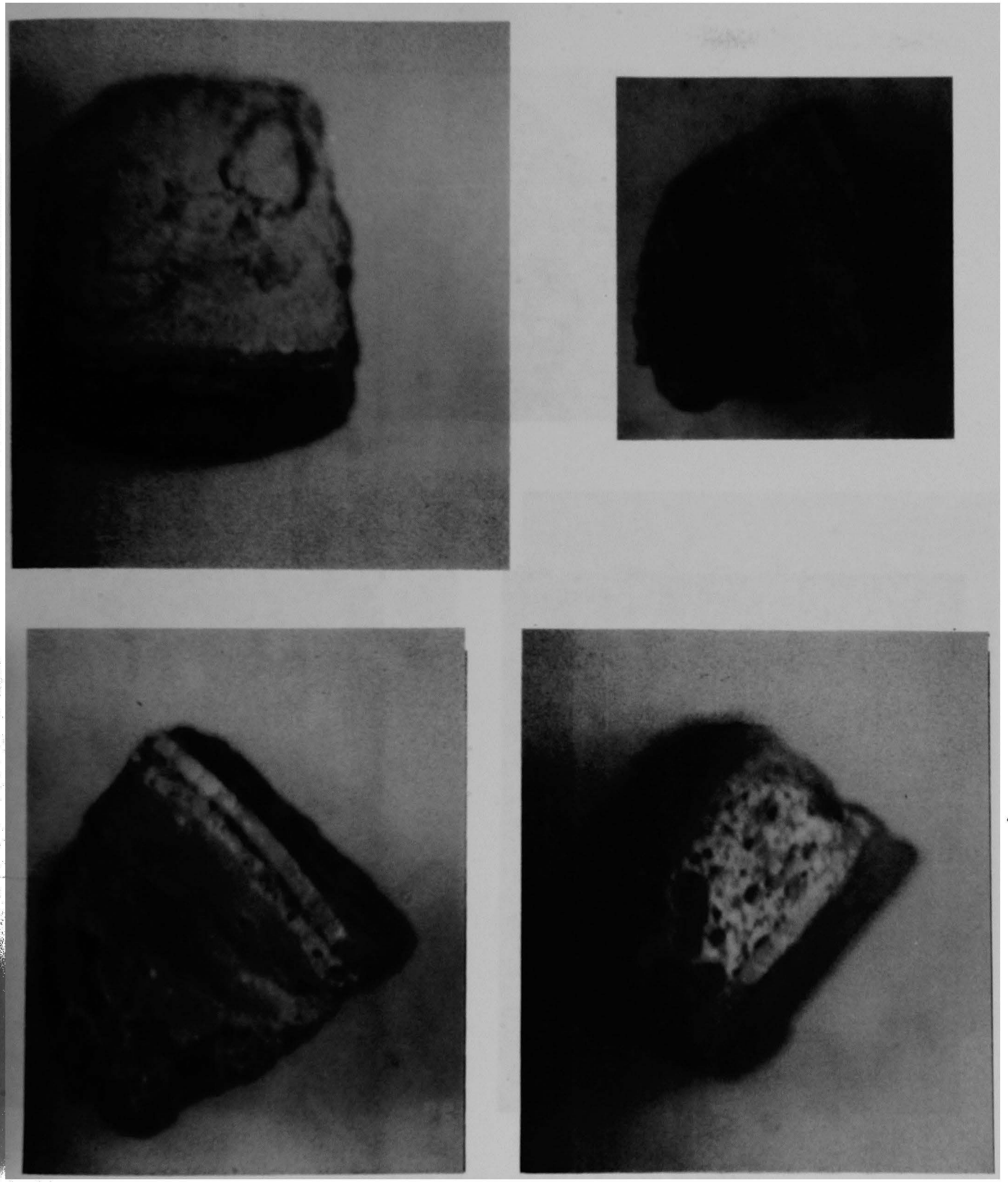

Figure B-6. Sample 6 Photographic Survey Results.

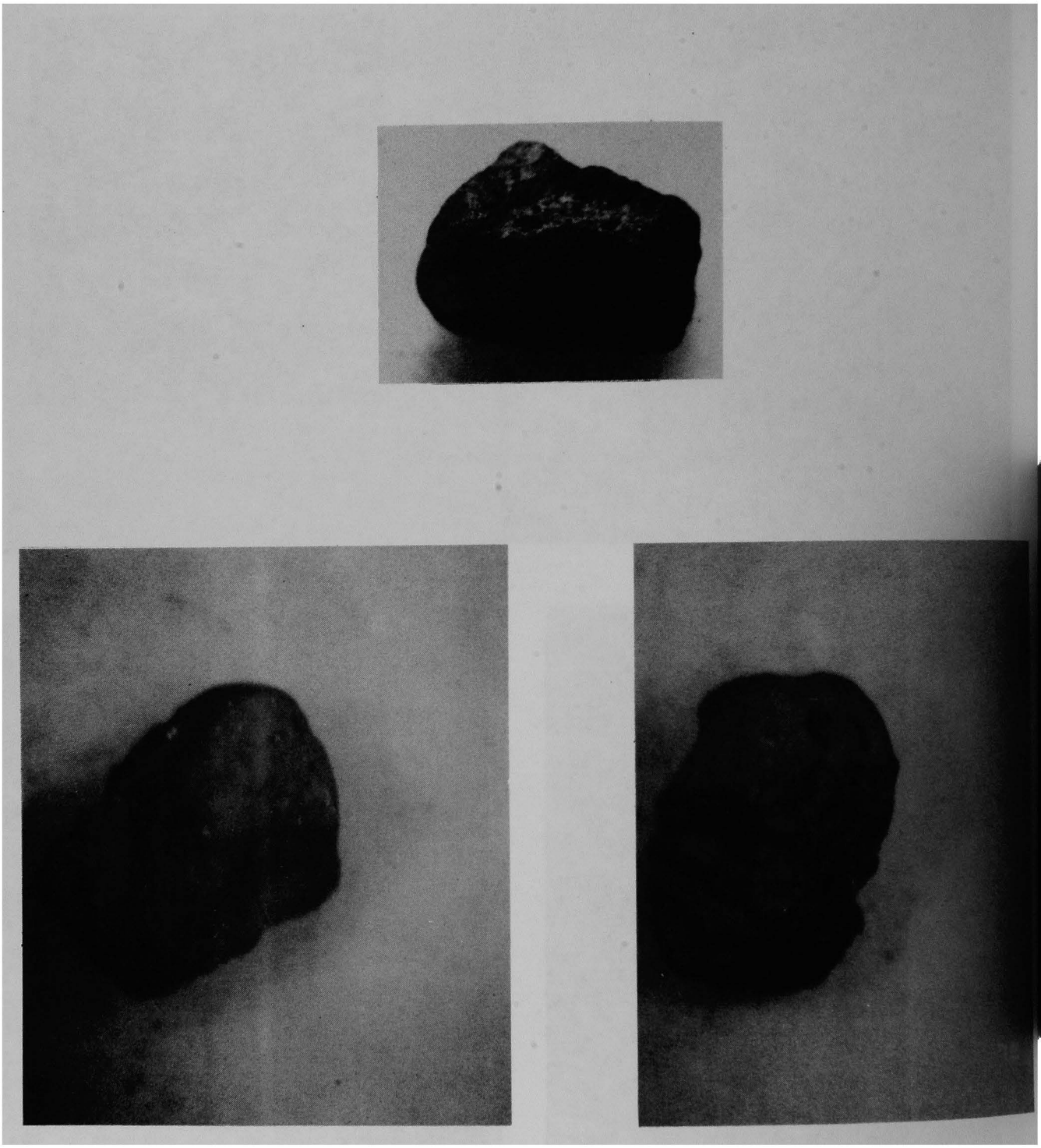

Figure B-7. Sample 7 Photographic Survey Results.

Figure B-8. Sample 8 Photographic Survey Results.

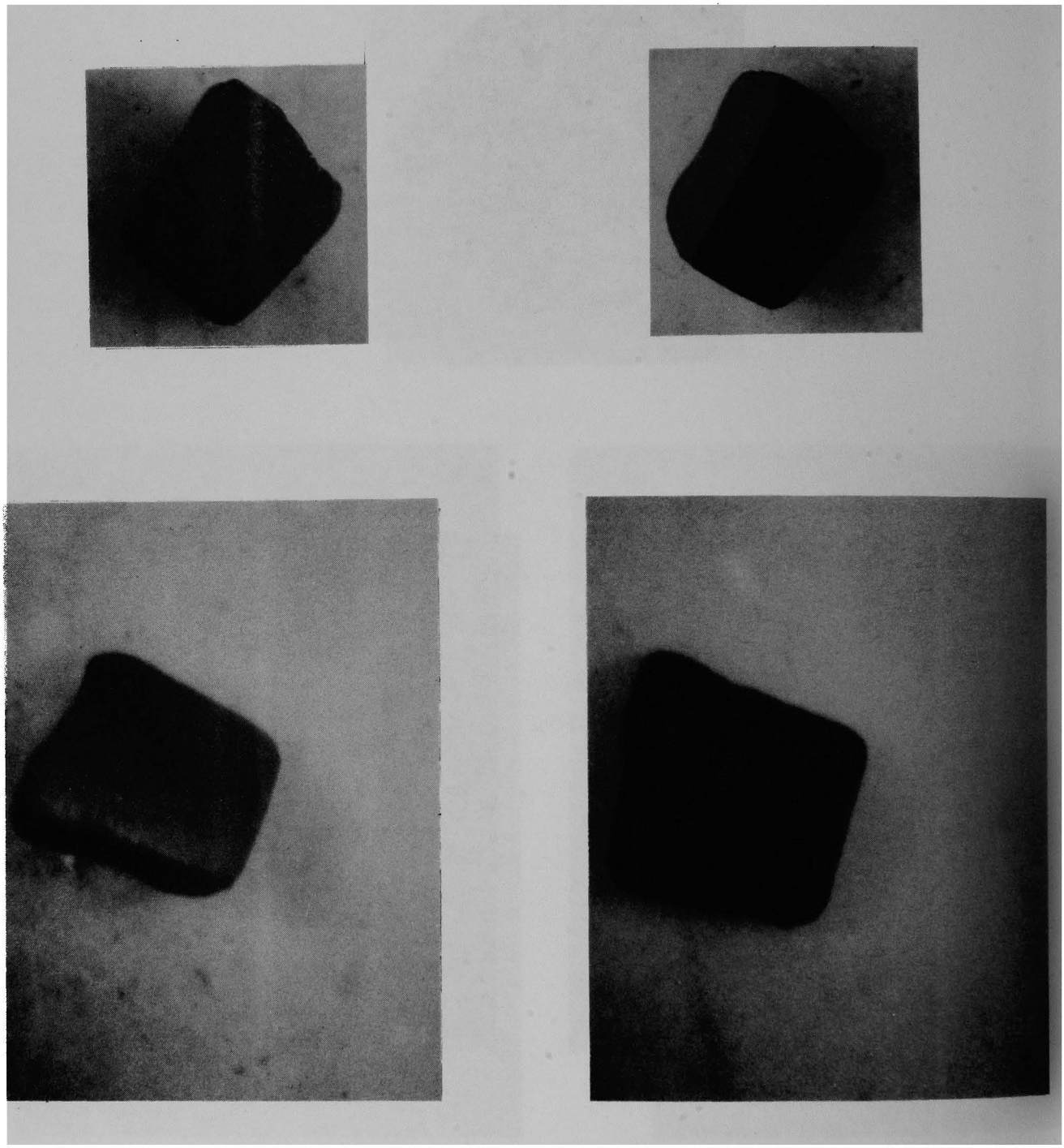

Figure B-9. Sample 9 Photographic Survey Results.

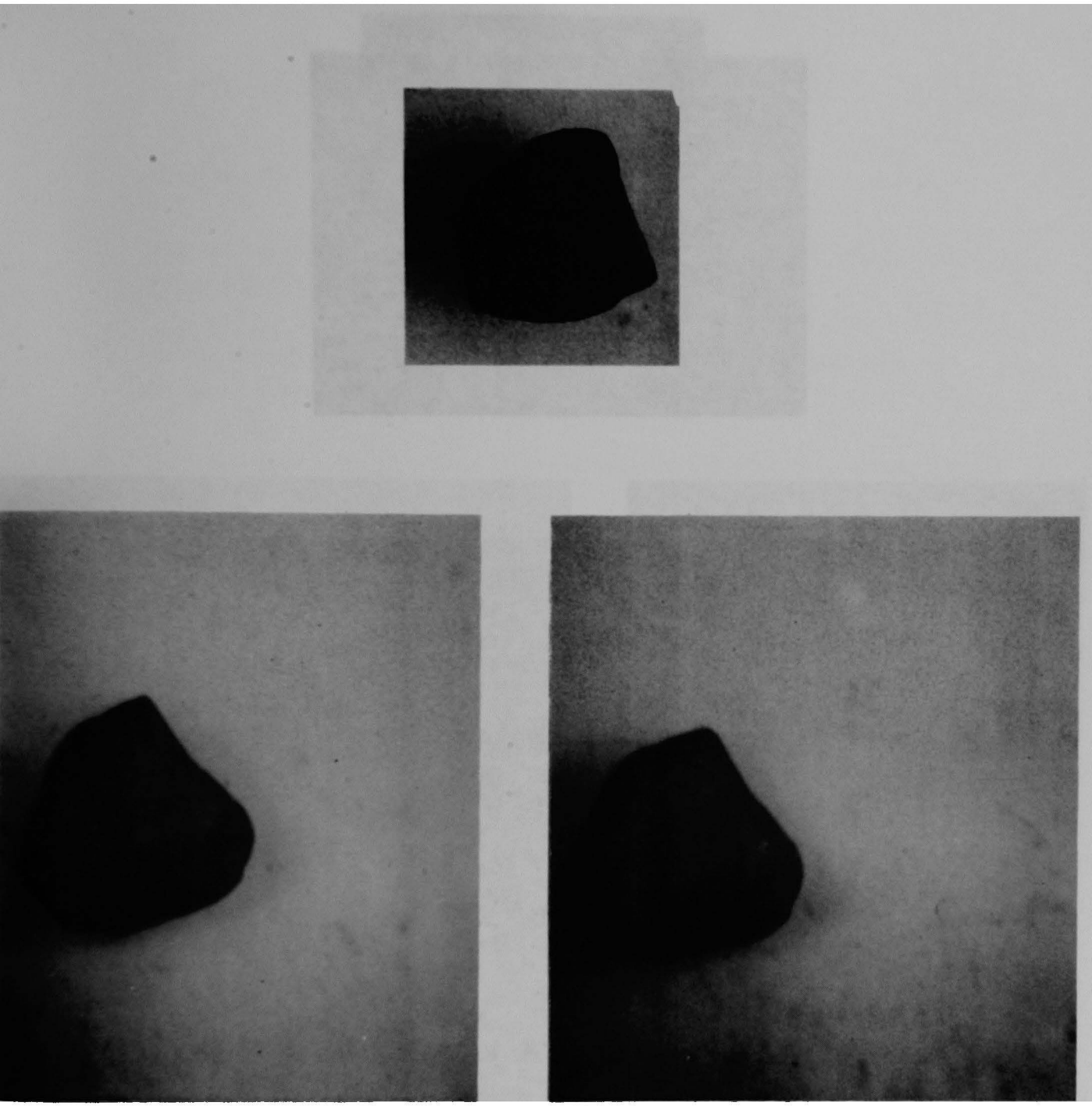

Figure B-10. Sample 10 Photographic Survey Results.

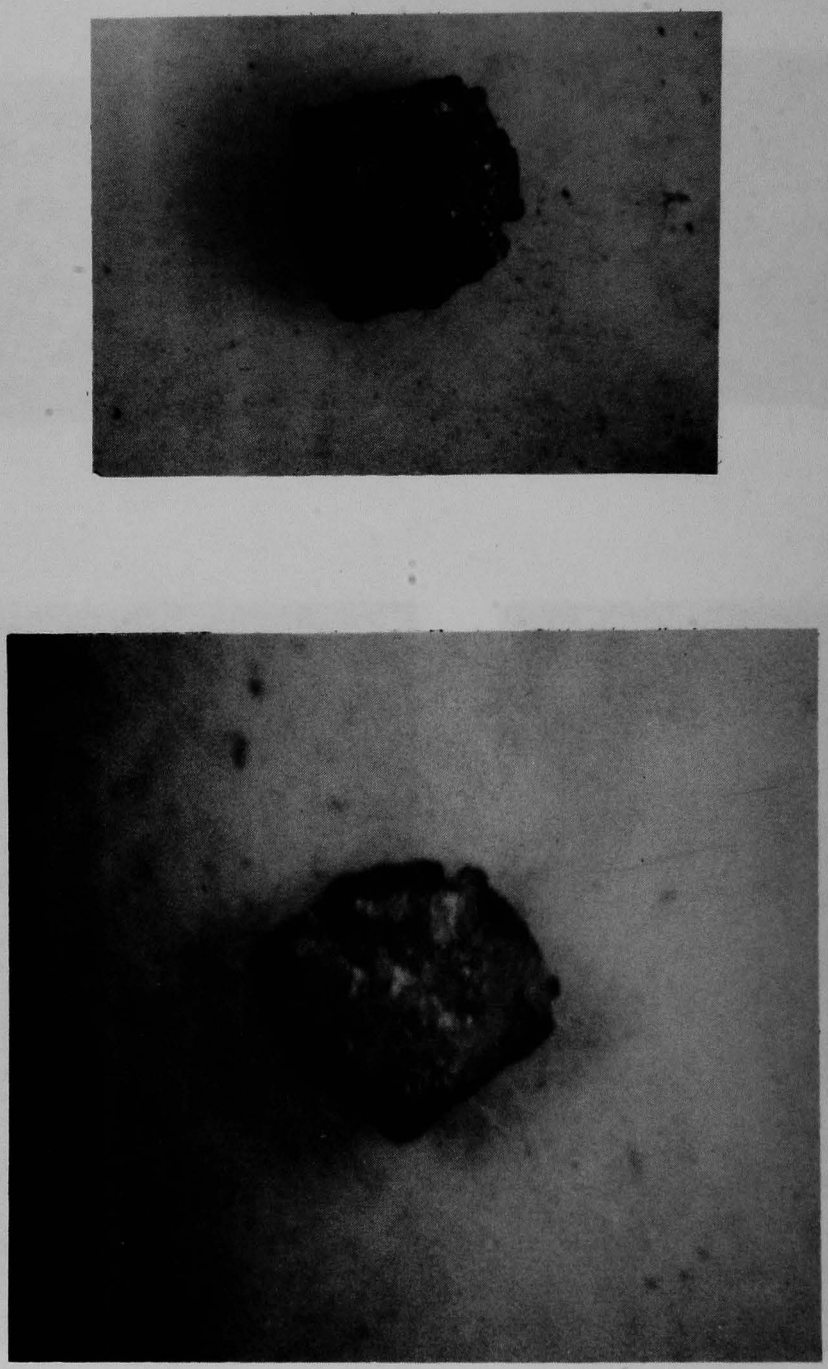

Fibure B-11. Sample 11 Photographic Survey Results.

Figure B-12. Sample 12 Photographic Survey Results.

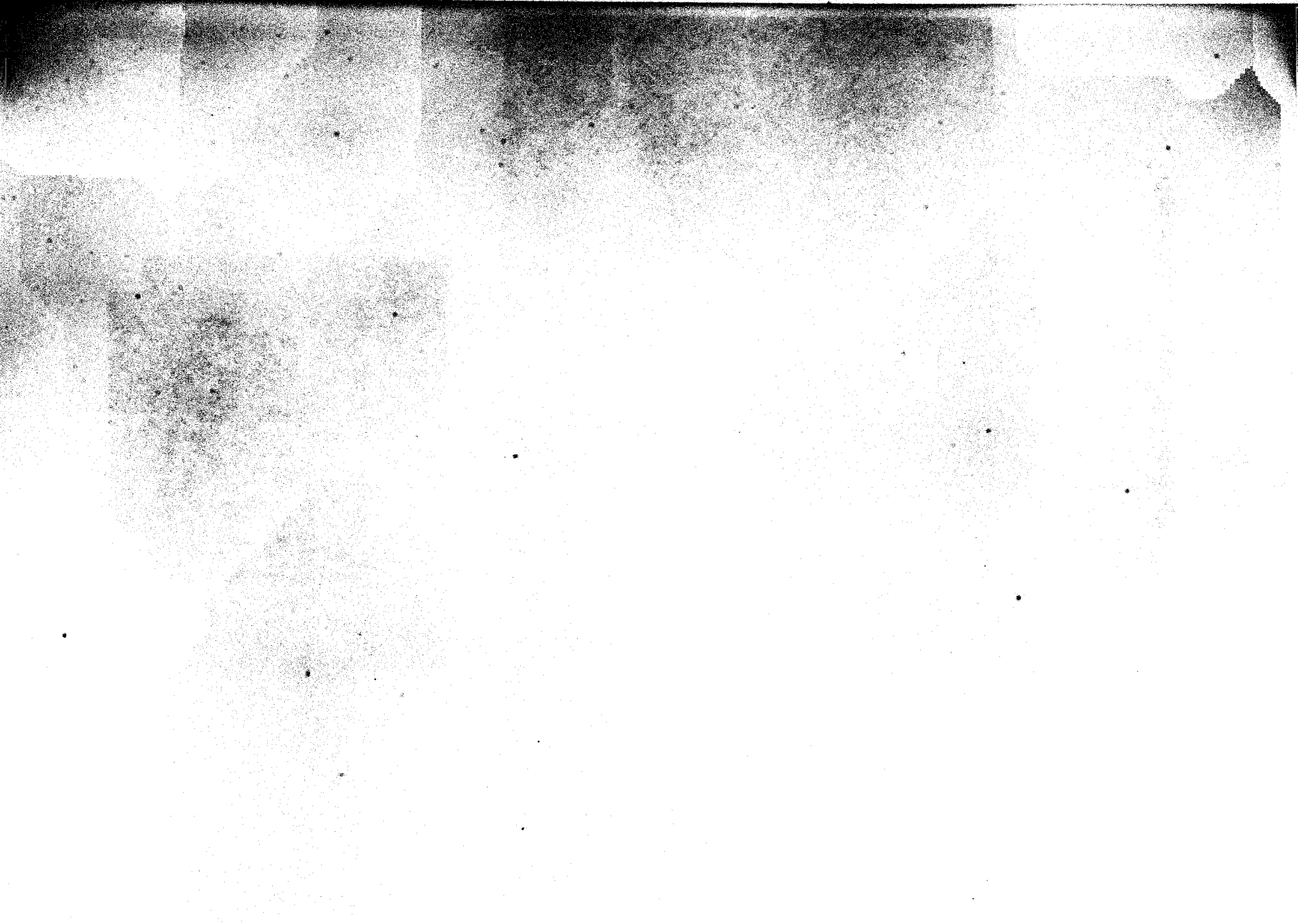

APPENDIX C

SAMPLE SECTIONING, MOUNTING AND POLISHING PROCEDURAL OUTLINE

1. Mount sample in cup of graphite holder using molten methyl methacrylate.

2. Section sample in graphite holder in proper orientation using a slow speed diamond saw.

3. Remove methyl methacrylate from sample by immersion in acetone in ultrasonic cleaner.

4. Glue particle (cut side down) to the cup in the copper mounting jacket (see sketch).

5. Assemble jacket bottom (containing cup), remainder of copper jacket with aluminum outer body.

6. Seal mounting press ram below sample with silicon rubber insert.

7. Pour molten Pb, Sn, Bi alloy into sample body. Ensure level is above sample body and allow to solidify.

8. Place second rubber insert above sample and close mounting press.

9. Apply heat and melt metal alloy. Apply pressure to mounting press and hold for 30 minutes. Allow press and sample to cool for 1 hour.

10. Remove specimen mount from press and grind through thin area on bottom of mount into cup using 60 grit SiC paper.

11. Grind specimen on 180, 240, 400, and 600 grit SiC papers using demineralized water.

12. Polish specimen using Syntron polisher with demineralized water in following sequence:

    a. Nylon cloth and 1.0 μ Al_2O_3 powder
    b. Nylon cloth and 0.3 μ Al_2O_3 powder
    c. Micro cloth and 0.05 μ Al_2O_3 powder

    Polish with each slurry for 3-4 hours.

13. Rinse specimen in demineralized water and cotton swab. Rinse with ethanol and blow dry.

14. Perform optical metallography.

15. Remove outer aluminum jacket and perform SEM/EDS examination.

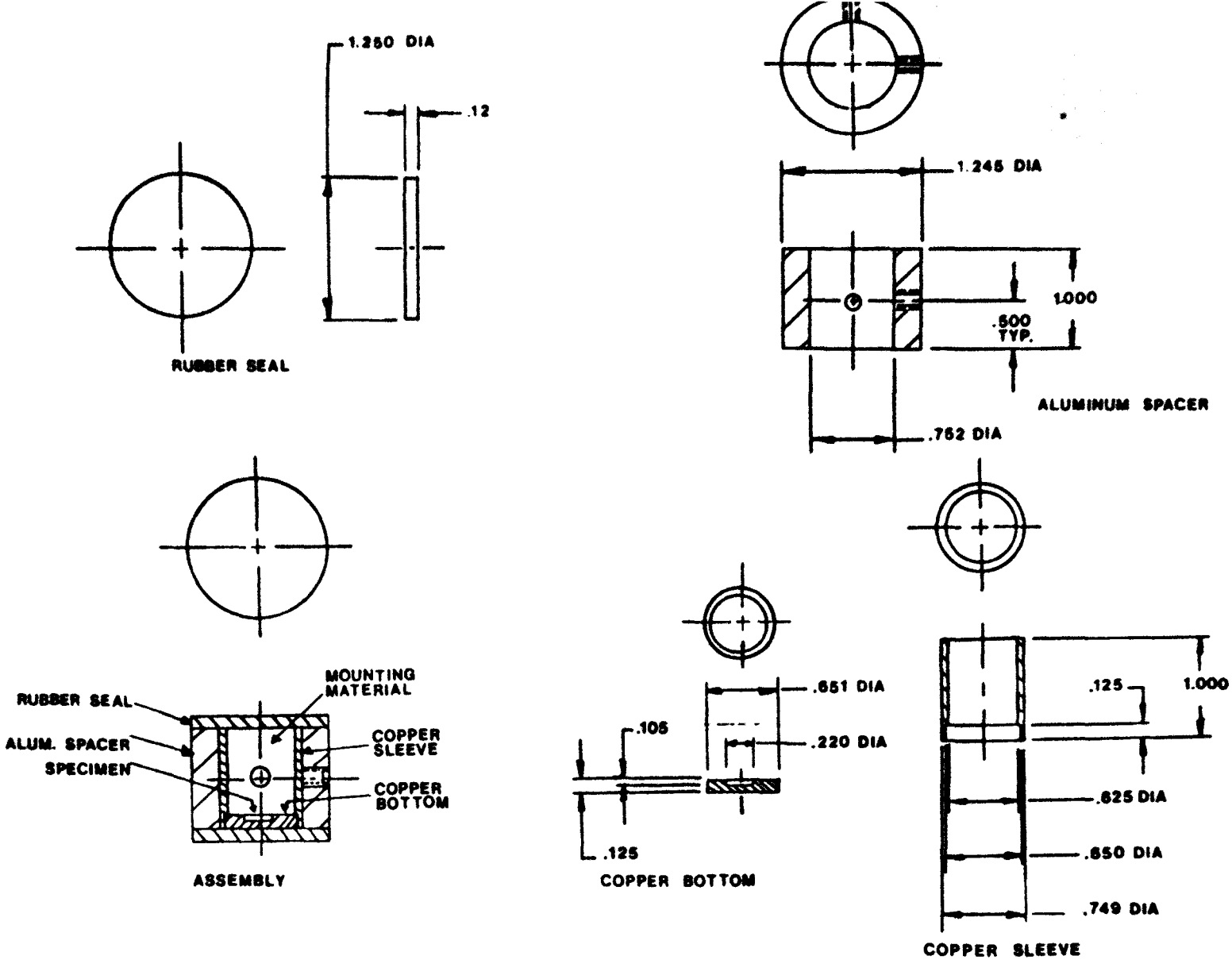

Figure C-1. Sketch of the specimen mount.

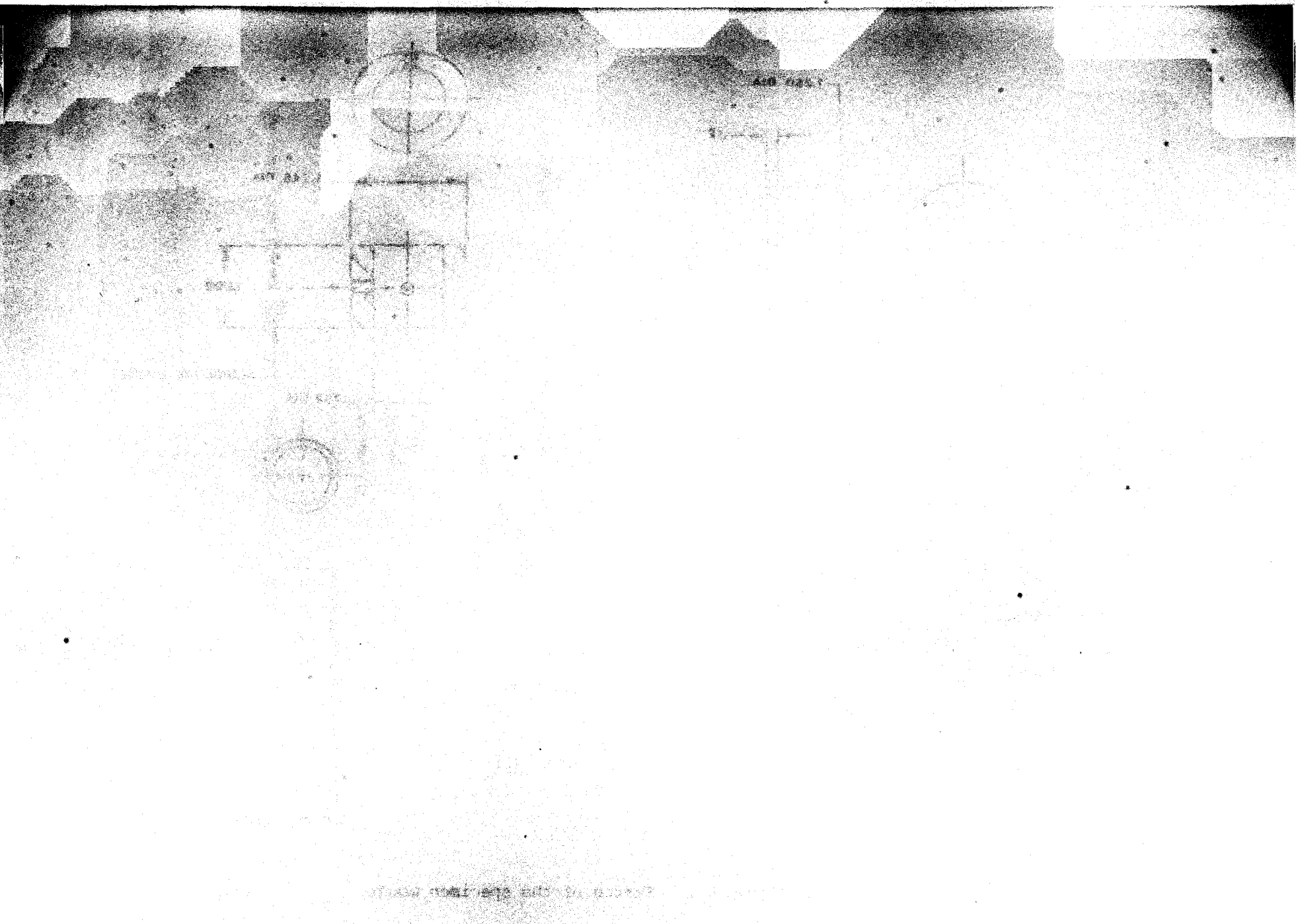

APPENDIX D

OPTICAL PHOTOMICROGRAPHS, SEM PHOTOGRAPHS, DOT MAPS, AND EDS SPECTRA

50X

Figure D-1. As polished optical photomicrograph of particle 1. Areas 1 and 2 examined in detail.

F539 Area 1 200X

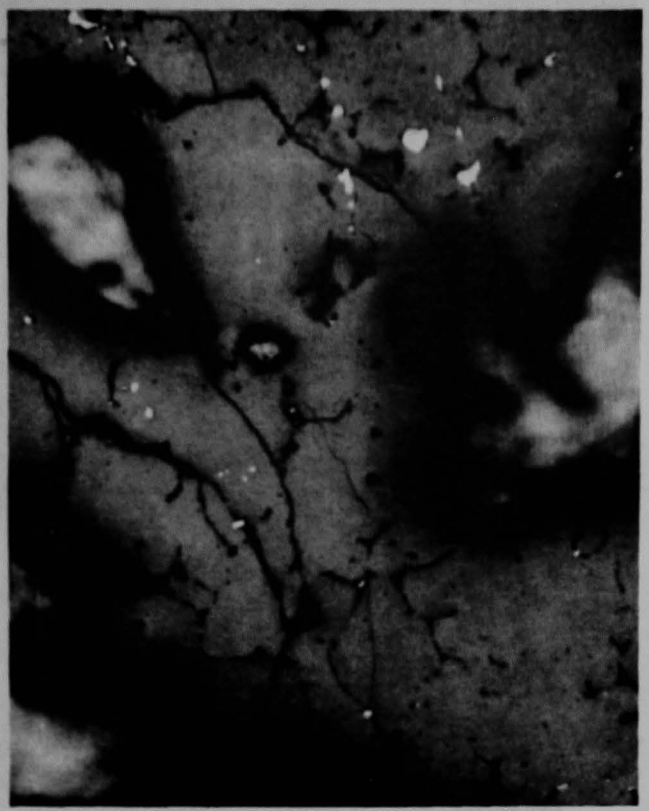

F540 Area 1 400X

F542 Area 2 200X

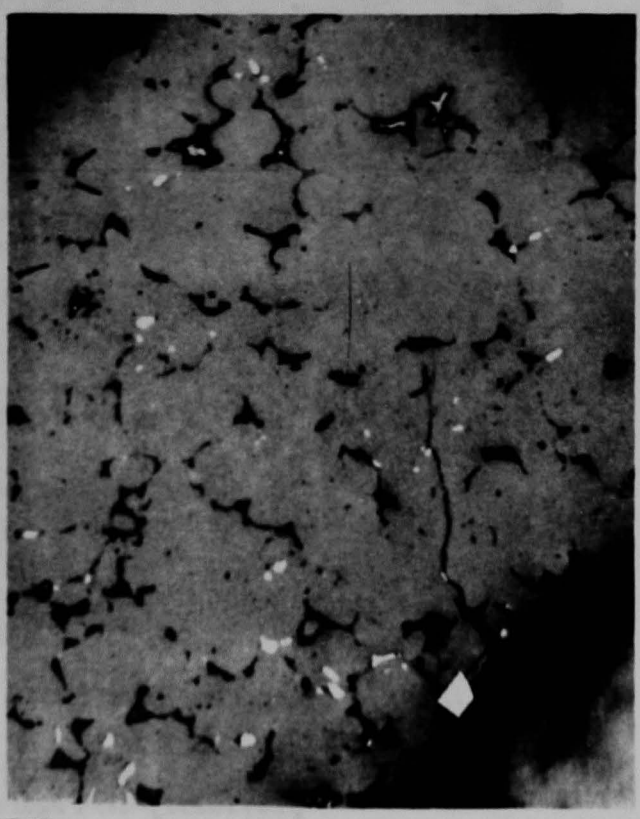

F543 Area 2 400X

Figure D-2. As polished high magnification optical photomicrographs of Areas 1 and 2 as noted in Figure D-1.

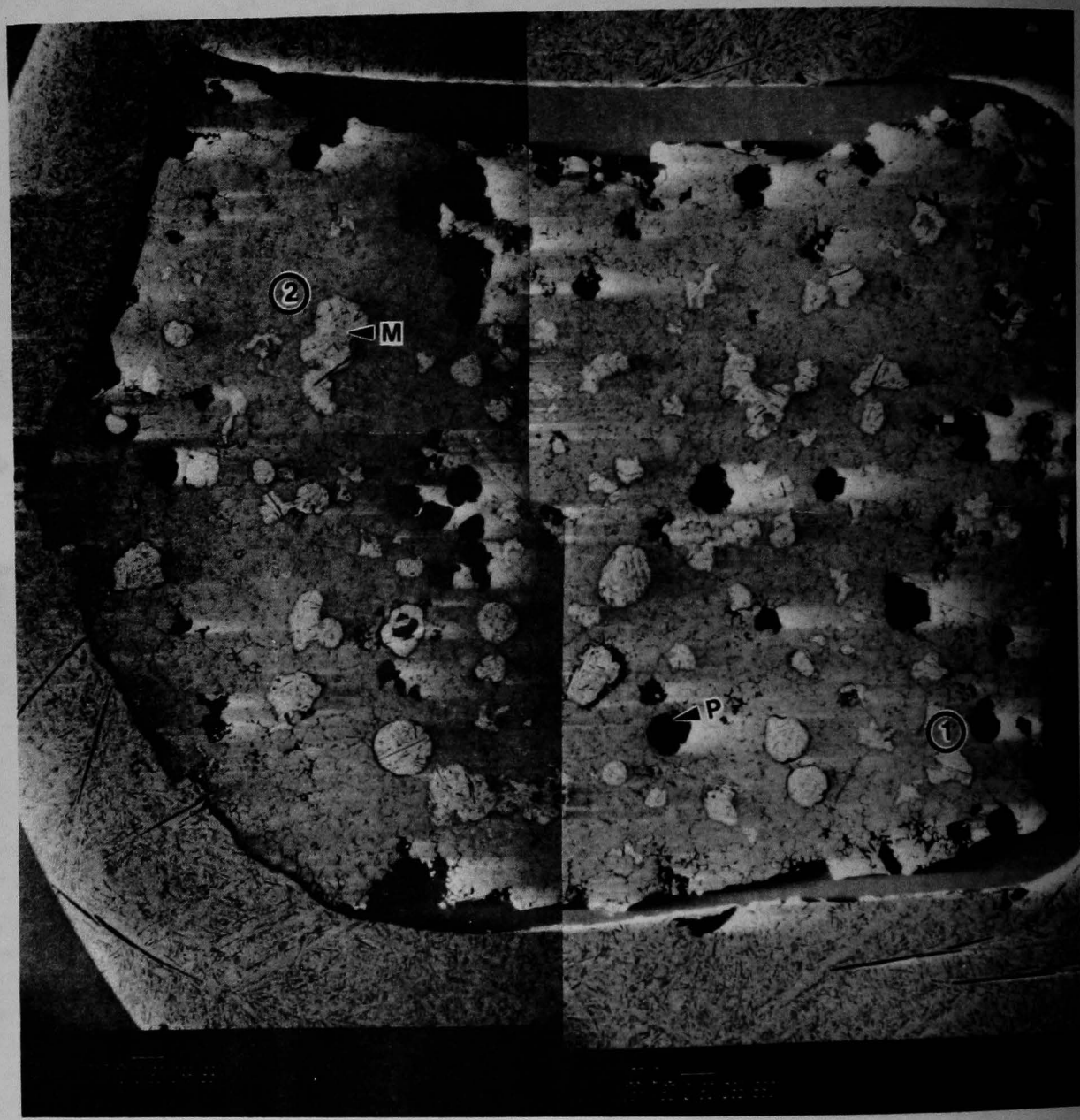

Figure D-3. BSE/SEM photo of particle 1. Areas 1 and 2 are those noted previously in Figures D-1 and D-2. Light areas adjacent to pores are artifacts caused by pore edges.

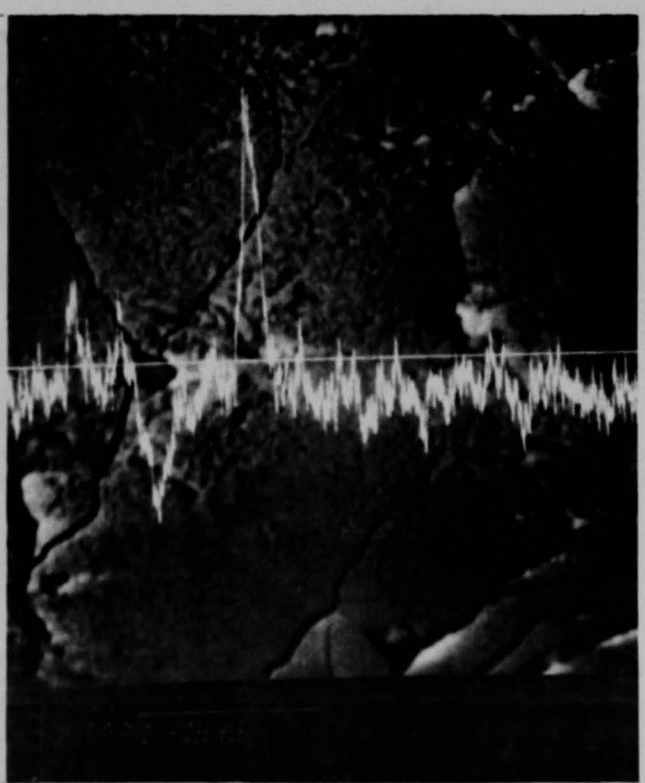

BSE/oxygen profile of area
near point 1 in photo 035 854.

Figure D-4. BSE/SEM Photos of Area 1.

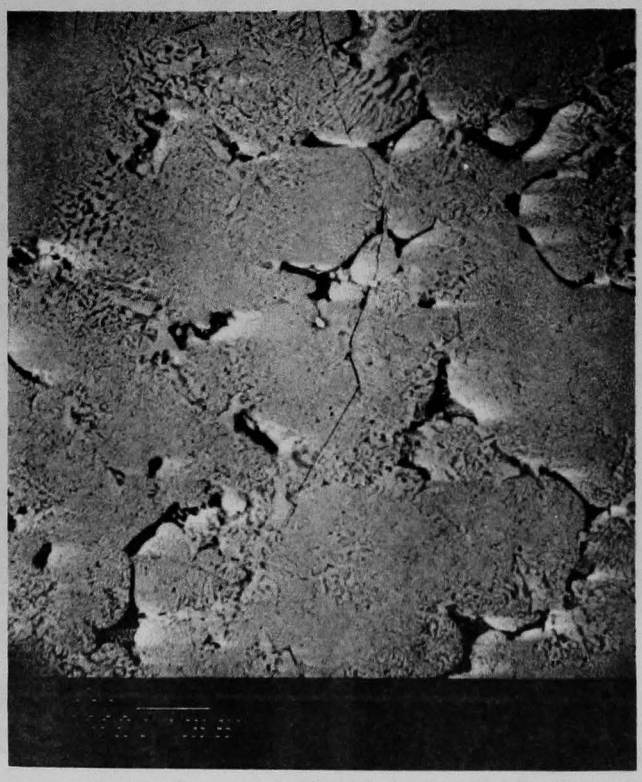

Figure D-5. BSE/SEM Photos of Area 2.

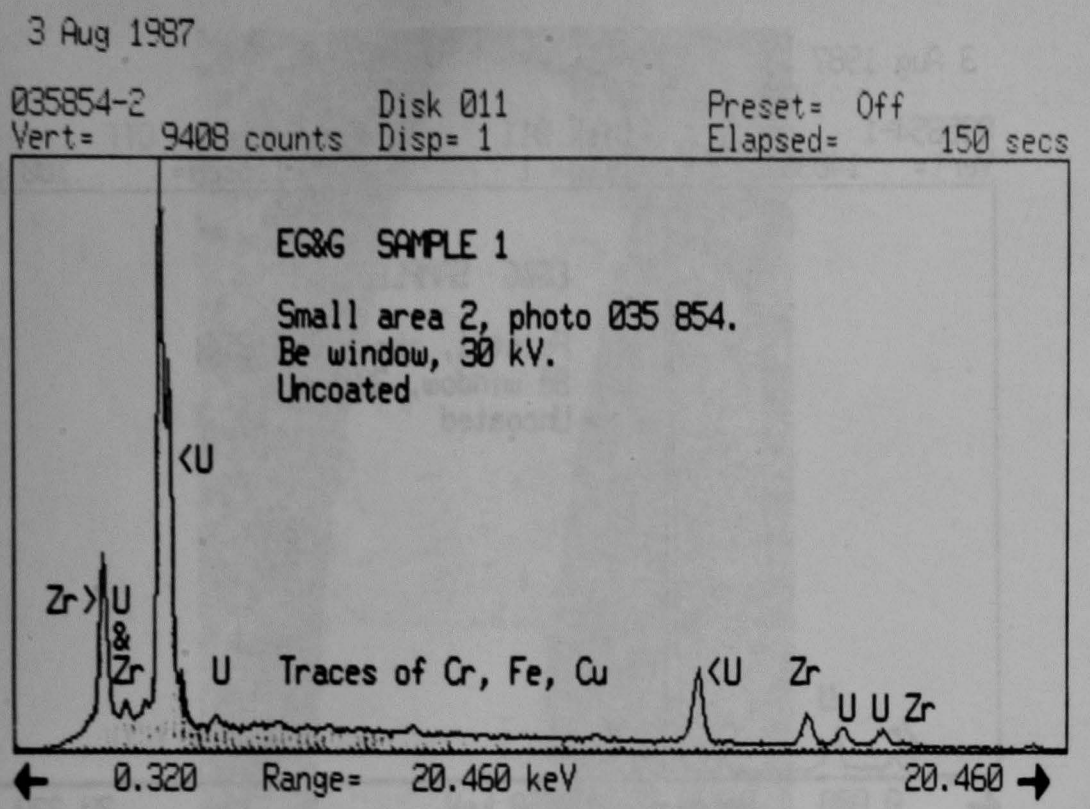

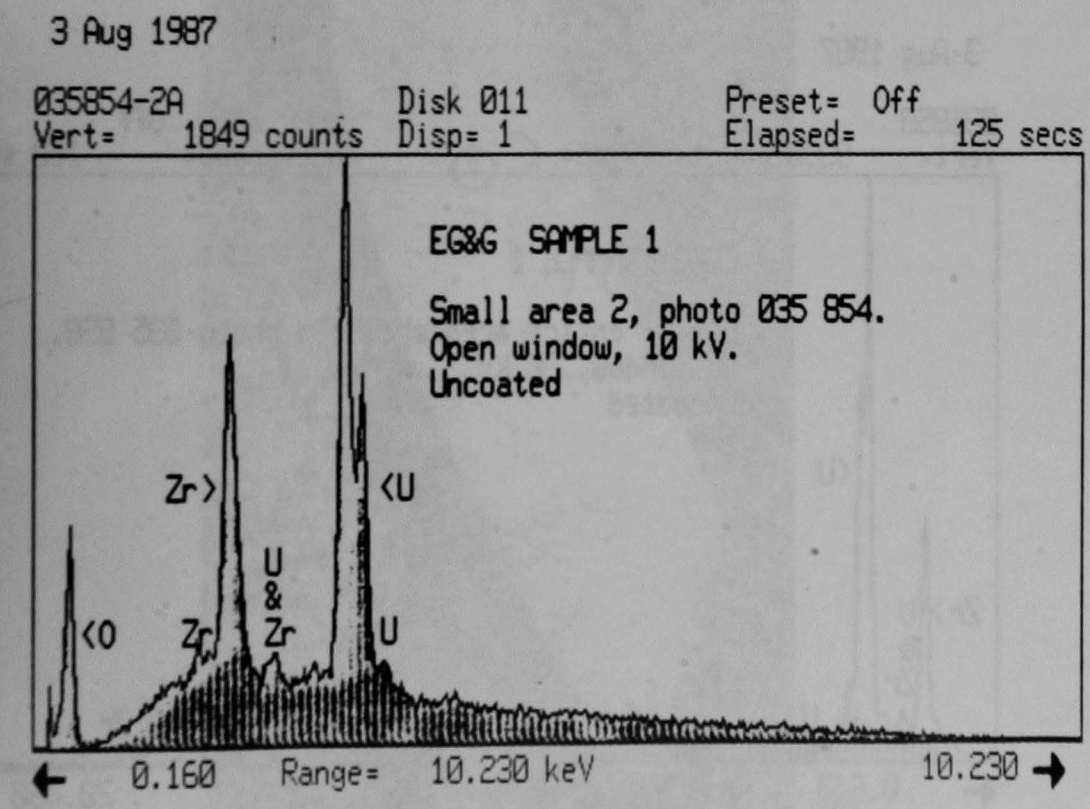

Figure D-6. EDS Spectra from Area 1.

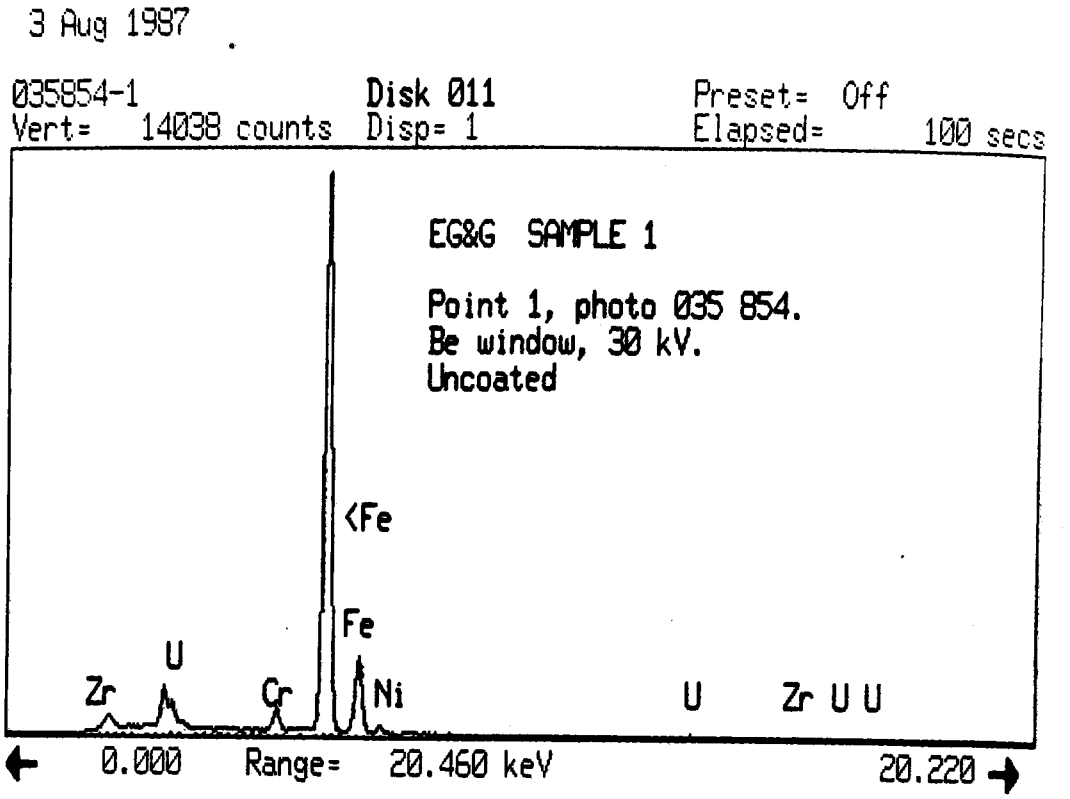

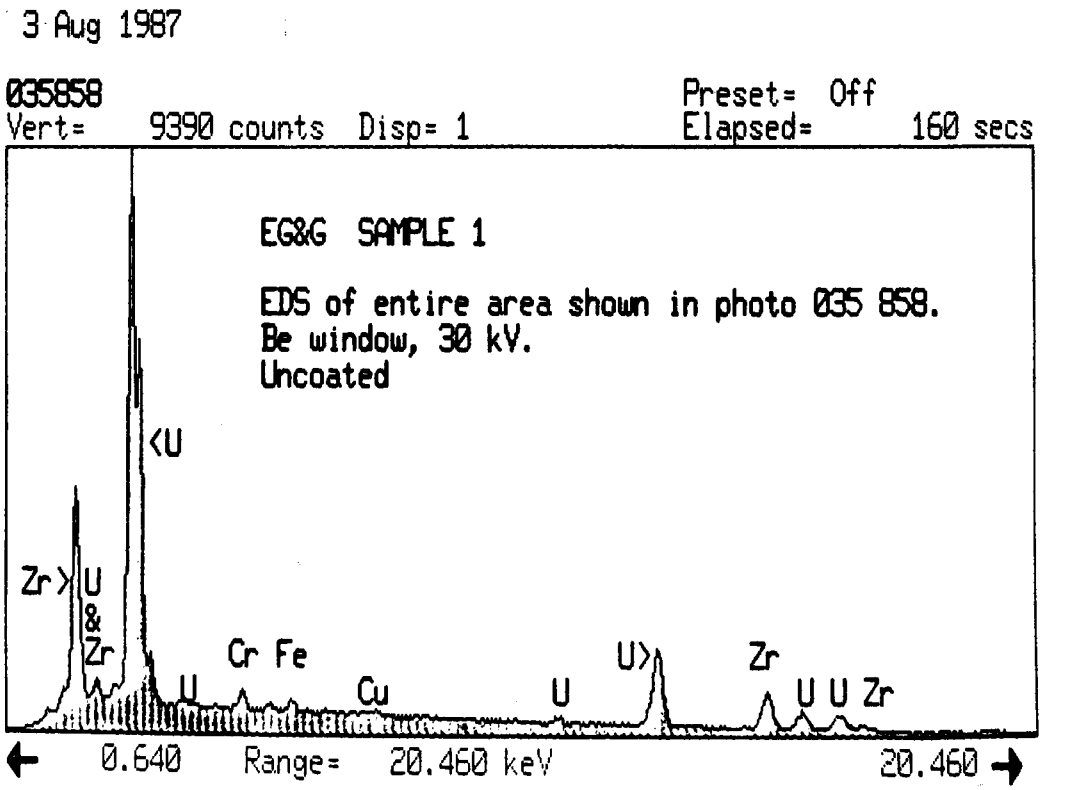

Figure D-7. EDS Spectra from Area 1 (upper) and Area 2 (lower).

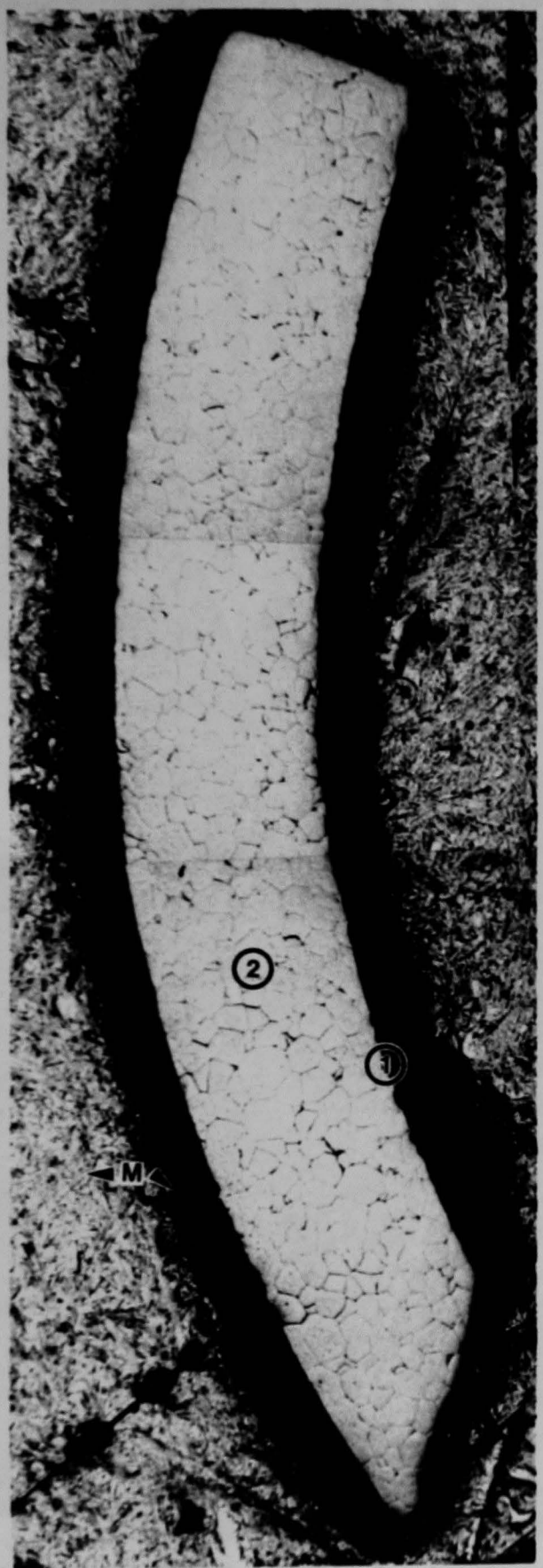

50X

Figure D-8. As polished optical photomicrograph of particle 2. Areas 1 and 2 examined in detail.

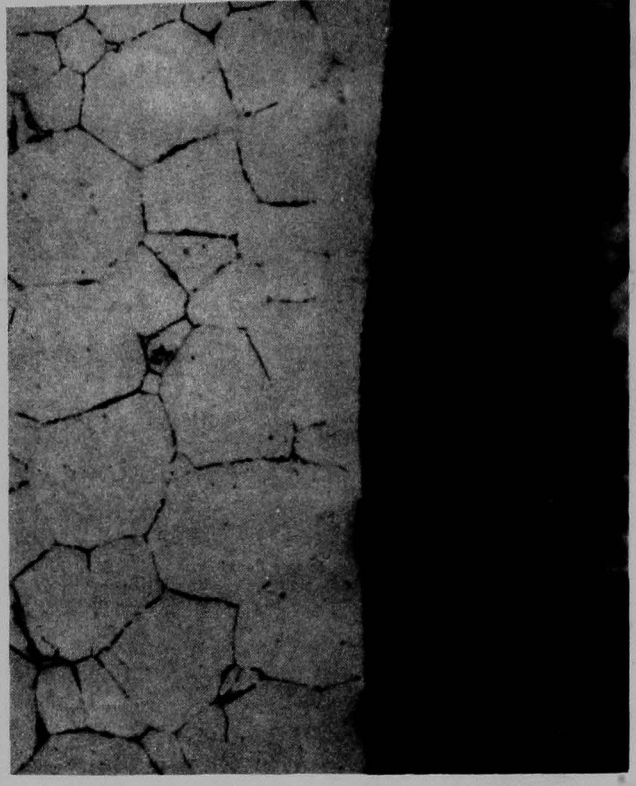

F545 Area 1 200X

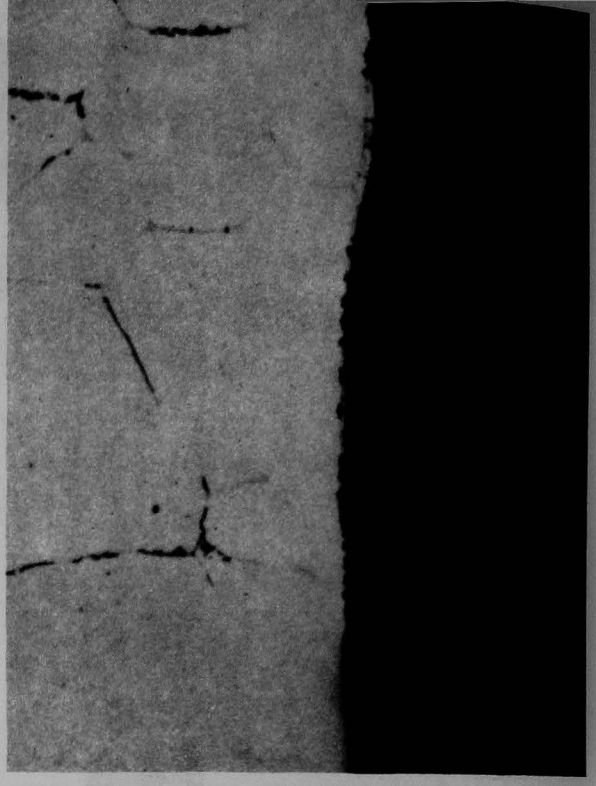

F546 Area 1 400X

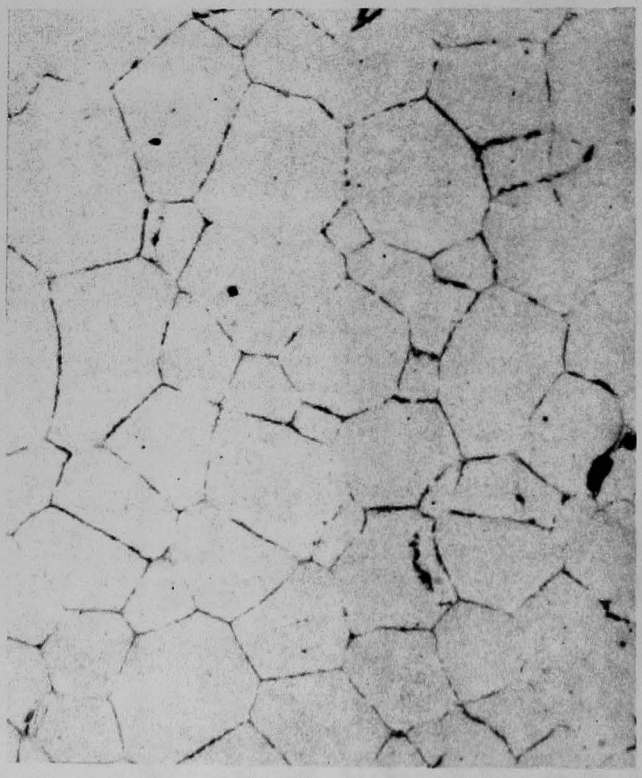

F548 Area 2 200X

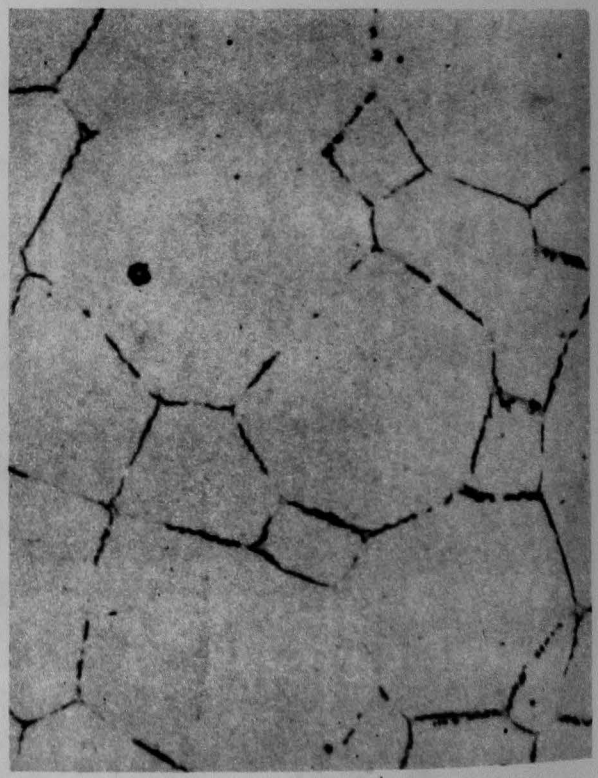

F549 Area 2 400X

Figure D-9. As polished high magnification optical photomicrographs of Areas 1 and 2 as noted in Figure 8.

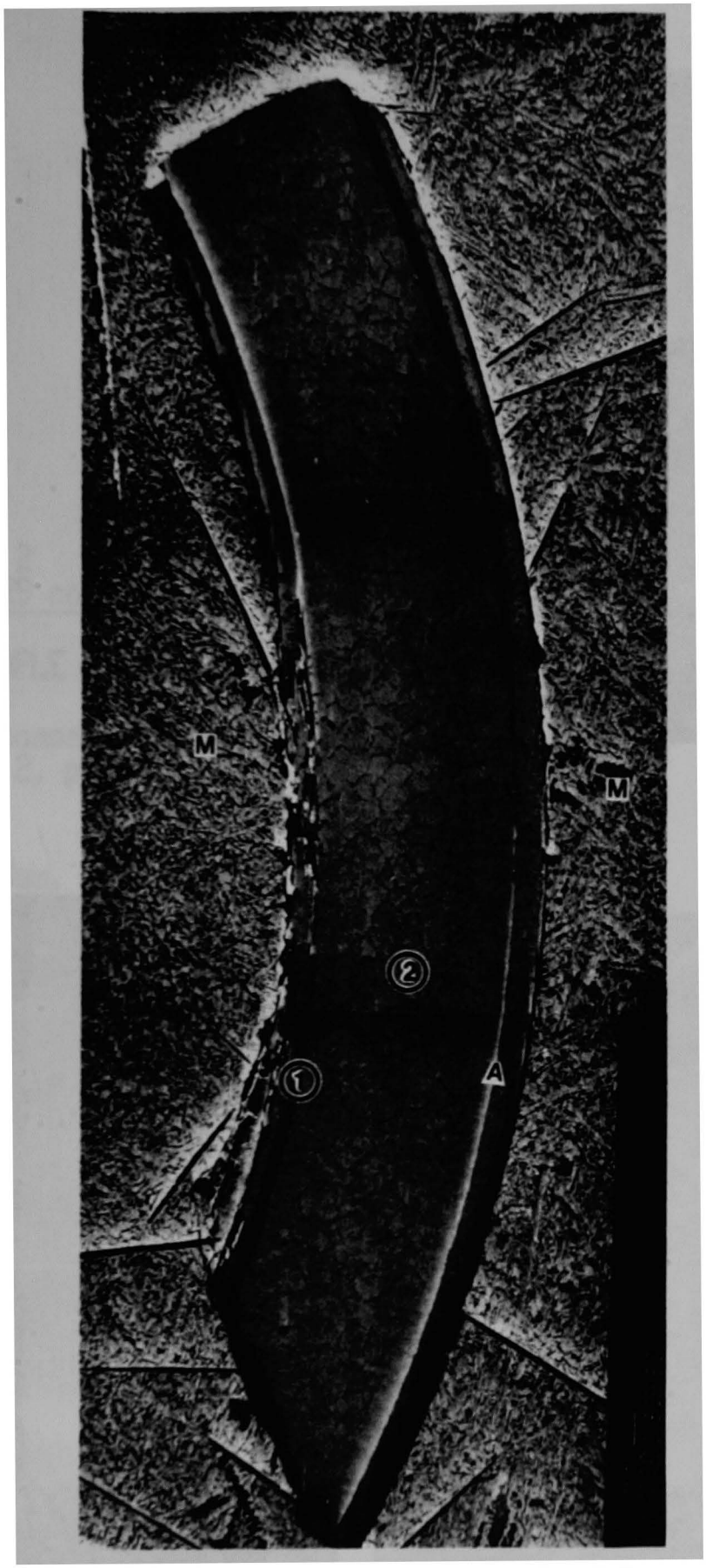

Figure D-10. BSE/SEM photo of particle 2. Areas 1 and 2 are those areas noted previously in Fig. D-8; Area A was used for EDS analysis.

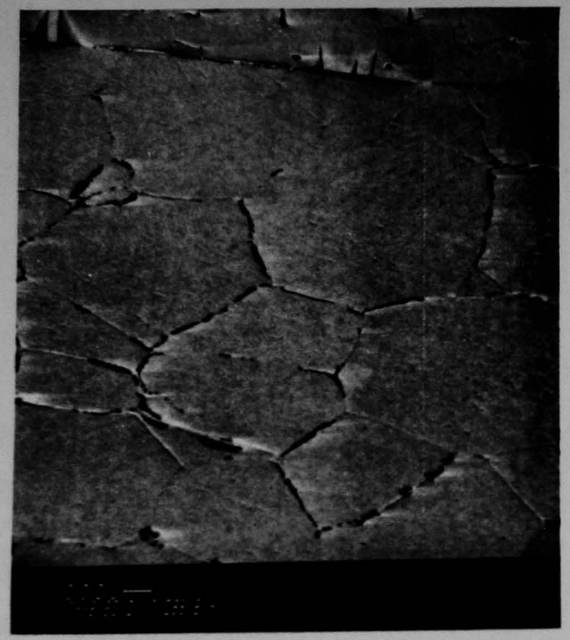

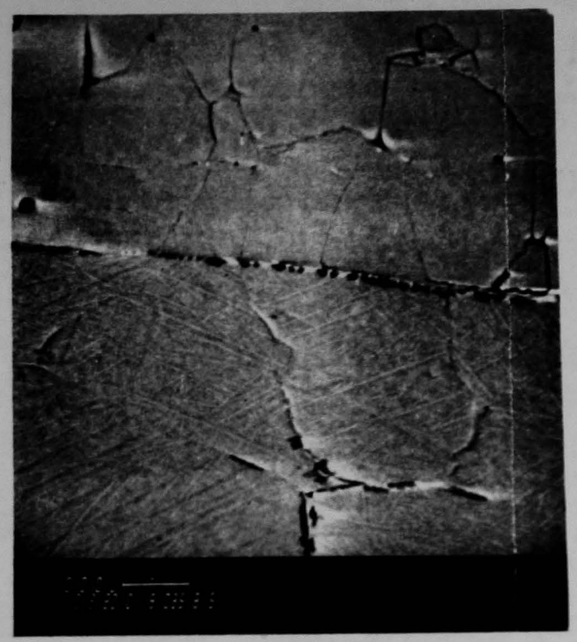

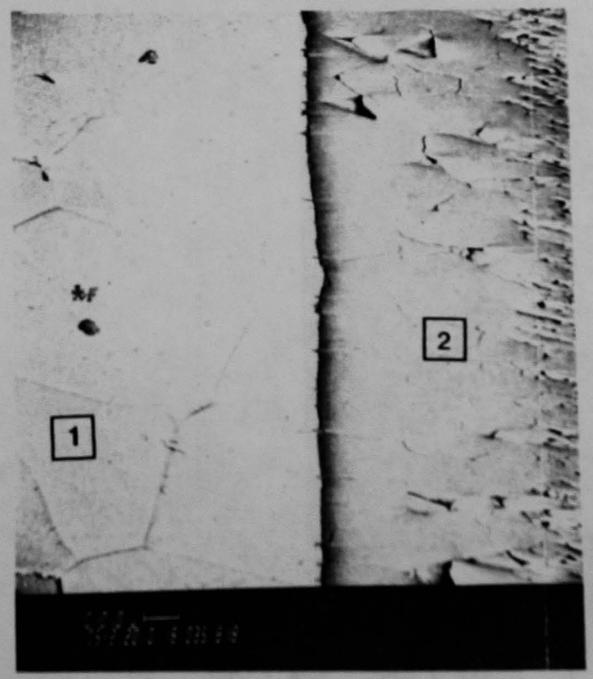

Area A as noted in Figure 10.

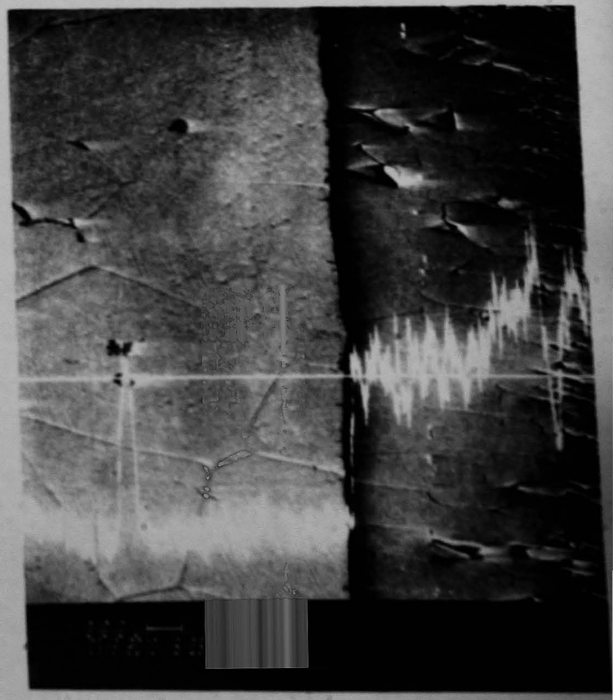

BSE/oxygen profile of 035 818, Area A.

Figure D-11. BSE/SEM photos of Area 1 (upper) and Area 2 (lower)

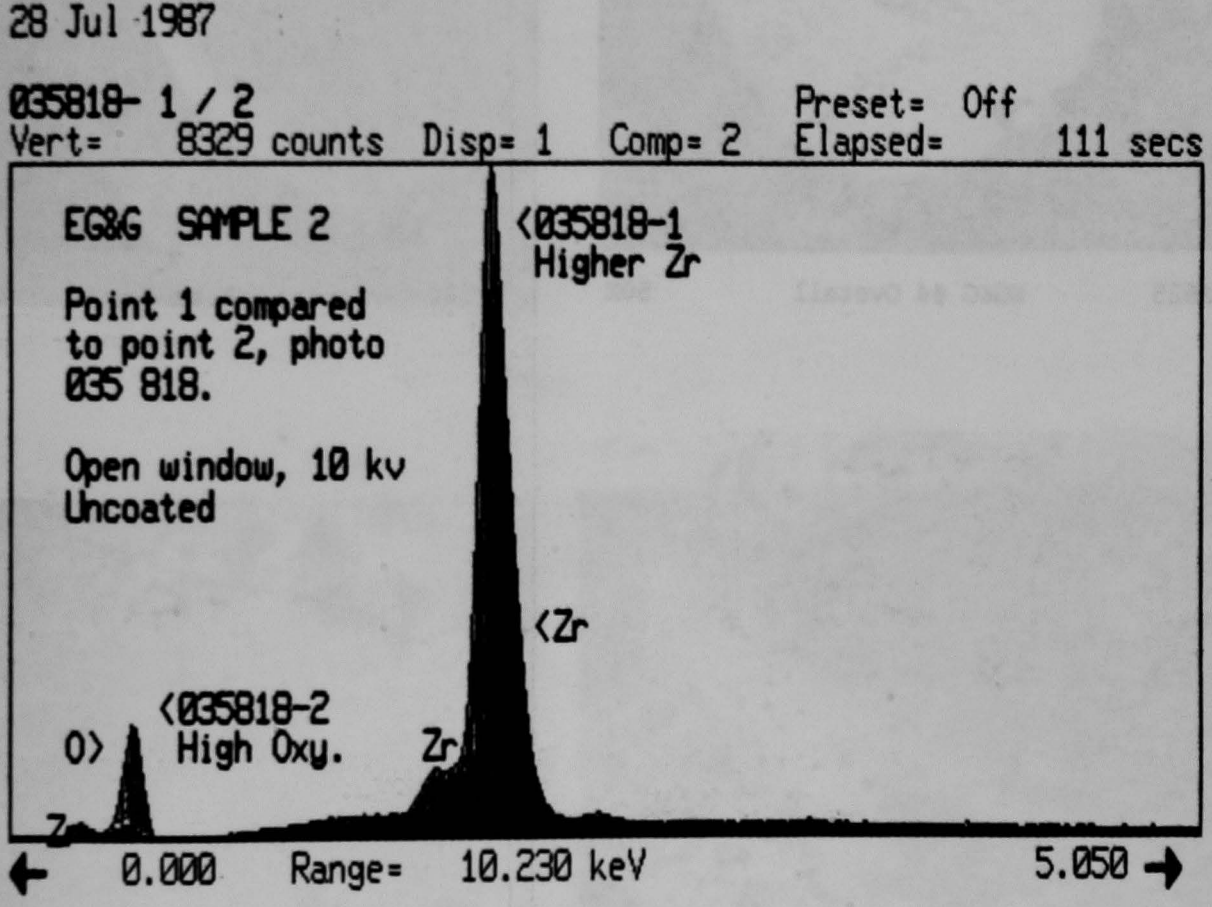

Figure D-12. EDS spectra of points 1 and 2 in photo 035 818, Figure D-11. Spectra are compared, showing higher oxygen in point 2.

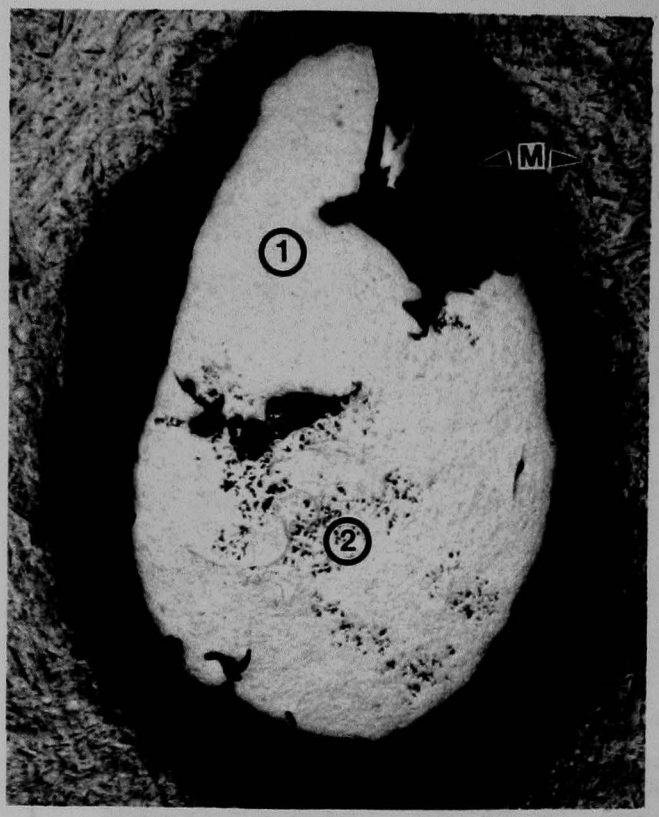

F525 EG&G #4 Overall 50X

F560 Area 1 200X

F563 Area 2 200X

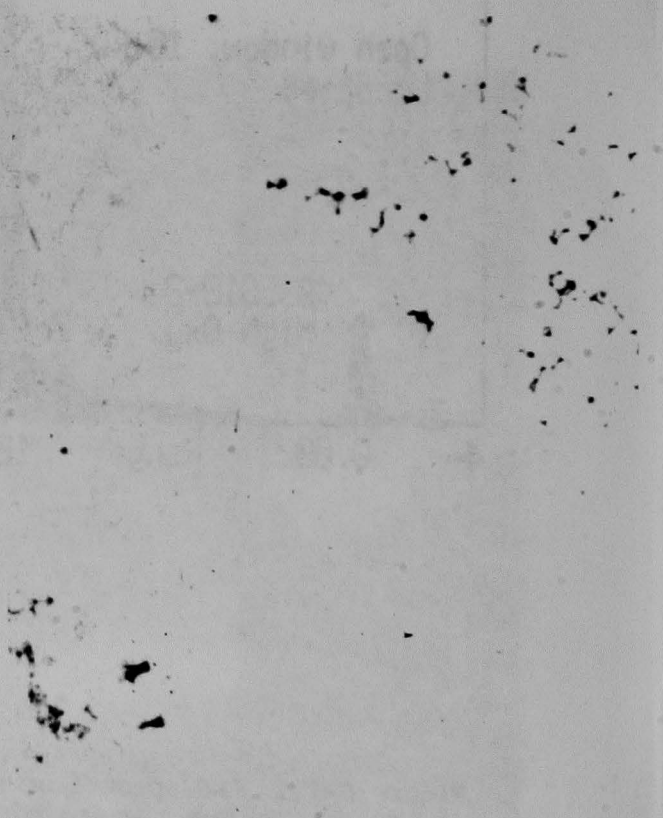

F564 Area 2 400X

Figure D-13. As polished optical photomicrographs of particle 4 with Areas 1 and 2 examined in detail.

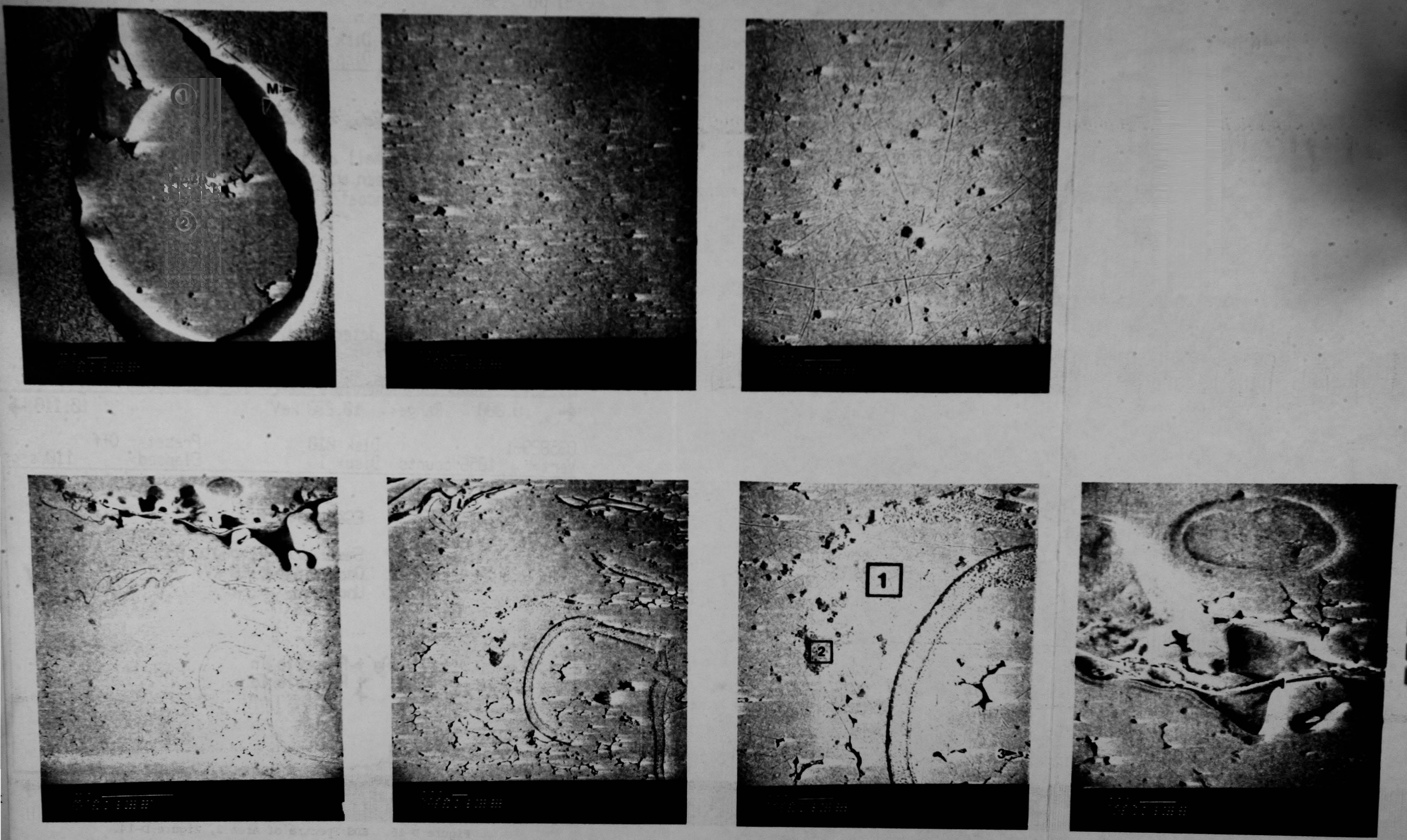

Figure D-14. BSE/SEM Photos of Area 1 (upper) and Area 2 (lower)

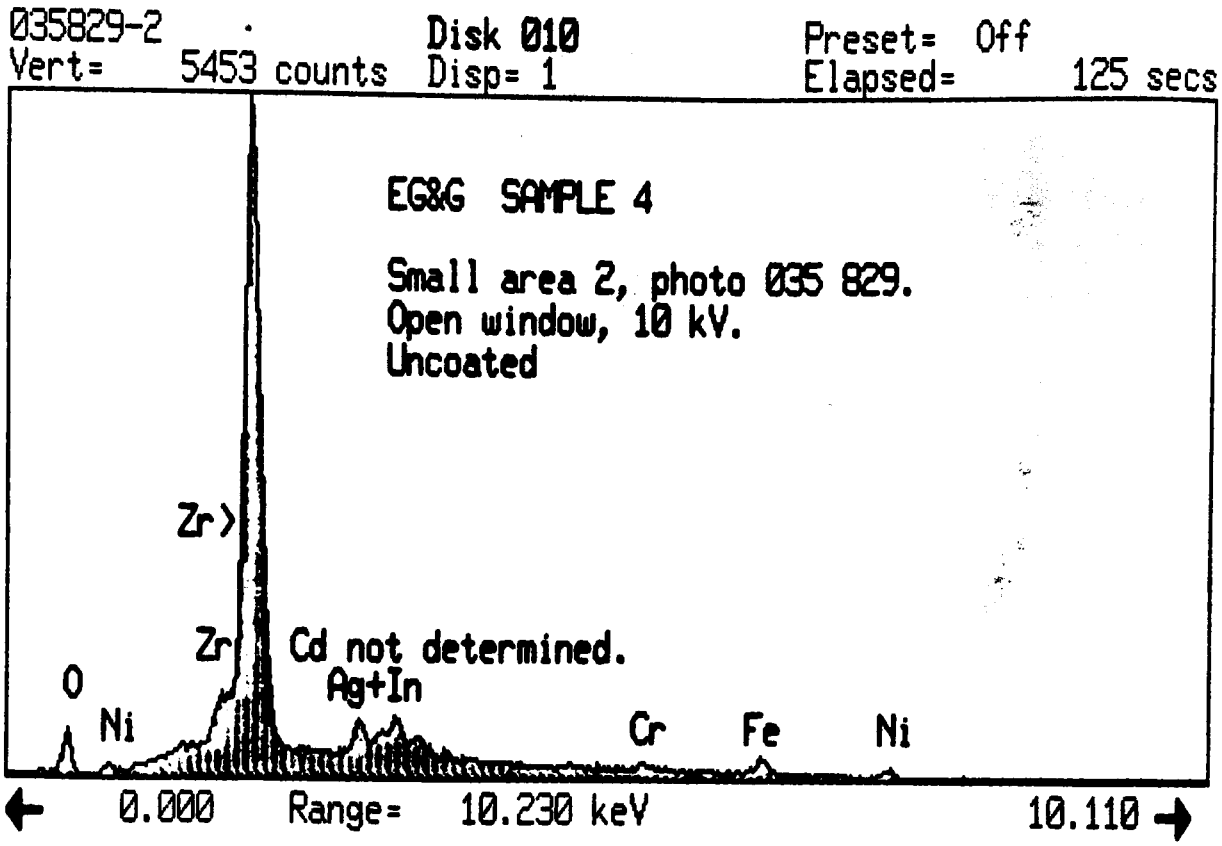

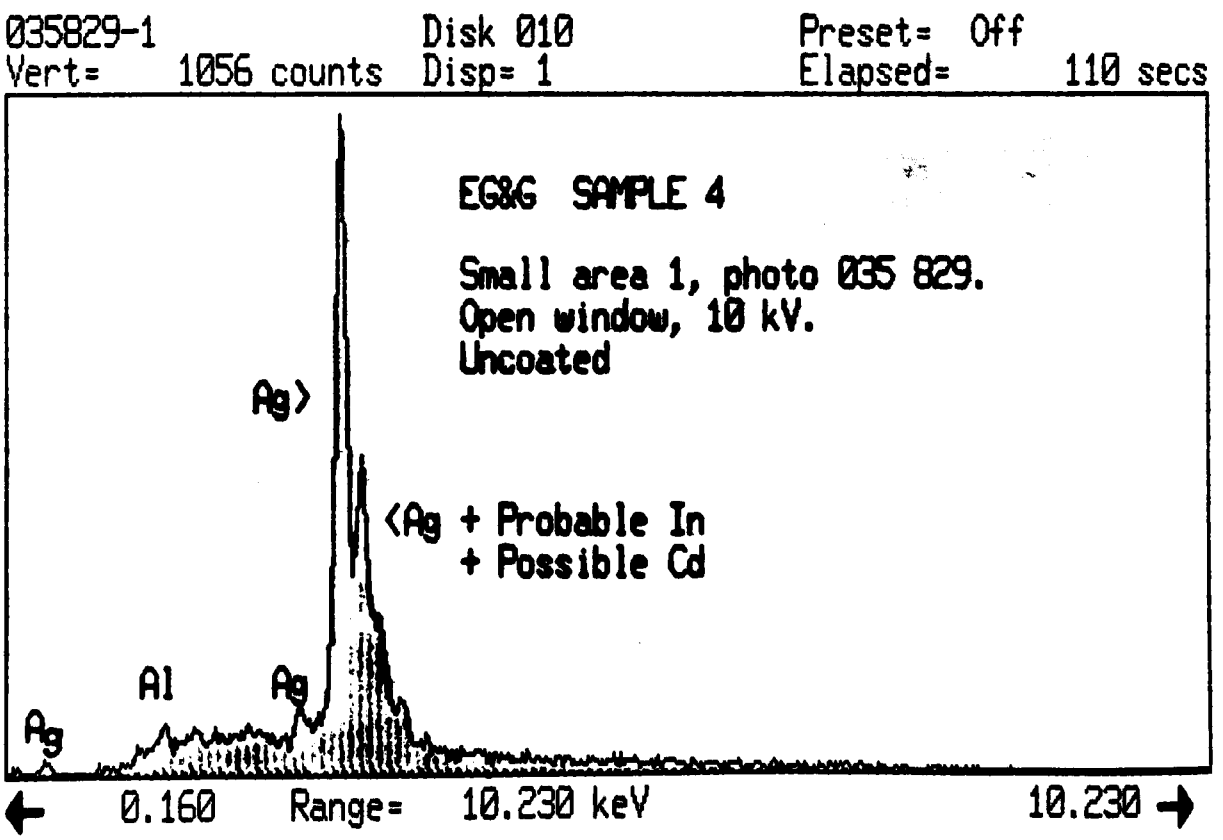

Figure D-15. EDS Spectra of Area 2, Figure D-14.

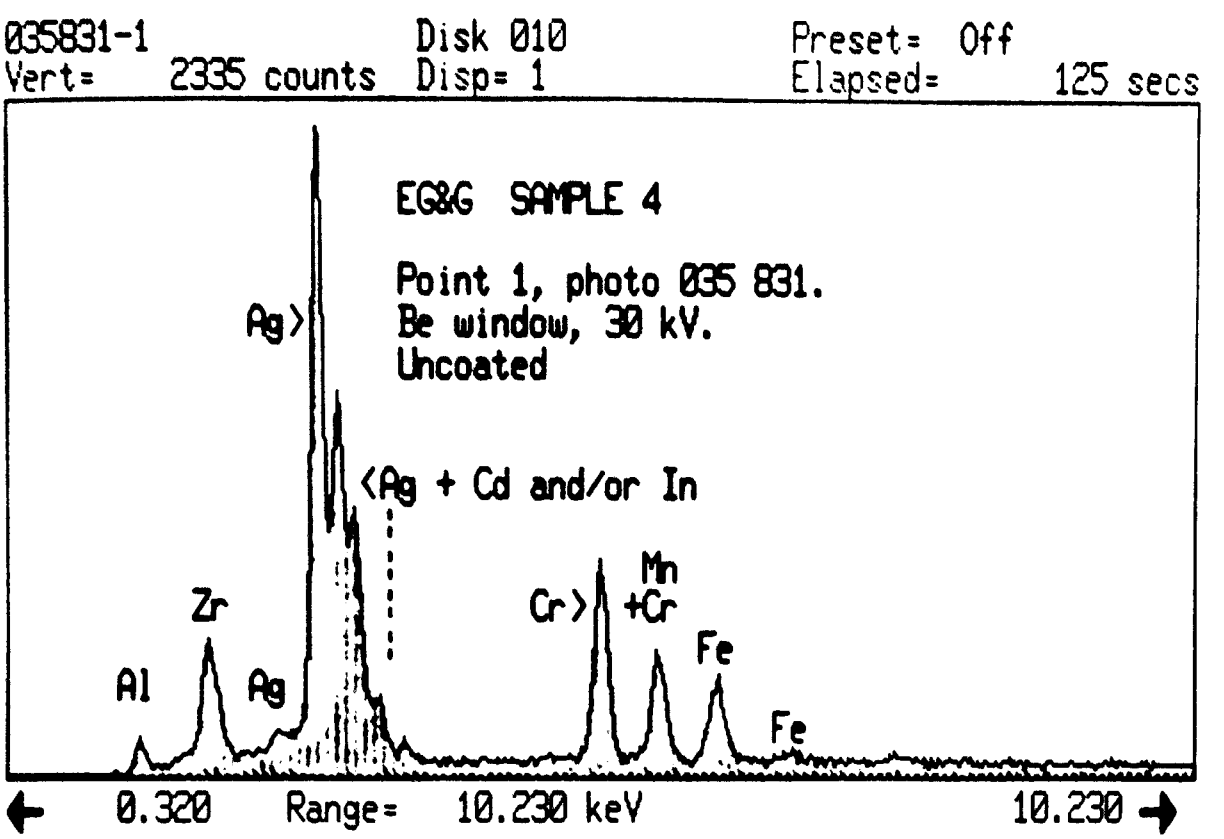

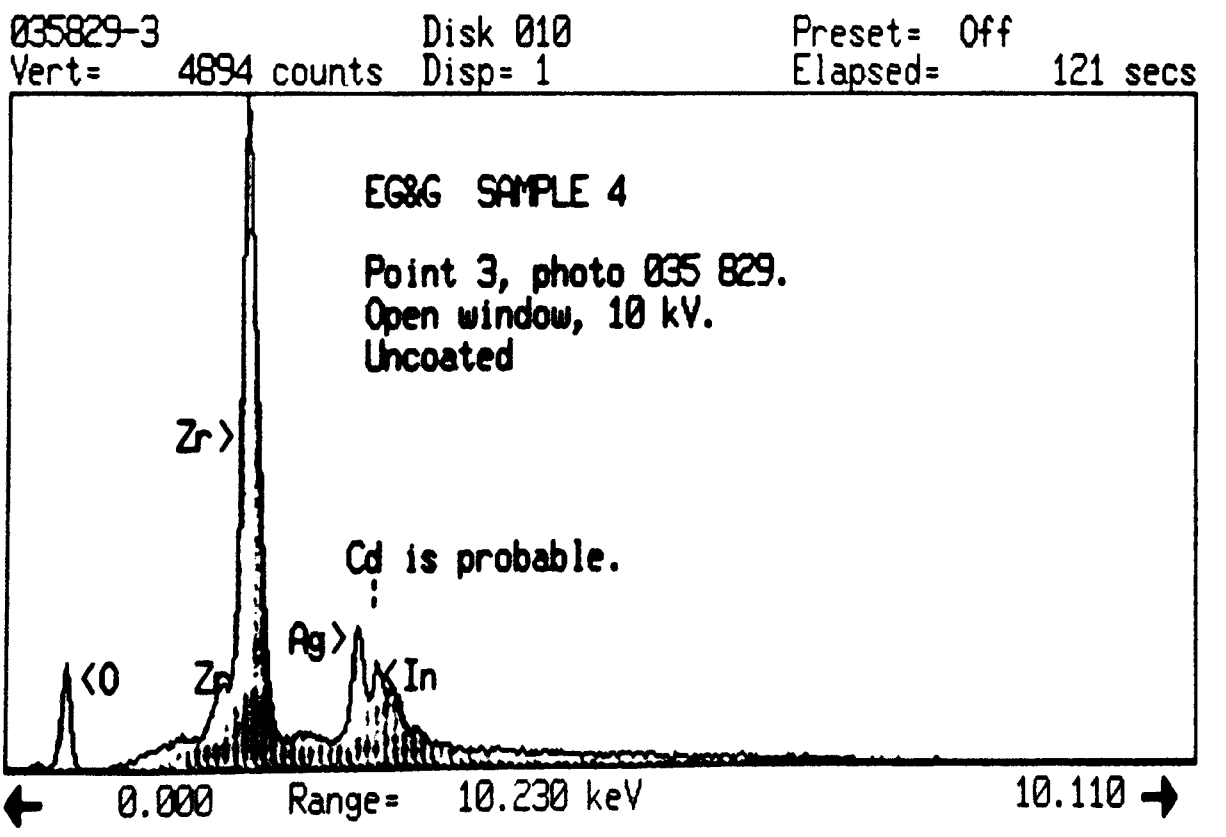

Figure D-15a. EDS Spectra of Area 2, Figure D-14.

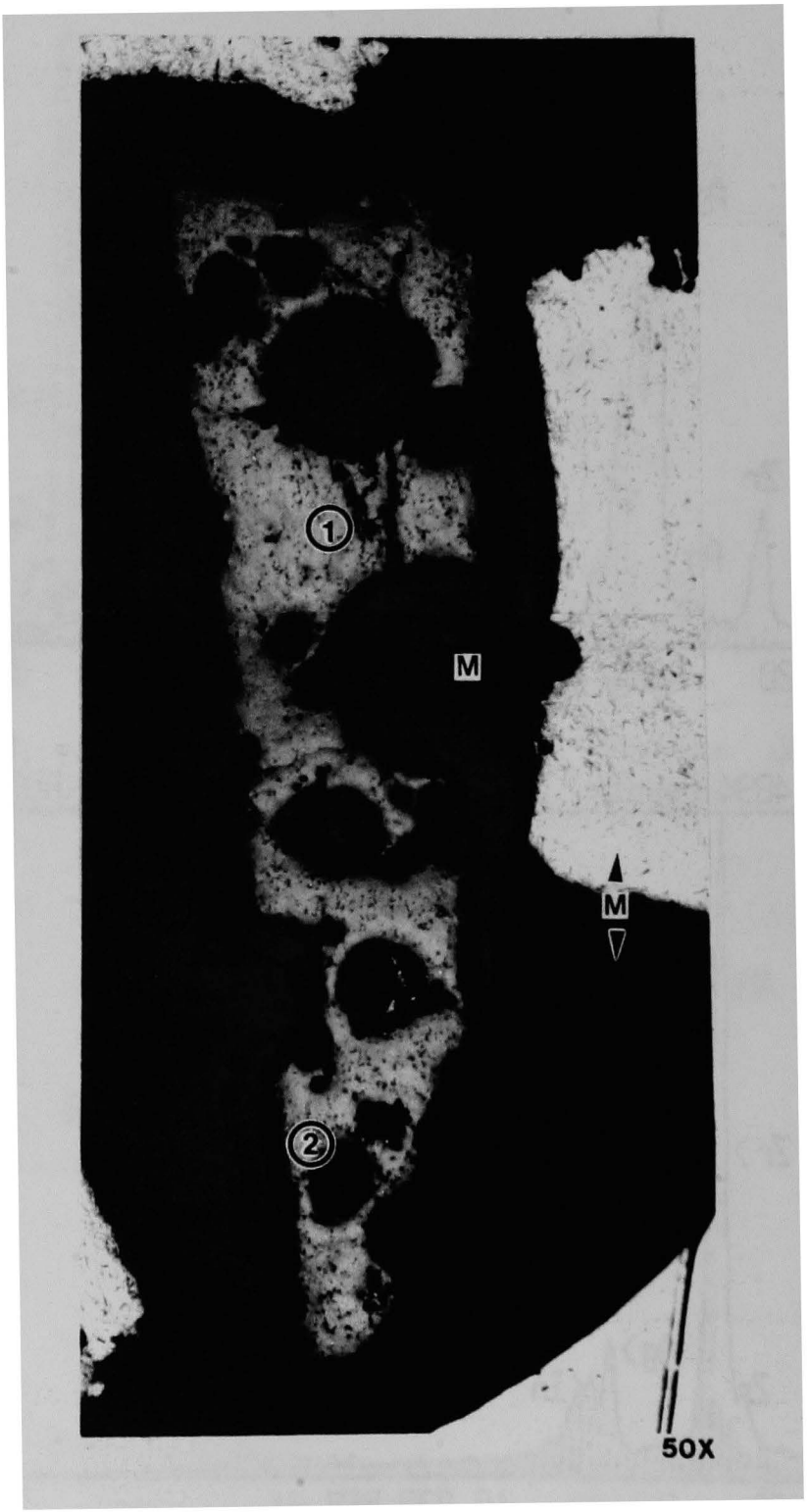

Figure D-16. As polished optical photomicrograph of particle Areas 1 and 2 examined in detail.

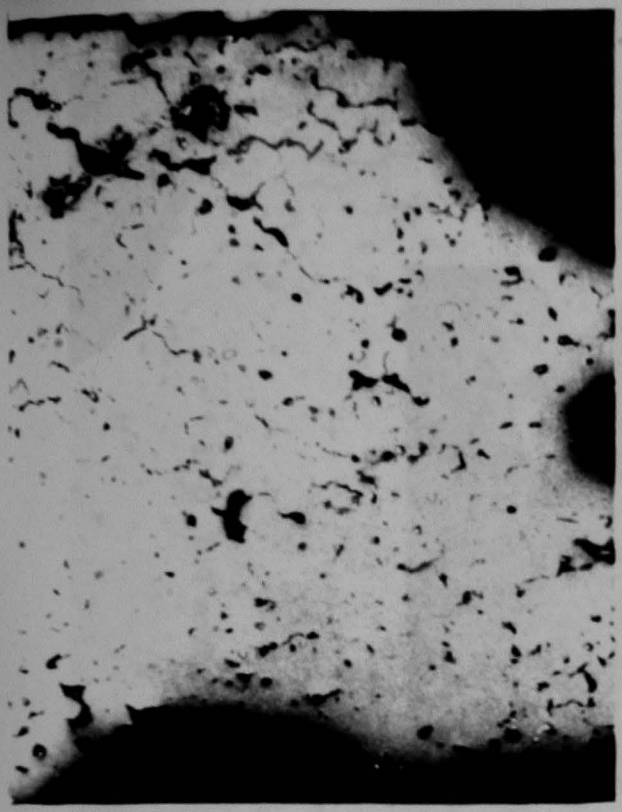

F467 Area 1

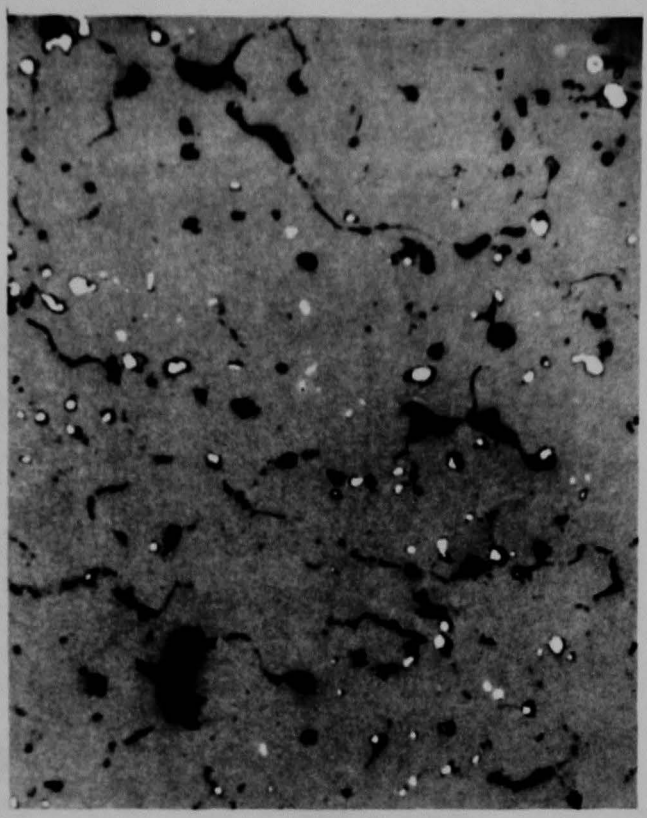

Area 1 400X

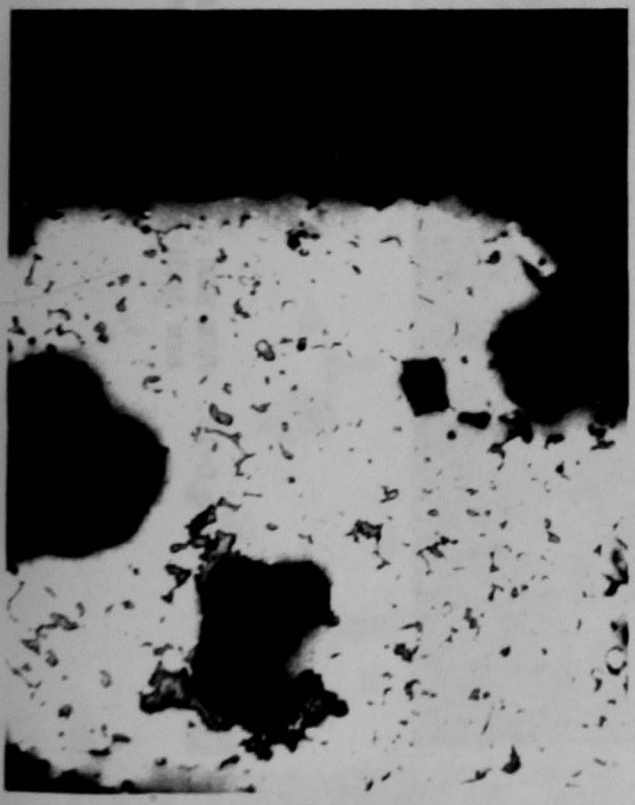

F470 Area 2 200X

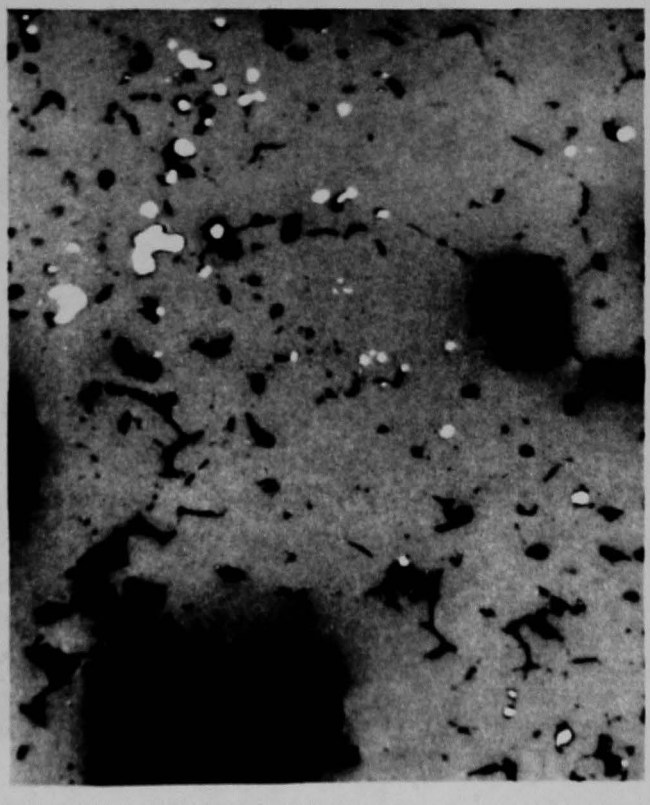

F471 Area 2 400X

Figure D-17. As polished high magnification photomicrographs of Areas 1 and 2 as noted in Fig. D-16.

Figure D-18. BSE/SEM photo of particle 5; Areas 1 and 2 from Fig. D-16 are indicated for reference.

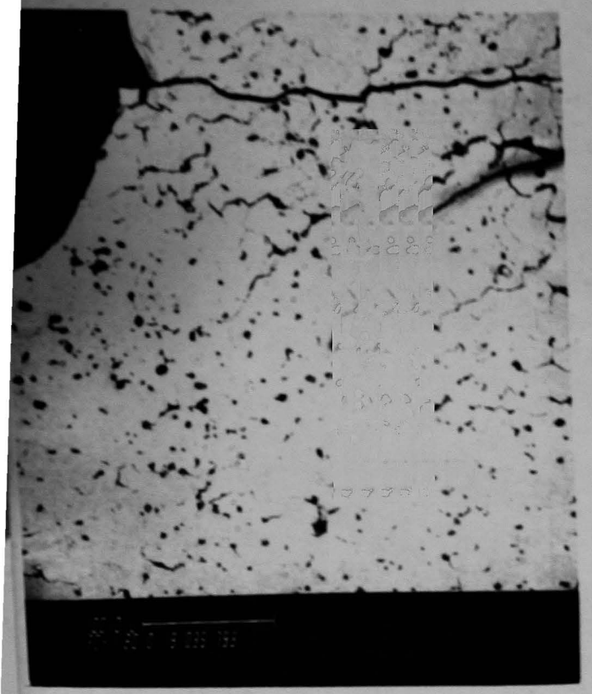

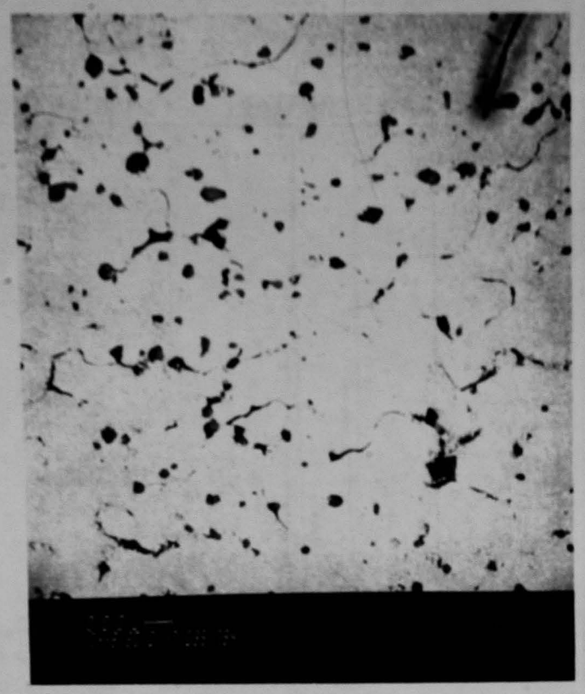

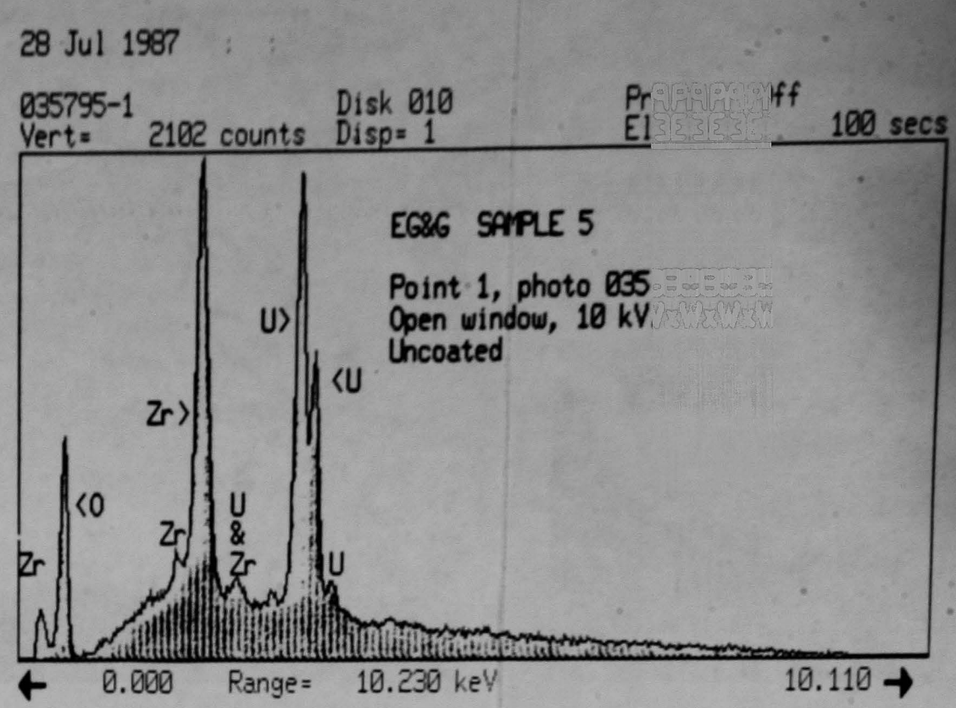

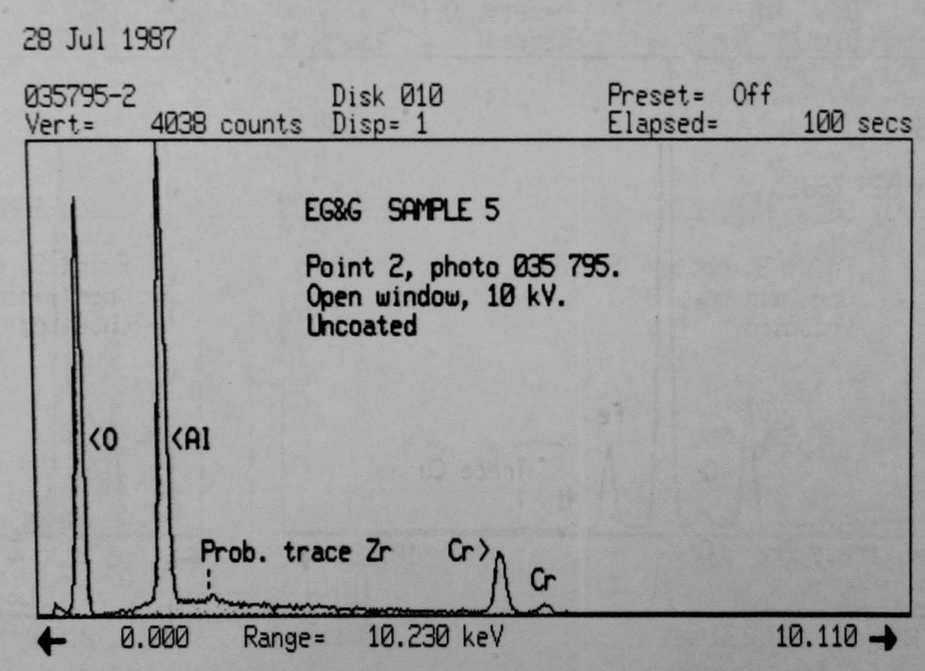

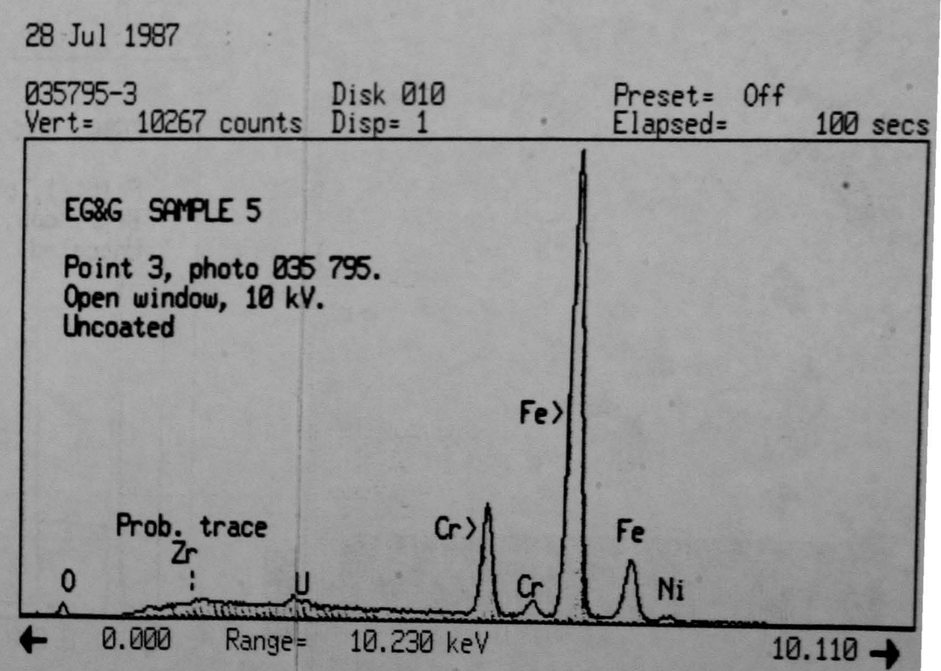

Figure D-19. BSE/SEM photos and EDS spectra from Area 1, Fig. D-18.

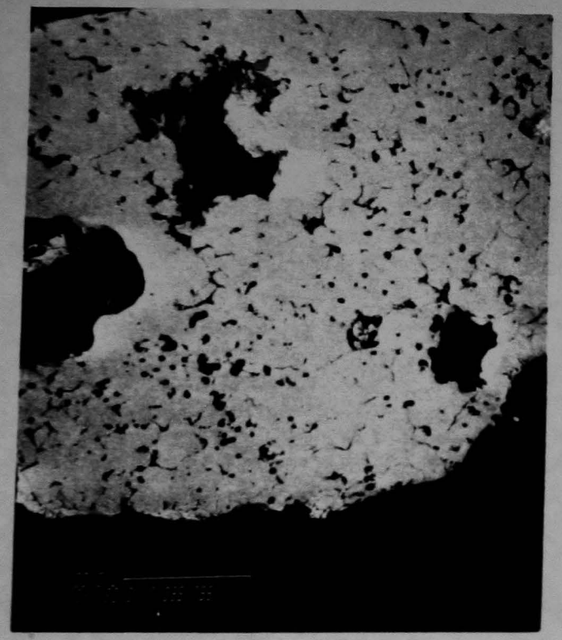

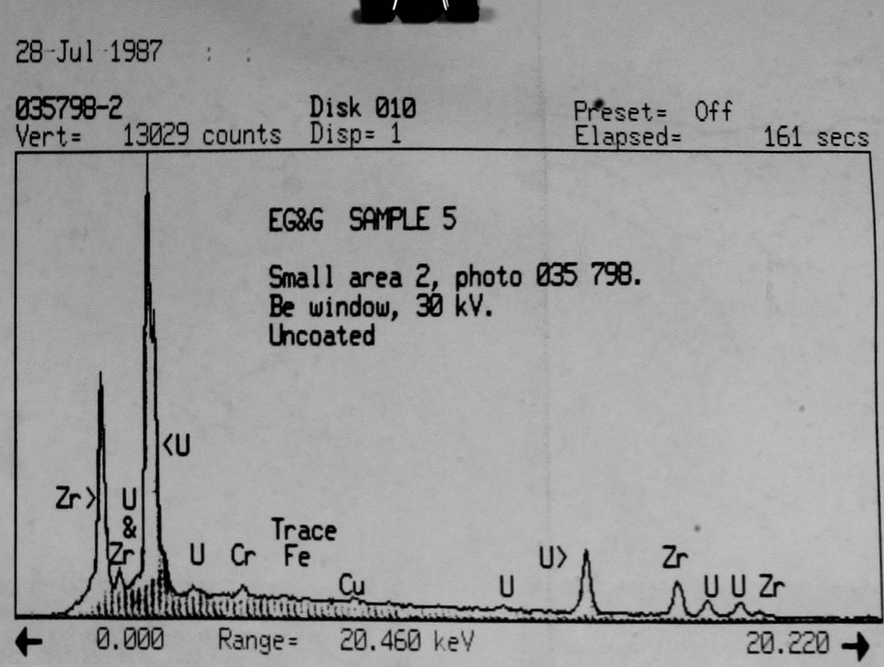

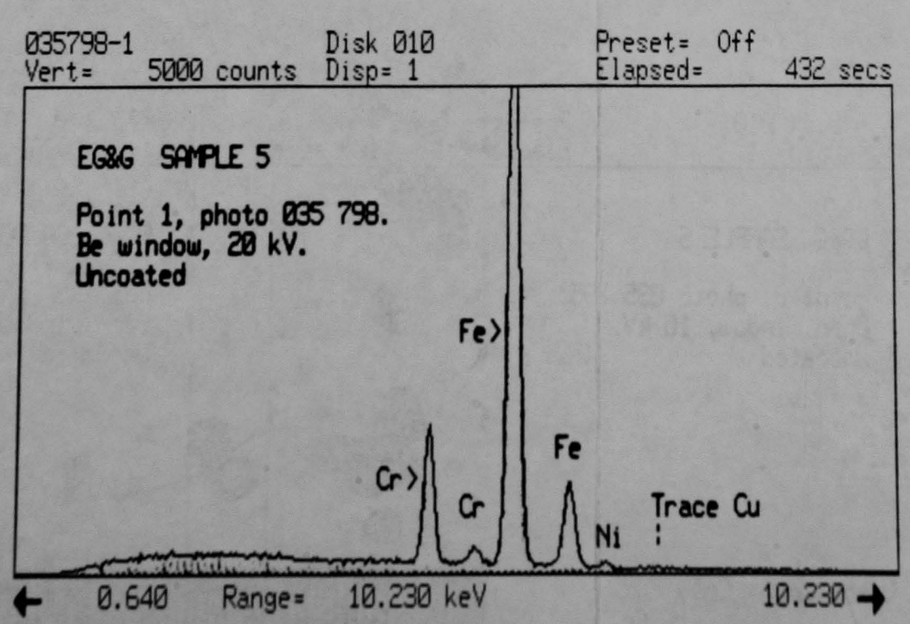

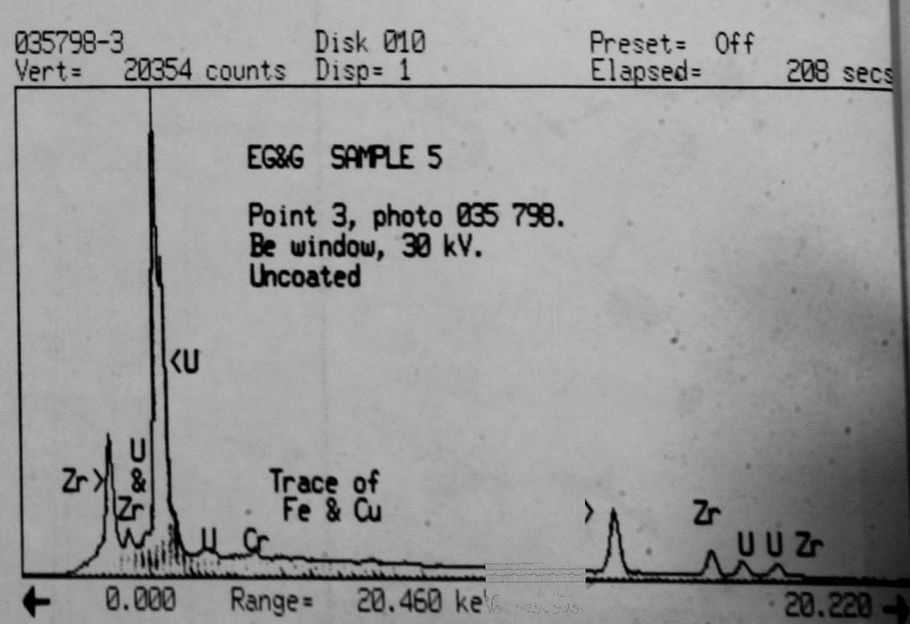

Figure D-20. BSE/SEM photos and EDS spectra from Area 2, Fig. D-18.

Figure D-21. As polished optical photomicrograph of particle 6. Areas 1 through 6 examined in detail.

Area 1

Area 2

Area 3

Area 4

Area 5

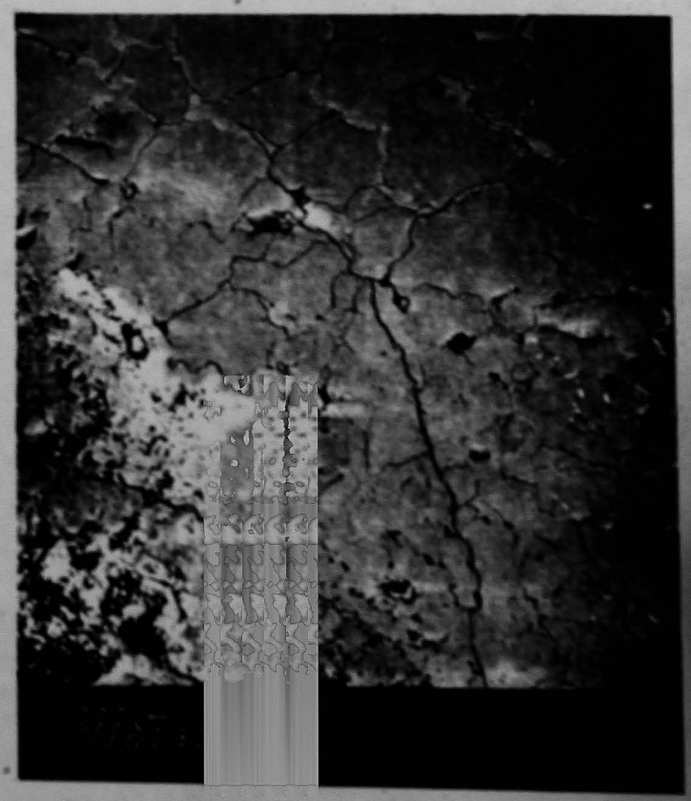

Area 6

Figure D-24. BSE/SEM photos of Areas 1 through 6 from Fig. D-23.

Area 1 200X

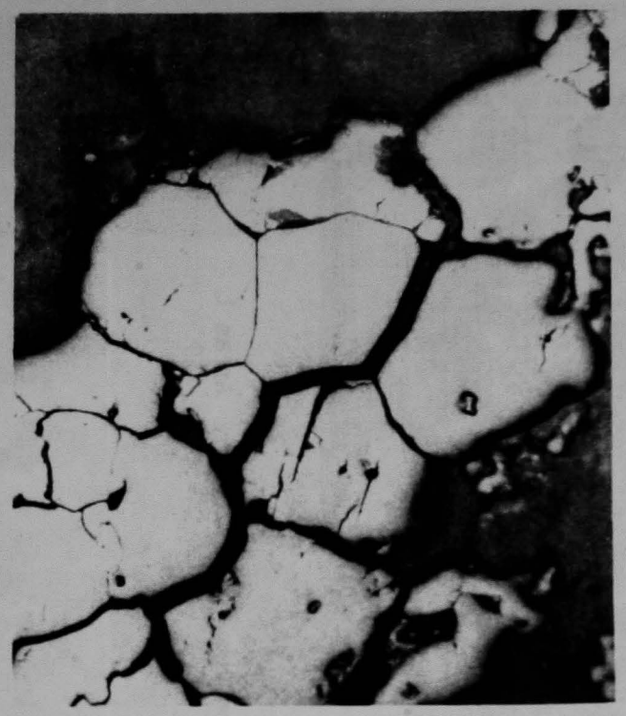

Area 2 200X

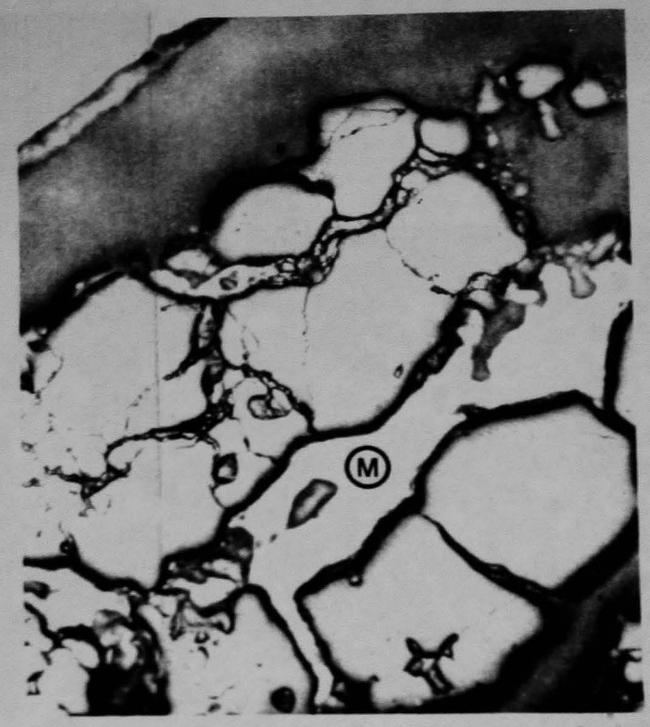

Area 3 200X

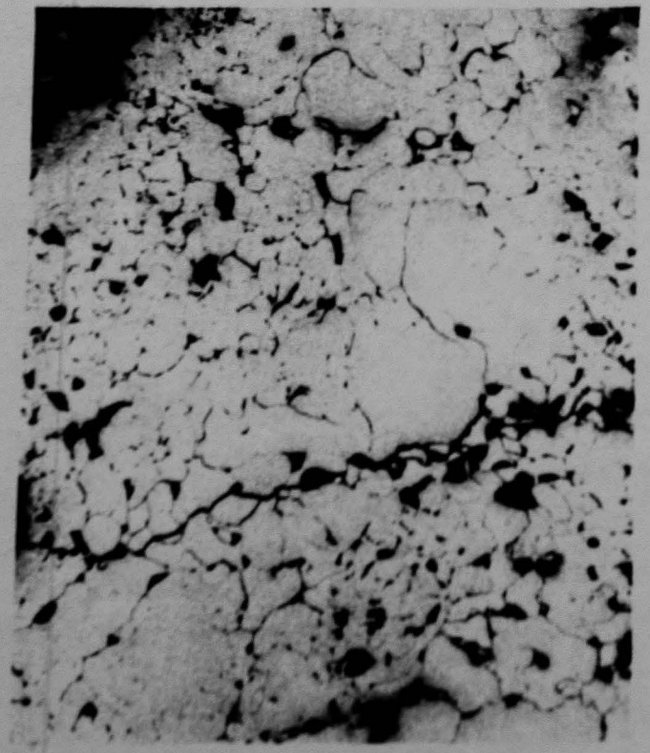

Area 4 200X

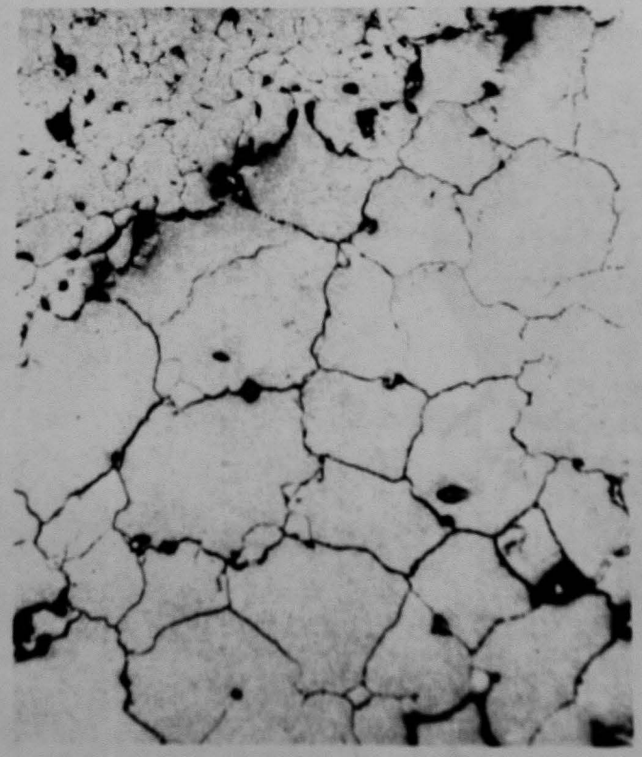

Area 5 200X

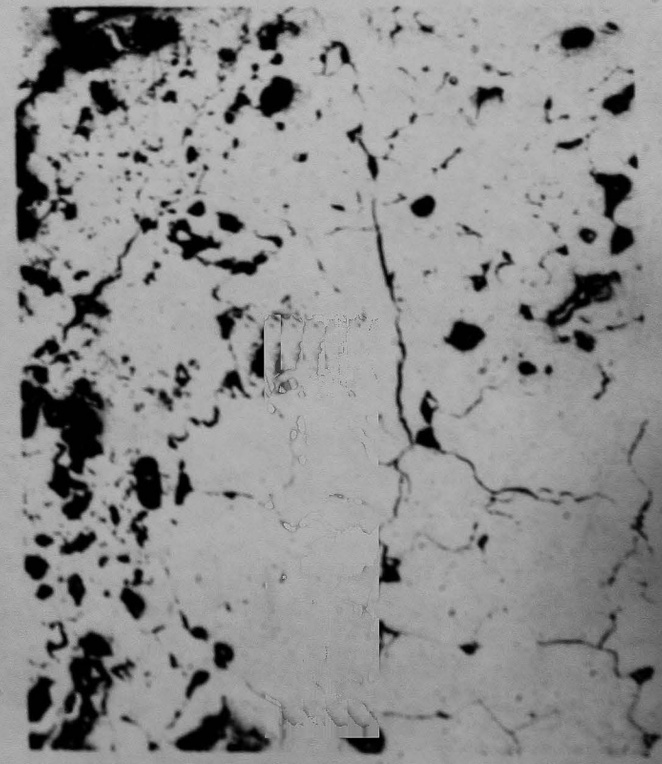

Area 6 200X

Figure D-22. As polished high magnification photomicrographs of Areas 1 through 6 as referenced in Figure D-21.

Figure D-23. BSE/SEM photo of particle 6. Areas 1 through 6 from Fig. D-21 are indicated. Areas A, B, and C were used for elemental dot maps.

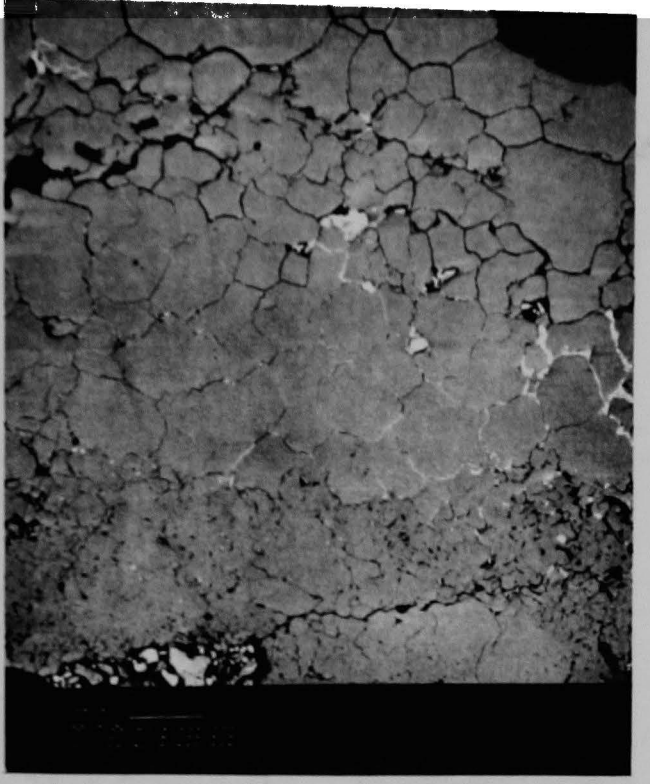

Area A

Zr Dot Map

U Dot Map

Figure D-25. Elemental dot maps of Area A in Fig. D-23.

Area B

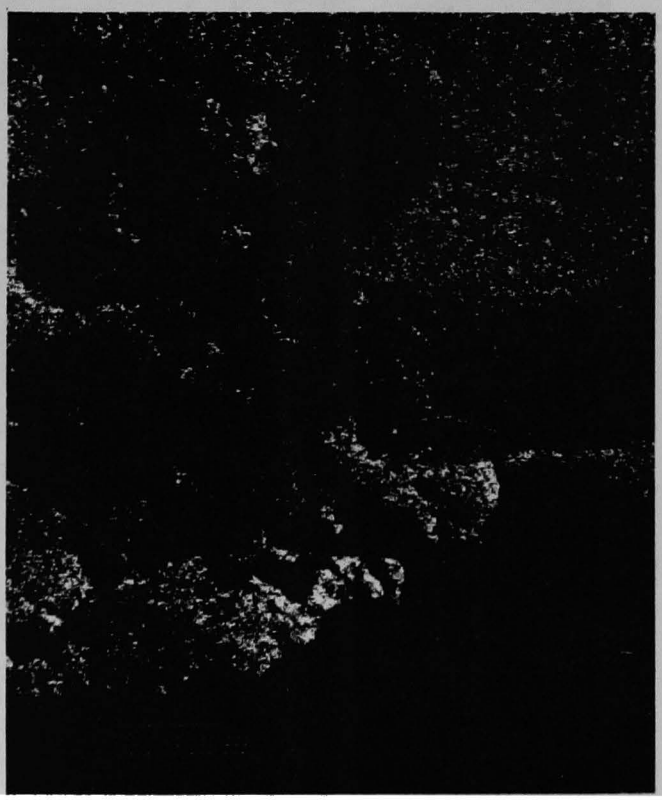

Zr Dot Map

U Dot Map

Figure D-25a. Elemental dot maps of Area B in Fig. D-23.

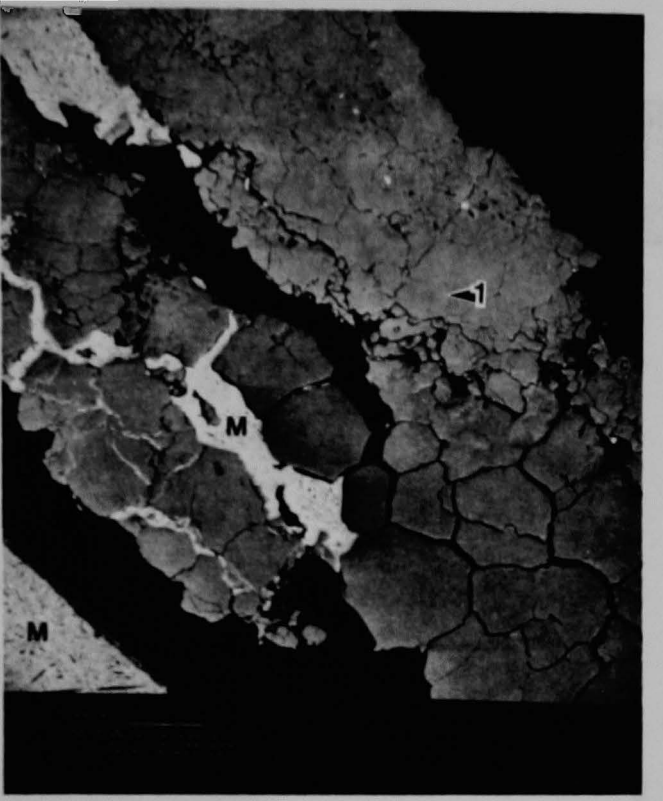

Area C

Zr Dot Map

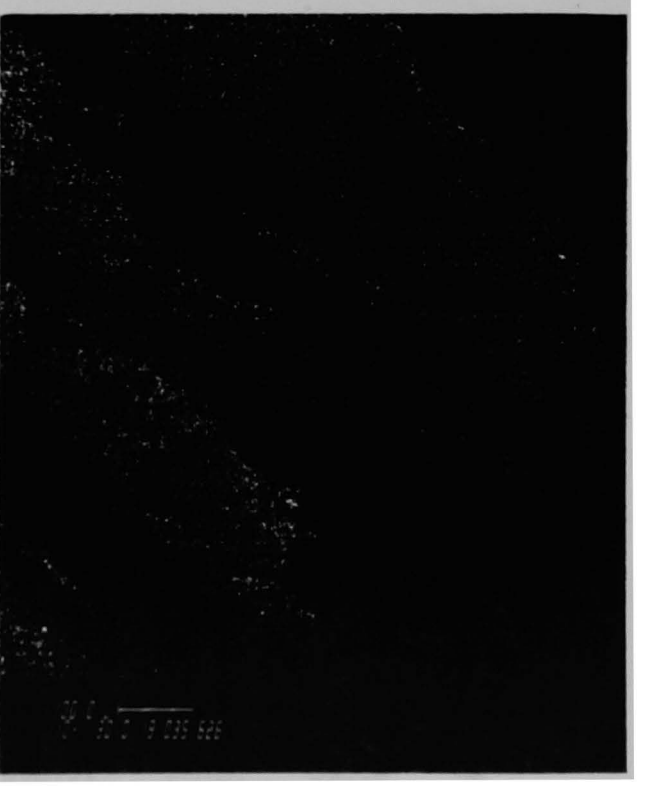

U Dot Map

Figure D-25b. Elemental dot maps of Area C in Fig. D-23. Point 1 in upper photo used for EDS analysis.

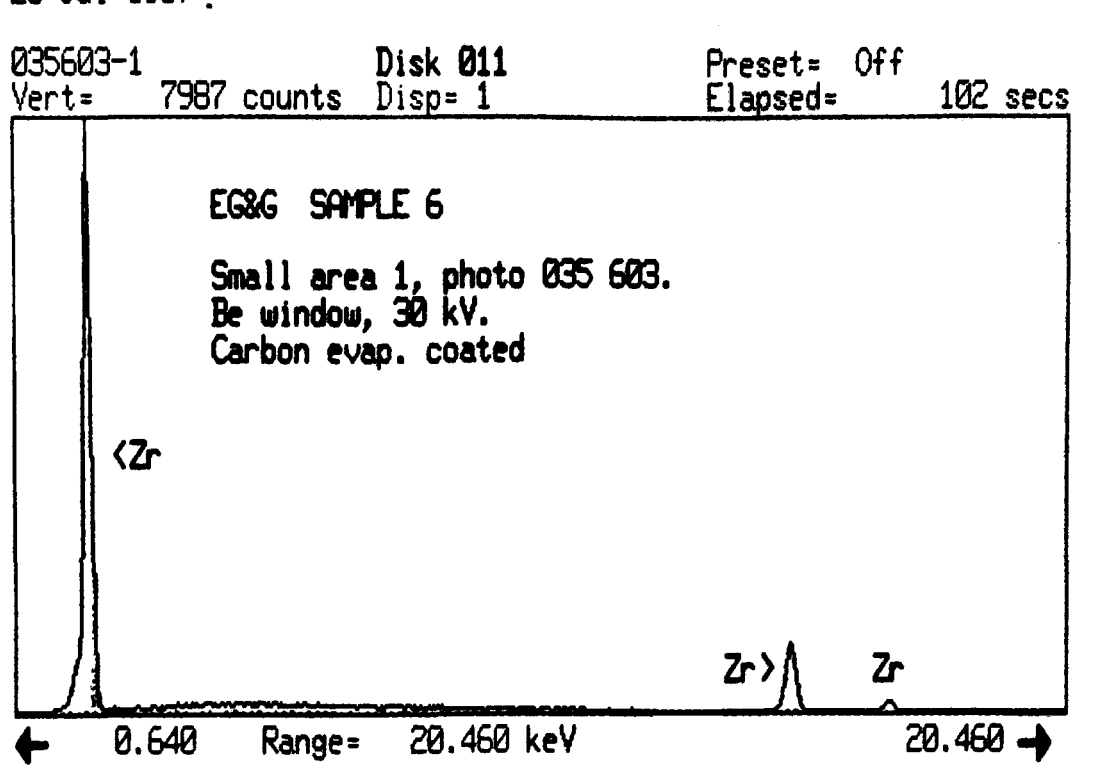

(Refer to Figure 24.)

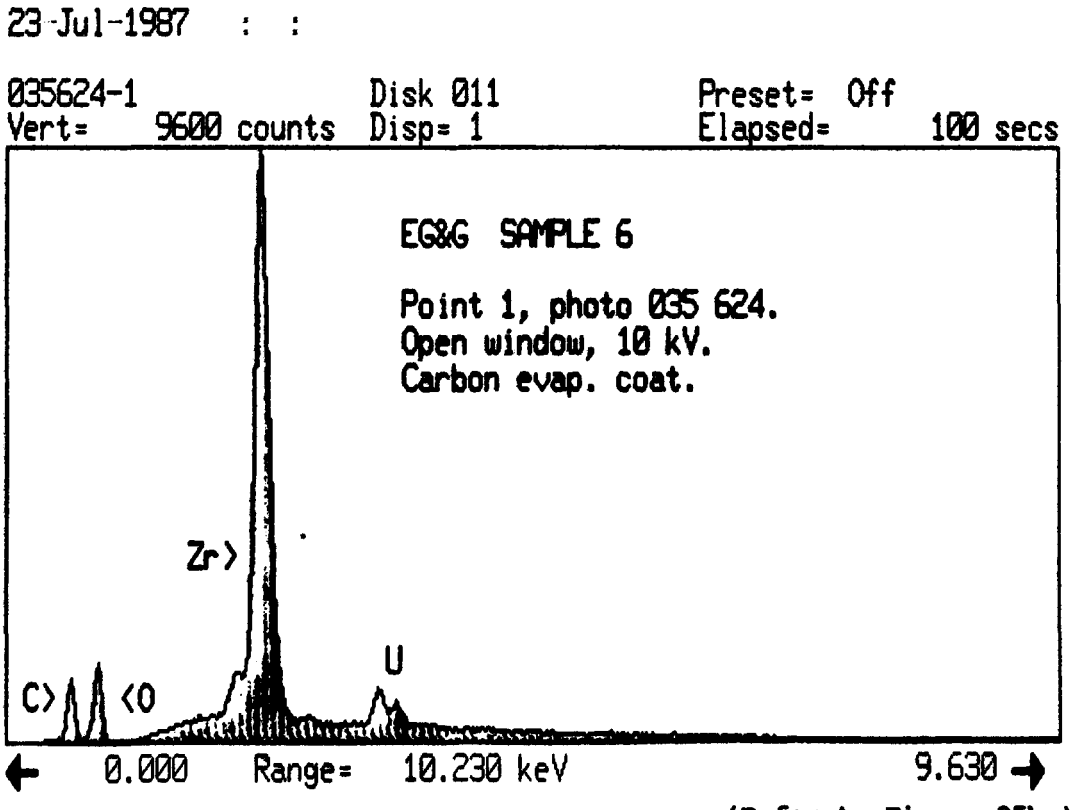

(Refer to Figure 25b.)

Figure D-26. EDS spectra from Area 3 in Fig. D-23.

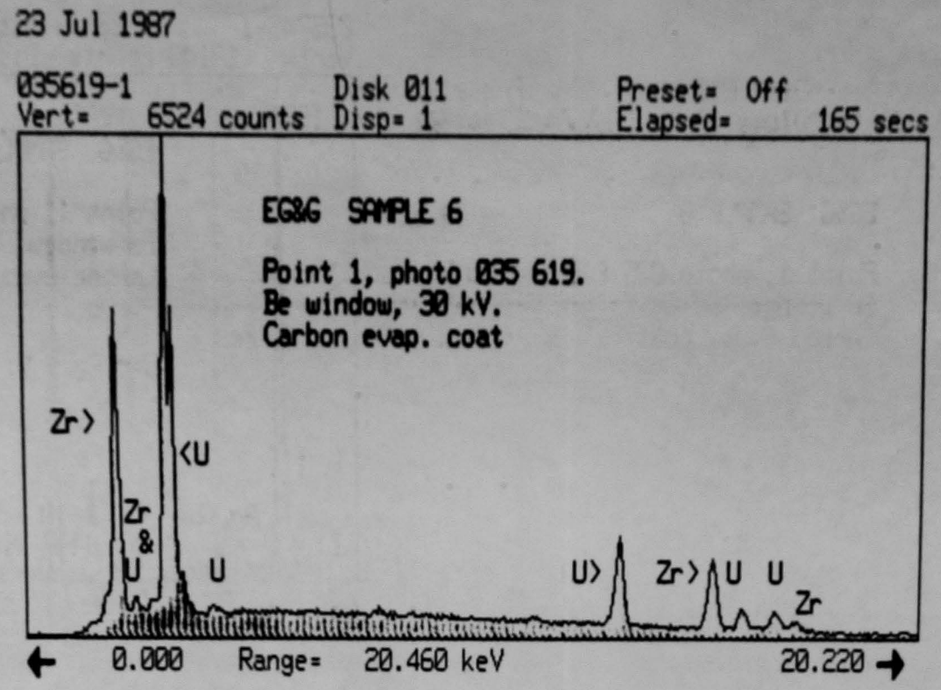

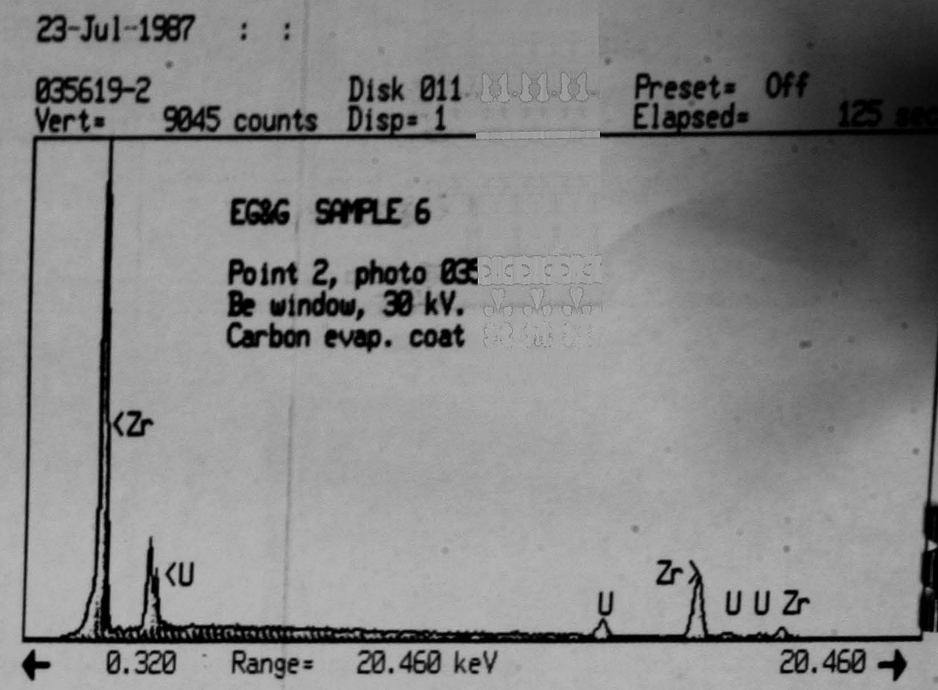

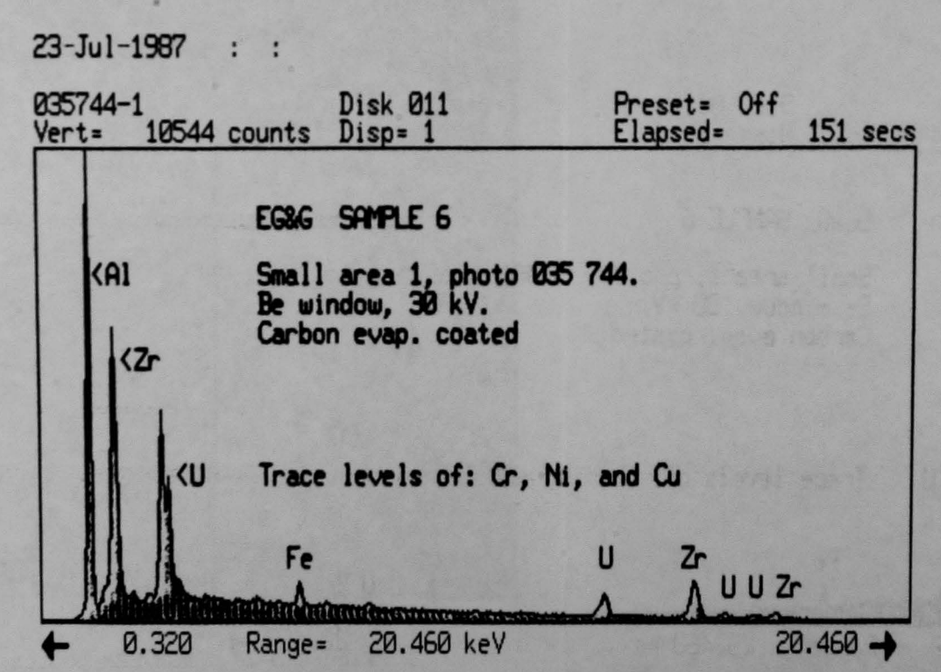

Figure D-27. BSE/SEM photos and EDS spectra from Area B in Fig. D-23.

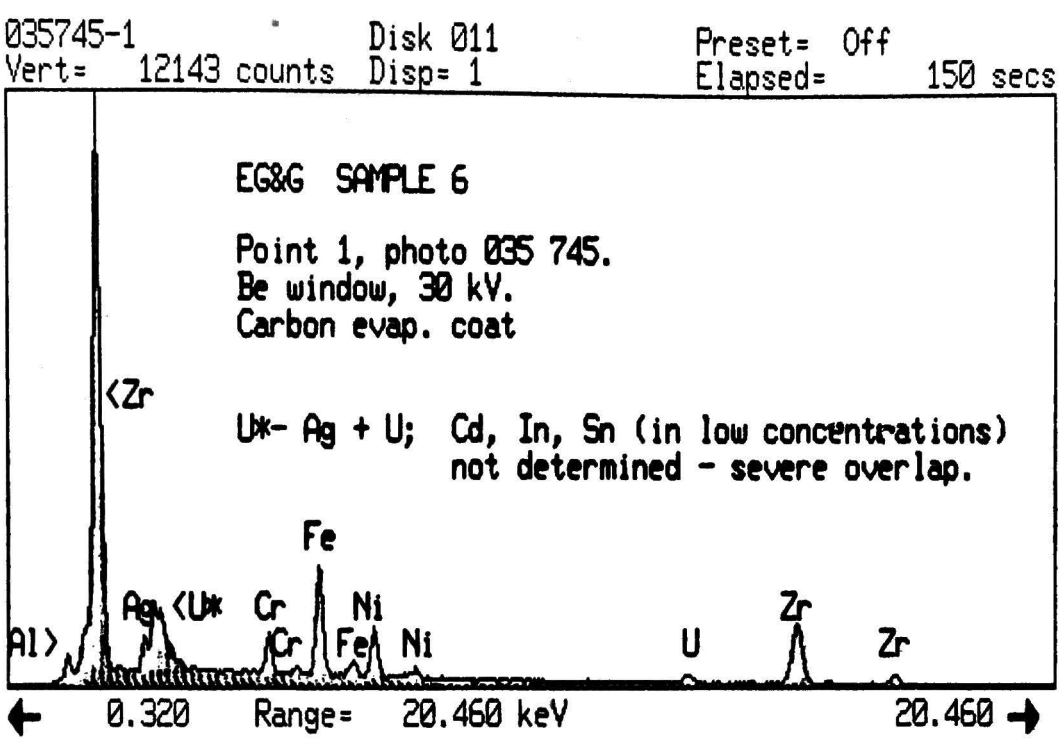

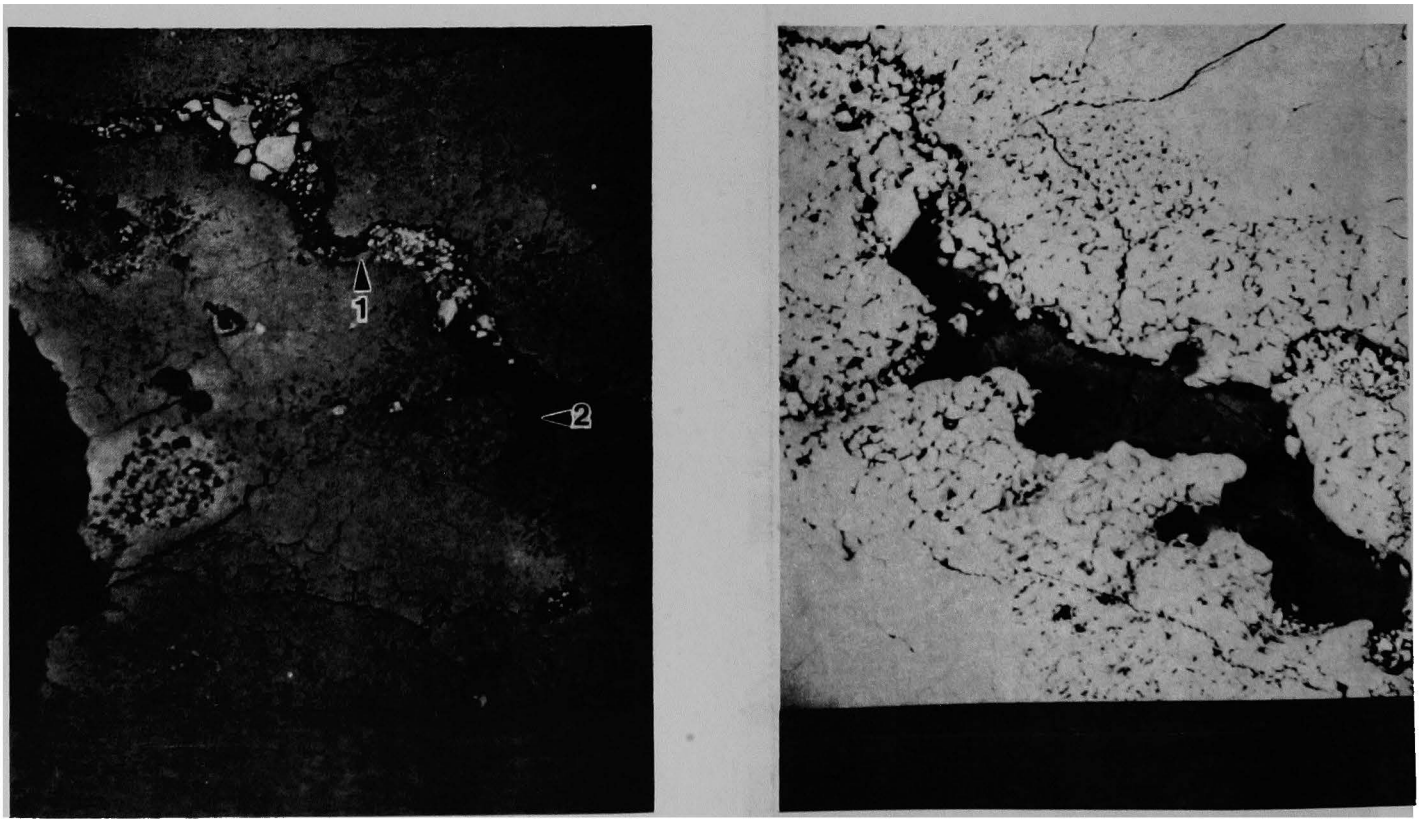

Figure D-28. BSE/SEM photos and EDS spectra from Area 4 in Fig. D-23. Point 2 in 035 745 is Fe; no spectra recorded.

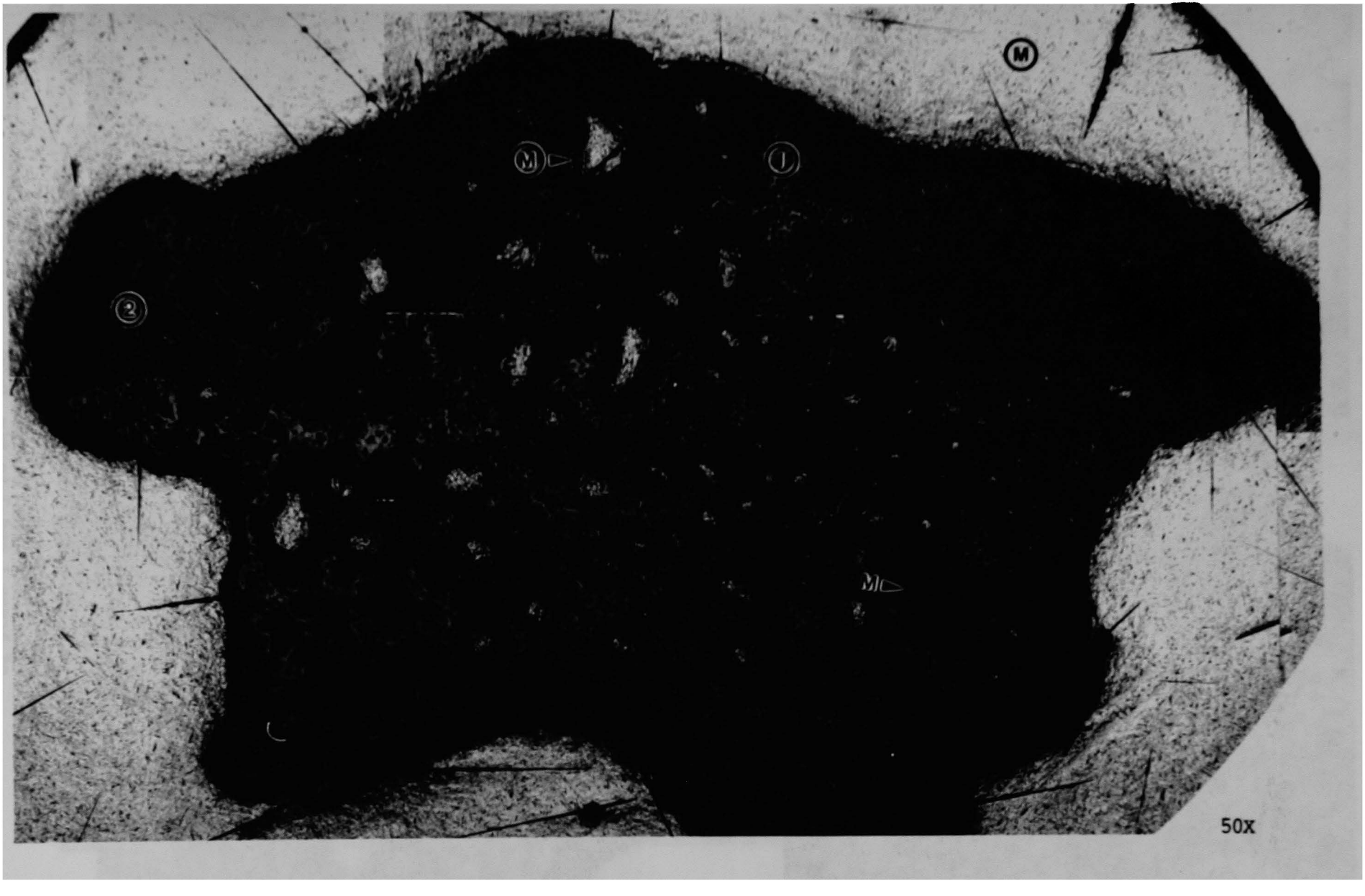

Figure D-29. As polished optical photomicrograph of particle 7. Areas 1 and 2 examined in detail.

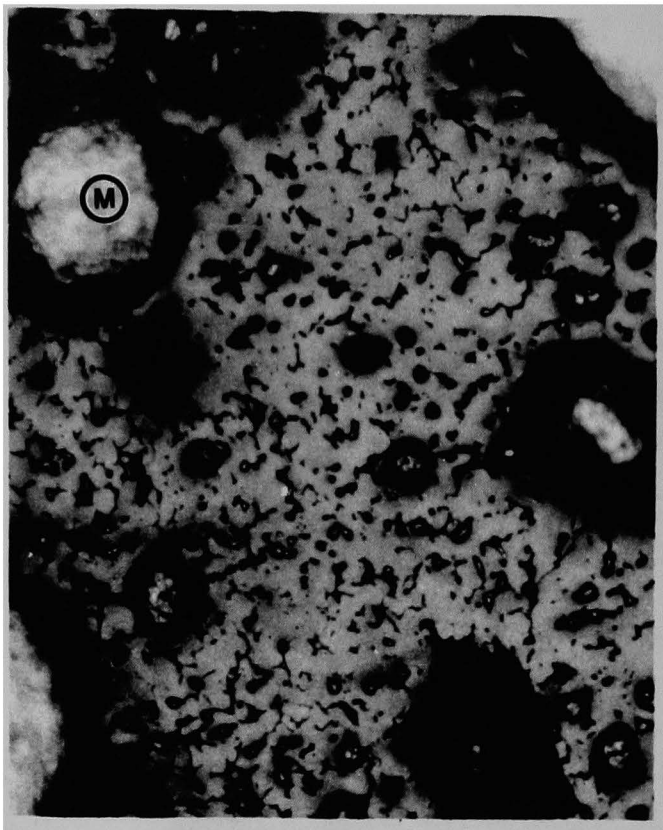

F566 Area 1 200X

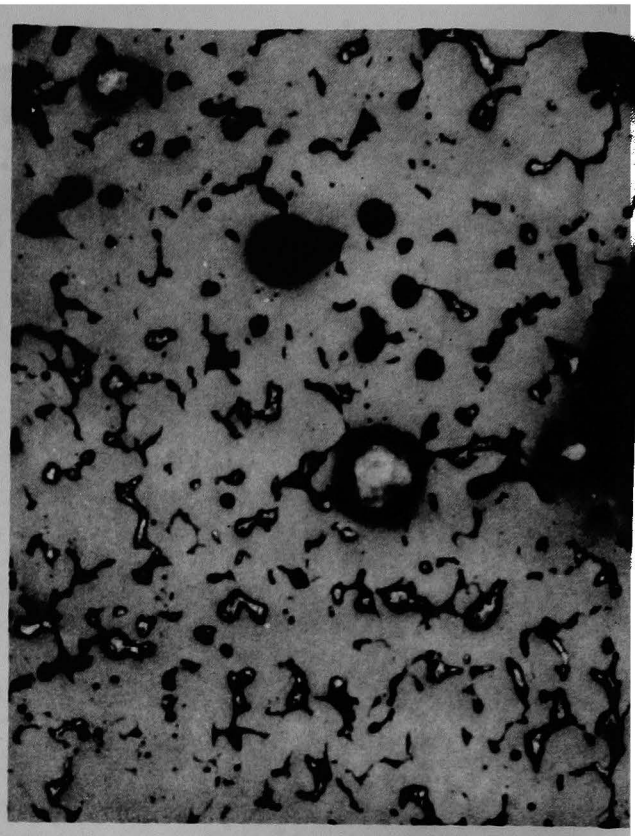

F567 Area 1 400X

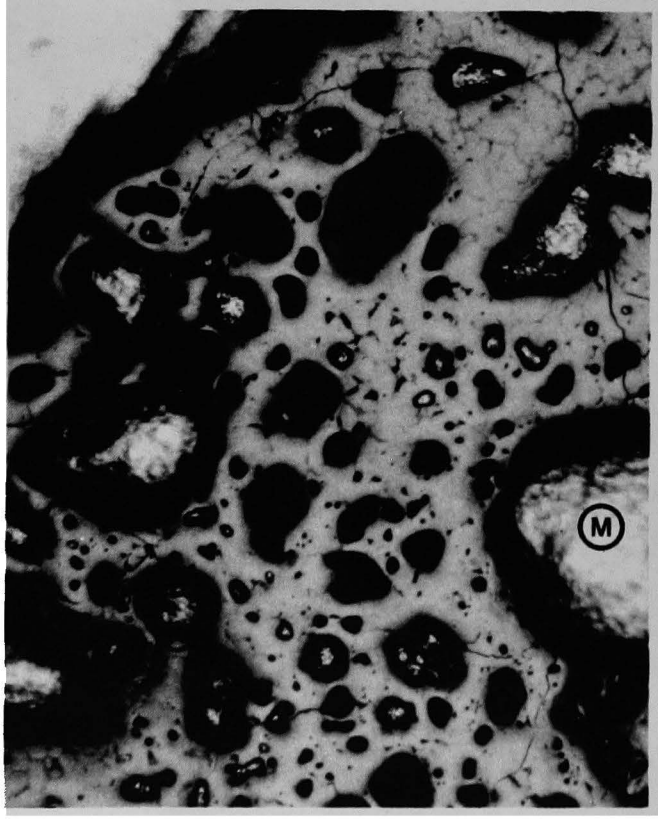

F569 Area 2 200X

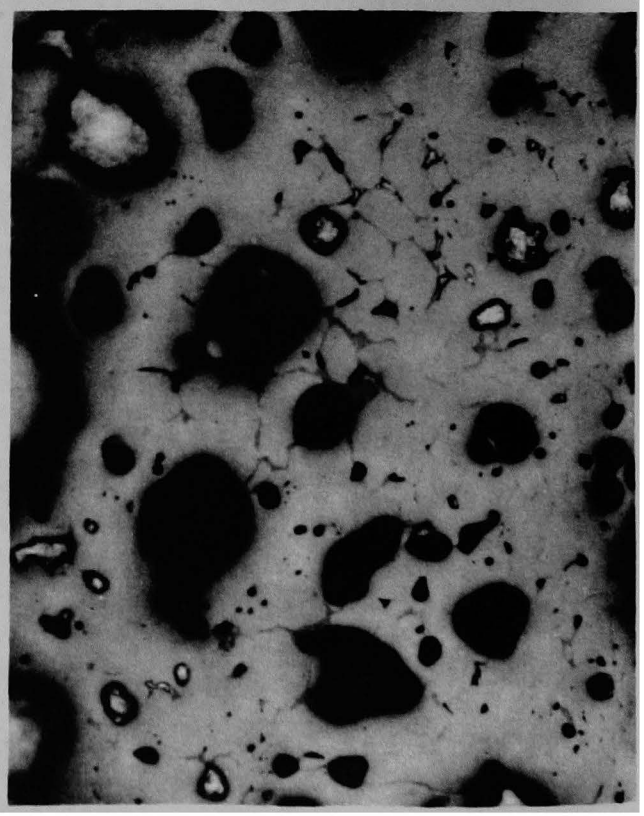

F570 Area 2 400X

Figure D-30. As polished high magnification optical photomicrographs of Areas 1 and 2 in Fig. D-29.

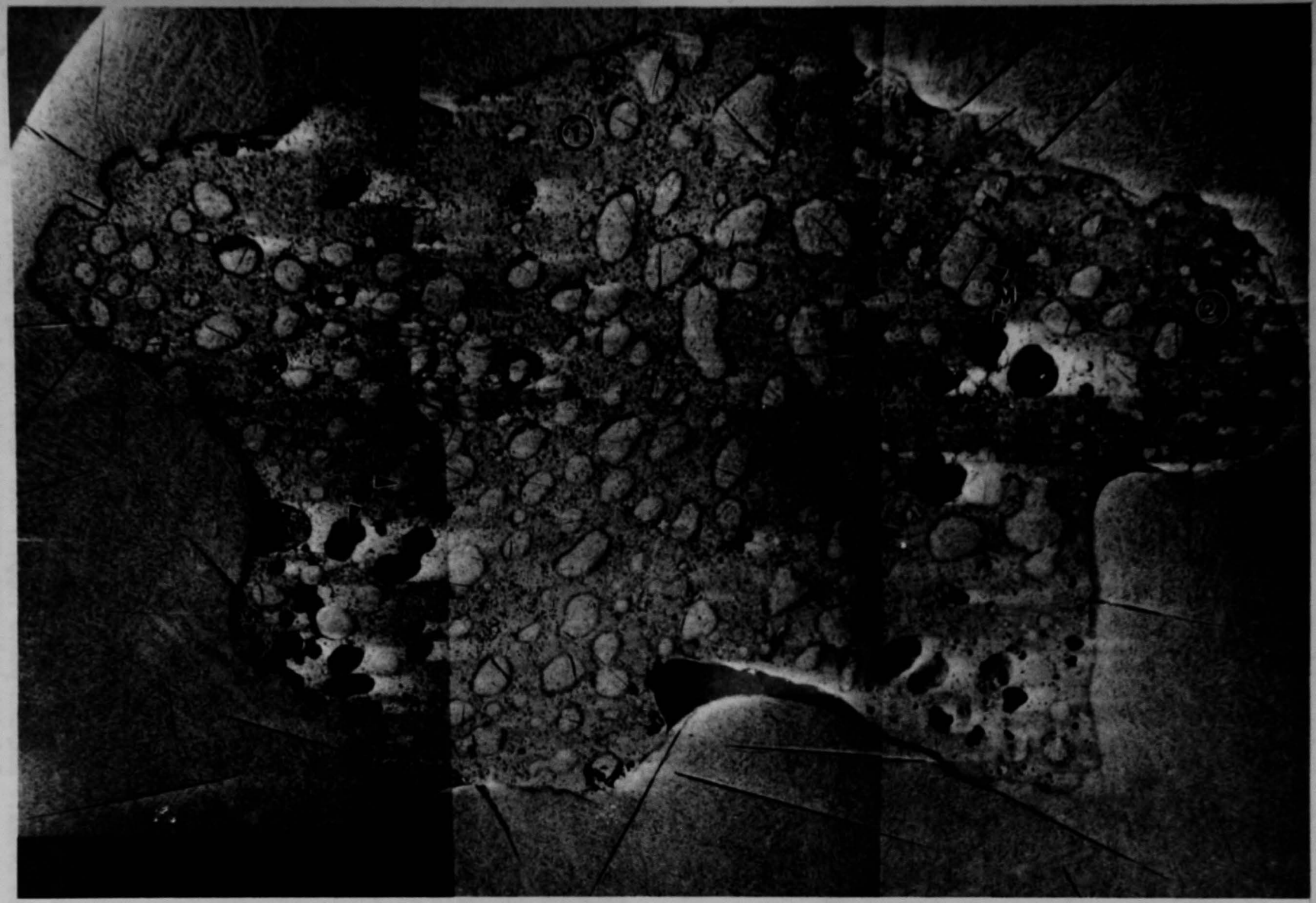

Figure D-31. BSE/SEM photos of particle 7; Areas 1 and 2 from Fig. D-29 are indicated.

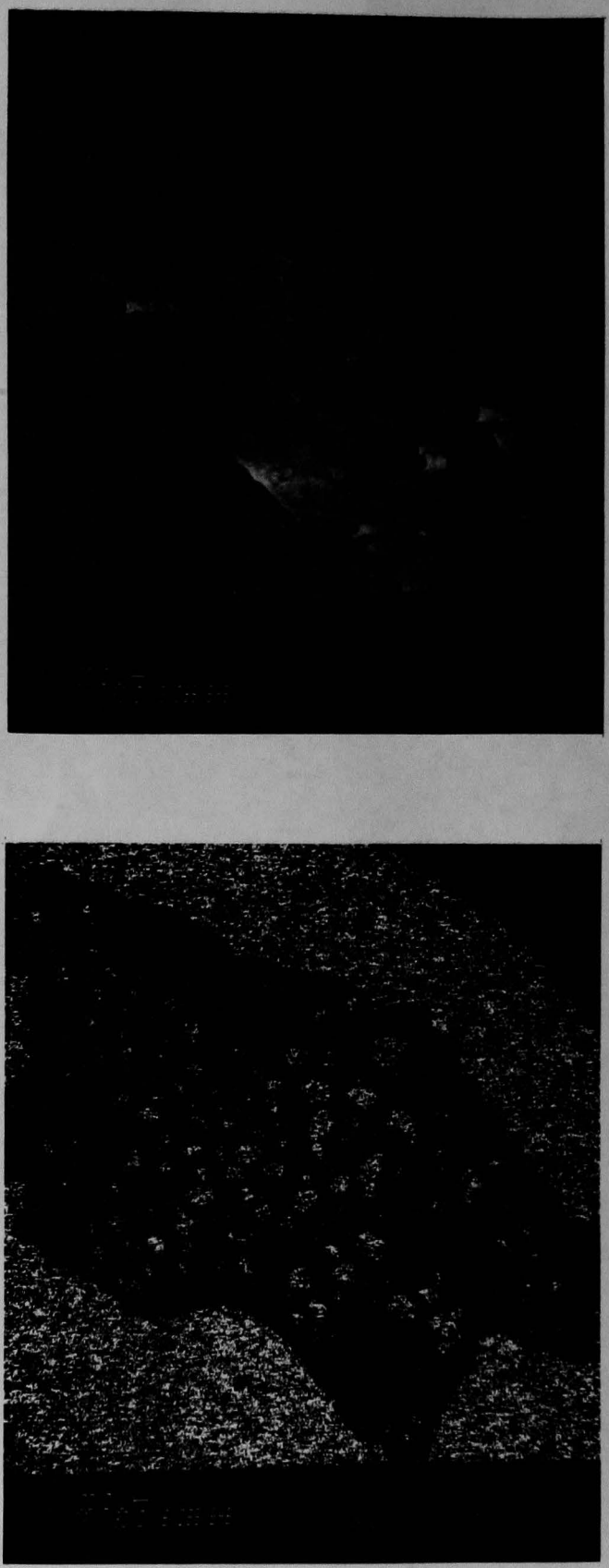

Figure D-31a. BSE/SEM photo (upper) and Pb/Bi dot map (lower) of particle 7. Dot map indicates mounting material in sample porosity.

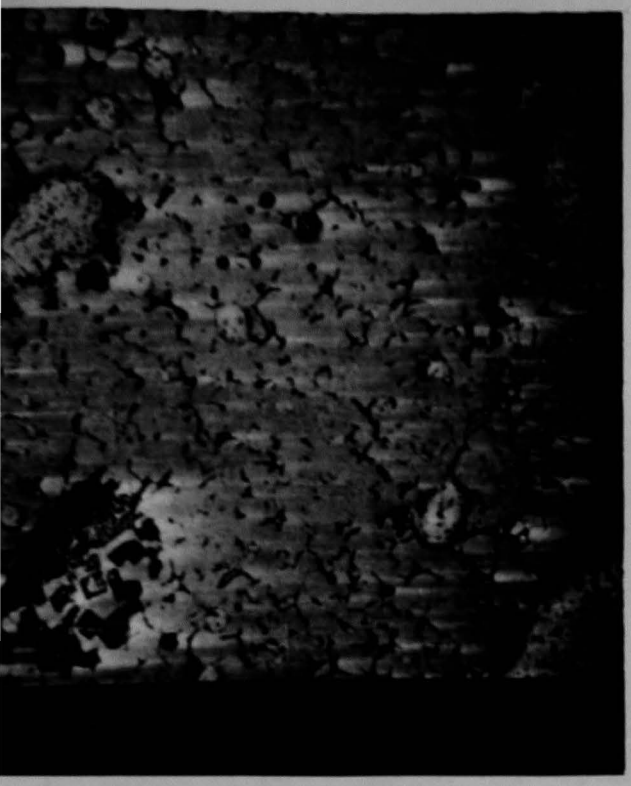

Overall, Area 1

Lower Left, 035 838

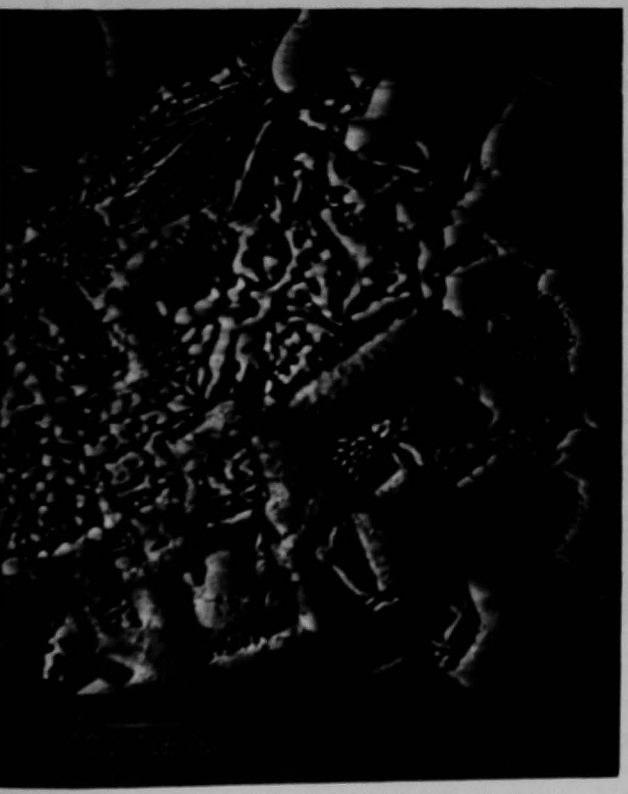

Center of 035 839

Left Center of 035 838

Figure D-32. BSE/SEM photos of Area 1 in Fig. D-31.

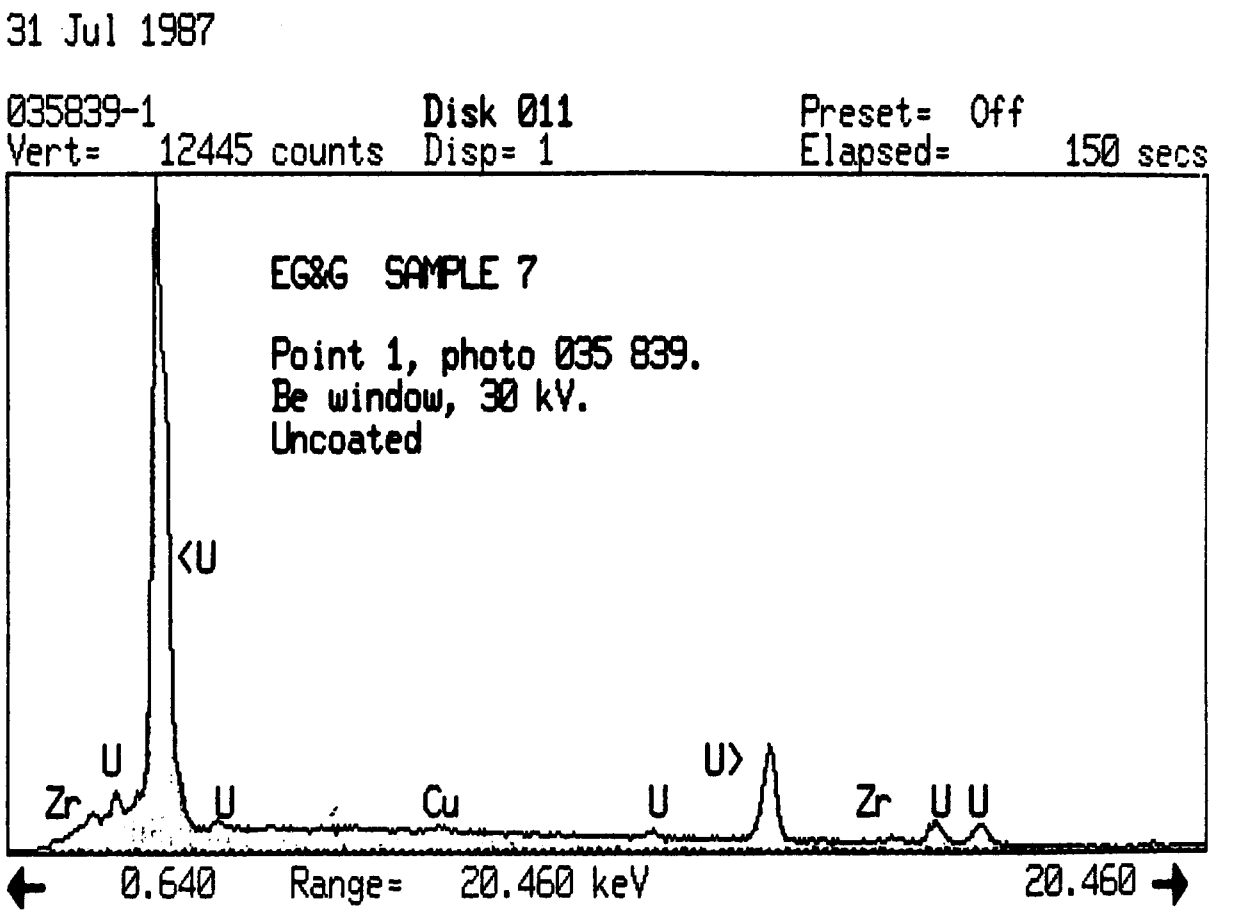

Figure D-32a. EDS spectra of point 1 in photo 035 839; refer to Fig. D-32.

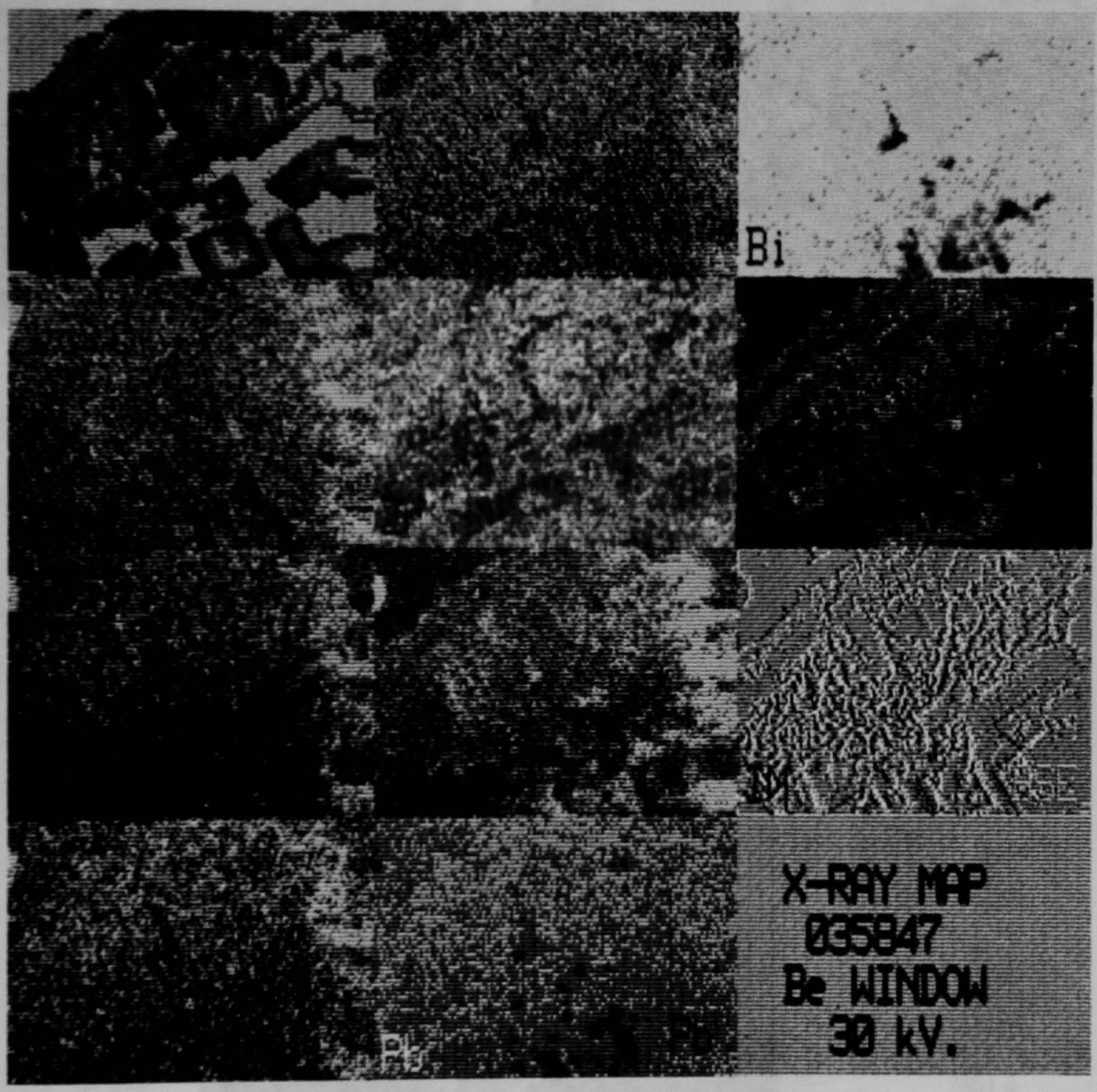

Figure D-32b. BSE/SEM photo and multi-element X-ray dot map of area shown in photo 035 840, Fig. D-32.

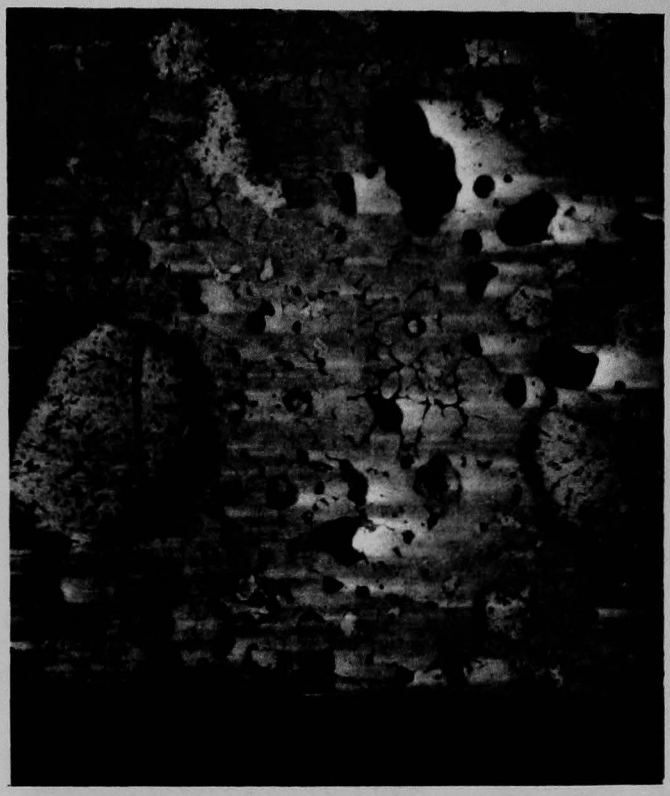

Overall, Area 2

Center of 035 842

Center of 035 843

Figure D-33. BSE/SEM photos of Area 2 in Fig. D-31.

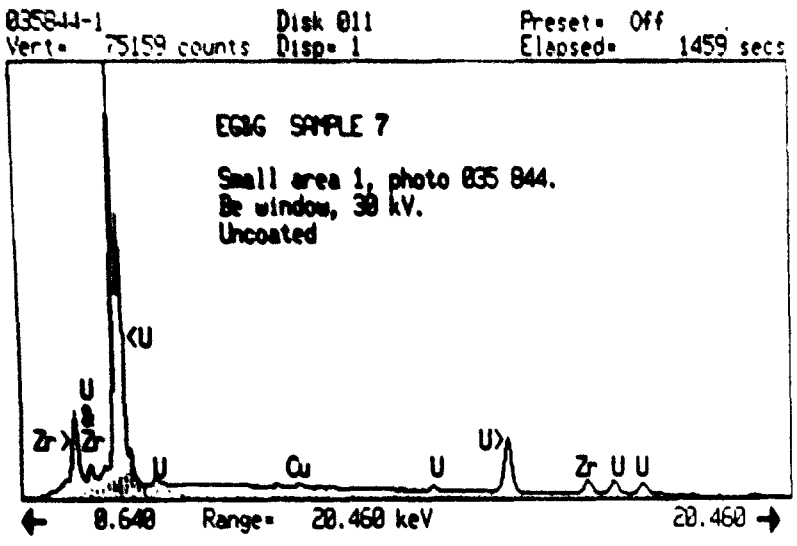

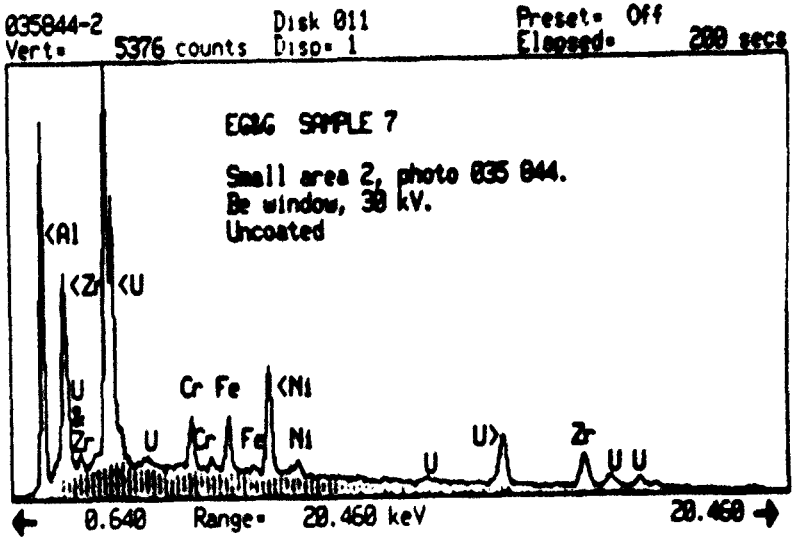

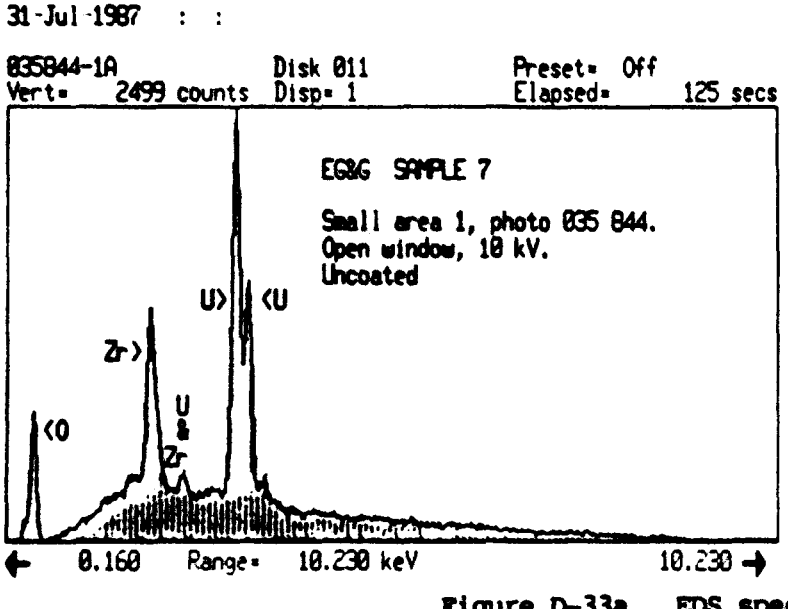

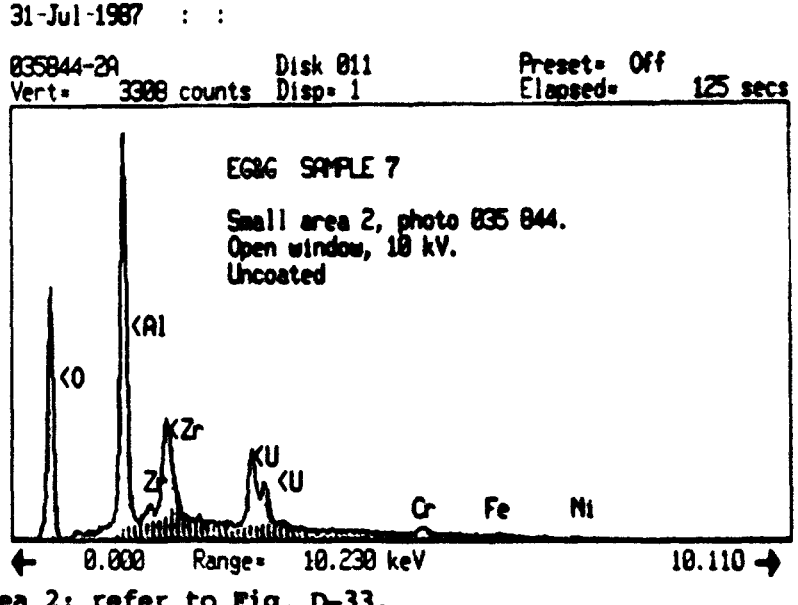

Figure D-33a. EDS spectra from Area 2; refer to Fig. D-33, photo 035 844.

F414 - F422

50X

Figure D-34. As polished optical photomicrograph of particle 8. Area 1 through 4 examined in detail.

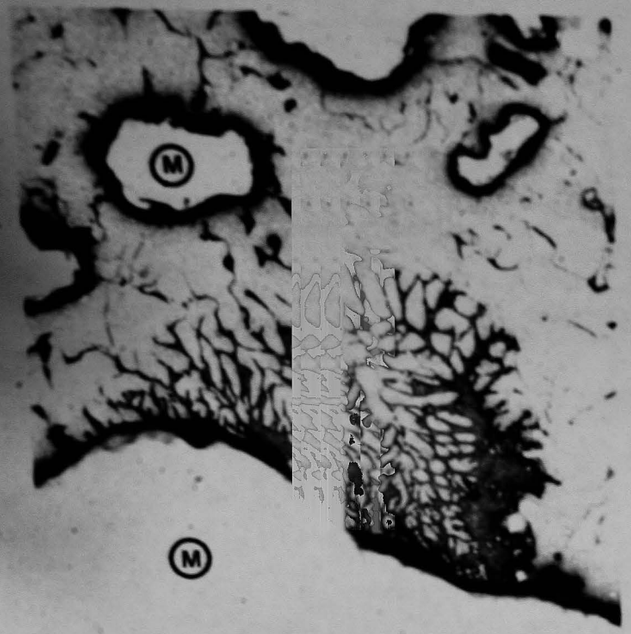

F455 Area 1 200X

F456 Area 1 400X

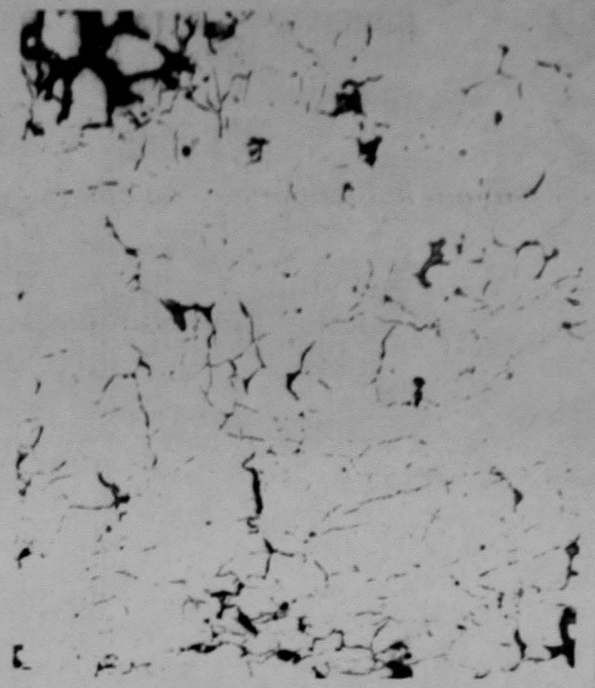

F458 Area 2 200X

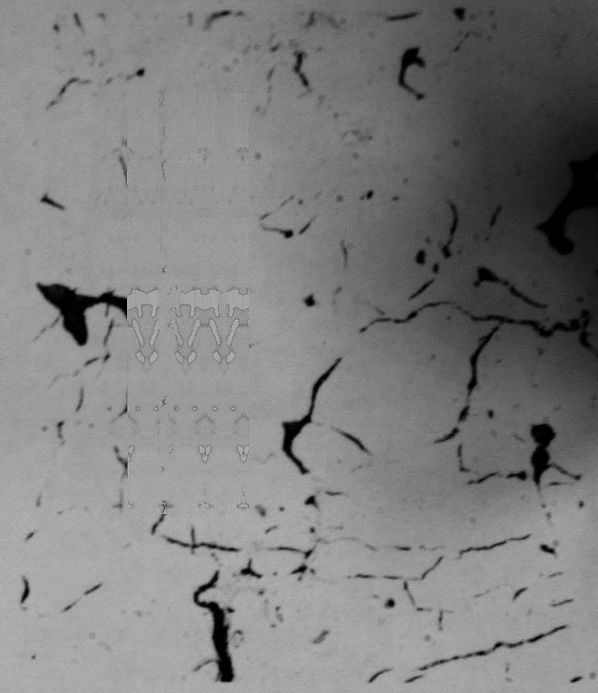

F459 Area 2 400X

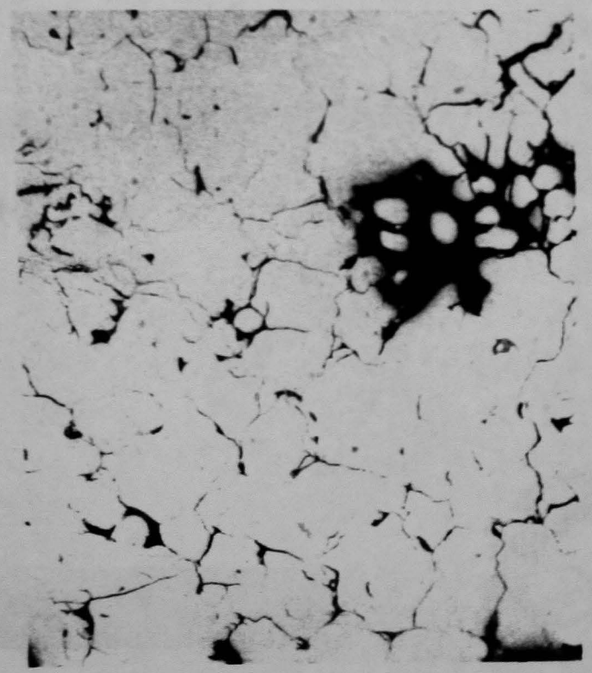

F461 Area 3 200X

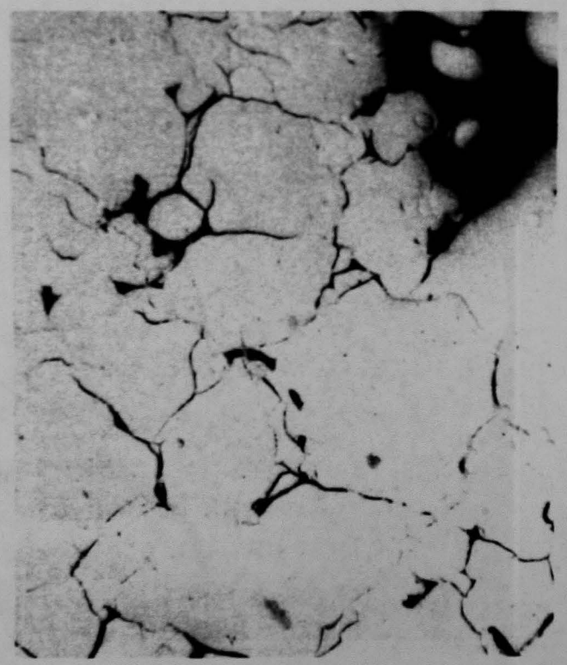

F462 Area 3 400X

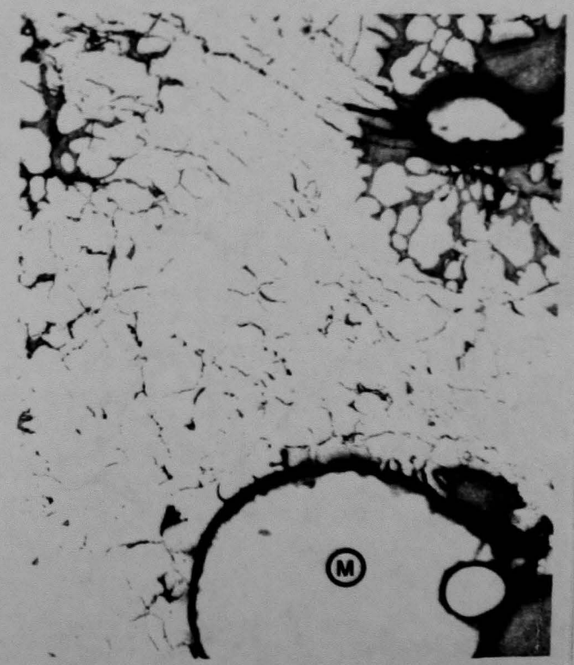

F464 Area 4 200X

F465 Area 4 400X

Figure D-35. As polished high magnification photomicrographs of Areas 1 through 4 from Fig. D-34.

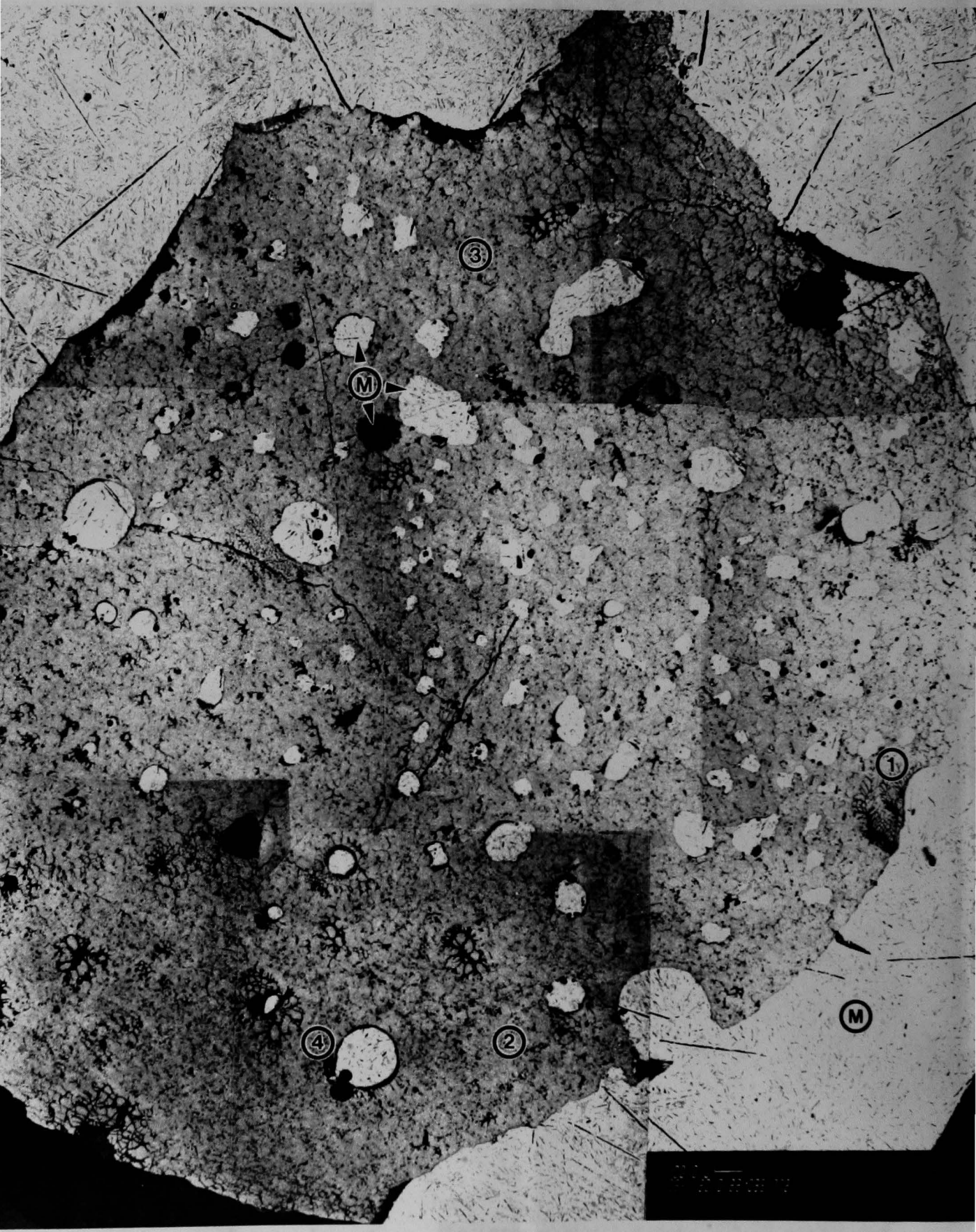

Figure D-36. BSE/SEM photo of particle 8. Areas 1 through 4 are indicated from Fig. D-34.

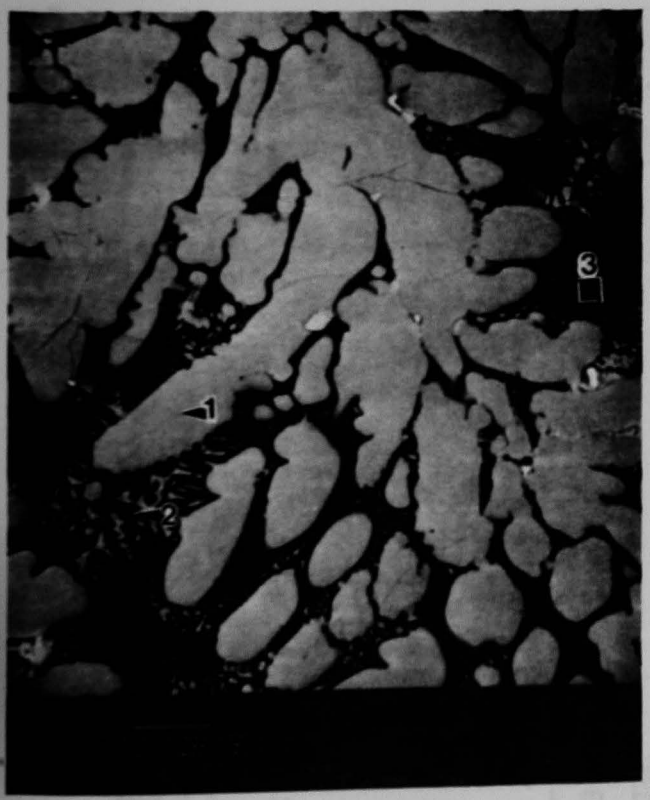

Figure D-37. BSE/SEM Photos of Area 1, Fig. D-36.

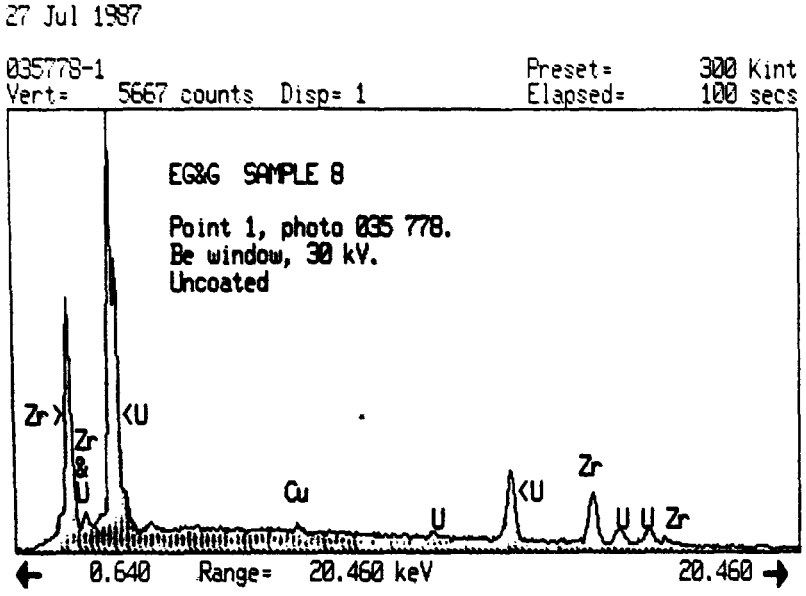

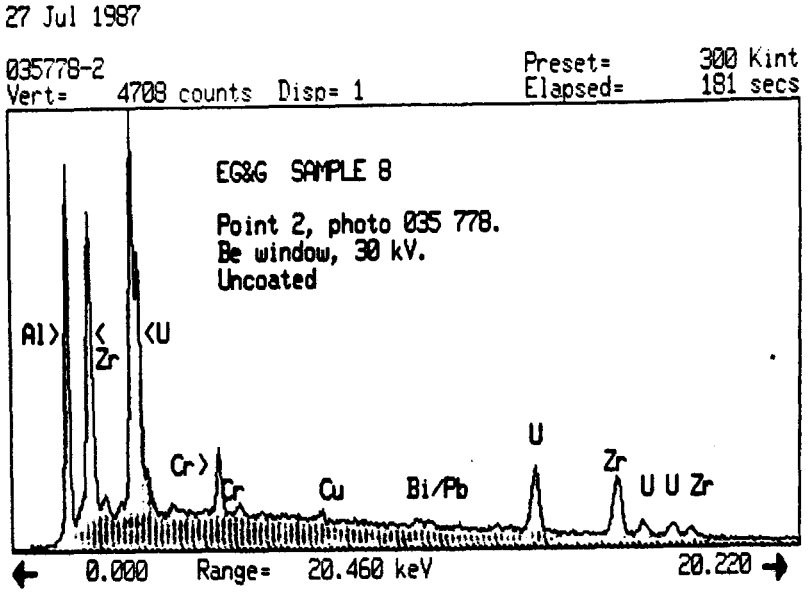

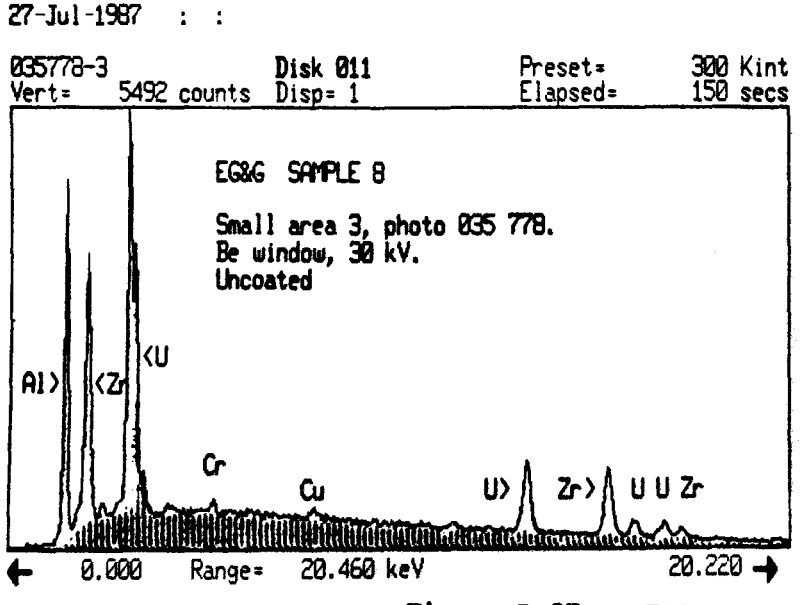

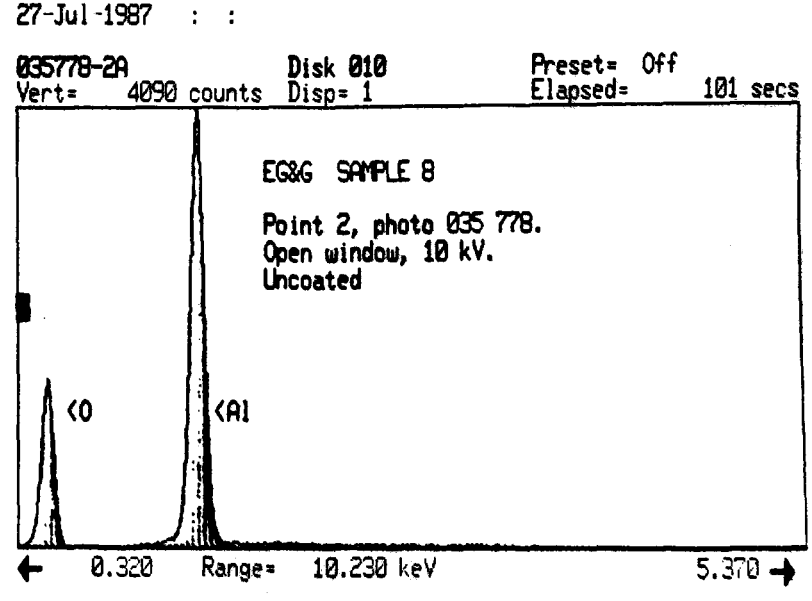

Figure D-37a. EDS spectra from Area 1 as indicated in Fig. D-36.

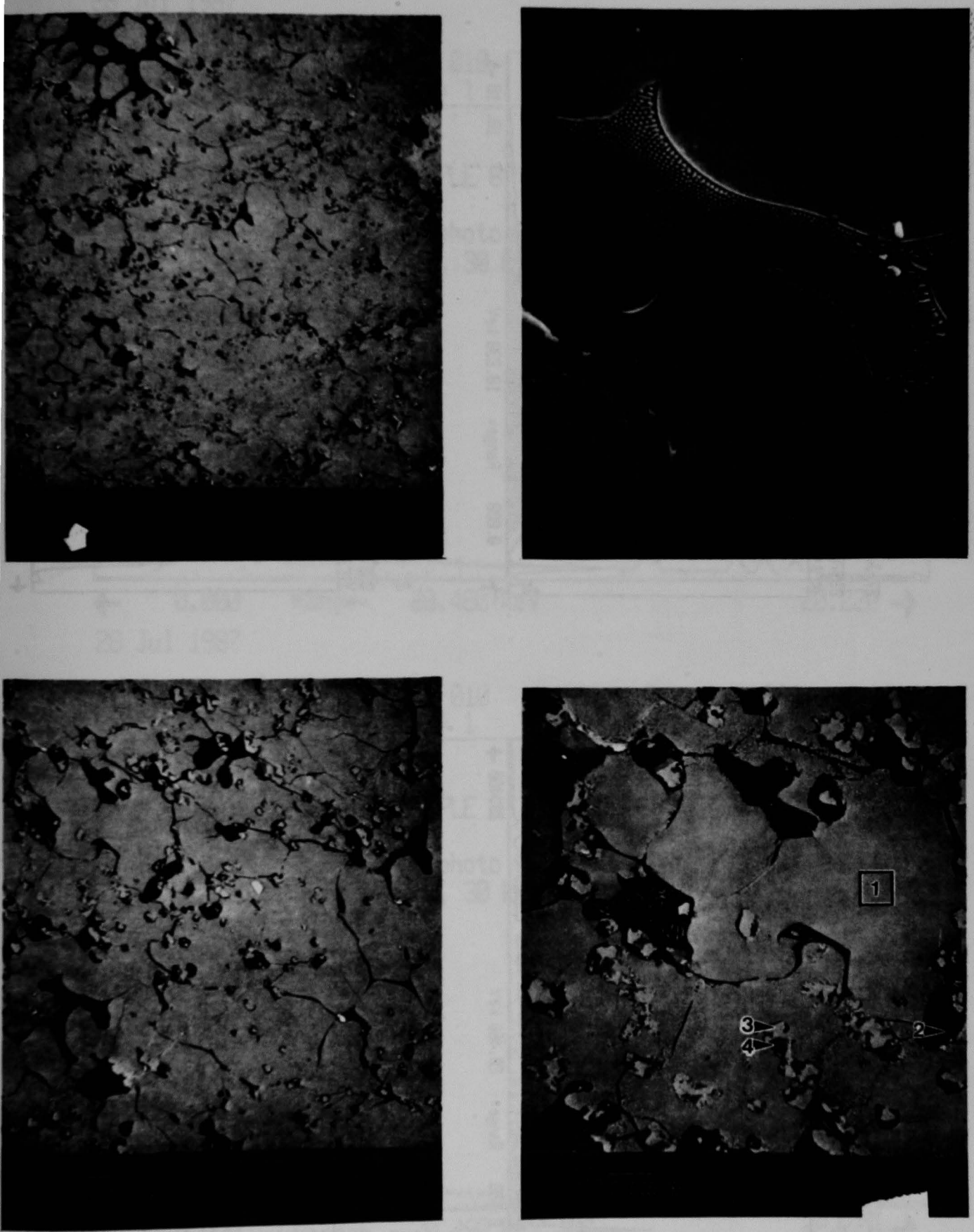

Figure D-38. BSE/SEM photos of Area 2, Fig. D-36.

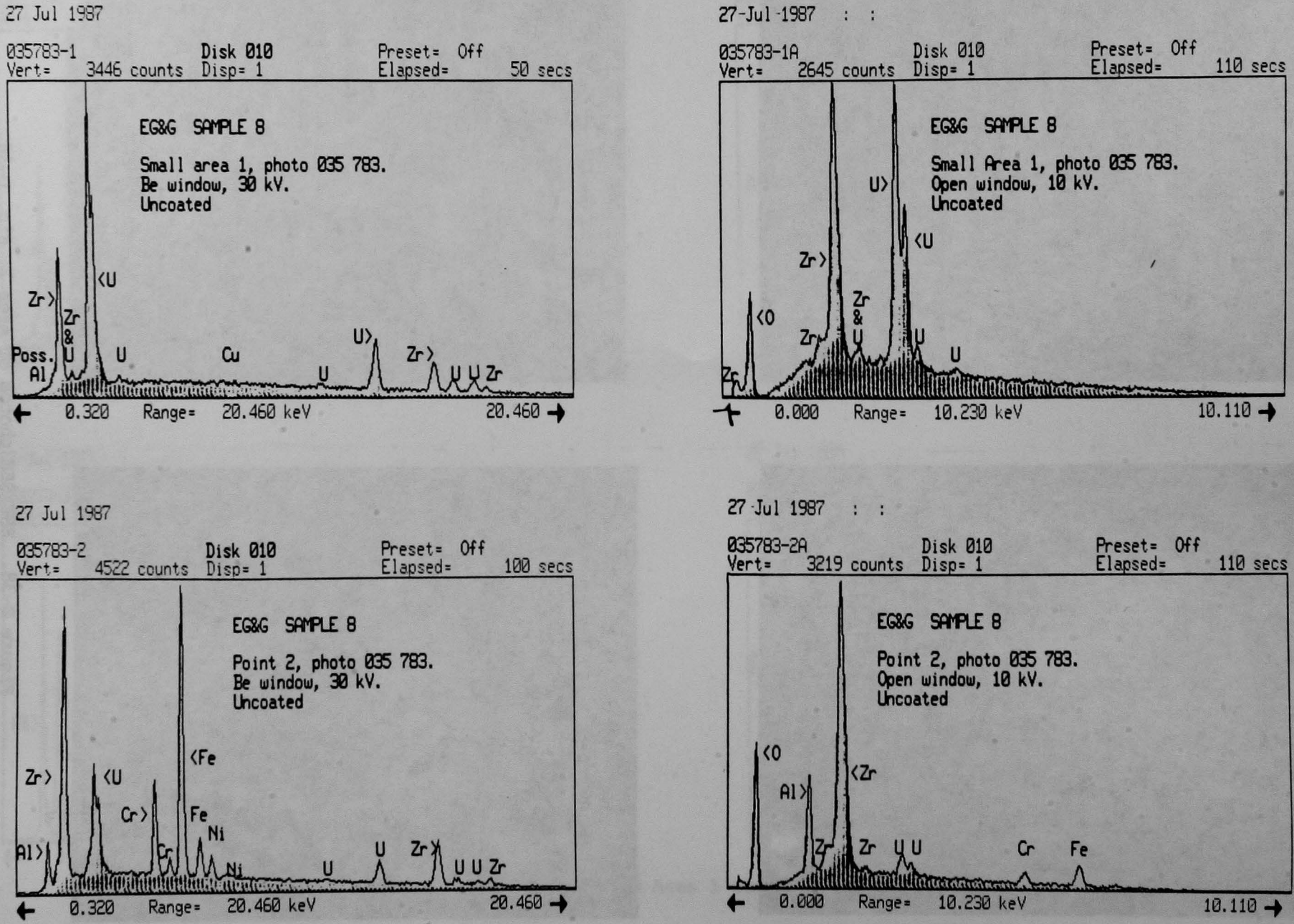

Figure D-38a. EDS spectra from Area 2 as indicated in Fig. D-38.

28 Jul 1987

035783-3 Disk 010 Preset= Off
Vert= 5933 counts Disp= 1 Elapsed= 55 secs

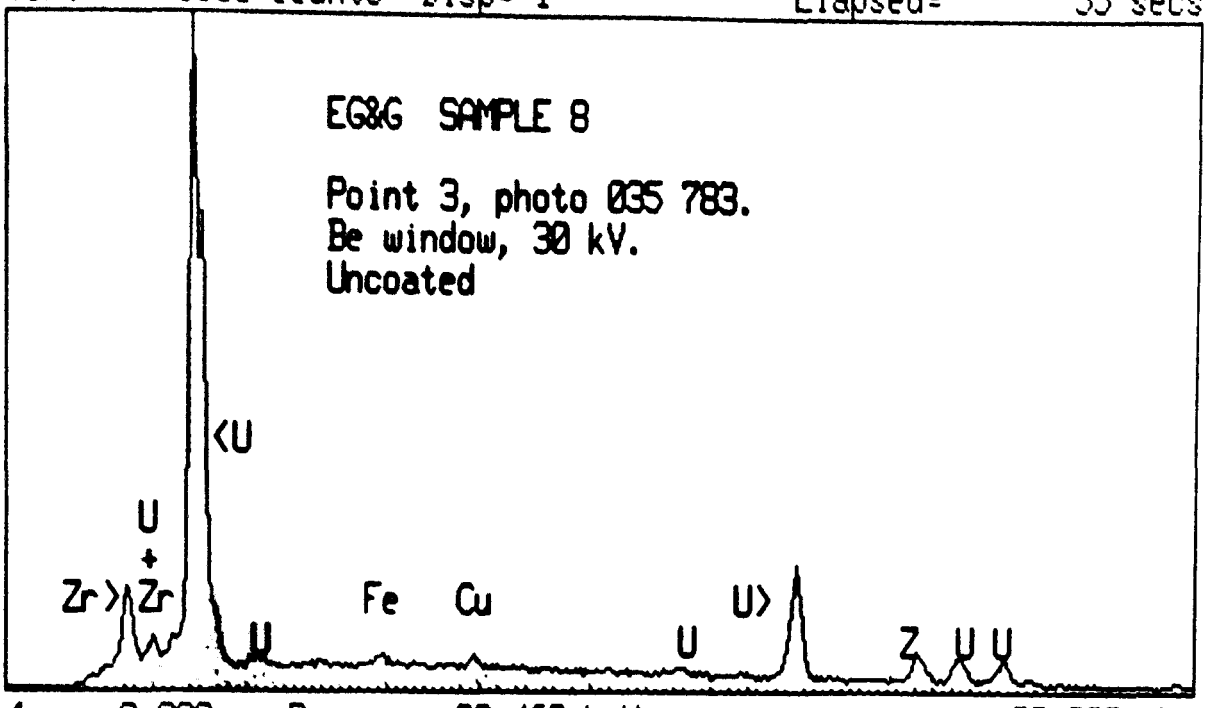

28 Jul 1987

035783-4 Disk 010 Preset= Off
Vert= 4211 counts Disp= 1 Elapsed= 55 secs

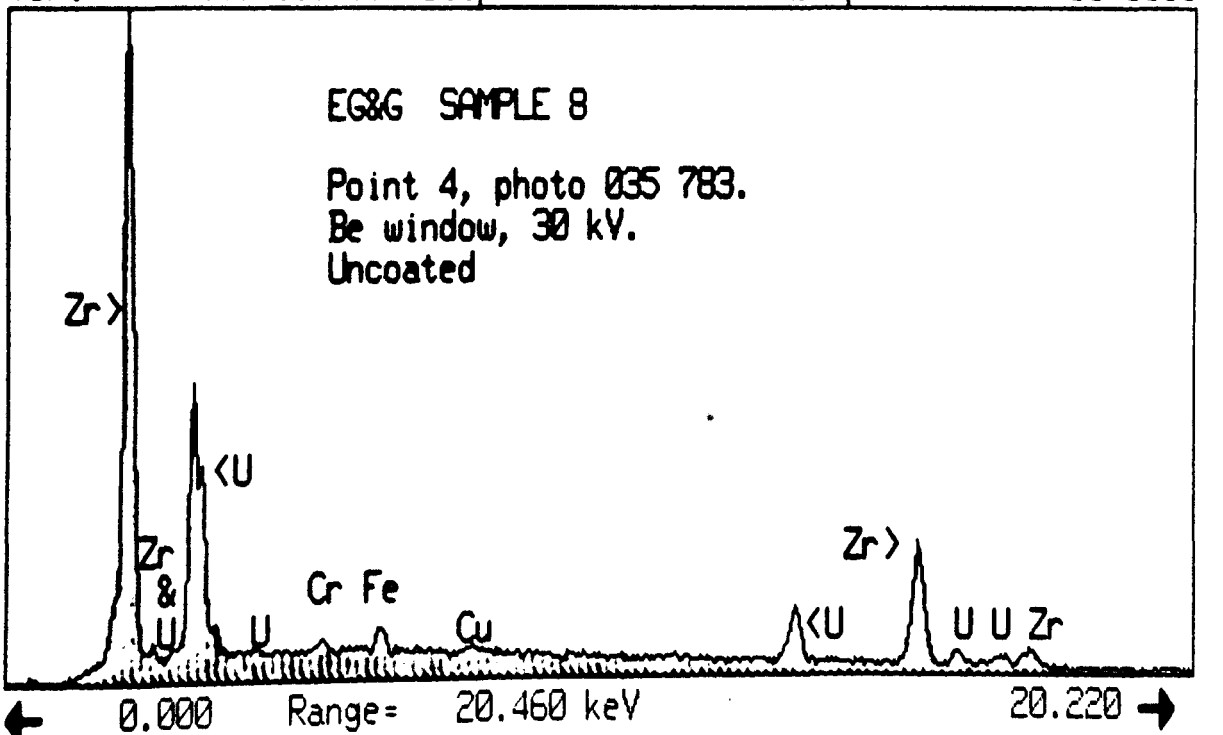

Figure D-38b. EDS spectra from Area 2 as indicated in Fig. D-38.

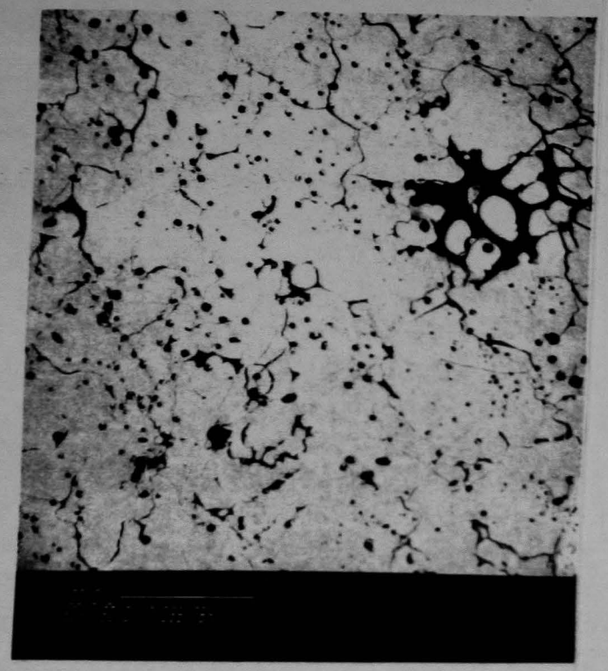

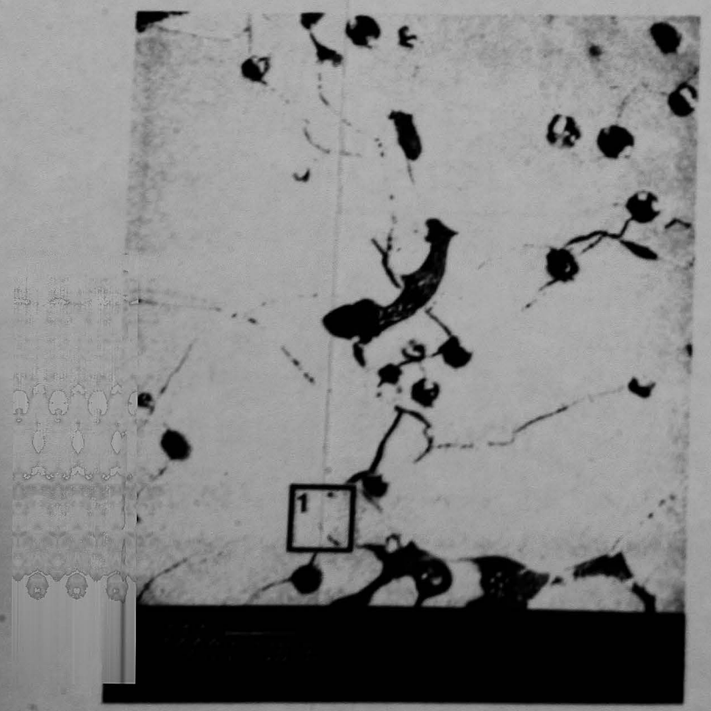

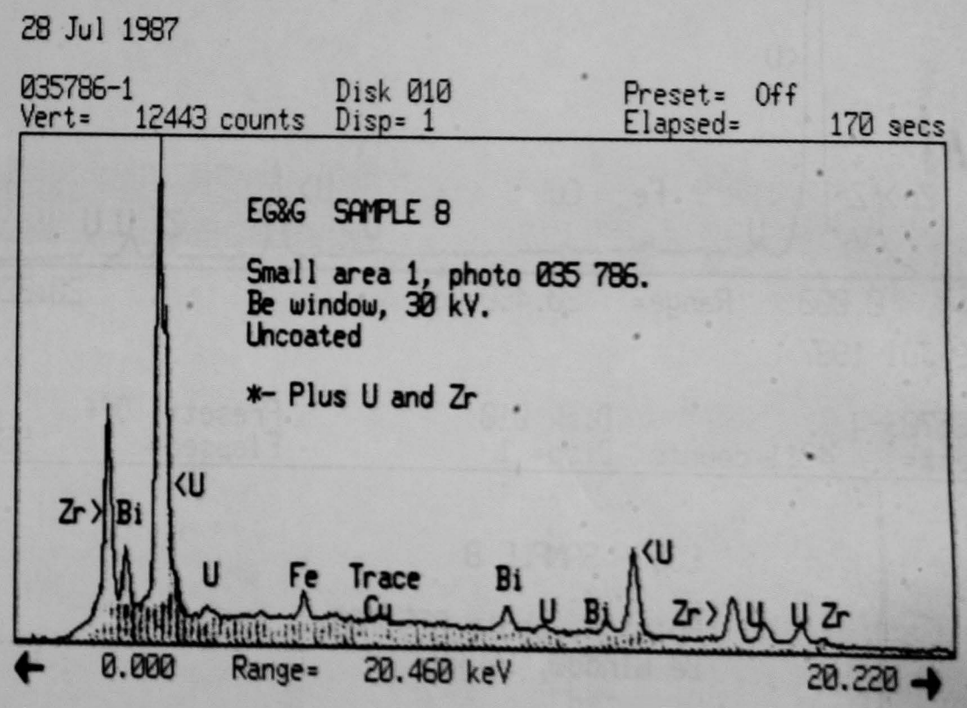

Figure D-39. BSE/SEM photos and EDS spectrum from Area 3, Fig. D-36.

Figure D-40. BSE/SEM Photos of Area 4, Fig. D-36.

Figure D-41. As polished optical photomicrograph of particle 11. Areas 1 and 2 are examined in detail.

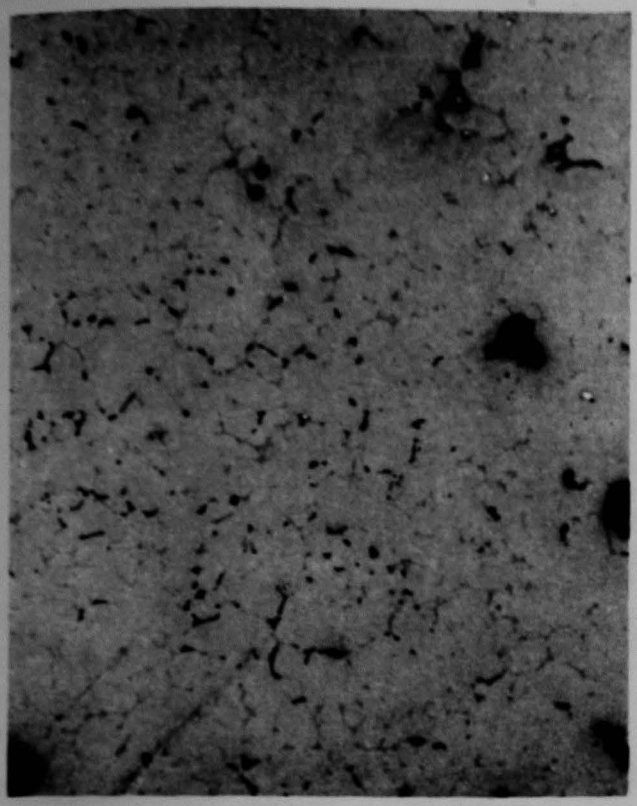

F440 Area 1 200X

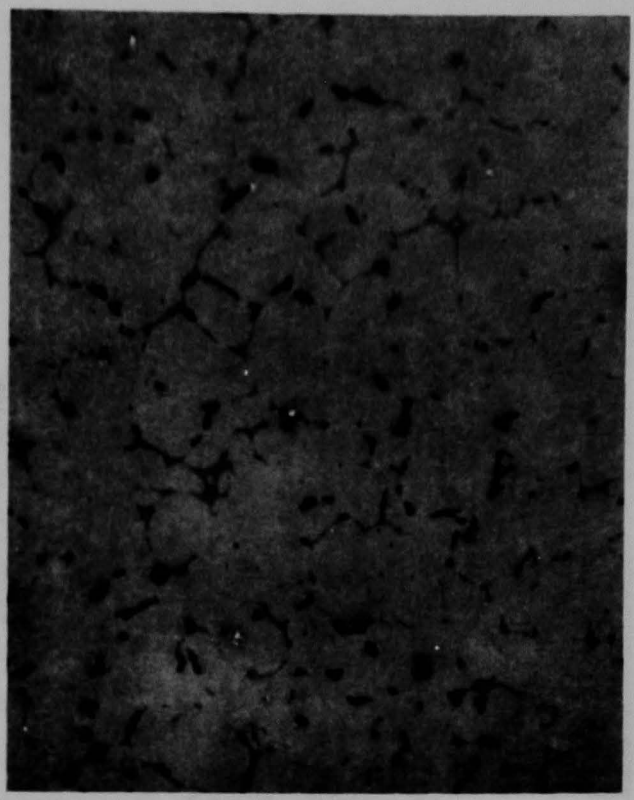

F441 Area 1 400X

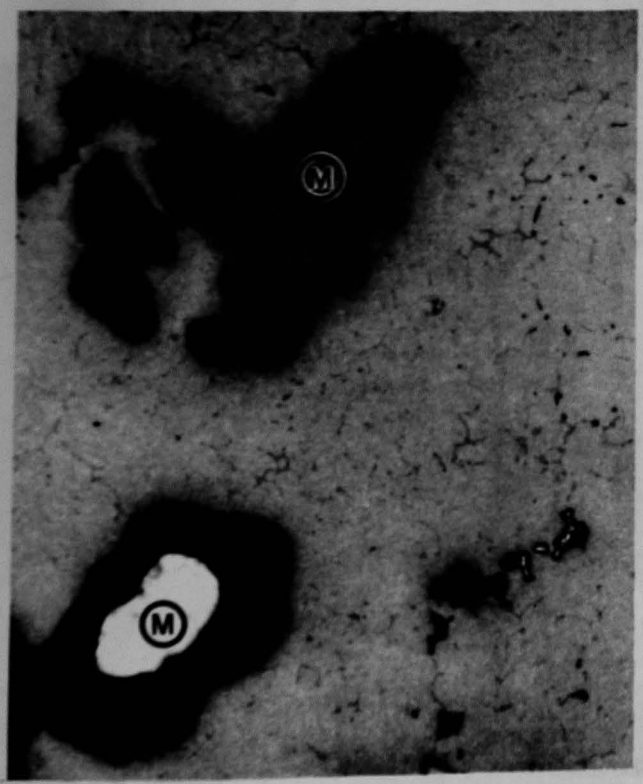

F443 Area 2 200X

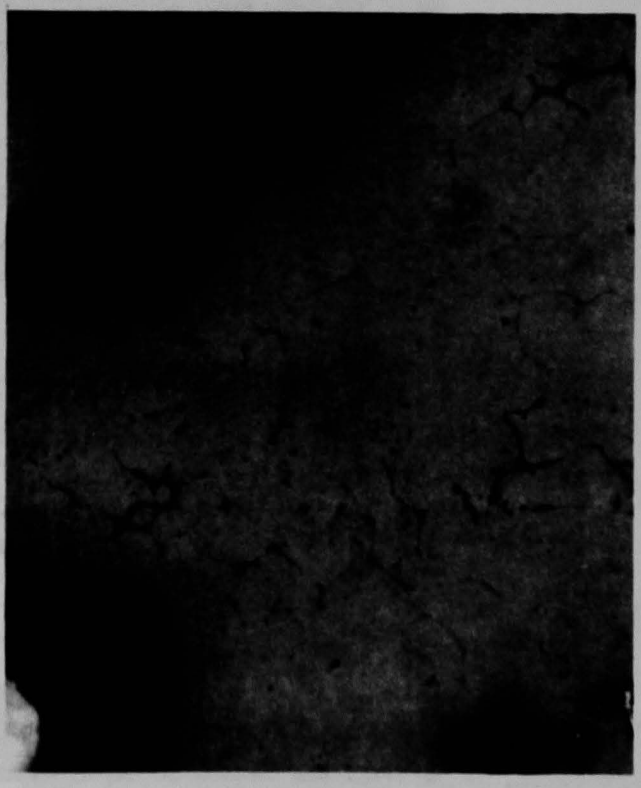

F444 Area 2 400X

Figure D-42. As polished high magnification photomicrographs of Areas 1 and 2 from Fig. D-41.

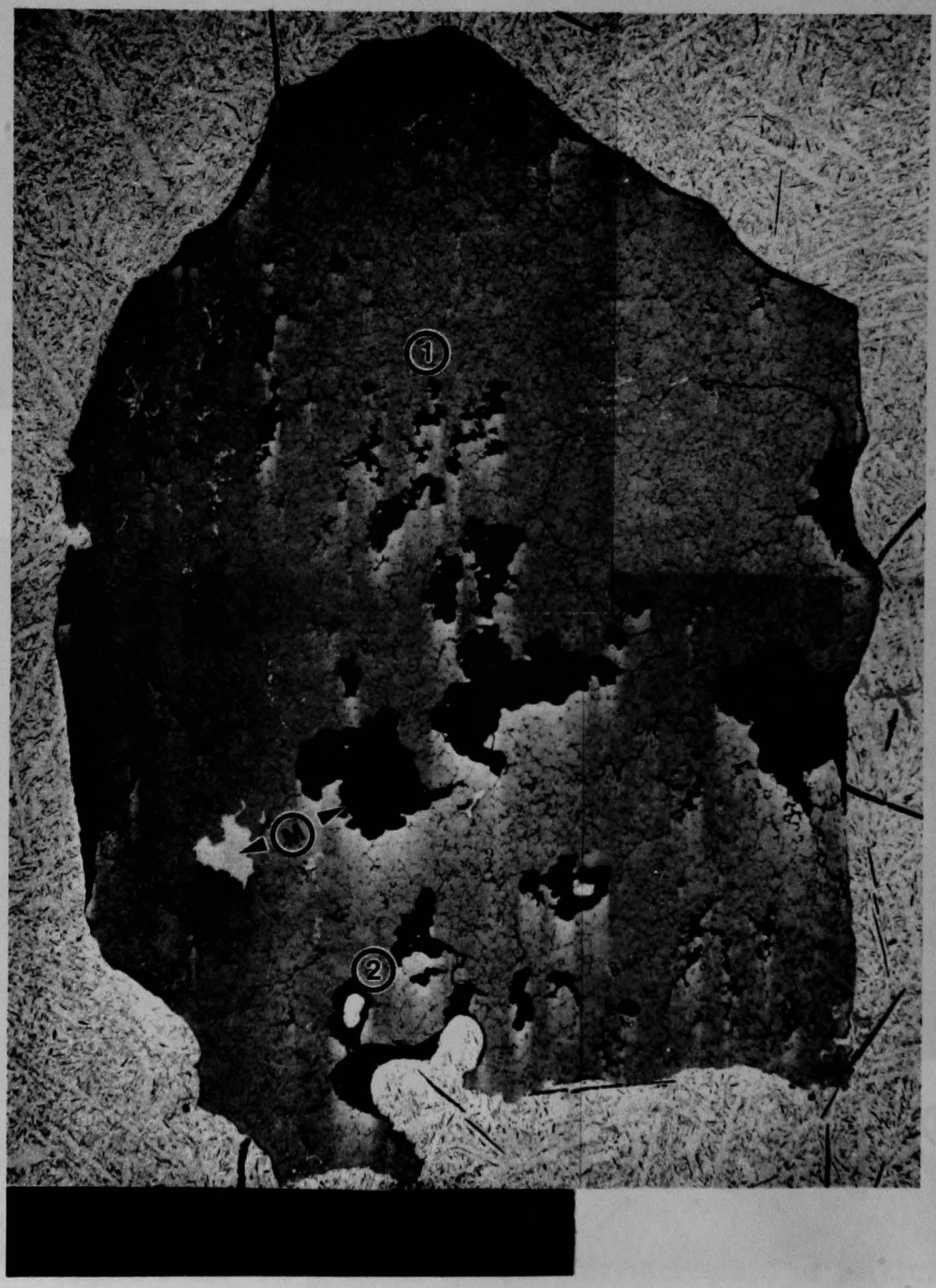

Figure D-43. BSE/SEM photo of particle 11 with Areas 1 and 2 from Fig. D-41 indicated.

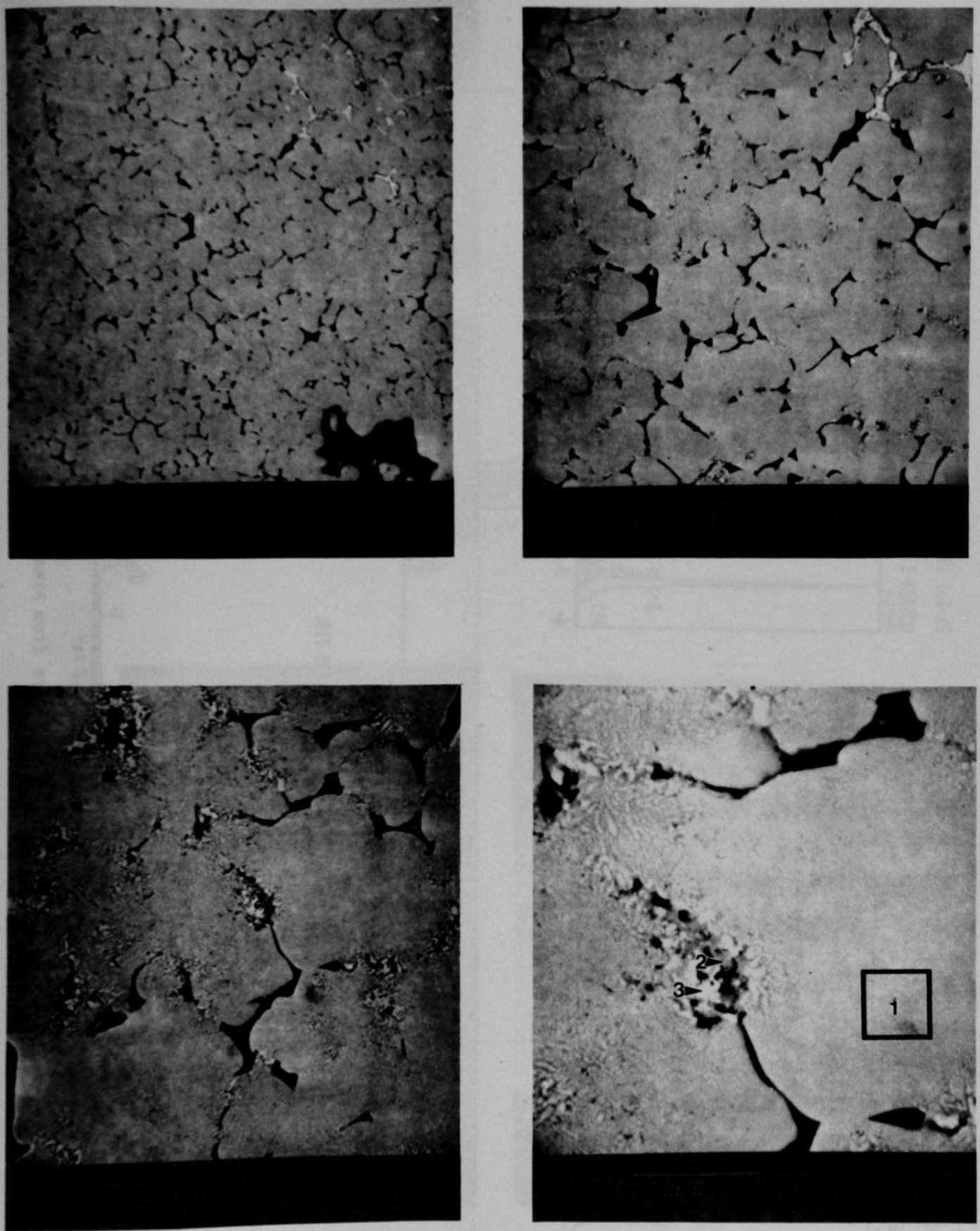

Figure D-44. BSE/SEM photos of Area 1, Fig. D-43.

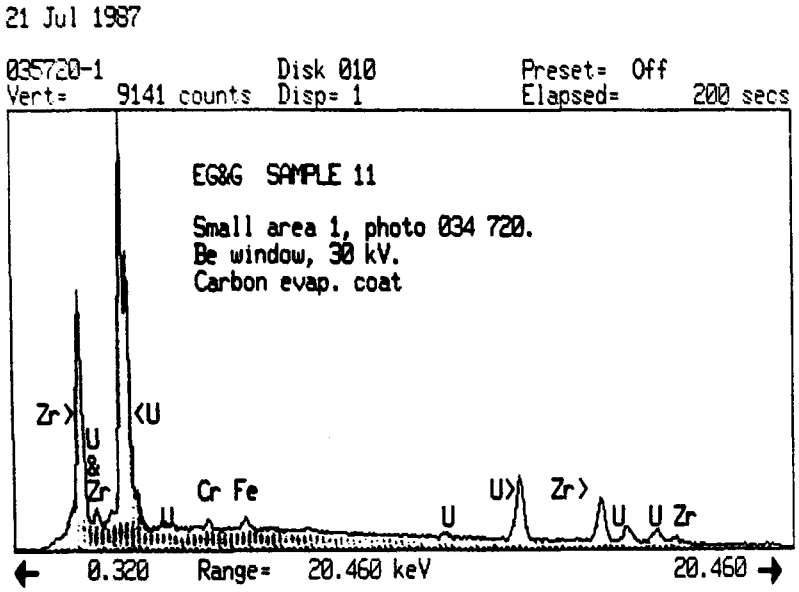

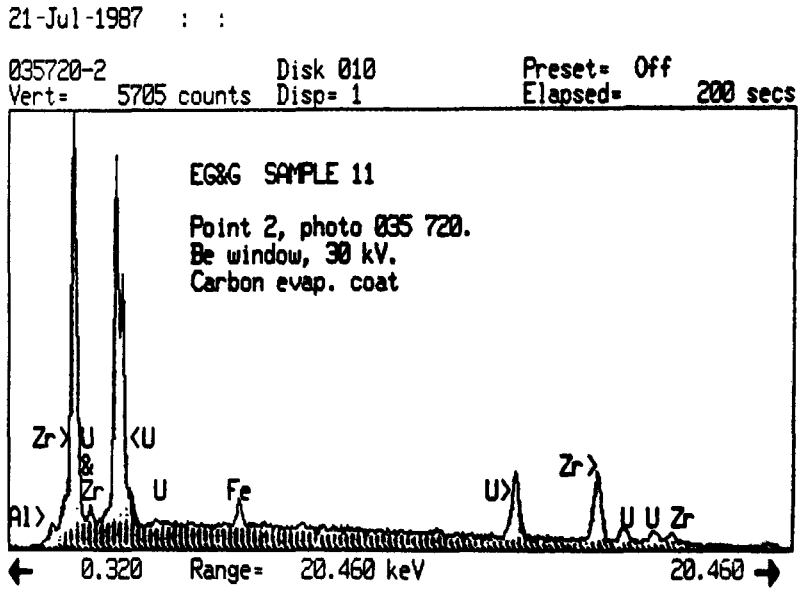

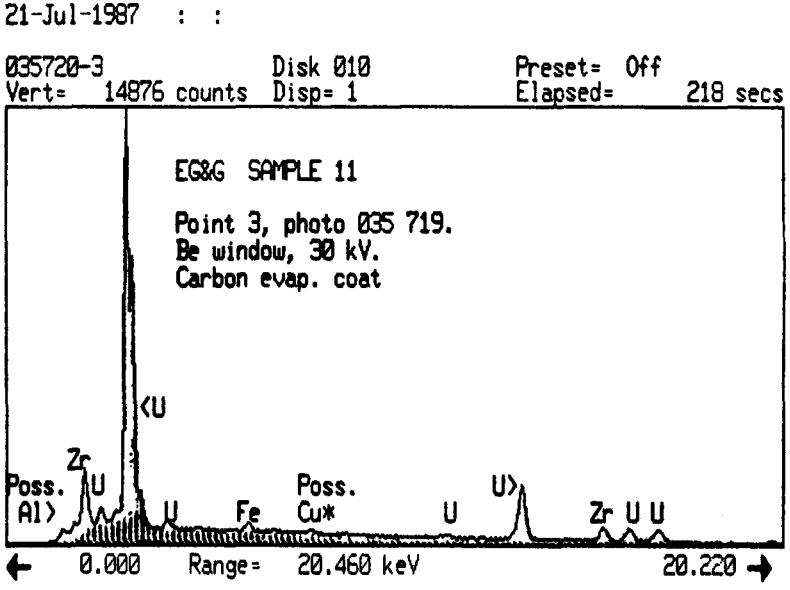

Figure D-44a. EDS spectra from Area 1 as indicated in Fig. D-44.

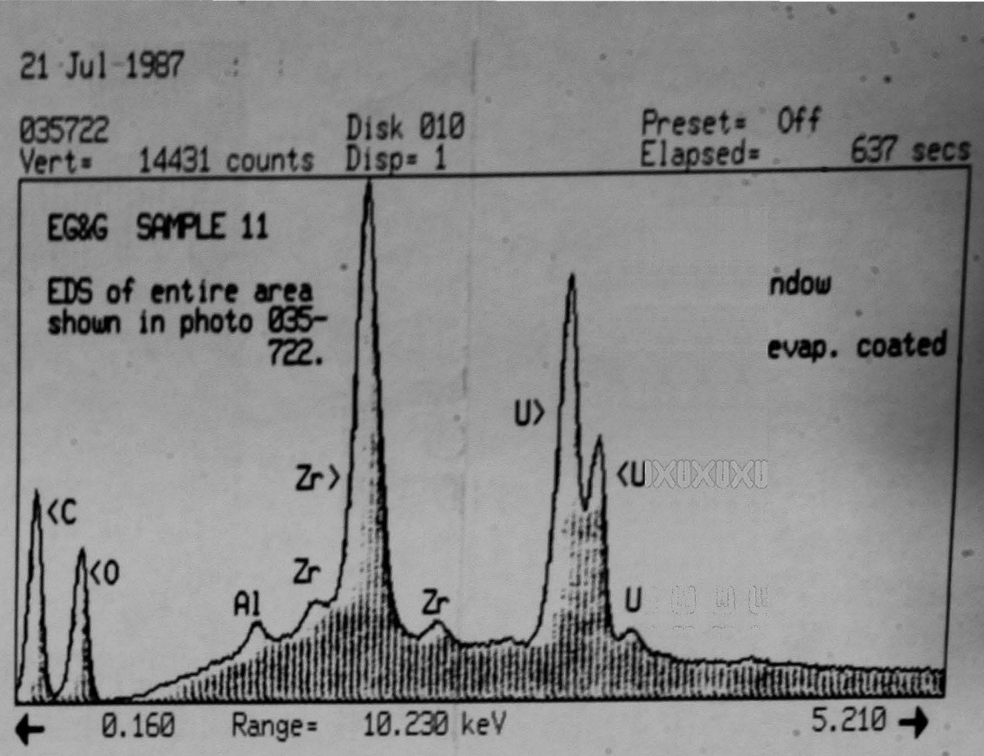

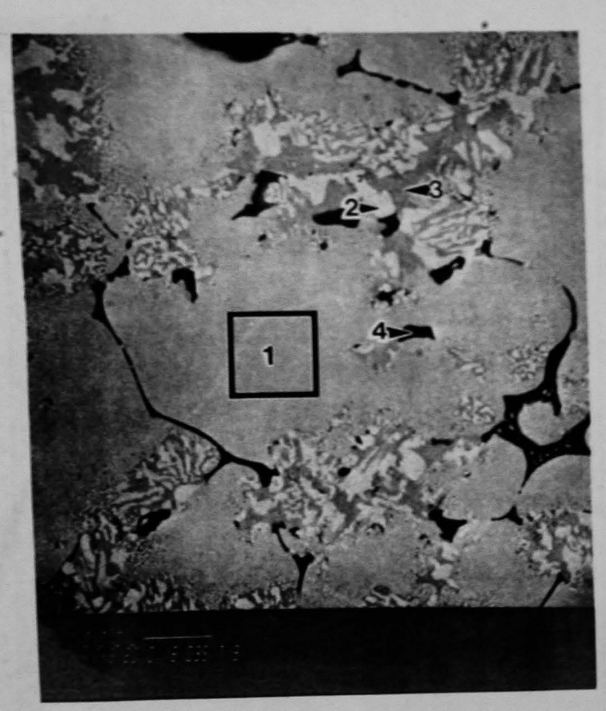

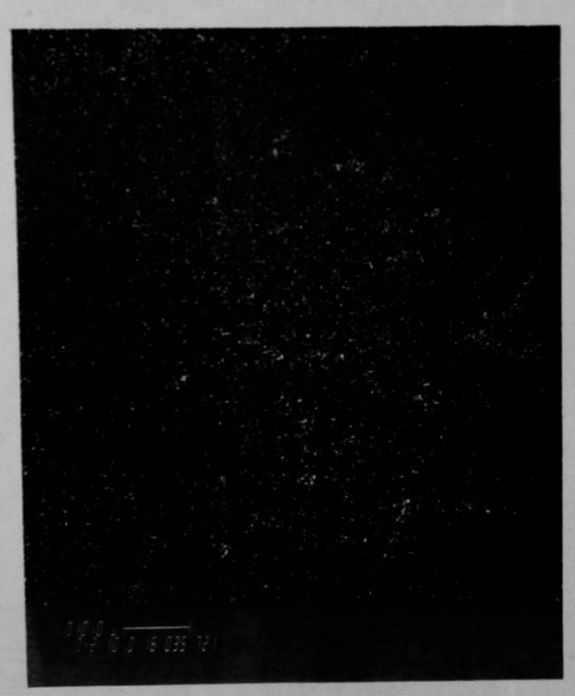

Oxygen Dot Map of 035 722

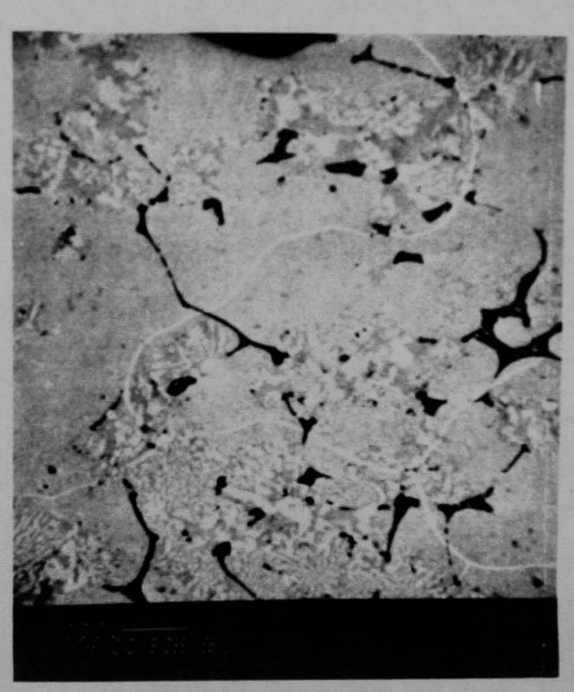

White lines are probable cracks in carbon coating.

BSE/Oxygen Profile of 035 722

Figure D-45. BSE/SEM photos and EDS spectra from Area 2, Fig. D-43.

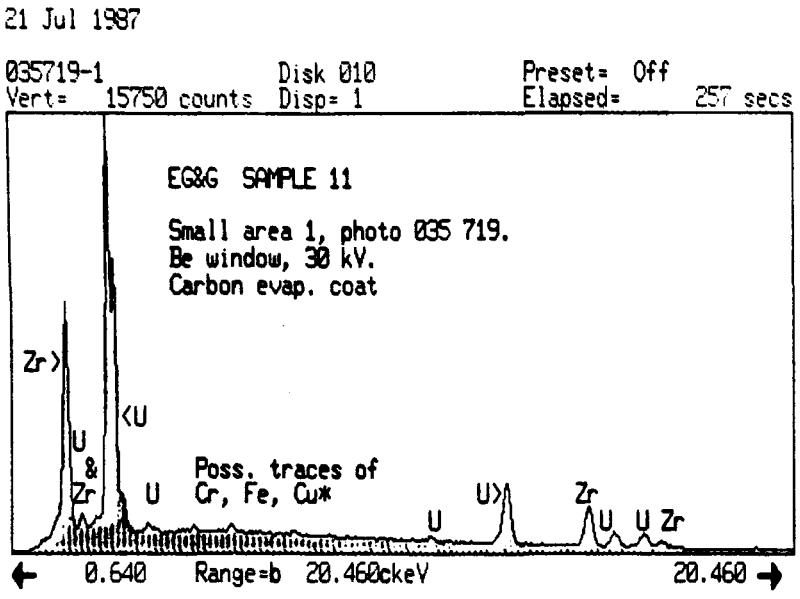

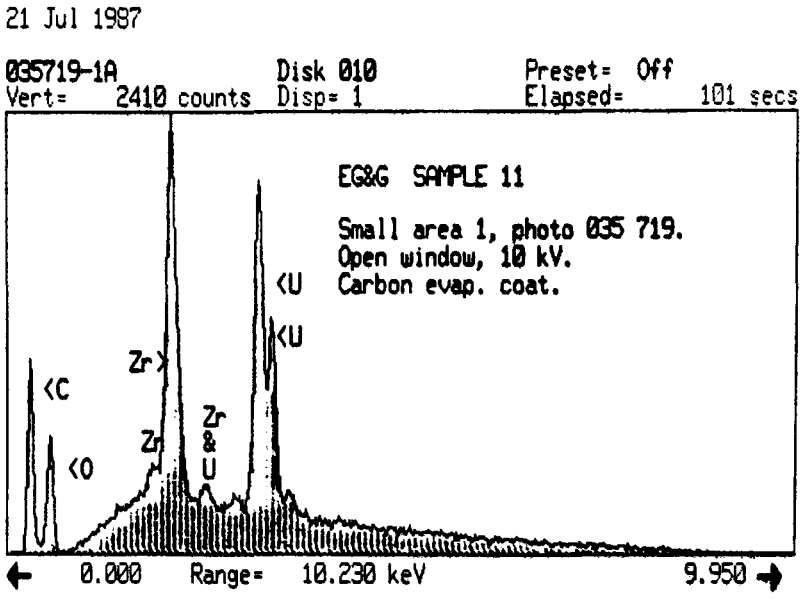

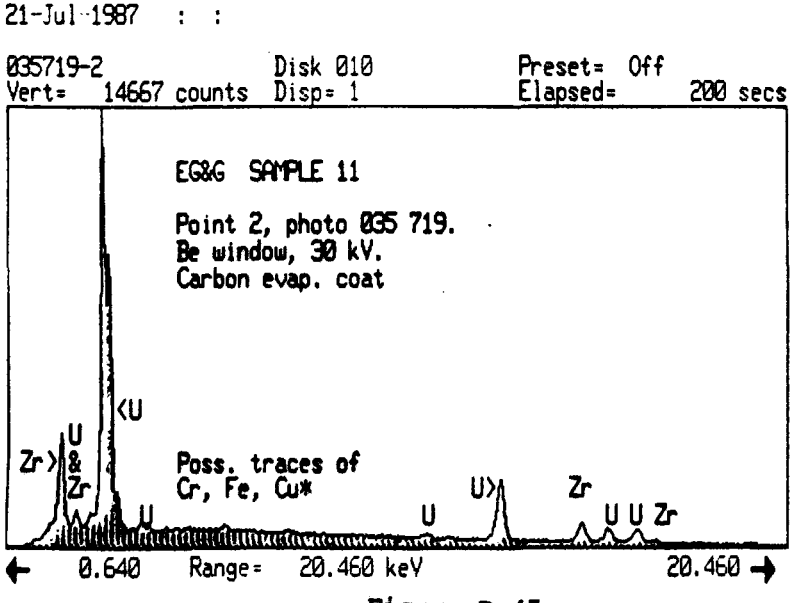

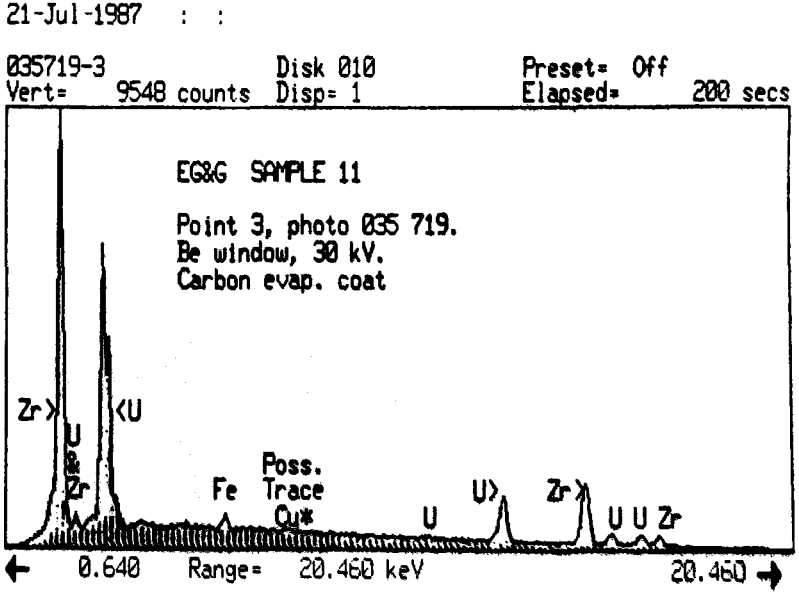

Figure D-45a. EDS spectra from Area 2 as indicated in Fig. D-45.

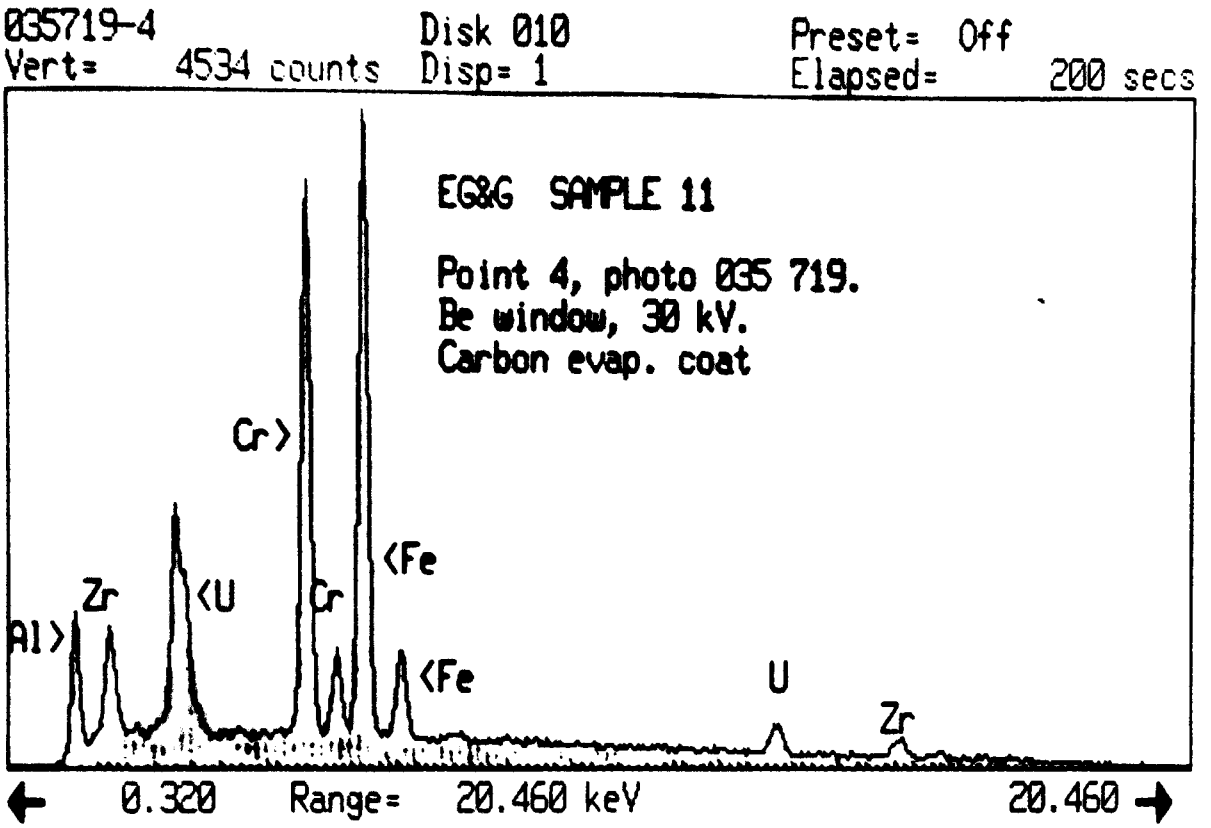

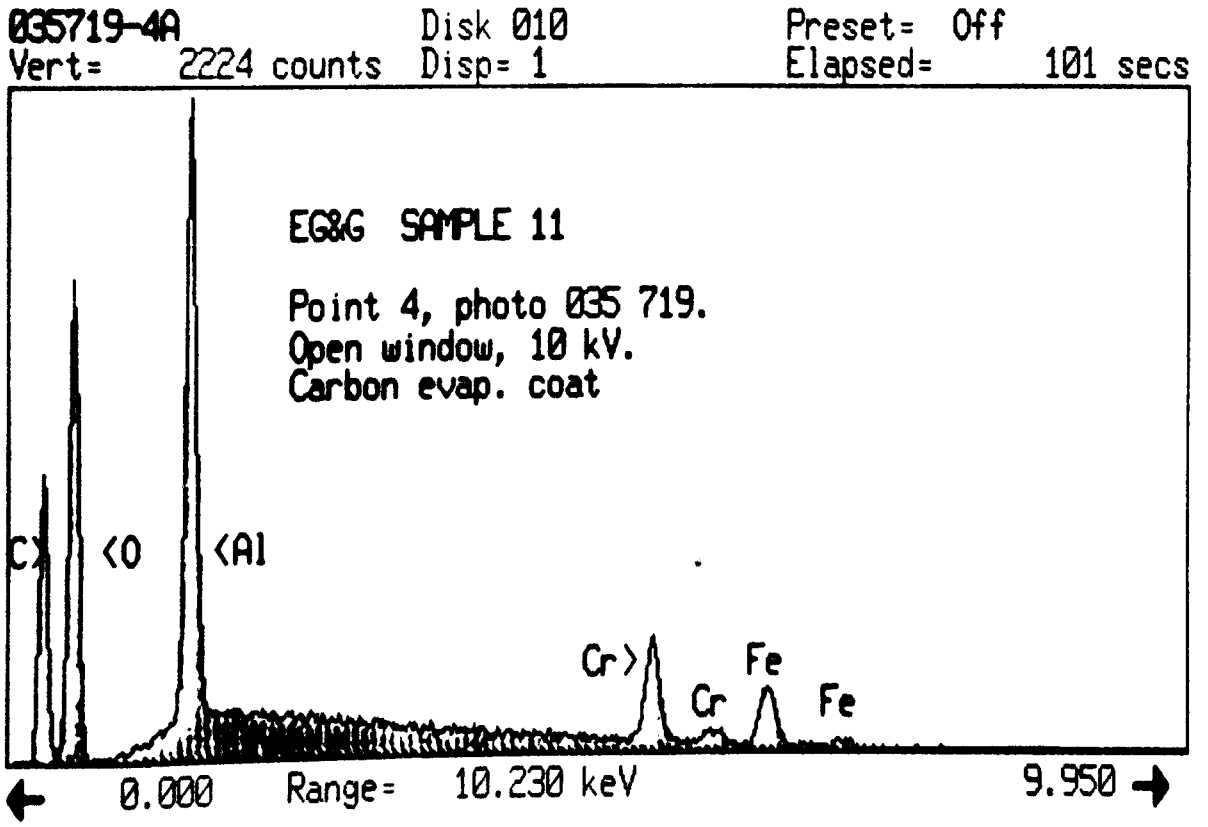

Figure D-45b. EDS spectra from Area 2 as indicated in Fig. D-45.

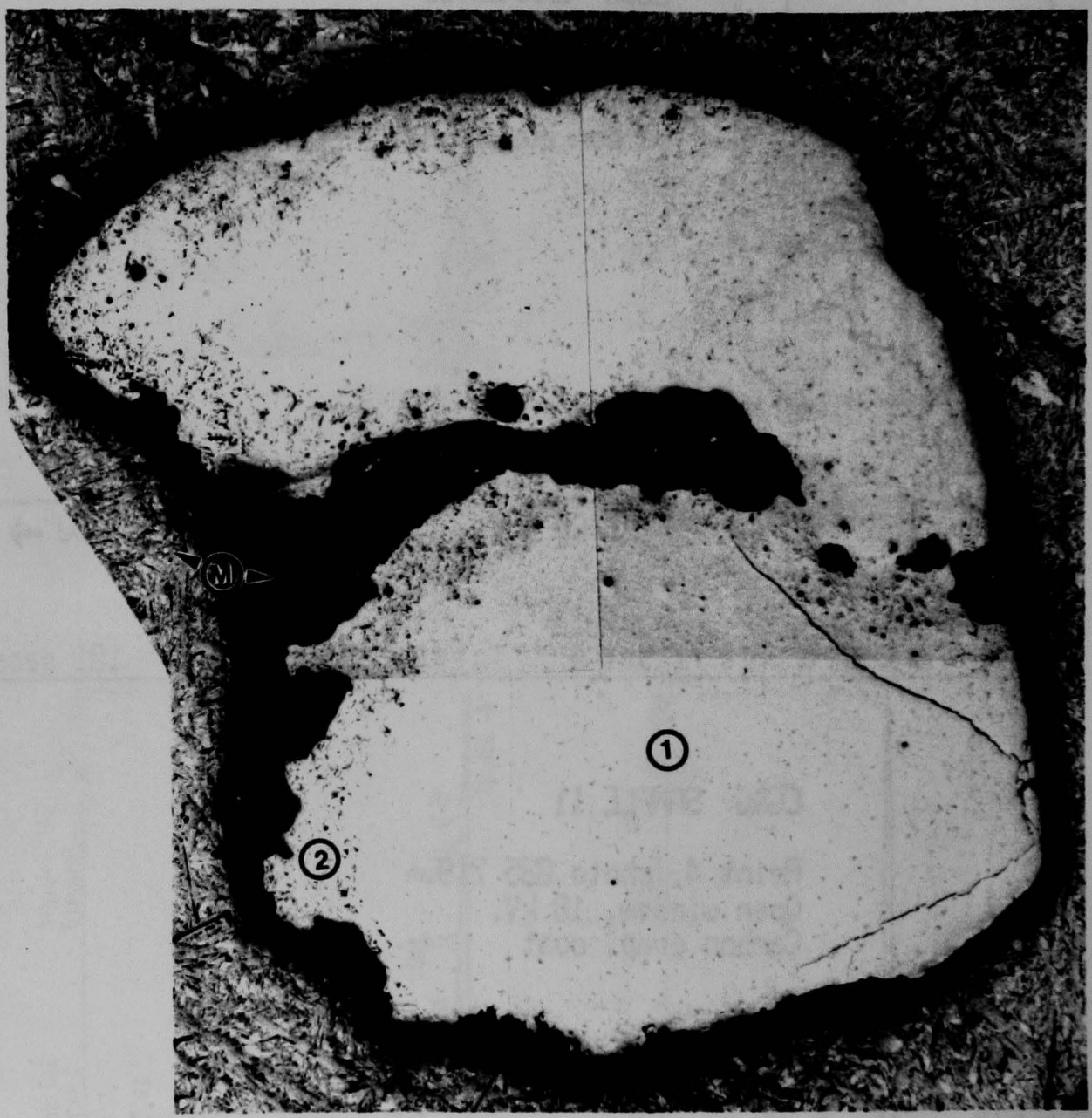

Figure D-46. As polished optical photomicrograph of particle 12. Areas 1 and 2 examined in detail.

F449 Area 1 200X

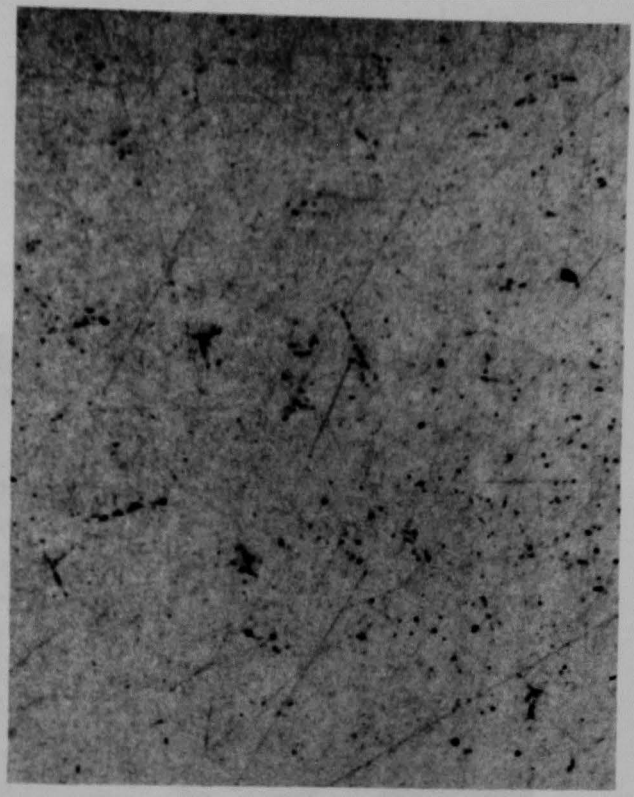

F450 Area 1 400X

F452 Area 2 200X

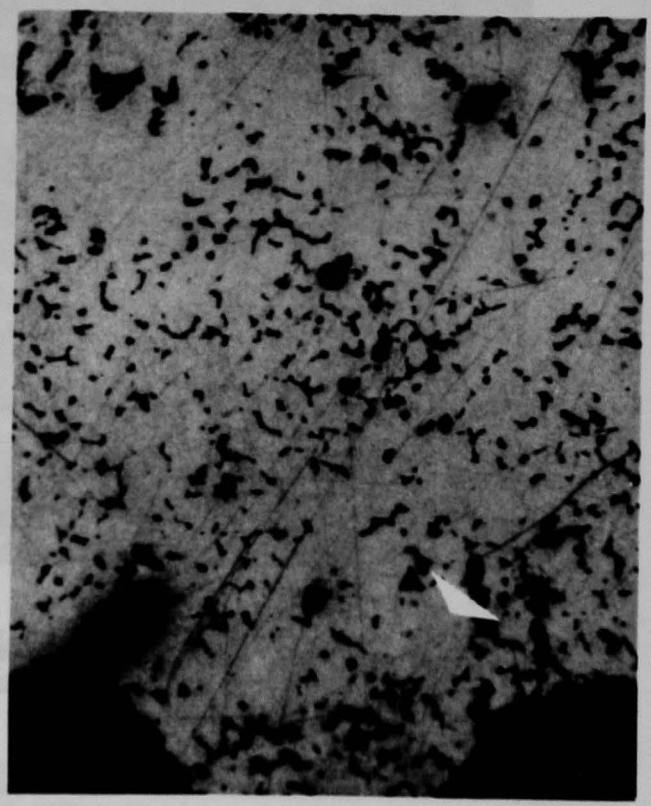

F453 Area 2 400X

Figure D-47. As polished high magnification photomicrographs of Areas 1 and 2 as noted in Fig. D-46.

Figure D-48. BSE/SEM photo of particle 12. Areas 1 and 2 from Fig. D-46 are indicated.

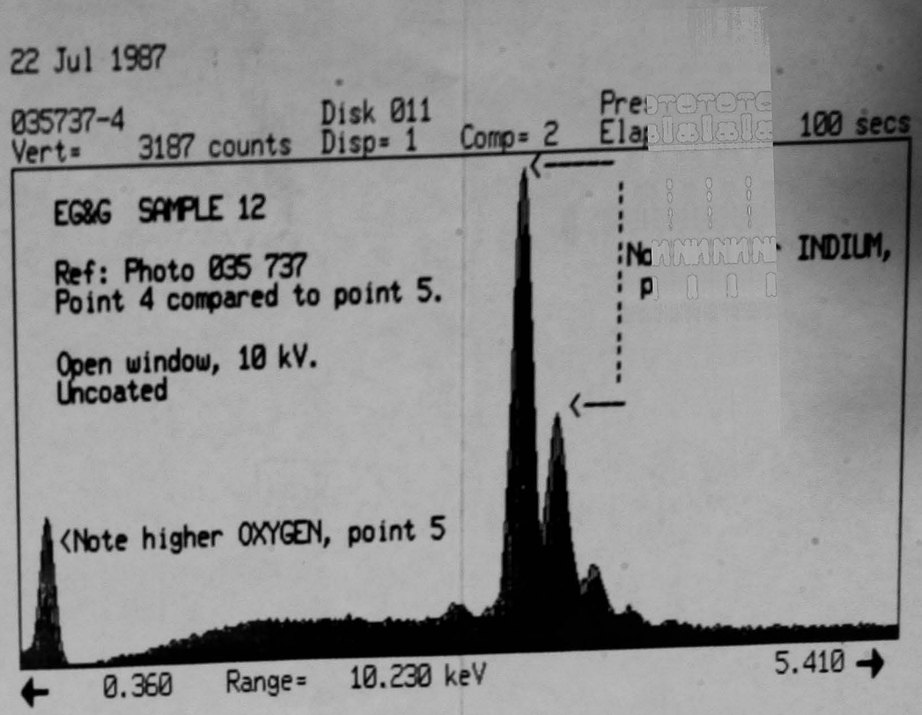

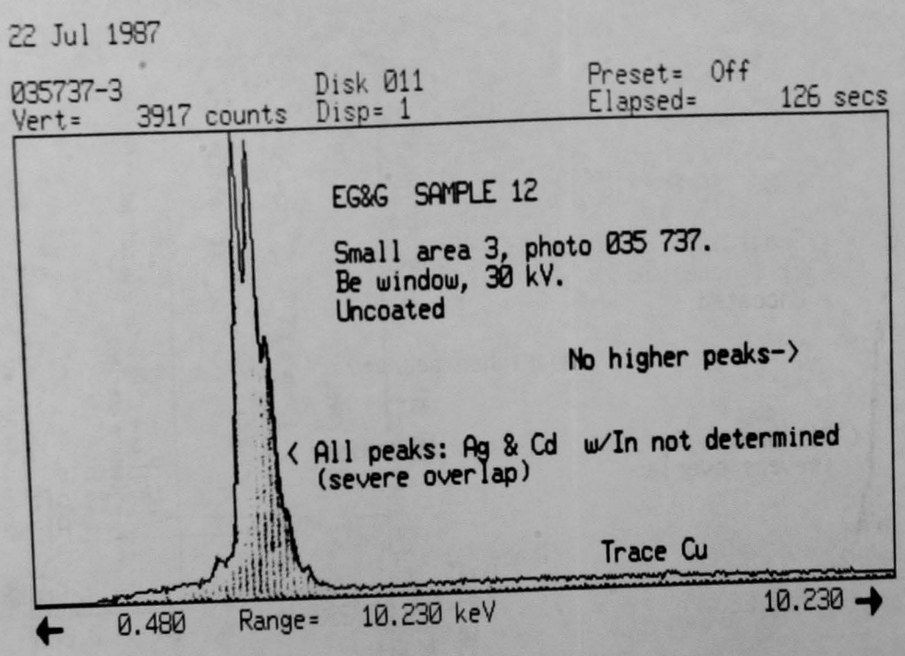

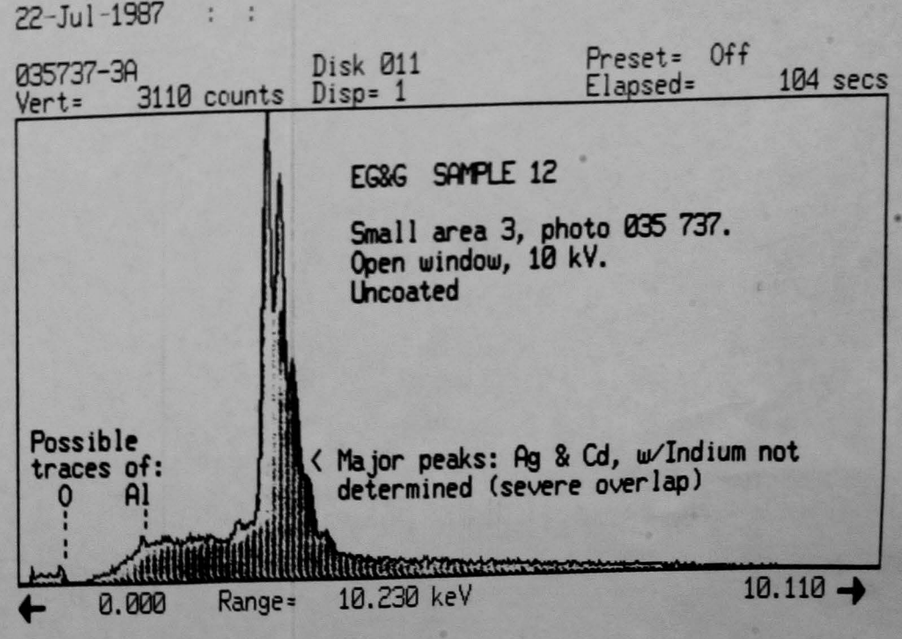

BSE/Oxygen Profile

Figure D-49. BSE/SEM photos and EDS spectra from Area 1, Fig. D-48.

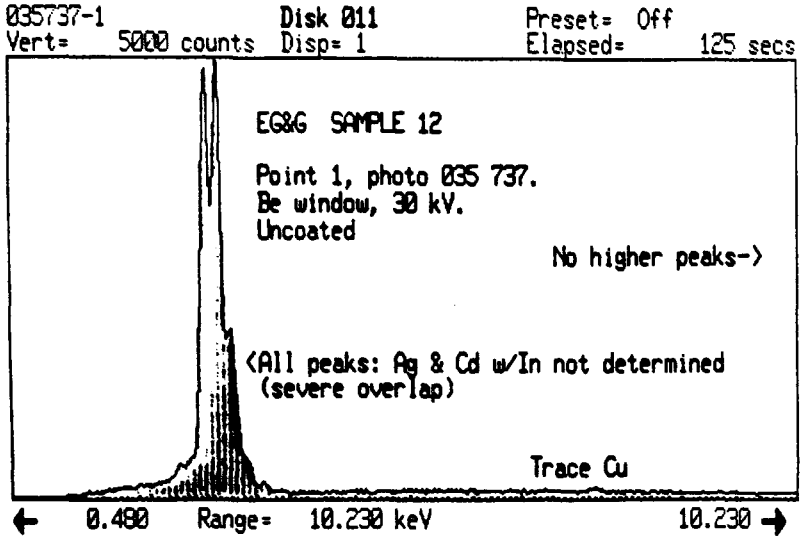

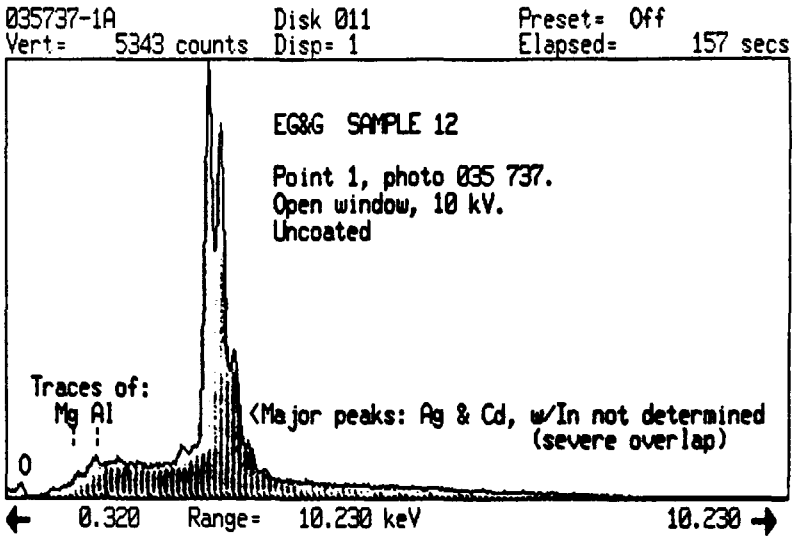

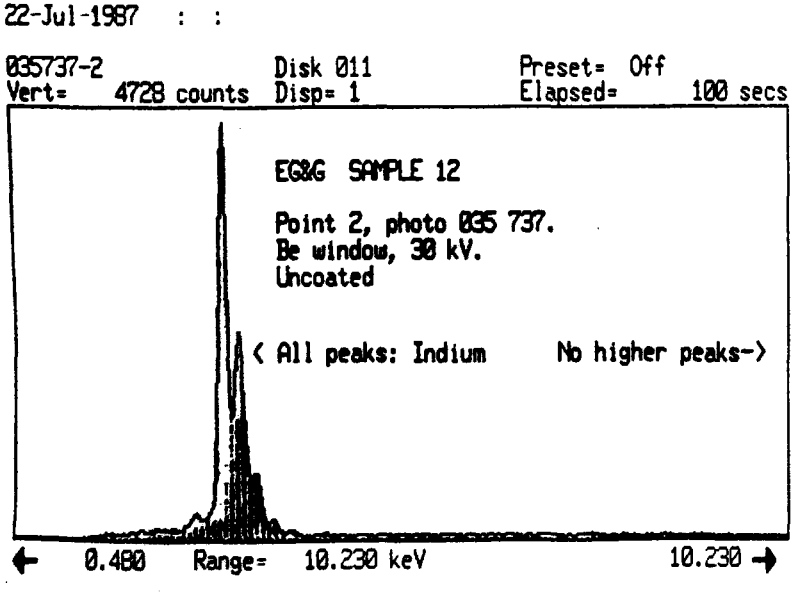

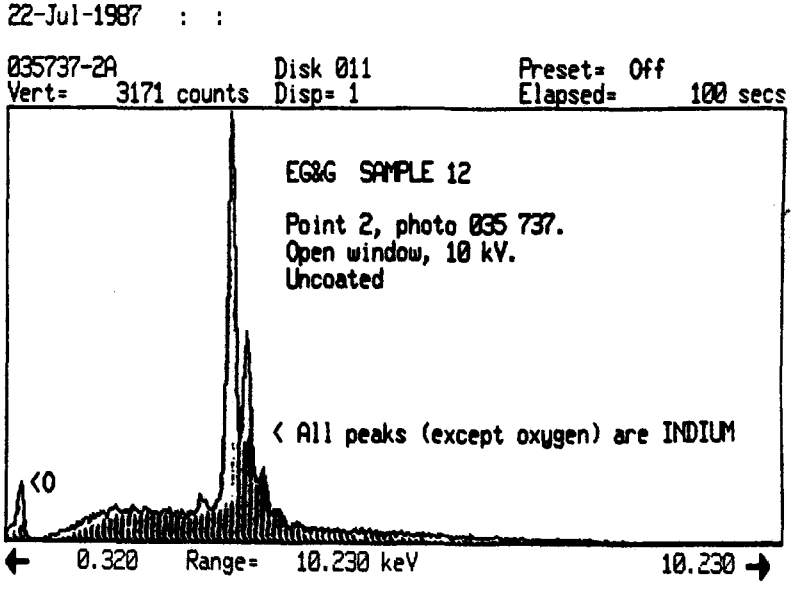

Figure D-49a. EDS spectra from Area 1 as indicated in Fig. D-49.

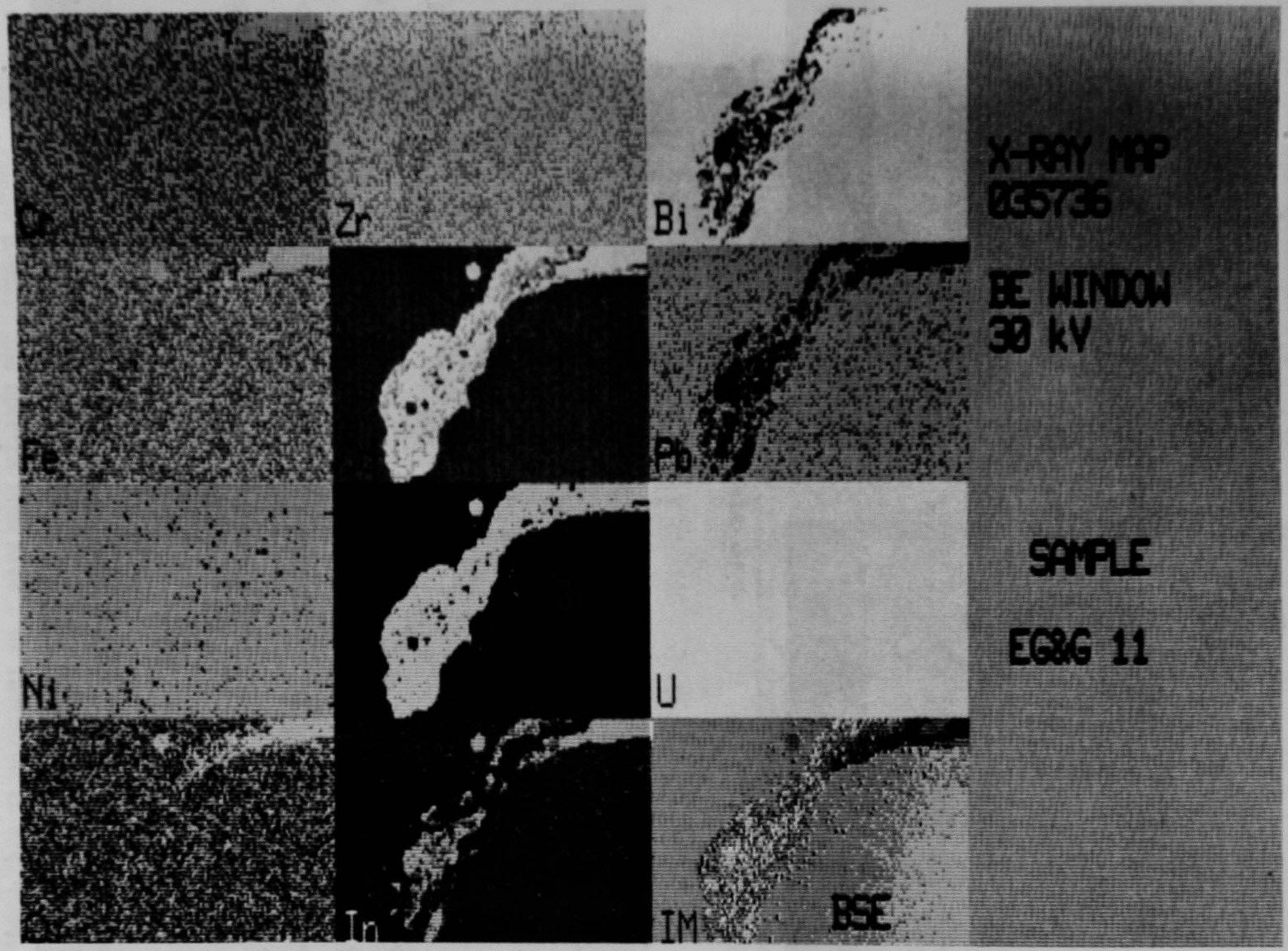

Figure D-49b. Multi-element X-ray dot map of Area 1 as shown in photo 035 736, Fig. D-49.

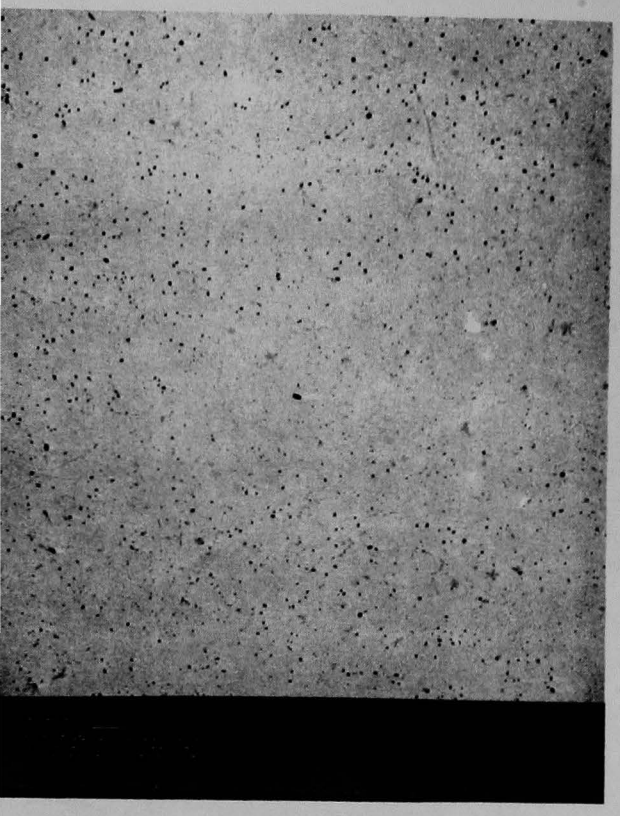

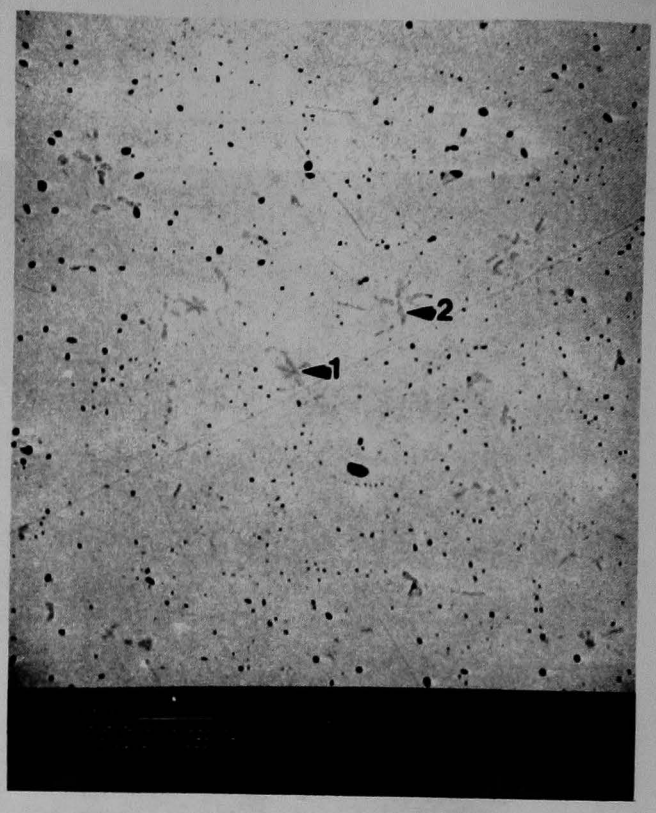

Area 1

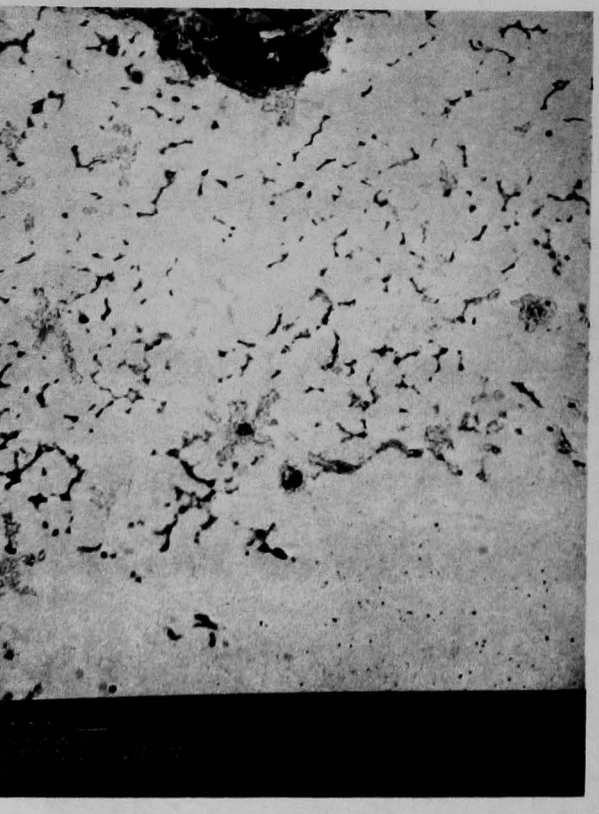

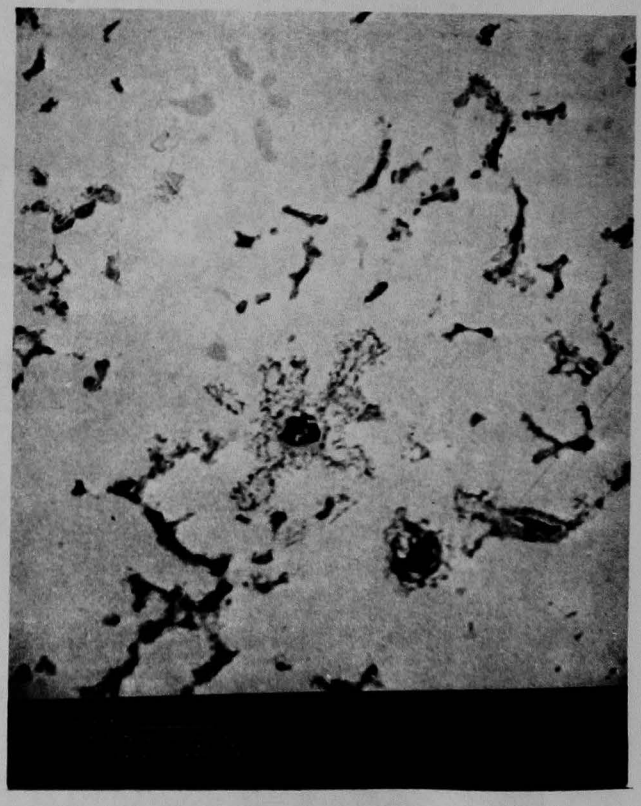

Area 2

Figure D-50. BSE/SEM photos from Areas 1 and 2, Fig. D-48.

22 Jul 1987

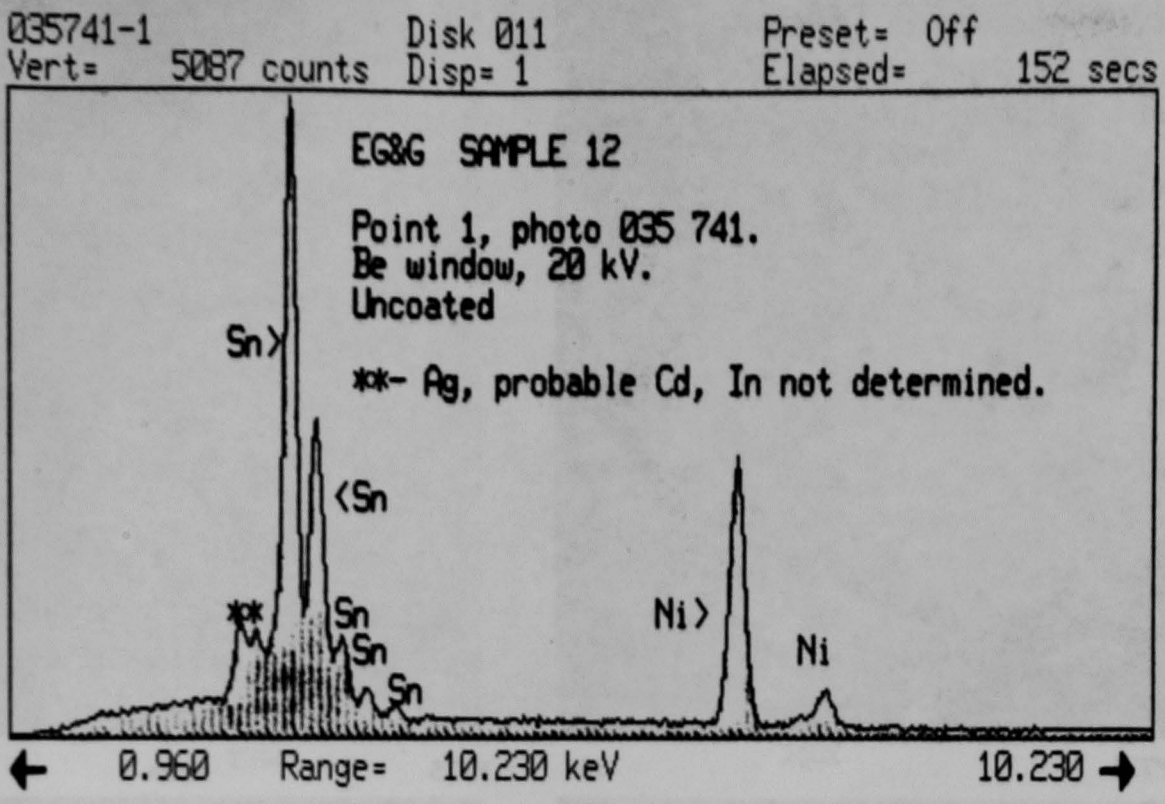

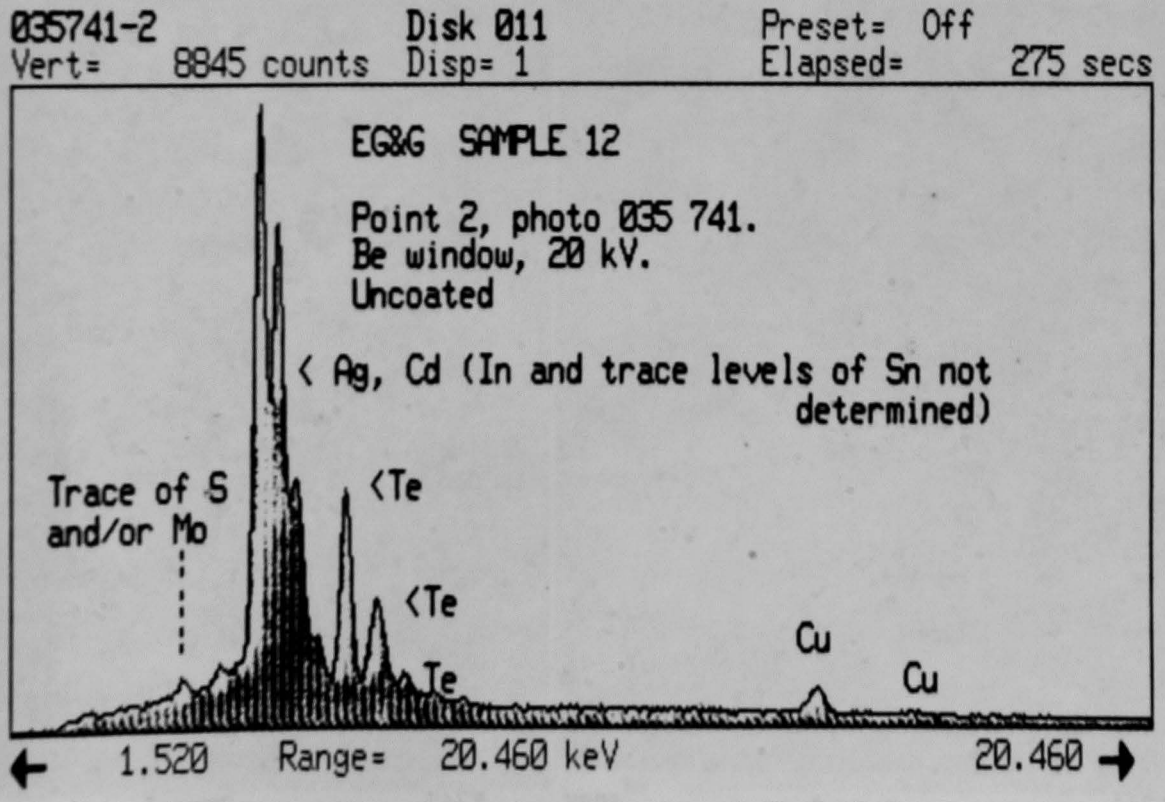

Figure D-50a. EDS spectra from Area 1 as indicated in Fig. D-50.

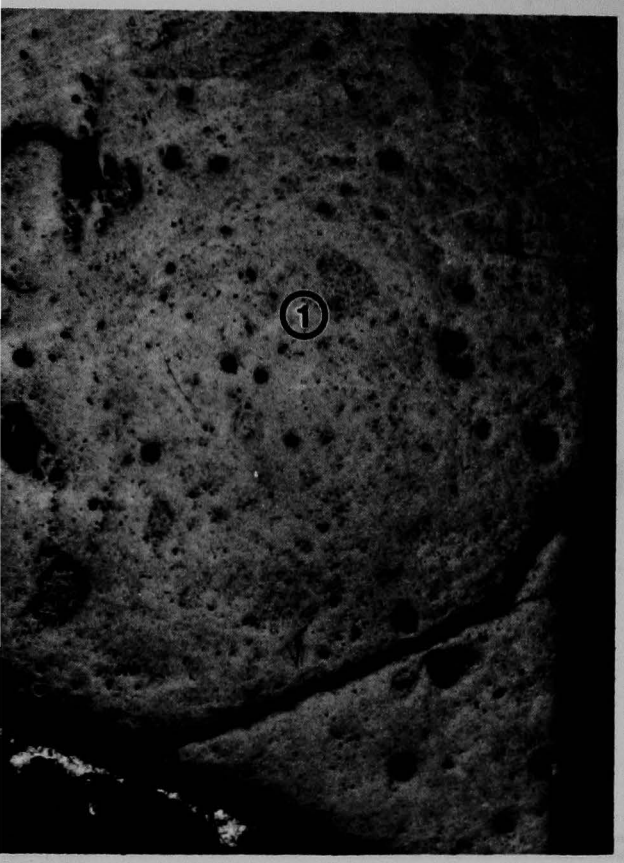

34 50X

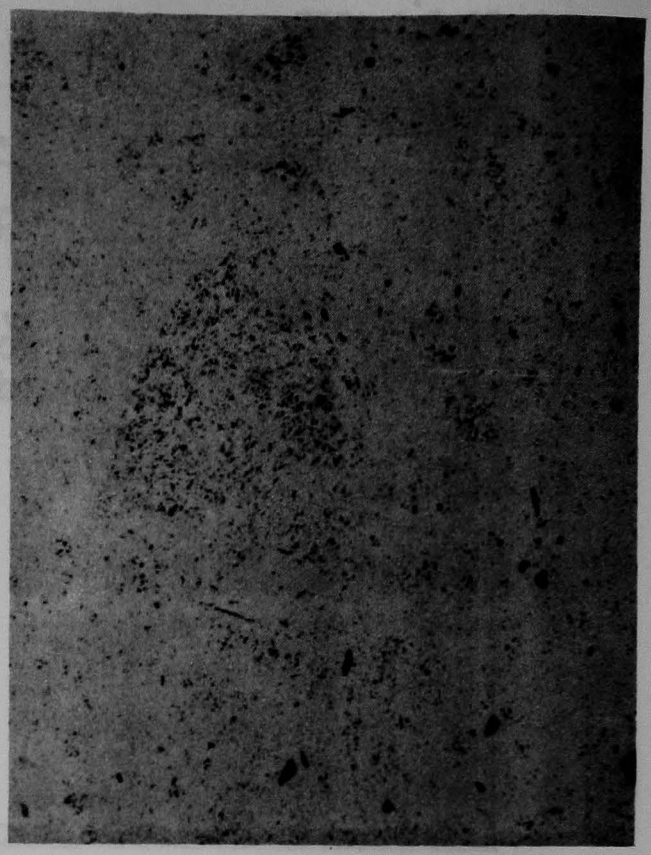

F735 Area 1 200X

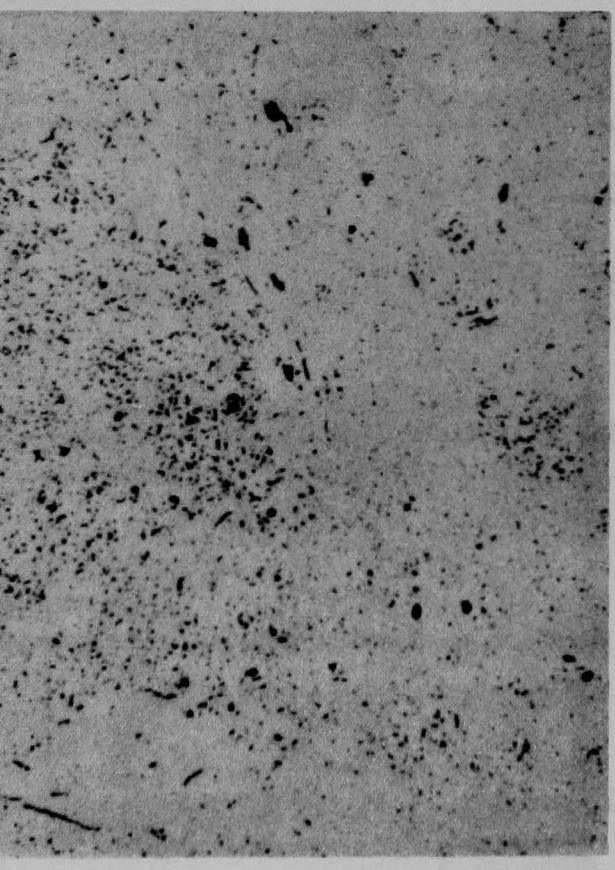

4 Area 1 400X

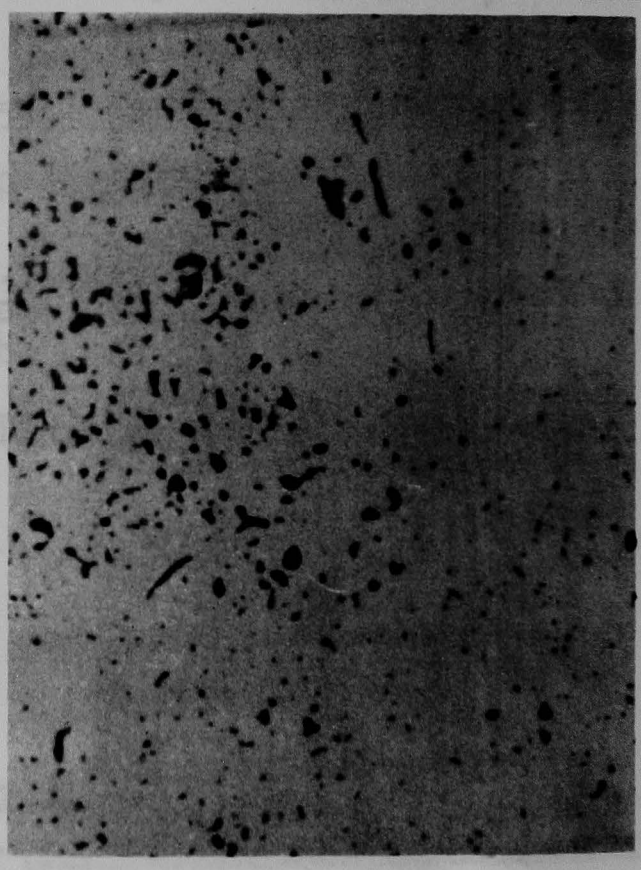

F745 Area 1 1000X

Figure D-51. As polished optical photomicrographs of particle 3.

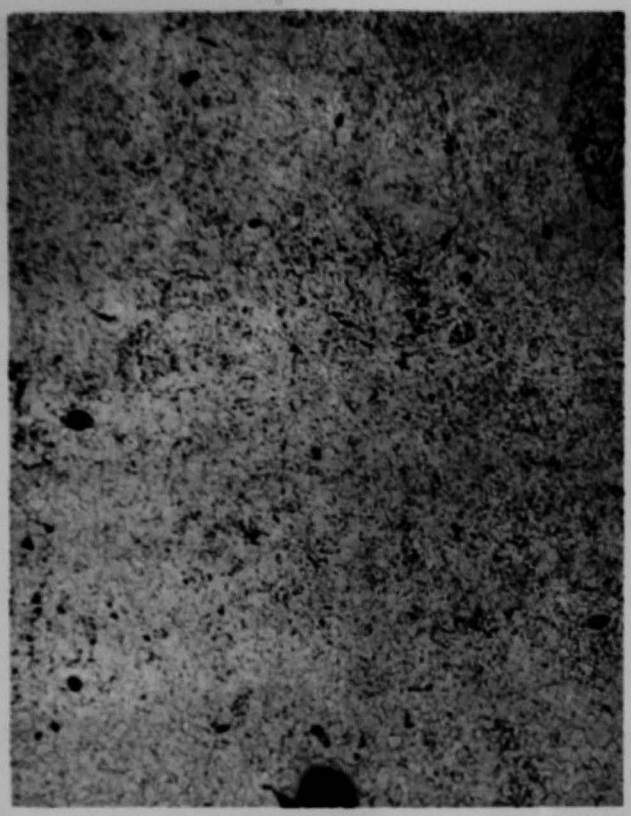

F755 200X

F756 400X

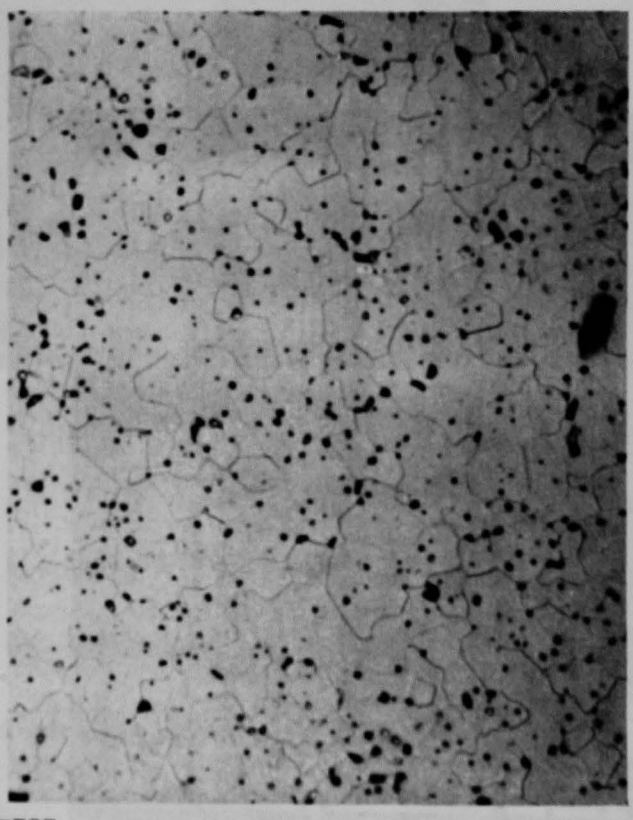

F757 1000X

Figure D-52. Optical photomicrographs of particle 3 in the etched condition (typical).

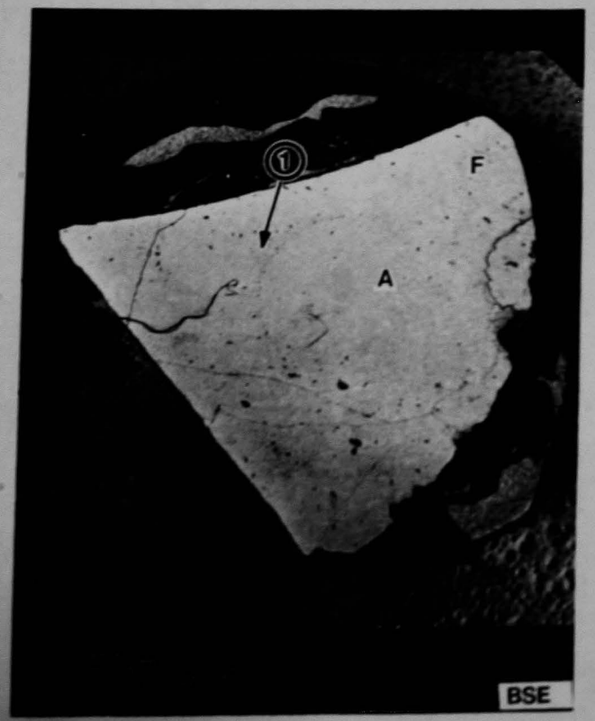

Light Microscopy Performed in Area 1

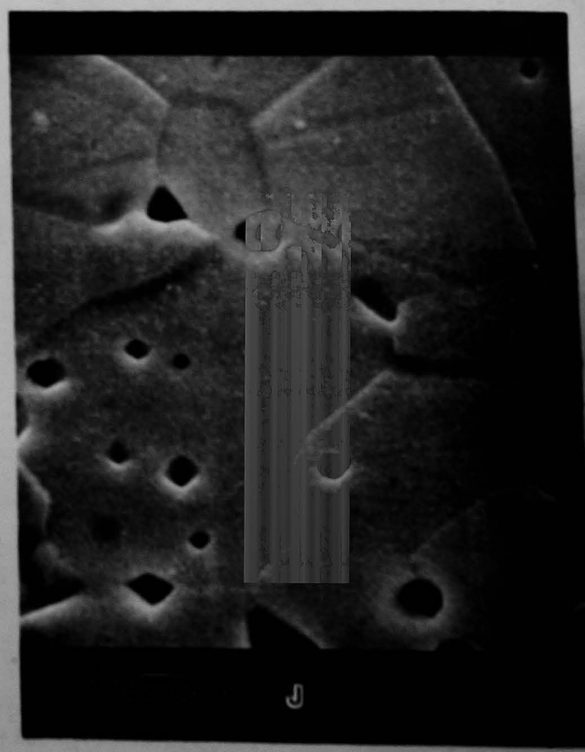

Figure D-53. SEM photomicrographs of particle 3.

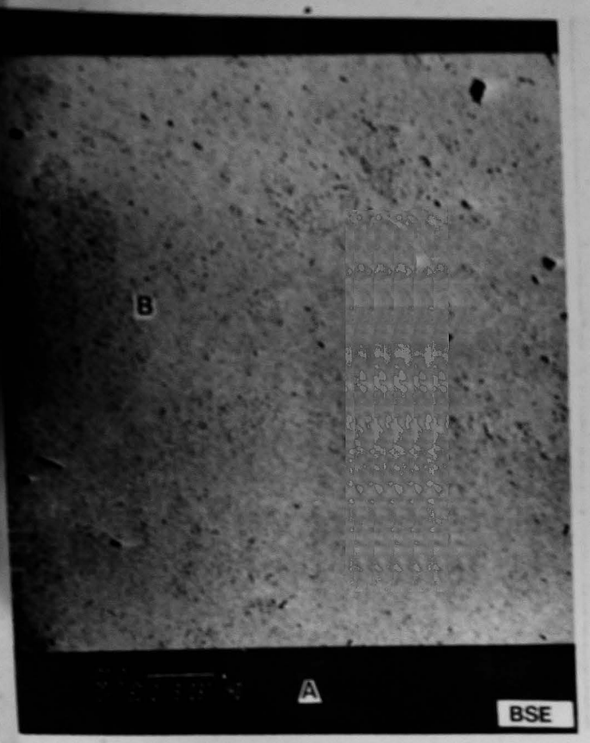

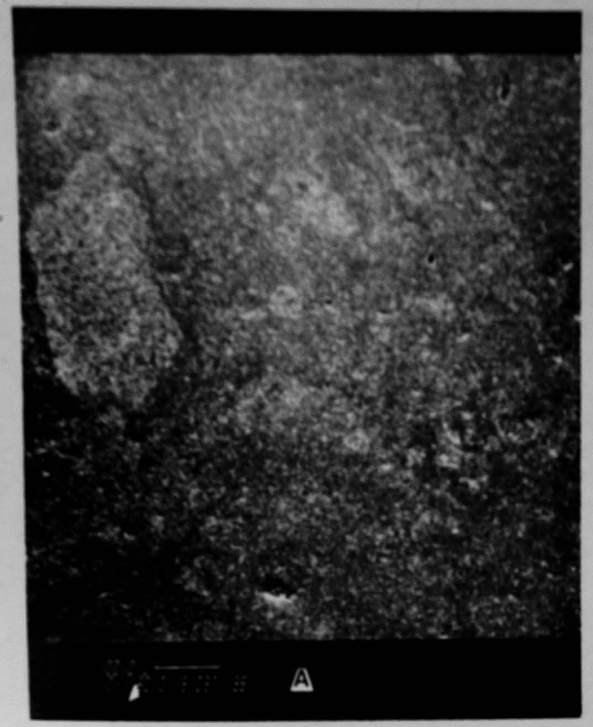

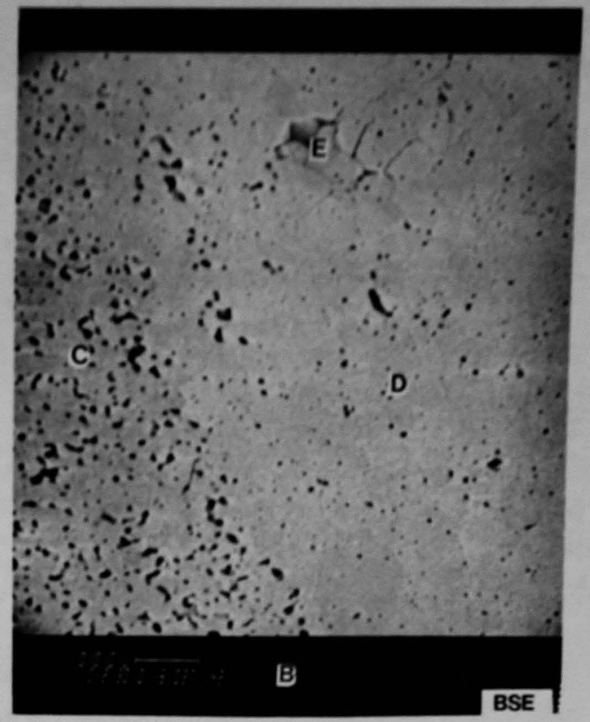

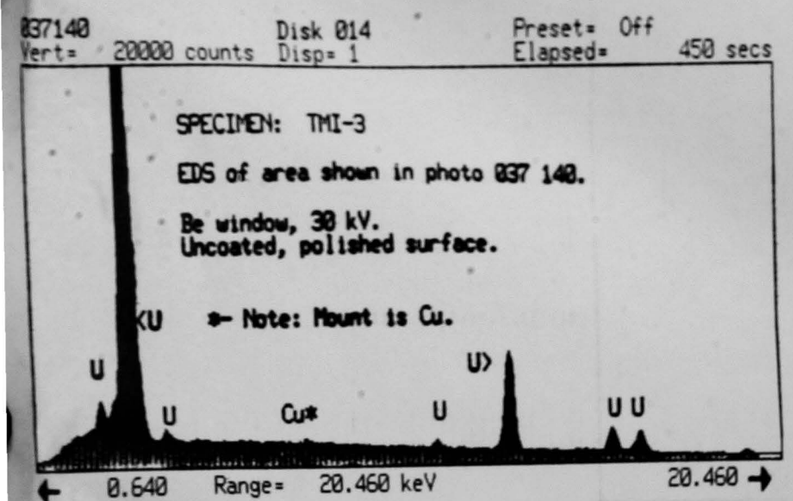

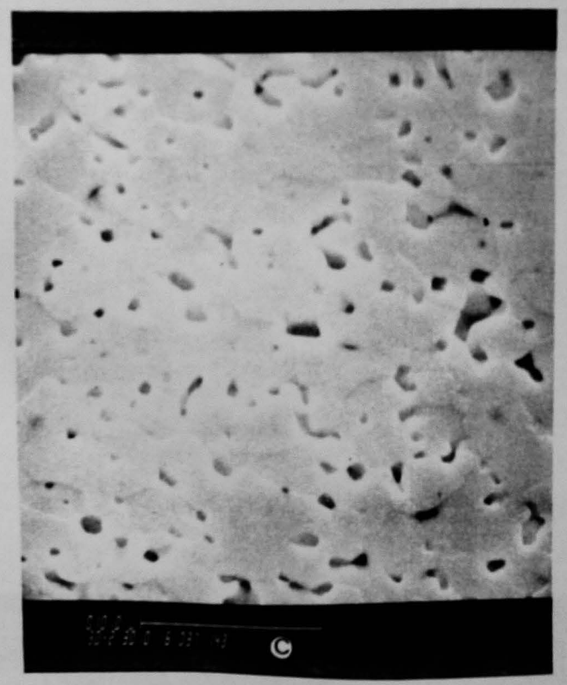

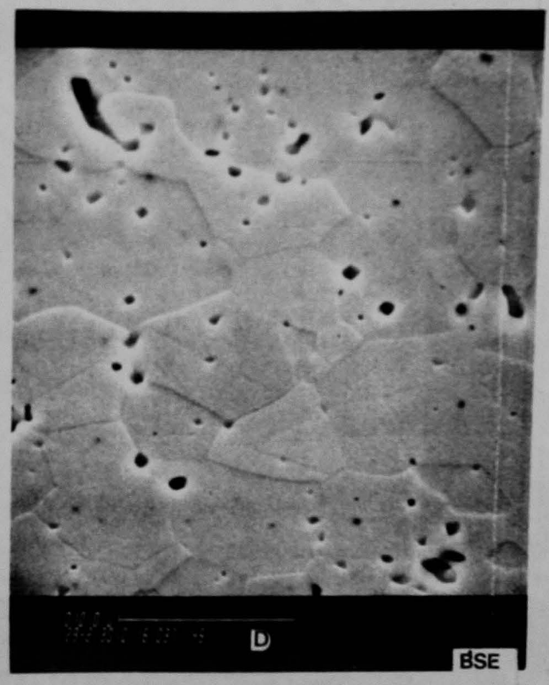

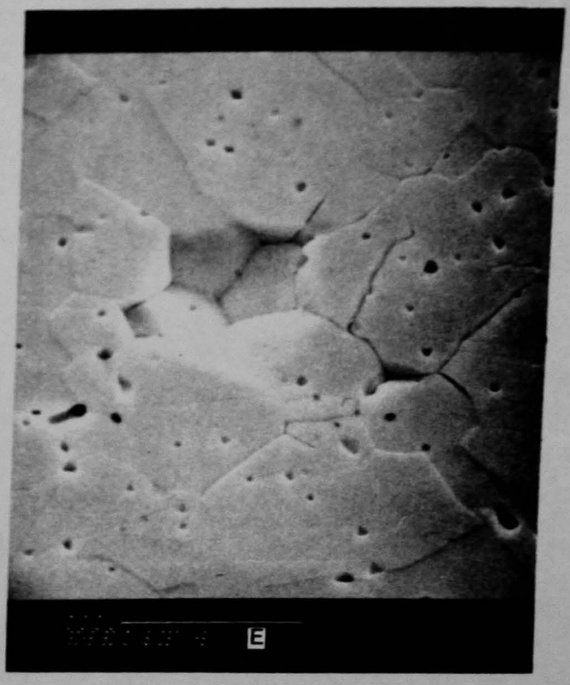

Figure D-54. SEM photomicrographs and EDS spectra of particle 3.